



**Manchester  
Metropolitan  
University**

---

Austin, Catrin Rebeca (2018) Role of MCRP in the clinical management and the pathophysiology of the acute coronary syndromes. Doctoral thesis (PhD), Manchester Metropolitan University.

---

**Downloaded from:** <https://e-space.mmu.ac.uk/621118/>

**Usage rights:** Creative Commons: Attribution-Noncommercial-No Derivative Works 4.0

Please cite the published version

<https://e-space.mmu.ac.uk>

# ROLE OF MCRP IN THE CLINICAL MANAGEMENT AND THE PATHOPHYSIOLOGY OF THE ACUTE CORONARY SYNDROMES

CATRIN REBECA AUSTIN

A thesis submitted in partial fulfilment of the  
requirements of the  
Manchester Metropolitan University for the degree  
of Doctor of Philosophy

School of Healthcare Science  
Faculty of Science and Engineering  
Manchester Metropolitan University  
2018

## Abstract

**Introduction:** The rise in emergency department admissions for chest pain necessitates a quicker and more specific test for the different acute coronary syndromes. For a non-ST elevated myocardial infarction (NSTEMI) diagnosis, the current Gold Standard requires at least one cTn (cTn) value above the 99<sup>th</sup> percentile of a reference population across 12h of serial testing. Current research suggests serum levels of monomeric C-reactive protein (mCRP) and ultra-high-sensitive cTn assays may rule out NSTEMI more rapidly.

**Aims:** To develop a novel immunoassay for mCRP for use on clinical samples to assess its diagnostic accuracy for NSTEMI. The Singulex Clarity and the Abbott iSTAT point of care hs-cTnI assays were assessed against the standard laboratory assay from Roche® Diagnostics hs-cTnT assay for NSTEMI diagnosis using non-kinetic (0h, 3h and max values) and kinetic ( $\Delta_{\text{absolute}}$ ,  $\% \Delta_{\text{baseline}}$  and  $\% \Delta_{\text{mean}}$ ) values and in combination with H-FABP and ECG ischaemia.

**Methods:** A competitive immunoassay for mCRP was optimised, which became an ELISA with a commercial anti-CRP detection antibody. Diagnostic tests calculated the clinical sensitivity, specificity, positive predictive value and negative predictive value for non-kinetic and kinetic values with the aim of creating the highest clinical sensitivity possible for NSTEMI rule out. Patients were grouped into 3 risk groups and cut-offs were optimised for each group. Predictor composites of 0h cTn, cTn deltas, ECG ischaemia and H-FABP were used for NSTEMI diagnosis and prediction of 3 different composite outcomes at 30 days. Cox regression assessed the assays' and risk factors' utility in 30-day MACE prediction.

**Results:** The mCRP immunoassay was not sensitive enough for physiological mCRP concentrations (LoD 2  $\mu\text{g/ml}$ ) and the inter-assay imprecision was too great to be clinically useful. The Roche and Singulex assays showed 100% sensitivity and NPV for kinetic values in intermediate risk groups and predictor composites. The Singulex assay had 100% sensitivity for non-kinetic values also but the iSTAT assay did not perform well as a rule out diagnosis tool. Singulex  $\Delta_{\text{absolute}}$  and prior angina were independent predictors for 30-day MACE.

**Discussion:** The mCRP immunoassay had problems because the antibody was not commercially produced, had to be used at high concentrations and therefore is not suitable for a competitive immunoassay. The Singulex assay could be used for early rule out but its variability could limit its clinical utility. The iSTAT assay is a useful tool for identifying high-risk patients quickly and all assays performed better when patients were split into risk groups by 0h cTn levels. Multi-faceted diagnostic tools are becoming more prominent for NSTEMI diagnosis and rule out.

## Acknowledgements

Firstly, I would like to thank Glenn and Stuart for providing great technical support in the labs across many issues and protocols.

I also extend my gratitude to Nicola who went through CRP purifying techniques with me. It was a pleasure to share a bench.

To the Science & Engineering Research Degrees admin team I would like to say thank you for dealing with all sorts of requests and always doing everything to help until a solution is found.

To my supervisors Dr Sarah Jones and Prof Mark Slevin, I would like to thank for sharing opportunities, knowledge, and techniques with me during my project.

I would like to thank Dr Richard Body for coordinating sample data from the MRI and for his advice.

Dr Jason Ashworth I would like to thank for help in guiding me through the immunoassay development, continued support throughout this process and for always having an open door.

To my friends and family I would ask forgiveness for only talking about troponin and SPSS for the last six months but also a huge thank you for your support and calls for me to rest. I would like to extend a further gratitude to my mother, father and sister whose many forms of support have helped me to progress through this process and onto another exciting adventure.

Finally, I would like to thank my DoS Dr Garry McDowell for all the help and guidance throughout my doctorate and for encouraging me to think for myself. I have learnt so much and will take what I have learnt through to my next post. I am truly grateful.

## Table of Contents

Abstract.....	ii
Acknowledgements.....	iii
List of tables .....	viii
List of figures.....	x
List of abbreviations.....	xiii
Chapter 1: Introduction to mCRP and CTn.....	xvi
1.1 Introduction .....	1
1.2 Atherosclerosis and its role in the development of ACS.....	3
1.2.1 Atherosclerosis as an inflammatory disease.....	3
1.3 mCRP as a causative Biomarkers for ACS .....	8
1.3.1 CRP .....	9
1.3.2 Dissociation from pCRP to mCRP .....	10
1.3.3 Different effects of pCRP & mCRP .....	13
1.3.4 mCRP in ACS diagnosis .....	18
1.4 Current AMI diagnosis.....	20
1.4.1 Risk stratification.....	20
1.5 Molecular characteristics of cTn .....	21
1.5.1 cTn immunoassays .....	22
1.5.2 cTn in ACS diagnosis.....	23
1.5.3 Kinetic and non-kinetic cTn values in ACS diagnosis.....	26
1.6 Molecular characteristics of H-FABP .....	27
1.7 Project Aims .....	28
1.7.1 Assay development.....	29
1.7.2 mCRP Clinical Study.....	29
1.7.3 cTn Clinical Study .....	30
Chapter 2: Materials and Methods.....	31
2.1 Materials .....	32
2.1.1 Immunoassay development materials.....	32
2.2 Methods.....	33
2.2.1 Immunoassay development methods .....	33
2.2.2 Competitive immunoassay development .....	33
2.2.3 Sandwich ELISA development.....	40
2.2.4 Diagnostic and prognostic analysis of three contemporary assays .....	42
Chapter 3: Immunoassay development.....	47
3.1 Competitive immunoassay development .....	48

3.1.1 Preliminary competitive immunoassay .....	48
3.1.2 Immunoassay with competition from mCRP removed.....	49
3.1.3 No competition introduced with alternative mCRP-biotin concentrations.....	50
3.1.4 Addition of 0.05% Tween to wash buffer .....	51
3.1.5 Reduction in range of mCRP-biotin standards to below 60 µg/ml .....	52
3.1.6 Addition of BSA as blocking buffer.....	53
3.1.5 BSA-mCRP interaction.....	54
3.1.6 Possible antibody-avidin and plate-avidin non-specific binding.....	57
3.1.7 Milk protein vs BSA as blocking buffer .....	61
3.1.8 Antibody coating buffer™ and Monster Block™ .....	63
3.1.9 Possible interaction between mCRP and Monster Block™ .....	64
3.1.10 mCRP-biotin conjugate competing with non-labelled mCRP standards.....	65
3.1.11 Experimentation of mCRP incubation time at 24h and 48h at room temperature	
3.1.12 Experimentation of mCRP incubation time at 24h and 48h at 4°C.....	68
3.1.13 Using a mixing plate to pre-equilibrate the mCRP-biotin and competing mCRP.	70
3.2 Sandwich ELISA for the determination of mCRP concentration .....	71
3.2.1 Monoclonal anti-human CRP antibody ab24462 as detection antibody .....	71
3.2.2 Polyclonal anti-human CRP antibody ab19175 as detection antibody.....	73
3.2.3 Non-repeatability of the sandwich ELISA with polyclonal anti-human CRP antibody ab19175 .....	74
Chapter 4: Diagnosis of NSTEMI with non-kinetic cTn values .....	78
4.1 Baseline characteristics of included patients.....	79
4.2 Baseline cTn levels of AMI and no AMI groups.....	80
4.3 Distribution of cTn 0h and 3h values .....	81
4.4 Diagnostic accuracy of 0h, 3h and maximum values of cTn for AMI diagnosis .....	83
4.5 Diagnostic accuracy of 0h, 3h and max cTn values in important patient subgroups ..	86
Chapter 5: Diagnosis of NSTEMI with kinetic cTn deltas .....	89
5.1 Mean $\Delta_{\text{absolute}}$ according to the Roche, Singulex and iSTAT assays .....	91
5.2 Mean $\% \Delta_{\text{baseline}}$ according to the Roche, Singulex and iSTAT assays.....	93
5.3 Mean $\% \Delta_{\text{mean}}$ according to the Roche, Singulex and iSTAT assays.....	94
5.4 Distribution of cTn $\Delta_{\text{absolute}}$ , $\% \Delta_{\text{baseline}}$ and $\% \Delta_{\text{mean}}$ in AMI and no AMI groups.....	95
5.5 Diagnostic accuracy of cTn $\Delta_{\text{absolute}}$ , $\% \Delta_{\text{baseline}}$ and $\% \Delta_{\text{mean}}$ for AMI diagnosis .....	99
5.6 AMI diagnosis with $\% \Delta_{\text{baseline}}$ and $\% \Delta_{\text{mean}}$ with fixed cut-offs.....	102
5.7 Diagnostic accuracy of $\Delta_{\text{absolute}}$ , $\% \Delta_{\text{baseline}}$ and $\% \Delta_{\text{mean}}$ cTn deltas based on baseline cTn	103
5.8 Diagnostic accuracy of baseline cTn in predictor composites with cTn deltas, acute ischaemia, and H-FABP diagnosis for AMI diagnosis for cardiac-associated conditions .....	107

5.9 Diagnostic accuracy of absolute and relative cTn deltas in important patient subgroups	113
Chapter 6: Does non-kinetic cTn predict 30-day outcome?	119
6.1 Baseline characteristics of the 30-day MACE and 30-day no MACE patients	120
6.2 Baseline cTn concentrations of different 30-day composite outcomes	122
6.3 30-day composite MACE prediction by cTn 0h, 3h and max values according to the Roche, Singulex and iSTAT assays	124
6.4 30-day AV1 prediction by cTn 0h, 3h and max values according to the Roche, Singulex and iSTAT assays	128
6.5 30-day AV2 prediction by cTn 0h, 3h and max values according to the Roche, Singulex and iSTAT assays	132
6.6 Comparison of the 0h cut-offs of the Roche, Singulex and iSTAT assays as event predictors	136
Chapter 7: Does kinetic cTn predict 30-day outcome?	140
7.1 $\Delta_{\text{absolute}}$ of different 30-day composite outcomes	141
7.2 $\% \Delta_{\text{baseline}}$ of different 30-day composite outcomes	143
7.3 $\% \Delta_{\text{mean}}$ of different 30-day composite outcomes	145
7.4 30-day composite MACE prediction by cTn $\Delta_{\text{absolute}}$ , $\% \Delta_{\text{baseline}}$ and $\% \Delta_{\text{mean}}$ according to the Roche, Singulex and iSTAT assays	147
7.5 30-day AV1 prediction cTn $\Delta_{\text{absolute}}$ , $\% \Delta_{\text{baseline}}$ and $\% \Delta_{\text{mean}}$ according to the Roche, Singulex and iSTAT assays	151
7.7 Prediction of 30-day composite MACE with baseline cTn in predictor composites with cTn $\Delta_{\text{absolute}}$ , $\% \Delta_{\text{mean}}$ or $\% \Delta_{\text{baseline}}$ , acute ischaemia, and H-FABP	159
7.8 Univariate and multivariate analysis for cTn as measured by the Roche, Singulex and iSTAT assays and of cardiovascular risk factors for composite MACE at 30 days	165
7.9 Comparison of the $\Delta_{\text{absolute}}$ cut-offs of the Roche, Singulex and iSTAT assays as event predictors	167
Chapter 8: Discussion	171
8.1 mCRP immunoassay development	172
8.1.1 8c10 mCRP antibody clone	172
8.1.2 mCRP and mammalian blocking buffers association	173
8.1.3 Hydrophobicity of mCRP	174
8.1.4 Future work for mCRP immunoassays	175
8.2 cTn in the diagnosis of NSTEMI and prediction of 30-day MACE	178
8.2.1 AMI diagnosis by cTn values at 0h and 3h	178
8.2.2 Diagnostic accuracy of cTn $\Delta_{\text{absolute}}$ , $\% \Delta_{\text{baseline}}$ and $\% \Delta_{\text{mean}}$ for AMI diagnosis	184
8.2.3 Diagnostic accuracy of $\Delta_{\text{absolute}}$ , $\% \Delta_{\text{baseline}}$ and $\% \Delta_{\text{mean}}$ cTn deltas based on baseline cTn	188
8.2.4 Absolute relative deltas with fixed cut-offs based on %CV	193
8.2.5 Diagnostic value of baseline cTn in predictor composites with cTn deltas, acute ischaemia, and H-FABP diagnosis for AMI diagnosis according to the 3 assays	194

8.2.6 Prediction of 30-day MACE with cTn 0h & 3h samples.....	198
8.2.7 Prediction of 30-day MACE with cTn $\Delta_{\text{absolute}}$ , $\% \Delta_{\text{baseline}}$ and $\% \Delta_{\text{mean}}$ .....	202
8.2.8 Prediction of 30-day MACE using baseline cTn in predictor composites with cTn deltas, acute ischaemia, and H-FABP diagnosis for AMI diagnosis for cardiac-associated conditions	207
8.2.9 Limitations.....	211
8.2.10 Future work.....	211
8.3 Conclusion.....	214
Appendix I.....	218
Appendix II.....	234
References.....	243



## List of tables

Table 1.3.3 – The different functions of pCPR and mCRP in inflammation.....	15
Table 4.1 Baseline characteristics of the patients.....	78
Table 4.4 Diagnostic accuracy of 0h, 3h and max cTn values for AMI diagnosis .....	85
Table 4.5 Diagnostic accuracy of 0h, 3h and max cTn values in patient subgroups using ROC curve analysis.....	86
Table 5.5 Diagnostic accuracy of cTn $\Delta_{\text{absolute}}$ , $\% \Delta_{\text{baseline}}$ and $\% \Delta_{\text{mean}}$ after 3 hours from presentation for AMI diagnosis.....	101
Table 5.6 Diagnostic accuracy of absolute relative deltas with cut-offs at 10% for AMI diagnosis.....	102
Table 5.7.1 Diagnostic accuracy of cTn $\Delta_{\text{absolute}}$ , $\% \Delta_{\text{baseline}}$ and $\% \Delta_{\text{mean}}$ after 3h grouped by baseline levels for AMI diagnosis according to the Roche assay.....	104
Table 5.7.2 Diagnostic accuracy of cTn $\Delta_{\text{absolute}}$ , $\% \Delta_{\text{baseline}}$ and $\% \Delta_{\text{mean}}$ after 3h grouped by baseline levels for AMI diagnosis according to the Singulex assay.....	105
Table 5.7.3 Diagnostic accuracy of cTn $\Delta_{\text{absolute}}$ , $\% \Delta_{\text{baseline}}$ and $\% \Delta_{\text{mean}}$ after 3h grouped by baseline levels for AMI diagnosis according to the iSTAT assay.....	106
Table 5.8.1 Diagnostic accuracy of baseline cTn in predictor composites with cTn deltas, acute ischaemia, and H-FABP for AMI diagnosis according to the Roche assay .....	108
Table 5.8.2 Diagnostic accuracy of baseline cTn in predictor composites with cTn deltas, acute ischaemia, and H-FABP for AMI diagnosis according to the Singulex assay.....	110
Table 5.8.3 Diagnostic accuracy of baseline cTn in predictor composites with cTn deltas, acute ischaemia, and H-FABP for AMI diagnosis according to the Singulex assay.....	112
Table 5.9 Diagnostic accuracy of absolute and relative cTn deltas in patient subgroups using ROC curve analysis.....	114
Table 6.1 Baseline characteristics of 30-day MACE positive and 30-day MACE negative patients.....	121
Table 6.3 30-day composite MACE prediction by cTn 0h, 3h and max values according to the Roche, Singulex and iSTAT assays.....	127
Table 6.4 30-day AV1 prediction by cTn 0h, 3h and max values according to the Roche, Singulex and iSTAT assays.....	131
Table 6.5 30-day AV2 prediction by cTn 0h, 3h and max values according to the Roche, Singulex and iSTAT assays.....	135
Table 7.4 30-day composite MACE prediction by cTn $\Delta_{\text{absolute}}$ , $\% \Delta_{\text{baseline}}$ and $\% \Delta_{\text{mean}}$ according to the Roche, Singulex and iSTAT assays.....	150

Table 7.5 30-day AV1 prediction cTn $\Delta_{\text{absolute}}$ , $\% \Delta_{\text{baseline}}$ and $\% \Delta_{\text{mean}}$ according to the Roche, Singulex and iSTAT assays.....	154
Table 7.6 30-day AV2 prediction cTn $\Delta_{\text{absolute}}$ , $\% \Delta_{\text{baseline}}$ and $\% \Delta_{\text{mean}}$ according to the Roche, Singulex and iSTAT assays.....	158
Table 7.7.1 Prediction of 30-day composite MACE with baseline cTn in predictor composites with cTn $\Delta_{\text{absolute}}$ , $\% \Delta_{\text{mean}}$ or $\% \Delta_{\text{baseline}}$ , acute ischaemia, and H-FABP with cTn according to the Roche assay.....	160
Table 7.7.2 Prediction of 30-day composite MACE with baseline cTn in predictor composites with cTn $\Delta_{\text{absolute}}$ , $\% \Delta_{\text{mean}}$ or $\% \Delta_{\text{baseline}}$ , acute ischaemia, and H-FABP with cTn according to the Singulex assay.....	162
Table 7.7.3 Prediction of 30-day composite MACE with baseline cTn in predictor composites with cTn $\Delta_{\text{absolute}}$ , $\% \Delta_{\text{mean}}$ or $\% \Delta_{\text{baseline}}$ , acute ischaemia, and H-FABP with cTn according to the iSTAT assay.....	164
Table 7.8.1 Univariate Cox proportional hazard analyses of cardiovascular risk factors predicting 30-day composite MACE.....	166
Table 7.8.2 Roche univariate Cox proportional hazard analyses of predicting 30-day composite MACE.....	166
Table 7.8.3 Singulex univariate Cox proportional hazard analyses of predicting 30-day composite MACE.....	166
Table 7.8.4 iSTAT univariate Cox proportional hazard analyses of predicting 30-day composite MACE.....	167
Table 7.8.5 Multivariate Cox proportional hazard analyses of predicting 30-day composite MACE.....	167

## List of figures

Figure 1.2.1.1 Diagram of shear stress changes around atheromas.....	4
Figure 1.2.1.2 Diagram of leukocyte infiltration through the vascular endothelium.....	5
Figure 1.2.1.3 Diagram of monocyte infiltration into the vascular tunica intima and vSMC migration from the tunica media into the intima.....	6
Figure 1.2.1.4 Stable and unstable plaque conformation.....	7
Figure 1.3 Atheroma development from foam cell infiltration through to plaque rupture....	8
Figure 1.3.2 The mechanism that leads to pCRP dissociation creating mCRP.....	10
Figure 1.3.3 Space-filling model of the 2 faces of pCRP.....	17
Figure 2.2.2 Diagram of the mCRP competitive immunoassay.....	33
Figure 2.2.3 Diagram of the mCRP sandwich ELISA.....	40
Figure 2.2.4.3.1 Mean single site repeatability %CV of cTnI Singulex assay.....	46
Figure 2.2.4.3.2 Mean multi-site repeatability %CV of cTnI Singulex assay.....	46
Figure 3.1.1 Preliminary competitive immunoassay for the determination of mCRP concentration in serum.....	48
Figure 3.1.2 Association between antibody concentrations, mCRP-biotin concentrations and absorbance.....	49
Figure 3.1.3 Association between antibody concentrations with alternative mCRP-biotin concentrations and absorbance.....	50
Figure 3.1.4 The effect of 0.05% Tween in CRP buffer as a wash buffer.....	51
Figure 3.1.5 Smaller range of mCRP-biotin concentrations in an immunoassay without competition to determine where rises in absorbance occur.....	52
Figure 3.1.6 Use of 0.05% Tween in CRP buffer for wash cycles and the effect of varying BSA concentrations.....	53
Figure 3.1.7 Possible BSA-mCRP interaction by using different BSA concentrations.....	56
Figure 3.1.8 Assessing possible antibody-avidin non-specific binding.....	59
Figure 3.1.8.1 Assessing possible avidin-BSA binding.....	60
Figure 3.1.9 Comparing milk protein and BSA as blocking buffers.....	62
Figure 3.1.10 Comparison between coating plates with antibody with and without Antibody Coating Buffer™ and possible interaction between mCRP and Monster Block™ .....	63
Figure 3.1.11 Assessing mCRP-Monster Block™ interaction with no antibody present.....	64
Figure 3.1.12 Competitive assay between mCRP-biotin and unlabelled mCRP standards....	66
Figure 3.1.13 Competitive immunoassay with 24h and 48h mCRP incubation time at room temperature.....	67

Figure 3.1.14 Competitive immunoassay with 24h and 48h mCRP incubation time at 4°C...	69
Figure 3.1.15 Pre-mixing of mCRP-biotin and mCRP and the effect of absorbance on the mixing plate.....	70
Figure 3.2.1 Development of sandwich ELISA for mCRP concentration determination using monoclonal antibody ab24462. ....	72
Figure 3.2.2 Sandwich ELISA for the determination of mCRP concentration with polyclonal antibody ab19175. ....	73
Figure 3.2.3 Poor repeatability of the mCRP ELISA with ab19175.....	75
Figure 4.2 Mean baseline cTn concentrations according to the Roche, Singulex and iSTAT assays.....	80
Figure 4.3 Distribution in histograms of cTn values in AMI and no AMI groups according to the Roche, Singulex and iSTAT assays.....	82
Figure 4.4 ROC curve of cTn 0h, 3h and max values according to the Roche, Singulex and iSTAT assays for AMI diagnosis.....	84
Figure 4.5 ROC curves for the diagnostic accuracy of 0h, 3h and max values of the Roche, Singulex and iSTAT assays for AMI diagnosis in important patient subgroups.....	88
Figure 5.1 Mean $\Delta_{\text{absolute}}$ cTn concentrations according to the Roche, Singulex and iSTAT assays.....	92
Figure 5.2 Mean $\% \Delta_{\text{baseline}}$ cTn concentrations according to the Roche, Singulex and iSTAT assays.....	93
Figure 5.3 Mean $\% \Delta_{\text{mean}}$ cTn concentrations according to the Roche, Singulex and iSTAT assays.....	94
Figure 5.4.1 Distribution of cTn deltas in AMI and no AMI groups according to the Roche assay.....	96
Figure 5.4.2 Distribution of cTn deltas in AMI and no AMI groups according to the Singulex assay. ....	97
Figure 5.4.3 Distribution of cTn deltas in AMI and no AMI groups according to the iSTAT assay.....	98
Figure 5.5 ROC curves of cTn $\Delta_{\text{absolute}}$ , $\% \Delta_{\text{baseline}}$ and $\% \Delta_{\text{mean}}$ according to the Roche, Singulex and iSTAT assays for AMI diagnosis. ....	100
Figure 5.9 ROC curves for the diagnostic accuracy of $\Delta_{\text{absolute}}$ , $\% \Delta_{\text{baseline}}$ and $\% \Delta_{\text{mean}}$ according to the Roche, Singulex and iSTAT assays for AMI diagnosis in important patient subgroups .....	114
Figure 6.2 Median cTn values at baseline by different 30-day prognoses according to the Roche, Singulex and iSTAT assays.....	123
Figure 6.3 ROC curve of cTn 0h, 3h and maximum values according to the Roche, Singulex and iSTAT assays for 30-day composite MACE.....	125

Figure 6.4 ROC curve of cTn 0h, 3h and maximum values according to the Roche, Singulex and iSTAT assays for 30-day AV1 prediction.....	129
Figure 6.5 ROC curve of cTn 0h, 3h and maximum values according to the Roche, Singulex and iSTAT assays for 30-day AV2 prediction.....	133
Figure 6.6 Kaplan-Meier curves for the prognostic value of the 0h cTn sample values for composite MACE prediction between high and low cTn groups according to the Roche, Singulex and iSTAT assays.....	137
Figure 7.1 Median cTn $\Delta_{\text{absolute}}$ by different 30-day prognoses according to the Roche, Singulex and iSTAT assays.....	142
Figure 7.2 Median cTn $\% \Delta_{\text{baseline}}$ by different 30-day prognoses according to the Roche, Singulex and iSTAT assays.....	144
Figure 7.3 Median cTn $\% \Delta_{\text{mean}}$ by different 30-day prognoses according to the Roche, Singulex and iSTAT assays. ....	146
Figure 7.4 ROC curve of cTn $\Delta_{\text{absolute}}$ , $\% \Delta_{\text{baseline}}$ and $\% \Delta_{\text{mean}}$ according to the Roche, Singulex and iSTAT assays for 30-day composite MACE.....	148
Figure 7.5 ROC curves of cTn $\Delta_{\text{absolute}}$ , $\% \Delta_{\text{baseline}}$ and $\% \Delta_{\text{mean}}$ according to the Roche, Singulex and iSTAT assays for 30-day AV1.....	152
Figure 7.6 ROC curves of cTn $\Delta_{\text{absolute}}$ , $\% \Delta_{\text{baseline}}$ and $\% \Delta_{\text{mean}}$ according to the Roche, Singulex and iSTAT assays for 30-day AV2.....	156
Figure 7.9 Kaplan-Meier curves for the prognostic value of the $\Delta_{\text{absolute}}$ for 30-day composite MACE prediction between high and low cTn groups according to the Roche, Singulex and iSTAT assays.....	168
Figure 8.2.1 The effect of adjusting diagnostic cut-offs on diagnostic sensitivity and specificity.....	182

## List of abbreviations

$\Delta_{\text{absolute}}$  – absolute change in cTn

$\% \Delta$  – relative change in cTn

$\% \Delta_{\text{baseline}}$  – relative to baseline change in cTn

$\% \Delta_{\text{mean}}$  – relative to mean change in cTn

ACS – acute coronary syndrome

Akt – protein kinase B

AMI – acute myocardial infarction

AUC – area under curve

AV1 – adverse events 1

AV2 – adverse events 2

BSA – bovine serum albumin

CAD – coronary artery disease

CABG – coronary artery bypass graft

CD36 – cluster of differentiation 36

CHF – chronic heart failure

CI – confidence interval

CK-MB – creatine kinase, muscle and brain forms bound

CRP – C-reactive protein

cTn – cardiac troponin

$\text{cTn}_{\text{low}}$  – lowest possible baseline cTn concentration for effective  $\% \Delta$  based on the functional sensitivity

CV – coefficient of variation

CXCL1 – chemokine (C-X-C motif) ligand-1

CXCL4 – chemokine (C-X-C motif) ligand-4

CXCL7 – chemokine (C-X-C motif) ligand-7

ECG – electrocardiogram

ELISA – enzyme-linked immunosorbent assay

eNOS – endothelial nitric oxide synthase

FGF – fibroblast growth factor

FS – functional sensitivity

h-FABP – human fatty acid binding protein  
hs-cTn – high sensitivity cardiac troponin  
HRP – horseradish peroxidase  
HUVEC – human umbilical vein endothelial cell  
ICAM-1 – intercellular adhesion molecule-1  
IFN- $\gamma$  – interferon- $\gamma$   
IGF-1 – insulin-like growth factor-1  
IL-1 – interleukin-1  
IL-6 – interleukin-6  
JAK – Janus kinase  
JAM-1 – junctional adhesion molecule-1  
LDL – low-density lipoprotein  
LoD – limit of detection  
LOX-1 – lectin-like oxidised low-density lipoprotein receptor-1  
LPC – lysophosphatidylcholine  
MACE – major adverse coronary events  
MACS – Manchester acute coronary syndromes  
MCP-1 – monocyte chemoattractant protein  
mCRP – monomeric C-reactive protein  
MMPO – matrix metalloproteinase  
MP – microparticle  
MPO – myeloperoxidase  
NICE – National Institute for Health and Care Excellence  
NO – nitric oxide  
NPV – negative predictive value  
NSTEMI – non-ST-elevation myocardial infarction  
oxLDL – oxidised low-density lipoprotein  
PAPP-A – pregnancy-associated plasma protein-A  
pCRP – pentameric C-reactive protein  
PCI – percutaneous coronary intervention  
PDGF – platelet-derived growth factor

PI3K – phosphoinositide 3 kinase  
PIGF – placental growth factor  
PPV – positive predictive value  
PSGL – P-selectin glycoprotein ligand-1  
RCV – reference change value  
ROC – receiver operating characteristic  
skTNT – skeletal troponin T  
STAT - signal transducer and activator of transcription  
STEMI – ST-elevation myocardial infarction  
TMB - 3,3',5,5'-tetramethyl benzidine  
TF – tissue factor  
TGF – transforming growth factor  
TIMI – thrombolysis in myocardial infarction  
TLR4 – Toll-like receptor-4  
TSSO – time since symptom onset  
TnC – troponin C  
TnI – troponin I  
TnT – troponin T  
UA – unstable angina  
VCAM-1 – vascular cell adhesion molecule-1  
vSMC – vascular smooth muscle cell



## **Chapter 1: Introduction to mCRP and cardiac troponin**

## 1.1 Introduction

With the number of people admitted to the emergency department (ED) in the UK increasing and many present with chest pain, there is a call to differentiate those in need of immediate attention and those who are not at significant risk of acute coronary syndrome (ACS). As many as 85% of patients who present to the ED do not suffer an acute myocardial infarction and are needlessly kept in the ED waiting for an acute myocardial infarction (AMI) exclusion or, perhaps worse, delaying diagnosis of another syndrome or disease. Currently, when a patient presents with chest pain an electrocardiogram (ECG) is taken immediately to confirm or rule out an ST-elevation myocardial infarction (STEMI). However, absence of ST segment elevation is not sufficient to rule out ACS.

In the case of a negative ECG, a blood test is used to assess the likelihood of a non-STEMI (NSTEMI). The Gold Standard biomarker is currently cardiac troponin (cTn) to diagnose AMI (7, 8). The rise and fall in cTn is used as an indicator of AMI but is insufficiently sensitive to safely rule out AMI until 12 hours after presentation. An AMI is diagnosed if serum cardiac cTn concentration is above the 99<sup>th</sup> percentile in at least one of the measurements taken over the 6-12 hour hospital stay. However, this does not take into account conditions that cause a chronic rise in serum cTn such as heart failure and hypertrophic cardiomyopathy. Even new thinking of using an absolute or relative rise in cTn over a shorter period of time causes problems as non-ischaemic disease such as pericarditis and myocarditis cause an acute rise in cTn (9). This is because cTn is a marker of cardiac cell death instead of direct marker of an infarct.

Moreover, as cTn is a measure of an event that has already happened, its use as an ACS predictor has been limited thus far. The problem lies with the cause of cTn release, which is that it is only released due to cardiac necrosis. Another possible approach would be to measure markers that rise earlier such as those involved in vascular inflammation or plaque rupture, such as monomeric C-reactive protein (mCRP) and human fatty acid binding protein (h-FABP), and use them in combination with cTn. Their benefits have been noted by earlier studies but their use in conjunction with clinical risk stratification of an unselected group of patients have not.

The development of ACS is the outcome of progressive atherosclerosis, which in itself is an inflammatory process. Instead of focusing on the outcome of a myocardial infarct, attention has now turned to markers that cause plaque rupture and therefore AMI. One such marker is C-reactive protein (CRP), which in a recent meta-analysis was shown to be a predictor of long-term cardiovascular mortality 72 hours post-event (10). CRP is a pentraxin consisting of five identical non-covalently linked subunits in its pentameric form, pCRP, but its monomeric form, mCRP, arises by pCRP dissociating on circulating microparticles (MPs) and activated platelets under flow (11). The isoforms have already been shown to rise in AMI and unstable angina pectoris (UAP). Due to the opposing roles pCRP and mCRP take part in vascular inflammation, a pCRP:mCRP ratio may have greater utility.

## 1.2 Atherosclerosis and its role in the development of ACS

The primary cause of ACS is ischaemia at rest from a lack of adequate blood flow to the myocardium. Although there can be many causes of this ischaemia, such as acute coronary vasospasm, the vast majority of patients suffer with atherosclerosis-related ACS such as STEMI (30%), NSTEMI (25%) and unstable angina (38%) (12).

Atherosclerosis causes a thickening of the arteries and a change in cellular composition resulting from lipid accumulation, cell proliferation and transformation over a number of years (13). Normally a gradual process, ruptures cause a large and rapid transformation of the atheroma. The centre of the plaque has no or very restricted blood flow, which leads to the development of a necrotic core. Plaque rupture exposes the necrotic core to the blood that initiates the clotting cascade and a thrombus develops. Repair of plaques develops its size by enveloping the thrombus and inward remodelling of the artery into the lumen restricts blood flow, which is when symptoms begin to occur. If a thrombus is present in a coronary artery and large enough, ACS will develop, a medical emergency that requires immediate treatment to prevent further necrosis to the myocardium.

### 1.2.1 Atherosclerosis as an inflammatory disease

The initiation of atherosclerosis is not well understood. In the first instance, an inflammatory response is required to begin atherosclerosis and the association of low-density lipoprotein (LDL) to the vessel wall either initiates or propagates this response of the endothelium (14). This, as well as high shear stress, causes endothelial activation and more LDL is allowed into the tunica intima of the affected site creating a burden on the vascular smooth muscle cells (vSMCs) in the tunica media, which causes the wall to become less compliant through oxLDL-

mediated vSMC transformation (15). Along with the loss of function of the endothelium and cell transformation, the increased inflammatory profile of the area causes an increase in blood flow and cell number and leukocyte infiltration. A number of cardiovascular risk factors, such as hypertension, hyperlipidaemia, oxidative stress and diabetes, increase LOX-1 expression in the endothelial cells that further increases the LDL uptake (16). This process is upregulated by the binding of CRP to LOX-1, further increasing oxLDL uptake, a process that increases endothelial upregulation of CRP expression creating a strong local positive feedback loop (17). To compound this process, anti-atherogenic endothelial nitric oxide synthase (eNOS) and nitric oxide (NO), a powerful vasodilator, are downregulated by LDL, a decrease in shear stress, cytokines and CRP.

Although the decrease in shear stress does not conform with the traditional cardiovascular risk factor of hypertension, the shape of an atheroma allows low shear stress to occur downstream of the plaque with the endothelium upstream of the plaque experiencing high levels of shear stress (18) as seen in figure 1.2.1.1. Its own remodelling initiating further plaque progression in different areas of the artery due to high shear stress (19). However, the role of high shear stress is debated and is considered now as possible cardioprotective except at sites of inflammation but oscillating shear stress could

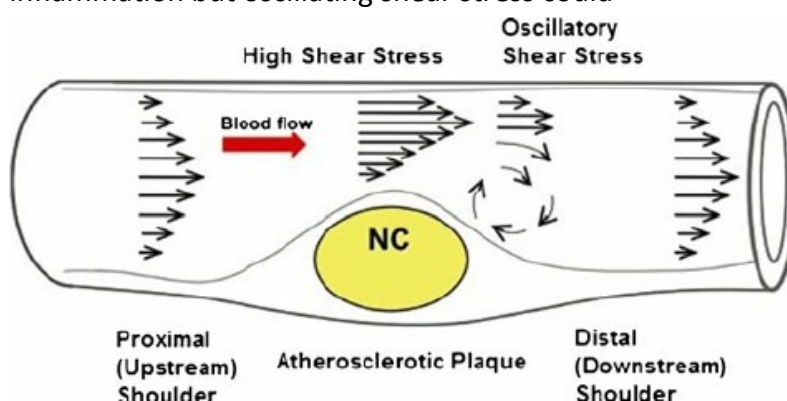


**Figure 1.2.1.1** Diagram of shear stress changes around atheromas. The blood flow is restricted by the imposing atheroma increasing wall shear stress experienced at and upstream of the atheroma. The re-expansion of the lumen downstream causes oscillatory shear stress (2).

downregulated PI16, an endothelial cell migration inhibitor (20). This increases the inflammatory profile of the atheroma further.

The migration of endothelial cells is important for leukocyte infiltration through the endothelium and into the intima (21). As seen in figure 1.2.1.2, a product of endothelial dysfunction is the expression of leukocyte receptors P- and E-selectins, which has been found to be upregulated by the presence of leukocytes themselves along with endothelial-derived chemoattractants (22) that attract more leukocytes. The selectins cause a loose association between the endothelium and the L-selectin and PSGL on leukocytes, which begin to roll and slow along the apical surface of the endothelium. At this point, the leukocytes undergo a slight conformational change due to the rolling and become flatter, increasing their surface area. The increased blood flow prevents the shearing force from dragging leukocytes into the middle of the blood flow. Both these actions allow firmer adhesion to the endothelium and binding to vascular cell adhesion molecule (VCAM)-1 and intercellular adhesion molecule (ICAM)-1. Monocytes have specific receptors for binding such as CXCL1,

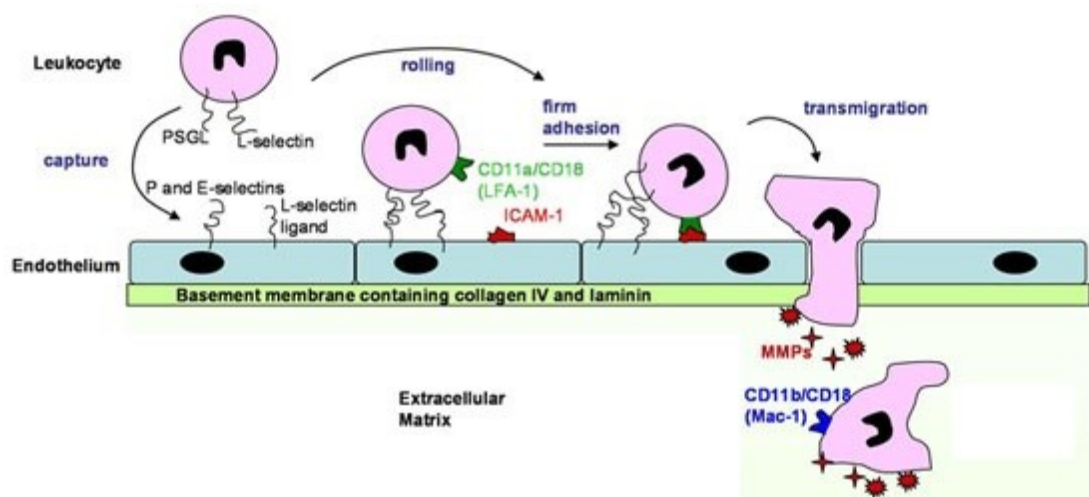


**Figure 1.2.1.2** Diagram of leukocyte infiltration through the vascular endothelium. Matrix metalloproteinases (MMPs) degrade the basement membrane and leukocytes can enter the tunica intima proper (2).

CXCL4, CXCL7 and CCL5. Transmigration is complete by the movement of leukocytes through the endothelium in areas where gap junctions have been weakened because of changes to VE-cadherin and dimerization of JAM-1 increases endothelial permeability (23).

Once in the intima of the endothelium, the monocytes differentiate into macrophages that uptake LDL and release cytokines, as seen in figure 1.2.1.3. The migration of vSMC from the media to the intima is induced through the interleukin (IL)-6/interferon (IFN)- $\gamma$  pathway. Here, the JAK/STAT pathway (24) and CD36 and TLR4-mediated oxLDL downregulation of contractile proteins initiates the vSMCs' transition from a contractile to a reparatory phenotype (25) and TNF- $\alpha$ -promoted vSMC proliferation increases atheroma size further. PDGFs, FGFs and TGFs promotes extracellular matrix synthesis that includes collagen, which initiates the

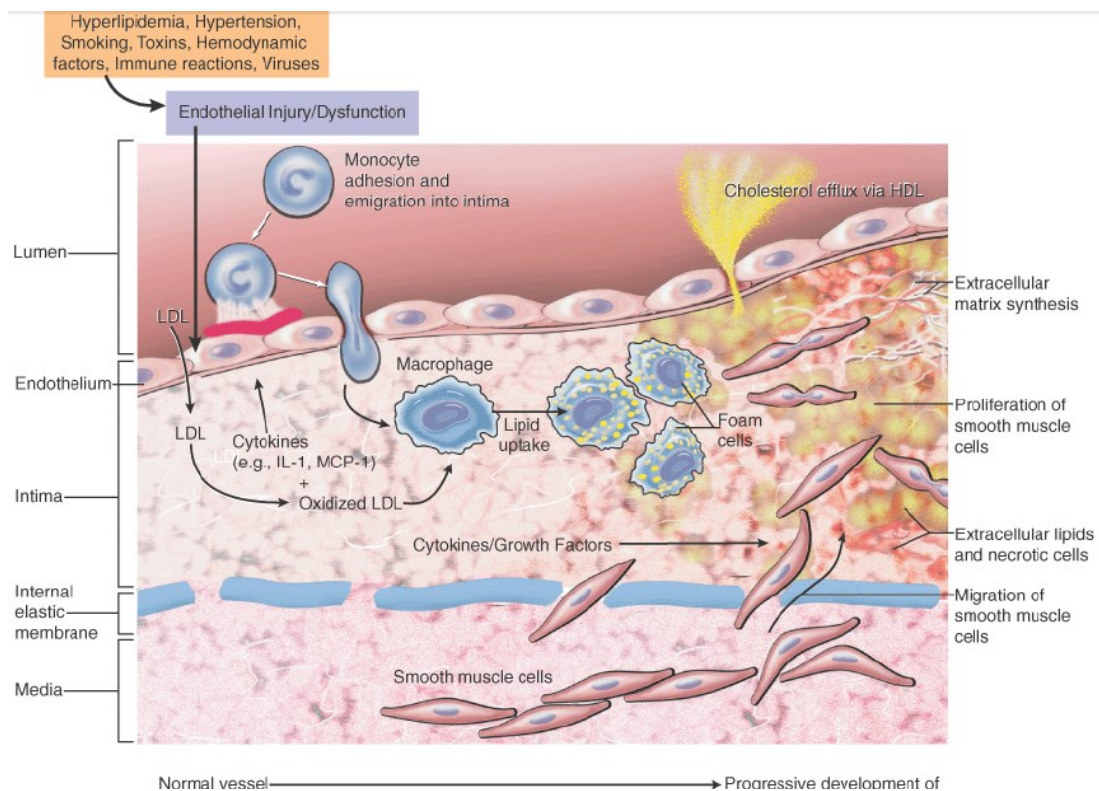


**Figure 1.2.1.3** Diagram of monocyte infiltration into the vascular tunica intima and vSMC migration from the tunica media into the intima(1).

thrombin/thromboxane platelet aggregation pathway (26), leading to thrombosis and possible artery occlusion.

If the resulting thrombosis is asymptomatic and no treatment occurs then the thrombosis is repaired and is added to the atheroma. This results in a stronger atheroma overall but is the cause of inward remodelling, which leads to stenosis.

Even though stenosis reduces blood flow by narrowing the lumen, the thicker fibrous cap generated by multiple rupture-repair cycles protects the atheroma from further rupture. An unstable plaque has a thin fibrous cap, a large lipid-laden necrotic core with many macrophages and foam cells, and vasa-vasorum neovascularisation leading to intra-plaque haemorrhage (27, 28). Stable plaques have more stabilising smooth muscle cells, a thick fibrous cap and a smaller lipid core (figure 1.2.1.4). The differences between stable and unstable plaque conformation mean that even though stable plaques lower blood flow leading to stable angina, the rupture risk of unstable plaques leading to more unstable angina

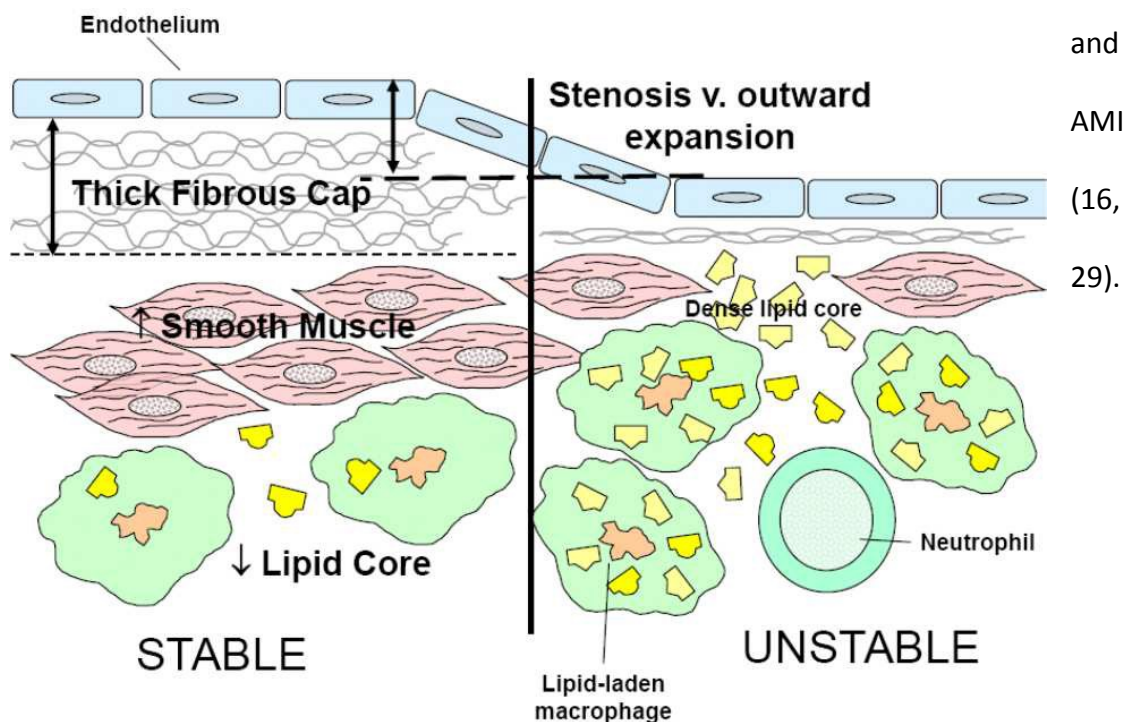
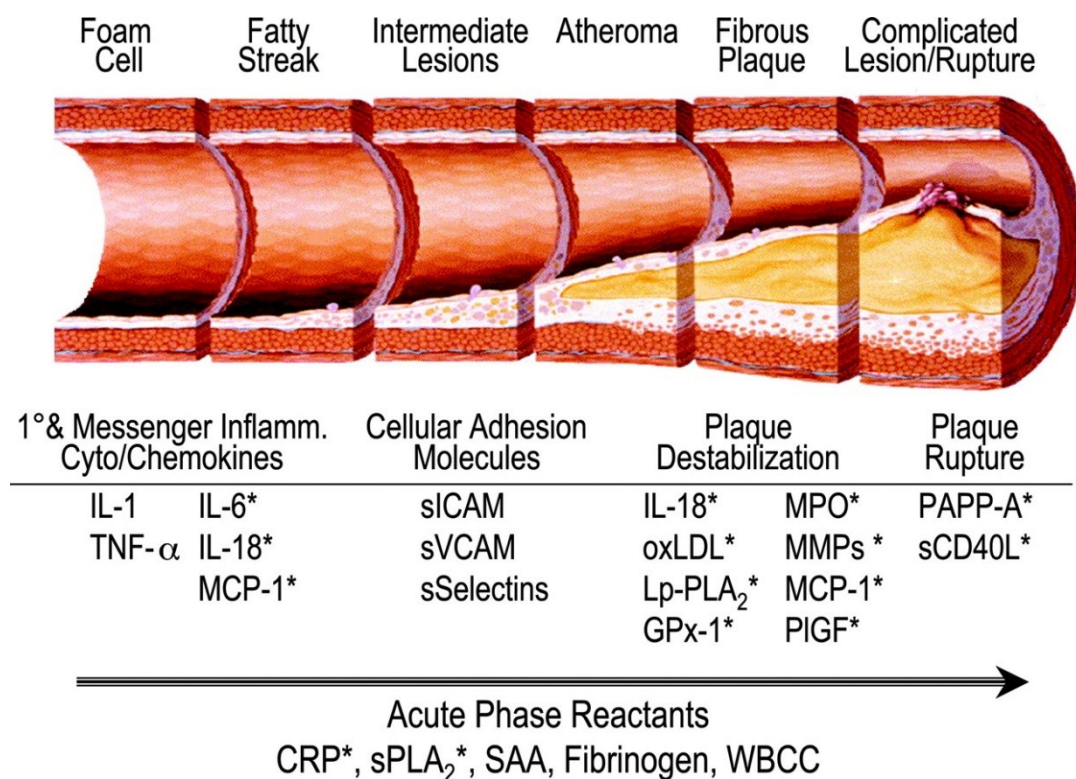


Figure 1.2.1.4 Stable and unstable plaque conformation.



### 1.3 mCRP as a causative Biomarkers for ACS

As mentioned above, in order to risk stratify patients into high- and low-risk groups attention has turned to factors that promote plaque destabilisation and possible rupture. The different biomarkers that have been identified target different parts of the atheroma cause its destabilisation, see figure 1.3.1. The dysfunctional endothelium causes an influx of monocytes and release inflammatory chemokines, cytokines and growth factors in the plaques as macrophages. Placental growth factor (PIGF) causes smooth muscle cells to migrate from the tunica media, into the intima and change from a protective, elastic phenotype to a collagen-producing cell (30). Pregnancy-associated plasma protein A (PAPP-A) promotes degradation of the fibrous cap via IGF-1 signalling (31) and has been shown to be an ACS predictor independent from CRP (32). Myeloperoxidase (MPO) appears to activate matrix



**Figure 1.3.1** Atheroma development from foam cell infiltration through to plaque rupture. Rupture is not an inevitability but the presence of these proteins could cause rupture. Their presence is increased by inflammation, increased blood pressure. Picture from (5)

metalloproteinases (MMPs) and impair MMP inhibitors (33, 34) which is deleterious for plaque stability as MMPs themselves promote extracellular matrix degradation (35) and it has been shown that an increase in MMP-9 is associated with future CV death (36). An increase in monocyte infiltration can cause instability and this is promoted by monocyte chemoattractant protein-1 (MCP-1), which has been shown to be increased in patients who have a higher risk of cardiac death but is not an independent predictor of coronary heart disease events (37). Recently, a small study showed that mCRP is elevated in AMI patient, but not angina patients (38), which means it might be of use as a clinical decision tool.

#### 1.3.1 CRP

CRP is principally produced and released from the liver in response to infection, inflammation and tissue injury. The protein is formed of 5 identical subunits covalently bonded around a central pore. Higher serum CRP concentration has been attributed to a higher cardiovascular disease and myocardial infarction risk (39). Primarily synthesised in hepatocytes in response to IL-6 and IL-1, pCRP forms part of the innate immune system (6) and interacts with the classical complement pathway (4). Raised CRP was found to be the best indicator for future adverse cardiovascular events in healthy, asymptomatic individuals (6, 39, 40). It has also been shown to be released from damaged endothelium (41). However, since this was before CRP was categorised into distinct forms, there may be discrepancy between which isoform was released from plaques. Therefore, there has been a growing body of research investigating the nature of mCRP production, its differences to pCRP and how mCRP may be used as a clinical decision algorithm for ACS, all of which will be discussed.

### 1.3.2 Dissociation from pCRP to mCRP

The dissociation process of CRP provides information on its function, where mCRP is most likely to affect and its possible role in ACS. As more data is published, it is becoming clear that dissociation allows the potential pro-inflammatory action of CRP to be released in the form of mCRP. Understanding the dissociation process will allow us to understand where, how and why mCRP is formed and crucially what this means for ACS diagnosis.

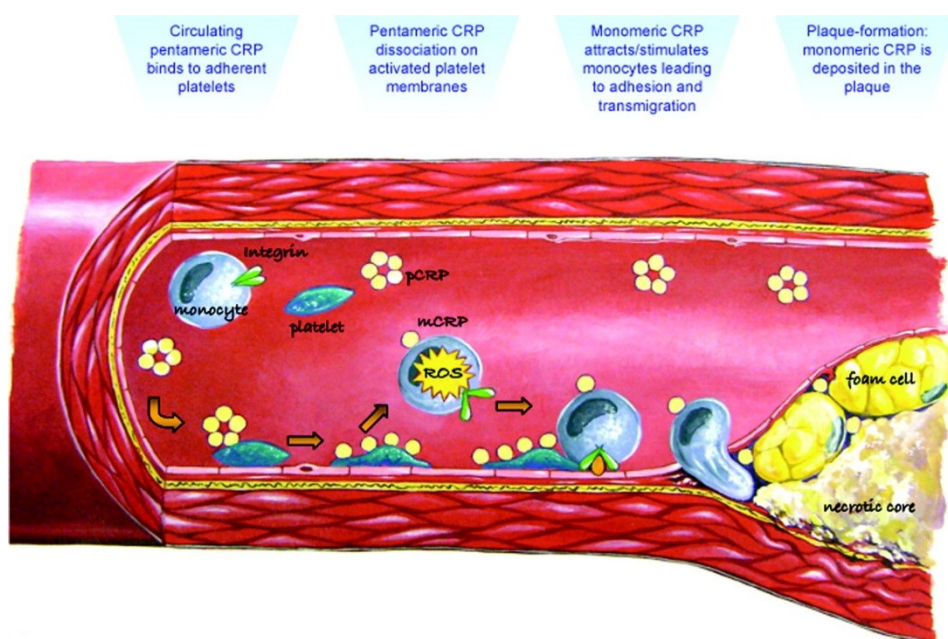


**Figure 1.3.2.1** The mechanism that leads to pCRP dissociation creating mCRP. pCRP is pictured as the yellow, 5-disk shape; mCRP as a single yellow disk. The green and blue platelet is shown to be adherent to the endothelium and facilitating pCRP dissociation in its active state. The platelet-mCRP deposit on the endothelium attracts and stimulates passing monocytes leading to their incorporation into the plaque. The mCRP will remain adhered to the monocyte when entering the plaque, which explains the presence of mCRP in damaged intima (6).

In fact, recent data have shown that it is the dissociated monomeric form that is active in the atheromas and produces the biggest changes to the endothelium in atherosclerotic progression (42, 43). However, in contrast to pCRP, mCRP is not found in the general circulation in healthy individuals as it is localised to sites of inflammation and has much slower solubility than pCRP (44). The facilitators for dissociation are activated platelets (11, 45), MPs (46) and endothelium (47). mCRP

might not be readily detected in the systemic circulation because it is such a strong localiser of the inflammatory process it will continue binding to the facilitator and promote atherosclerosis and thrombus generation. Figure 1.3.2.1 depicts the process surrounding atheromas.

Mechanisms of dissociation differ between platelets and MPs. On activated platelets, the dissociation of pCRP relies on a specific receptor that is expressed on the cell surface. Glycoprotein IIb-IIIa binds pCRP and promotes mCRP generation (48). However, this has not been the only proposed cell-surface receptor. Lipid rafts have also been considered and there is evidence to suggest that the proposition is accurate. By disturbing lipid raft conformation in human aortic endothelial cells with either methyl- $\beta$  cyclodextrin or nystatin the amount of IL-8 release was decreased (49). Again, this is evidence of a positive feedback loop concerning mCRP. In the interaction between mCRP and lipid raft, the interaction between cholesterol and amino acids 35-47 were of greatest importance (49). In pCRP, this motif is hidden in its core and is only exposed when dissociated into mCRP (49) and therefore could be central to mCRP signalling.

MPs facilitate dissociation through pCRP binding to lysophosphatidylcholine (LPS) in the lipid membrane. Habersberger et al (46) showed this by incubating MPs derived from THP-1 cells and human umbilical vein endothelial cells (HUVECs) with pCRP that produced mCRP. This action was inhibited pCRP membrane-binding by pre-treating the protein with 1,6 bis-phosphocholine, which binds to the pCRP phosphocholine binding site. The group also observed that the mCRP-containing MPs binding and releasing mCRP to activated HUVECs by specific staining. By

comparison with platelets, their functions are similar in that both cause dissociation and deliverance of mCRP but the mechanisms differ. Whether the difference in mechanisms provides a difference in mCRP function remains to be seen.

Understanding the differences could provide information concerning how best to diagnose ACS using mCRP.

Evidence that CRP is released from endothelial cells when stimulated with inflammatory cytokines displays a possible mechanism for a self-perpetuating cycle of increasing inflammation and atherosclerosis in a specific area (47). Especially as IL-6 and MCP-1 expression both increased, together increasing the plaque's size further and IL-6 promoting CRP expression. The infiltration of more monocytes into the plaque causes it to destabilise increasing the likelihood of rupture. Since mCRP associates with the membrane and causes an increase in VCAM-1 expression (46), it can be said that a higher mCRP presence could cause plaque rupture and infarction.

Furthermore, dissociation is increased during hypoxia, for instance during an AMI or stroke (50). The hypoxic environment provides a local area where hypoxic-reactive species can induce mechanisms that oppose the negative effects of oxygen depletion. One of these mechanisms is angiogenesis of neovessels. mCRP has been shown to stimulate cell migration and tube formation in endothelial cells (47) that, when occurring within plaques, destabilises atheroma cores leading to more MACEs (51-53). The small, fragile neovessels may haemorrhage introducing lipid-rich red blood cells into the plaque that will increase its necrotic core and pro-inflammatory profile from within (28, 54). These factors have a negative impact on the stability of

the core, which combined with increased monocyte infiltration could further rupture risk.

The dissociation is fuelled by intermolecular electrostatic forces becoming greater than intramolecular forces when pCRP is clustered on a lipid monolayer, as shown by Wang et al (55). The comparably weak intramolecular forces are overcome by intermolecular forces when the pentamers aggregate and are in close proximity. The salt bridges holding the pentamer together are broken creating a dimeric and trimeric isoform from the native molecule. The lipid surface allows this close proximity and perhaps a secondary catalyst to break down pCRP is not necessary. However, the interaction between pentamers has been shown to be stable at physiologically similar salt levels and does not induce spontaneous dissociation (56). Dissociation is not an instantaneous process but with 30-40% of pCRP dissociating within 1-2 hours of contact with the cell membrane, it is still a fast progression (57). It is this speed of dissociation that leads the thinking that mCRP might be a good biomarker not only for AMI but for risk stratification of patients who do not experience AMI upon presentation at the ED. Also, if it is proved to be a causative factor, detection in AMI would be earlier and risk stratification would be more reliable than biomarkers that assess myocardial damage.

### 1.3.3 Different effects of pCRP & mCRP

Before the knowledge that CRP had 2 distinct isoforms with opposing functions, any findings surrounding the isoforms were attributed to CRP as a singly functioning protein, which produced conflicting accounts on its activity. One of the activities that was falsely attributed to pCRP was that it was deposited in atherosclerotic

plaques (58) when in fact it was the dissociated form that was found in the damaged intima (47, 59). The failure to differentiate the two isoforms meant that pCRP was viewed as actively involved in atherosclerosis progression and as it is found in the general circulation, it was postulated that CRP could be accelerating or creating atheroma growth. This implied that pCRP has many more functions than in reality and from this inaccurate prognostic data would be inferred. In fact, it is the dissociation of pCRP to mCRP that exposes proinflammatory binding sites and allows association between mCRP and downstream proinflammatory effectors (54).

For instance, it has now been found that mCRP resides on the endothelium of the area of an infarct and on at risk areas of the endothelium (60). A myocardial ischaemia-reperfusion injury model was conducted in rats in the left anterior descending coronary artery to assess the effect of this model on mCRP deposition. Not only did the infarct area of the group with mCRP included in the injection group increase more than the sham-operated group, there was no increase in RNA expression of mCRP implying the CRP would arrive from the circulation and not from the cells' response to the reperfusion post-ischaemia.

pCRP	mCRP
Increase in IL-8 secretion in monocytes (61)	Increase in IL-8 and MCP-1 secretion in neutrophils and coronary artery endothelial cells (43, 50)
Increase in monocyte-endothelium interaction in human aorta and umbilical vein cells (62)	Increase in neutrophil-endothelium interaction (43)
Increase in apoptosis in endothelial progenitor cells (63, 64)	Delayed apoptosis of neutrophils (65)
Released from endothelium of vulnerable plaques (41)	Propagates platelet activation and thrombus growth (11)
Co-localises with macrophages, oxidised low-density lipoprotein (66)	Increases platelet-neutrophil interactions (43) and platelet-endothelium interactions (67)
Strong pro-inflammatory action (68)	Signals through classical complement pathway on necrotic cells (69)
Delayed plaque formation (70)	Increase in expression of adhesion molecules E-selectin, ICAM-1 and VCAM-1 (43)
	Increase in angiogenesis within atheromas leading to haemorrhage (50, 71)

**Table 1.3.3.1** The different functions of pCRP and mCRP in inflammation. Some of the effects appear to be contradictory especially concerning pCRP. These are due to a lack of distinction between pCRP and mCRP in earlier papers, an obstacle that has now been overcome with the understanding that the isoforms are different.

The different functions of the 2 isoforms have been detailed in table 1.3.3.1. As previously mentioned, exposure to mCRP will increase IL-8 and MCP-1 release from the endothelium will, as its name suggests, attract monocytes to the activated endothelium, and the adhesion molecules will cause an increase in monocyte infiltration and weaken the atheroma (42, 47). A much longer incubation period is required – 24 hours instead of 4 hours – for these proinflammatory effects are observed by pCRP on the endothelium suggesting that the pCRP is dissociating into



mCRP. As activated platelets and MPs are proinflammatory and are significant factors in mCRP generation, this localises mCRP action and further increases monocyte infiltration and platelet activation to a specific site in the endothelium (72).

The delay in apoptosis of neutrophils by mCRP (65) may serve to protect the cardiac tissue post-infarction but may accentuate apoptosis and increase degradation of the extracellular matrix by a continued inflammatory response resulting in further cardiac remodelling (73). However, differing effects in the complement cascade in necrotic cells by mCRP may yet prove to be cardioprotective (69). Nevertheless, the recruitment of monocytes and neutrophils to the endothelium will only cause a larger thrombus to form when the atheroma does rupture possibly leading to more complications (68).

Another factor contributing to this might be tissue factor (TF), which is exposed when a plaque is disrupted and is believed to initiate thrombus formation (74).

Through confocal microscopy, it has been shown that HUVECs incubated with mCRP increase expression of TF and the initial fibrin monolayer in clot formation is denser than that formed when incubated with pCRP (75). mCRP also promotes intra-plaque angiogenesis through the PI3K/Akt pathway (76) that causes haemorrhaging worsening thrombus formation upon plaque rupture. This along with inducing platelet activation and aggregation (11, 67) points towards a multi-causative role for mCRP in thrombus growth.

The problems surrounding the overlapping functions of mCRP and pCRP could be caused by the difficulty in preventing spontaneous pCRP dissociation *in vitro*, which may produce effects that only occur in the presence of mCRP. As seen in table 1, Meuwissen et al (66) reported through immunohistological staining that CRP was found within the plaques of stable angina (SA) and UA patients and MI patients. It was assumed that the CRP found was pCRP as the antibody used was not tested for specificity and the CRP found in the plaque could be mCRP. This seems likely considering plaques in cerebral arteries of stroke patients were found to contain

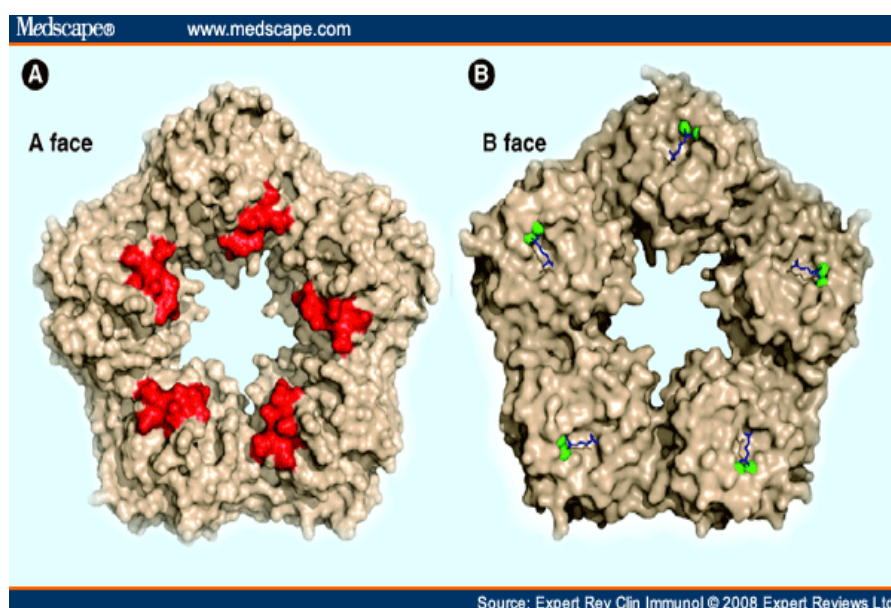


**Figure 1.3.3.2** Space-filling model of the 2 faces of pCRP. (A) This face shows the receptor binding face of CRP with the ridge helix binding site in red. The binding sites for Cq1 and FcγRs overlap meaning interaction with one will inhibit binding with the other. Taking the size of Cq1 and CRP into consideration, it appears that only 1 globular head binds to the pore. (B) The B face of the pentamer is shown with the positions of the binding sites for 2 calcium ions (green) and for phosphocholine (blue) (4).

mCRP, but not pCRP, by using validated antibodies that were specific for pCRP and mCRP (47).

Peisajovich et al (4) displayed that pCRP has overlapping binding sites for C1q of the complement system and FcγRs, as seen in figure 1.3.3.2. In addition, it has been suggested that the role of mCRP as a complement effector changes depending on its state. mCRP has reduced solubility compared to pCRP (44). mCRP

is most effective at activating the complement cascade via C1q when bound to LDLs or ox-LDLs. In fluid phase, mCRP binds to C1q and inhibits downstream signalling and therefore the complement cascade (50). This evidence indicates that the role of mCRP in complement is more complex and is dependent on other factors outside the cascade itself.

Alluding to the pores for calcium binding (figure 1.3.3.2), the existing knowledge on calcium-dependent binding to lysophosphatidylcholine (LPC) is being challenged (77). The binding to LPC is the facilitator for pCRP to mCRP dissociation and arguably the increase of its inflammatory properties. Previous studies reported that calcium was absolutely necessary for the binding of CRP (78, 79) and therefore the understanding of mCRP and its role in the complement cascade must be reviewed. Even though it is known that mCRP can attach to lipid rafts in the plasma membrane in a calcium independent manner (49), this new study shows the importance of understanding conformation and pH on the function of mCRP and hence its complex interactions with the complement cascade (80, 81).

#### 1.3.4 mCRP in ACS diagnosis

This information could be of great value in the use of mCRP as a clinical decision tool. Obradovic et al (82) have proposed that only when CRP and oxLDL are measured and both are elevated can ACS be prognosed. The rationale behind this was that pCRP blocked LDL binding to monocytes via the LOX-1 receptor and therefore attenuated the pro-atherogenic effects of the LDL. However, these effects did not occur when mCRP was dissociated from pCRP. In our aims, it is hypothesised that the ratio between pCRP and mCRP would provide a good clinical

decision tool for ACS. This ratio overcomes the pCRP-oxLDL association problem by virtue of mCRP opposing effects on LDL and its receptors.

Concerning mCRP detection alone, there have been studies that have linked more mCRP with MI (38, 44). With larger cohorts, it could be decided whether mCRP is a suitable addition to the diagnosis of ACS, particularly NSTEMI, and in prognosis of patients for developing major adverse coronary events (MACE) within the subsequent 30-days. The evidence above suggests that mCRP is the local effector of the CRP isoforms and could be used a specific biomarker because of this. Its specificity and sensitivity in ACS diagnosis is yet to be seen but if is effective, it would be of great value to add a causative biomarker to ACS diagnostics.

Above it has been shown how mCRP is formed and that its local formation is vital to its function. It also increases monocyte and neutrophil infiltration, thins the fibrous cap, increases thrombus size and intra-plaque haemorrhage that increase plaque vulnerability leading to ACS. In the next section, how AMI is currently diagnosed will be introduced along with the role that cTn plays in those diagnoses.

## 1.4 Current AMI diagnosis

The condition of NSTEMI is a pressure-based chest pain that lasts for 10 or more minutes with possible associated pain in either arms, neck or jaw. Pain in these areas independent of chest pain can also indicate NSTEMI. Typical symptoms that are present alongside chest pain are diaphoresis, dyspnea, abdominal pain, nausea and syncope. Less commonly, patients may present without chest pain but with nausea, vomiting, unexplained fatigue, syncope and diaphoresis (83). For these patients, their history and the clinical judgement of the physicians may be enough to consider these more uncommon symptoms as a possible NSTEMI. High risk groups include the elderly ( $\leq 75$  years old), male sex, presence of peripheral artery disease, positive family history of coronary artery disease, renal insufficiency, diabetes mellitus, prior MI and percutaneous coronary intervention (PCI) (84, 85). In these groups, atypical symptoms are more likely than other groups and can include epigastric pain, indigestion, and stabbing or pleuritic pain (86).

### 1.4.1 Risk stratification

NSTEMI needs to be separated from unstable angina diagnosis as the treatments are different but symptoms are very similar. In addition, the prognosis of NSTEMI is worse than that of unstable angina (UA) and at 6 months, mortality rates are equal or greater than those of STEMI patients (87). Furthermore, early interventions can provide short-term treatments but may lead to worse prognoses (88). At initial presentation, different risk factors in the patient's history such as sex, age, symptoms and a history of coronary artery disease (CAD), are used in combination with traditional symptoms of angina to assess how likely the prolonged chest pain is

due to stable chronic or acute ischaemia, instead of an alternative aetiology (89, 90).

The use of clinical risk scores can provide invaluable information on a patient's prognosis by using these risk factors to stratify patients by scoring certain factors (91). These include the Thrombolysis In Myocardial Infarction (TIMI) score, the HEART score and the Manchester Acute Coronary Syndromes (MACS) decision rule. The HEART score is more general and is useful to make accurate diagnostic stratifications without validation or invasive procedures (92, 93). TIMI also is non-invasive but has more focus on ischaemia than the HEART score (94). These aim to provide clinicians with a guide to how likely the patient is to experience MACE within a certain time.

A recent National Institute for Health and Care Excellence (NICE) strategy (95) has suggested to clinicians to use a validated tool, such as those mentioned above, to assess risk of MI and that if patients fall into the low-risk group that a single cTn test below the limit of detection (LoD) is sufficient to rule a patient out of NSTEMI. Observational studies have shown that using a sample at presentation may be a safe rule out tool when using the LoD of a hs-cTn assay (7, 96-102) and have significantly higher sensitivities and negative predictive values (NPVs) than the traditional cut-off at the 99<sup>th</sup> percentile when compared directly (103).

### 1.5 Molecular characteristics of cTn

cTn is a complex found in skeletal and cardiac muscle but not smooth muscle. It is bound to tropomyosin in between actin filaments in the muscle's sarcomeres and is vital to muscle contraction (104). In its relaxed state, tropomyosin will block the

attachment of the myosin cross bridge on the actin filaments by covering the binding sites preventing contraction (104). Action potentials stimulate the  $\text{Ca}^{2+}$  channels to open in the sarcoplasmic membrane and the  $\text{Ca}^{2+}$  ions bind to cTn changing its shape exposing its myosin binding sites (105). This causes myosin to bind to actin and, by releasing the ADP and  $\text{P}_i$ , induces a contraction stroke in the filament. The myosin head detaches once a new ATP molecule binds and the muscle is relaxed once more.

There are three forms of cTn, cTn C (TnC), cTn T (TnT) and cTn I (TnI) (106, 107). TnC is 18kDa (108) and binds to  $\text{Ca}^{2+}$  ions causing a conformational change to TnI (109, 110). TnT, 37 kDa (111), binds tropomyosin to form a cTn-tropomyosin complex and TnI at 23kDa (112) binds to actin to hold the complex in place on the thin filament. Only TnT and TnI have cardiac-specific forms and therefore useful as a cardiac biomarker (113) but TnC has no cardiac-specific isoform. There is only one cardiac isoform of TnI (106), cTnI, whereas there are several cTnT isoforms but only one is expressed in a healthy heart (114). Even though cTnT is cardiac-specific, in cases of chronic skeletal muscle injuries or renal disease cTnT can be expressed in skeletal muscle (115-118) lowering its utility as a cardiac biomarker somewhat.

#### 1.5.1 cTn immunoassays

The specificity of cTnI can be alluded to the expression pattern of cTnI and cTnT in foetal development. Skeletal forms of cTn are expressed in the foetal heart until late in development when cTnI and cTnT replace them (119, 120). cTnI is never expressed in other tissues during development (121) and it can be assumed that cells other than the myocardium cannot produce cTnI. In the case of cTnT, its four isoforms have significant cross reactivity with skeletal muscle TnT (skTnT), which

caused non-specific antibodies for use in assays to be created (122). Early cTn assays were not sensitive or specific enough to outperform CK-MB diagnosis and could only identify patients with AMI 6 hours after event (123, 124). The problem was solved by developing a highly specific monoclonal antibody that finds its epitope on the N-terminal of cTnT (125).

The development of the antibodies allowed the assays to become more and more sensitive to circulating cTn, which had exceeded CK-MB as the superior marker for AMI diagnosis (126, 127). Moreover, the consensus document released in 2000 of the Joint European Society of Cardiology and American College of Cardiology Committee to redefine MI (128) acknowledged the importance of biomarkers in the diagnosis of AMI as depending on ECG alone will result in a significant number of missed diagnoses. The combined use of ECG, CK-MB and cTn allowed faster diagnoses and options if differential diagnosis proves difficult. One such problem is an elevated serum cTn level at presentation meaning the rise and fall pattern may not be as clear as a patient whose cTn level is relatively low. By combining with the ECG, it is possible to ascertain if the patient is experiencing an ischaemic attack, for example ACS, or a non-ischaemic condition such as myocarditis (129).

#### 1.5.2 cTn in ACS diagnosis

It was recommended that cTn be the preferred MI biomarker due to its higher specificity for myocardial necrosis with CK-MB becoming a support marker for early diagnosis as it rises faster than cTn (128, 130), and it was later suggested that CK-MB does not add value to the diagnosis (131). Furthermore, the longer half-life of the cTns results in elevated cTn levels over a longer period of time (132, 133), which allows more patients to be identified as high-risk for subsequent MACE in



comparison to CK-MB (134-137). The increased clinical sensitivity of cTn is correlated to a higher concentration of cTn than CK-MB in the blood (138) meaning absolute increases in cTn are more marked. In addition, the normal reference range for cTn is much smaller than CK-MB as cTn is not detected in healthy patients and therefore any detected cTn in patients is regarded with clinical suspicion.

**Box 1: Definitions for cTn assays**

- *Limit of detection*: lowest detectable concentration that is above zero. A more sensitive assay will have a lower limit of detection.
- *Upper limit of normal*: for most assays, the upper limit of normal is set at the 95<sup>th</sup> percentile of the reference population (mean  $\pm$  2 SDs). For cTn assays, the cut off was set at 99<sup>th</sup> percentile (mean  $\pm$  3 SDs).
- *Coefficient of variation*: measures variability as a ratio between SD and mean in percent. Cut offs for cTn assays must have a CV < 10%.
- *Precision profile*: Used to determine at which concentration the 10% CV limit is reached.

The utility of cTn in ACS prediction may be because it is a specific measure of myocardial necrosis but why this aids in predicting future adverse cardiac events is still uncertain. It has been postulated that the low levels of cTn seen is as a result of thrombotic activity surrounding vulnerable plaques and the subsequent associated

emboli characterise areas of the coronary vasculature likely to rupture and therefore identify high-risk patients (139-143). It has been established that in unstable angina patients, sporadic necrosis in coronary arteries leads to higher risk of sudden cardiac death (144, 145).

As cTn was outperforming CK-MB and myoglobin in diagnosis, focus was changing from whether cTn was a more accurate biomarker to what cut-off would be best to implement. The consensus brought the 99<sup>th</sup> percentile as a recommendation to diagnose AMI in a healthy population (128) and the <10% CV was proposed as an

alternative (146). Imprecision profiles of assays available at the time yielded CVs lower than 10% at the 99<sup>th</sup> percentile or lower concentrations (147). The 99<sup>th</sup> percentile was useful for early rule out of AMI due to its low cut-off but yielded small PPVs (131) but conversely imprecision greater than 10% around the 99<sup>th</sup> percentile presents increased risk of misdiagnoses.

There are now many high-sensitivity cTn (hs-cTn) assays, all of which have different precision profiles, LoDs and 99<sup>th</sup> percentile cut-offs hence why guidelines for MI diagnosis are quoted as above and not at specific concentrations. hs-cTn assays are named as such if cTn can be detected in 50% of the population. The differences arise from the array of antibodies used in separate assays that have epitopes on diverse fragments of the circulating cTnI and cTnT (148-152). Each fragment will have different half-lives in the plasma, antibody-fragment affinity will differ (151) and the components of the assays will cause differing amounts of matrix effects in each (153, 154). The heterogeneity of the factors will affect the percentage recovery of the proteins in the plasma and the degree of detection by the antibodies causing each assay and its parameters to be particular to that assay.

It is for this reason that it is difficult to compare the performance of assays directly and for their diagnostic accuracies to be assessed individually, clinical sensitivity, specificity, positive predictive value (PPV) and NPV based on specific diagnostic cut-offs must be calculated. This allows the number of patients who will be identified correctly by a test to be quantified but these clinical parameters allow flexibility in how cut-offs are used in diagnosis.

### 1.5.3 Kinetic and non-kinetic cTn values in ACS diagnosis

For ACS diagnosis, a rule out diagnosis is a useful tool and is becoming more

**Box 2: Definitions for diagnostic tests (3)**

- *Sensitivity*: proportion of patients with the disease who are correctly identified by the test
- *Specificity*: proportion of patients without the disease who are correctly identified by the test
- *Positive predictive value*: Proportion of patients with a positive test who are correctly diagnosed as disease positive
- *Negative predictive value*: Proportion of patients with a negative test who are correctly diagnosed as being disease free

popular now with more sensitive hs-cTn

assays because they allow detection of very small concentrations of cTn (155).

Until the advent of hs-cTn assays, a

patient with negative cTn could be

confidently ruled out of AMI but a

positive hs-cTn can now be found in 50%

of the population. The concentration at

which cTn is considered safe for

different assays still remains up for

debate (7, 99, 100, 131, 156-162). Sampling at presentation allows for the

possibility of immediate AMI rule out and time between serial sampling has been

recommended to be reduced from 6h to 3h (163).

As well as non-kinetic values of cTn, changes between two cTn samples, or cTn

deltas, have been proposed to assess what degree of change constitutes an AMI

has occurred, as per international guidelines (164). Deltas allow the distinction

between acute and chronic causes of cTn rise, e.g. between AMI and chronic heart

failure (CHF) (165) Therefore, raised cTn is not specific enough to for it to be used

alone to diagnose AMI. Consequently, the rise and fall pattern must be observed

but how these increases and decreases apply to AMI diagnosis is debated (166-

169).

There are two main methods, the absolute delta, which is the change between two cTn samples expressed as an absolute value, or the relative delta, which is expressed as a percentage change. The later method can utilised in different ways, e.g. the change relative to the baseline cTn value, to the mean of the cTn values, to the minimum or maximum of the cTn values, and has been the delta tool of choice. However, with the advent of ever more analytically sensitive cTn assays, the absolute delta has been found to be more accurate for lower cTn levels, such as those cTn values found in NSTEMI (160).

### 1.6 Molecular characteristics of h-FABP

h-FABP is a small 15 kDa cytoplasmic protein released from cardiomyocytes in ischaemic conditions (170). It is involved in long chain fatty acid transportation and metabolism by moving fatty acids from the plasma membrane to the mitochondria for oxidation (171). h-FABP is found to be highly specific to the cardiomyocytes (172) and in only low levels in the skeletal muscle, small intestine, liver and kidneys (173, 174). It has been shown that it is 20 times more specific to the heart than myoglobin (172). In addition, it is very soluble, stable and has a low molecular weight (175, 176), all of which contribute to its rapid increase in systemic concentration (177), which has been reported to increase 30 minutes post-event (178) and returns to the reference population values within 24h (179).

The diagnostic utility for AMI diagnosis of h-FABP has previously been shown especially concerning early detection of h-FABP (180-187). The combination of h-FABP with cTn concentration, ECG ischaemia and cTn deltas has not yet been explored for the diagnosis of AMI and the prediction of MACE. As h-FABP is released

earlier into the bloodstream than cTn, it may allow faster diagnosis of AMI with early presenters and prevent more false negatives.

## 1.7 Project Aims

The aim of this project is to assess if mCRP and different cTn measurements can be used to rule in/rule out ACS.

The primary objective is to address the following research questions:

- In patients with suspected ACS, serial measurement of the ratio of mCRP to pCRP, cTn in addition to routine clinical and laboratory investigations, identify:
  - Patients at sufficiently low risk of AMI or MACEs within 30 days to enable safe early discharge, rule out *and*
  - Patients at high risk of AMI or MACE within 30 days that the diagnosis of ACS should be ruled in
- Our secondary objective is:
  - To derive and validate a clinical decision algorithm incorporating serial measurements of the above markers for the identification of patients at low and high risk of MACE within 30 days, including identifying optimal critical difference

The above aims will be achieved as detailed below.

### 1.7.1 Assay development

#### *Method*

mCRP concentration will be determined in patients' blood via a new immunoassay developed into a competitive format with a colorimetric testing step. Initial validation will determine antibody titre and assay linear range. Further validation will utilise industry standard guidelines for the validation of the immunoassay.

### 1.7.2 mCRP Clinical Study

#### *Method*

We will conduct a prospective diagnostic cohort study in patients presenting with possible ACS warranting hospital admission for further investigation. Patients must be >25 years of age and presenting with suspected cardiac chest pain that has occurred within 24 of coming to the ED. Patients with unequivocal evidence of STEMI who will be transferred for immediate percutaneous coronary intervention will be excluded. Also excluded will be those with renal failure requiring dialysis, suspected myocardial contusion or another medical condition requiring hospital admission. Comprehensive clinical, ECG and biochemical data will be recorded at the time of presentation using a custom designed case report form. We will collect whole blood samples for the measurement of mCRP/pCRP ratio by immunoassay. As part of routine clinical care, all patients will undergo diagnostic testing (reference testing) using a laboratory based cTn assay on arrival and at least 12 hours after symptom onset. A positive result will be any cTn level >99th percentile of a reference population. Patients will be followed up throughout their inpatient stay and after 30 days. The primary endpoint will be a composite of AMI and MACE within 30 days. We will determine the diagnostic accuracy of serial measurements

of mCRP/pCRP and cTn by calculating sensitivity, specificity, positive and negative predictive value. In addition we will derive and validate a clinical decision algorithm to rule out and rule in AMI. This analysis will include clinical findings in addition to data from mCRP, pCRP, the mCRP/pCRP ratio and cTn to define a clinical decision rule to determine short and long-term risks of AMI and/or MACE.

#### 1.7.3 cTn Clinical Study

For the following analyses, the fifth-generation Elecsys, Roche Diagnostics hs-cTnT assay, the Singulex Clarity™ cTnI assay and the Abbott Point of Care iSTAT cTnI assay will be assessed as tools for rule in and rule out of ACS. This will be explored in diagnosis and 30-day MACE prediction by:

- Using the 10% CV of each assay as cut-offs at presentation and 3h to assess utility as quick rule in or rule out
- Calculating the deltas between presentation and 3h samples as absolute deltas, relative to baseline deltas and relative to mean deltas, that will allow 100% sensitivity for rule out
- Using the baseline cTn concentrations to divide the cohort into high-, intermediate and low-risk groups and create group-specific cut-offs to assess if grouped improves diagnostic accuracy
- Using a novel risk score, which includes predictor variables of cTn, cTn deltas, ECG ischaemia and H-FABP

## **Chapter 2: Materials and Methods**



## 2.1 Materials

### 2.1.1 Immunoassay development materials

This section details the different reagents and equipment used in the immunoassay development. Any changes will be included in the results section.

CRP purchased from mybiosource.com (catalogue # MBS318375) in its native, pentameric form. mCRP obtained via urea chelation stored in a CRP buffer (140 mM NaCl, 20mM Tris-HCl, 2mM CaCl<sub>2</sub>, pH 7.5).

Plates used are Nunc-Immuno™ MicroWell™ Polysorp® flat bottom 96 well solid plates (catalogue # M0661-1CS, Sigma Aldrich).

mCRP antibody clone 8C10 was kindly gifted from Dr Potempa (47).

Mouse monoclonal anti-C reactive protein antibody [C6], HRP conjugated (ab24462, Abcam).

Goat polyclonal anti-C reactive protein antibody, HRP conjugated (ab19175, Abcam).

The mCRP-biotin conjugate was made as per the instructions using Lightning-Link® Biotin Conjugation Kit (Type A\*), 1-2mg scale (catalogue # 704-0015, Innova Biosciences).

Bovine serum albumin (BSA) was in the form of lyophilised powder, crystallised ≥96.0% (catalogue # A4503-100G, Sigma Aldrich).

Monster Block™ (obtained from ImmnuoChemistry Technologies, catalogue # 6295).

ImmunoPure® Streptavidin-HRP conjugated 5 mg (Prod # 29994, ThermoScientific).

3,3',5,5'-tetramethyl benzidine (TMB) 0.4g/L in aqueous solution (Prod #1854050, ThermoScientific) and peroxide solution, 0.02% in buffer (Prod #1854060).

## 2.2 Methods

### 2.2.1 Immunoassay development methods

This section details the different reagents and equipment used in the immunoassay development. Any changes or additional materials will be included in the results section.

### 2.2.2 Competitive immunoassay development

A competitive immunoassay was in development first, a diagram of the basic principles is provided in figure 2.2.2.

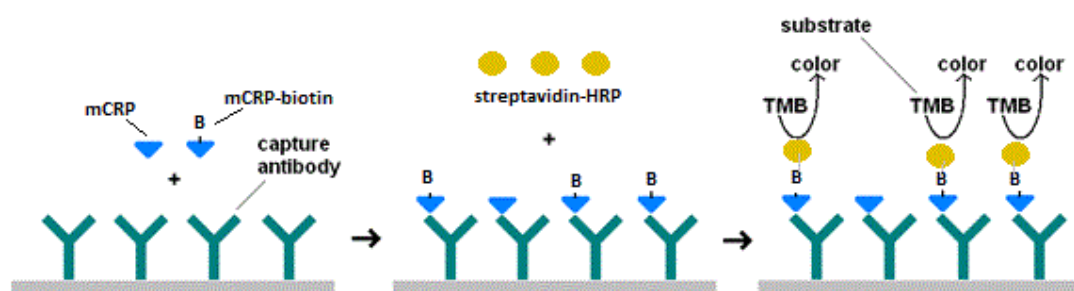


**Figure 2.2.2.** Diagram of the mCRP competitive immunoassay. The capture antibody, mCRP antibody clone 8C10, was coated on the wells. The mCRP and mCRP-biotin are added to the wells, then the streptavidin –HRP is added and binds to the biotin. TMB is added and the HRP changes the colour of the TMB from colourless to blue. The amount of colour change is measured by absorbance at 450 nm. The mCRP and mCRP-biotin compete to bind with available antibodies and therefore a higher mCRP concentration will result in a smaller absorbance reading. An array of standards was used per immunoassay to produce standard curves.

#### 2.2.2.1 First competitive immunoassay protocol

The plates were coated with the antibody overnight at 4°C at concentration 1:10 and 1:20 in CRP buffer. After aspirating, 3 x 5 minute washes with CRP buffer were conducted. Dilutions were made immediately before usage and diluted using CRP

buffer. 80 µl of CRP buffer was added to each well, and 10 µl of mCRP-biotin at concentrations 0-300 µg/ml. mCRP standards at 0-500 µg/ml were added immediately in triplicate and incubated overnight at 4°C. The solution was aspirated and 5 x 3 minute washes with CRP buffer were conducted. 0.1 µg/ml avidin-HRP was added and incubated for 30 minutes at room temperature. The solution was aspirated and wells washed as above. TMB and peroxide solutions were added and the reaction stopped after 10 minutes with 2M sulphuric acid. The plates were read by Synergy HT Microplate reader (BioTek).

#### *2.2.2.2 Immunoassay with competition from mCRP removed*

The plates were coated with the antibody overnight at 4°C at concentrations 1:10, 1:20, 1:30, 1:40, 1:50, 1:100 and 1:200 in CRP buffer. After aspirating, 3 x 5 minute washes with CRP buffer were conducted. Dilutions were made immediately before usage and diluted using CRP buffer. 80 µl of CRP buffer was added to each well, and 10 µl of mCRP-biotin at concentrations 0-200 µg/ml in triplicate and incubated overnight at 4°C. The solution was aspirated and 5 x 3 minute washes with CRP buffer were conducted. 0.1 µg/ml avidin-HRP was added and incubated for 30 minutes at room temperature. The solution was aspirated and wells washed as above. TMB and peroxide solutions were added and the reaction stopped after 10 minutes with 2M sulphuric acid. The plates were read by Synergy HT Microplate reader (BioTek).

#### *2.2.2.3 No competition introduced with alternative mCRP-biotin concentrations*

Protocol as previous but with mCRP-biotin concentrations 0-150 µg/ml.

#### *2.2.2.4 Addition of 0.05% Tween to wash buffer*

Protocol as previous but with 0.05% Tween in CRP buffer as wash buffer. Capture antibody concentration at 1:20.

#### *2.2.2.5 Reduction in range of mCRP-biotin standards to below 60 µg/ml*

Protocol as previous but with mCRP-biotin standards at 0-60 µg/ml.

#### *2.2.2.6 Addition of BSA as blocking buffer*

The plates were coated with the antibody overnight at 4°C at concentration 1:10 and 1:20 in CRP buffer. After aspirating, 3 x 5 minute washes with CRP buffer were conducted and 300 µl BSA at 0%, 0.5% and 2% added to the plate for 1 hour. BSA was aspirated and plates washed 3 x 5 minutes with 0.05% Tween. Dilutions were made immediately before usage and diluted using CRP buffer. 80 µl of CRP buffer was added to each well, and 10 µl of mCRP-biotin at concentrations 0-160 µg/ml were added in triplicate and incubated overnight at 4°C. The solution was aspirated and 5 x 3 minute washes with 0.05% Tween in CRP buffer were conducted. 0.1 µg/ml avidin-HRP was added and incubated for 30 minutes at room temperature. The solution was aspirated and wells washed as above. TMB and peroxide solutions were added and the reaction stopped after 10 minutes with 2M sulphuric acid. The plates were read by Synergy HT Microplate reader (BioTek).

#### *2.2.2.7 Possible BSA-mCRP interaction*

Plates were incubated with CRP buffer overnight at 4°C. After aspirating, 3 x 5 minute washes with 0.05% Tween were conducted before adding 100 µl BSA in CRP buffer at concentrations of 0%, 0.5% and 2% in quadruplicate incubated at room temperature for 2 hours. After aspirating, washes were performed as above. mCRP-biotin concentrations of 0, 5, 10, 15, 20, 25, 30, 40 µg/ml were diluted with CRP buffer and made with serial dilutions. 90 µl CRP buffer was placed into each well with 10 µl of mCRP-biotin and incubated overnight at 4°C. The solutions were aspirated and wells washed as above. 0.1, 0.05, 0.025 and 0 µg/ml Streptavidin-HRP

was added in duplicate and incubated for 30 minutes at room temperature. The solution was aspirated and wells washed as above. 80 µl of the mixed TMB and peroxide solution was added and the reaction stopped after 10 minutes with 2M sulphuric acid. The plates were read by Synergy HT Microplate reader (BioTek). The experiment was performed twice.

#### *2.2.2.8 Antibody-avidin and plate-avidin non-specific binding*

Plates were coated with 80 µl of antibody in an array of concentrations (1:40-1:500) diluted with CRP buffer incubated overnight at 4°C. 3 x 5 minute washes of 0.05% Tween before adding 100 µl BSA at concentrations 0%, 0.5% and 2% in quadruplicate incubated at room temperature for 2 hours. Plates were washed as above. 80 µl of avidin at concentrations at 0.1, 0.05, 0.025, 0 µg/ml were added to the plates for 30 minutes at room temperature. 80 µl of the mixed TMB and peroxide solution was added and the reaction stopped after 10 minutes with 2M sulphuric acid. The plates were read by Synergy HT Microplate reader (BioTek). The experiment was performed twice.

#### *2.2.2.9 Milk protein vs BSA as blocking agent*

Plates were coated with 80 µl antibody at concentrations 1:100, 1:200 or 1:400 and incubated at 4°C overnight. 3 x 5 minute 0.05% Tween washes were performed. 80 µl of 2% BSA and 5% and 10% milk were added and incubated for 2 hours at room temperature. Washes were performed as above. 10 µl of mCRP-biotin at concentrations 0-160 µg/ml and 90 µl of CRP buffer were added in duplicate and incubated overnight at 4°C and then washed as above. 80 µl of 0.1 µg/ml avidin were added to the plates for 30 minutes at room temperature. . 80 µl of the mixed TMB and peroxide solution was added and the reaction stopped after 10 minutes

with 2M sulphuric acid. The plates were read by Synergy HT Microplate reader (BioTek). The experiment was performed twice.

#### *2.2.2.10 Using antibody coating buffer and Monster Block™*

Plates were coated with 80 µl of either 1:200 antibody diluted in either antibody coating buffer or CRP buffer and incubated overnight at 4°C. Another plate was coated with 1:50 antibody with the antibody coating buffer and incubated as above. 3 x 5 minutes 0.05% Tween washes were performed and 300 µl of Monster Block™ was added to each well and incubated for 24 hours at room temperature. Washes were performed as above. 10 µl of mCRP-biotin of concentrations 0-160 µg/ml were added as 6 replicates to 90 µl of CRP buffer in wells and incubated overnight at 4°C on the plates of 1:200 antibody. The plate with 1:50 antibody had mCRP-biotin concentrations of 0-640 µg/ml and incubated as above. Washes were performed as above. 80 µl of 0.1 µg/ml avidin were added to the plates for 30 minutes at room temperature. 80 µl of the mixed TMB and peroxide solution was added and the reaction stopped after 10 minutes with 2M sulphuric acid. The plates were read by Synergy HT Microplate reader (BioTek). The experiment was performed twice.

#### *2.2.2.11 Possible interaction between mCRP and Monster Block™*

The plates were coated with Antibody coating buffer™ containing no antibody and incubated overnight at 4°C. After aspirating, 3 x 5 minute washes with 0.05% Tween were conducted before adding 300 µl Monster Block™ at 0%, 50% and 100% concentration (100% as concentration bought) for 24h at room temperature. Dilutions were made immediately before usage and diluted using CRP buffer. 80 µl of CRP buffer was added to each well, and 10 µl of mCRP-biotin at concentrations 0

µg/ml, 80 µg/ml and 120 µg/ml. mCRP standards at 0-80 µg/ml were added immediately in triplicate and incubated overnight at 4°C. The solution was aspirated and 5 x 3 minute washes with 0.05% Tween were conducted. 0.1 µg/ml avidin-HRP was added and incubated for 30 minutes at room temperature. The solution was aspirated and wells washed as above. TMB and peroxide solutions were added and the reaction stopped after 20 minutes with 2M sulphuric acid. The plates were read by Synergy HT Microplate reader (BioTek). The experiment was performed twice.

#### *2.2.2.12 mCRP-biotin conjugates competing for antibody availability with non-labelled mCRP standards*

The plates were coated with the antibody overnight at 4°C at concentration 1:50 in Antibody coating buffer. After aspirating, 3 x 5 minute washes with 0.05% Tween were conducted before adding 300 µl Monster Block™ for 24h at room temperature. Dilutions were made immediately before usage and diluted using CRP buffer. 80 µl of CRP buffer was added to each well, and 10 µl of mCRP-biotin at concentrations 0-200 µg/ml. mCRP standards at 0-70 µg/ml were added immediately in triplicate and incubated overnight at 4°C. The solution was aspirated and 5 x 3 minute washes with 0.05% Tween were conducted. 0.1 µg/ml avidin-HRP was added and incubated for 30 minutes at room temperature. The solution was aspirated and wells washed as above. TMB and peroxide solutions were added and the reaction stopped in half the wells after 10 minutes and 16 minutes in the other half with 2M sulphuric acid. The plates were read by Synergy HT Microplate reader (BioTek). The experiment was performed twice.

#### *2.2.2.13 Experimentation of mCRP incubation time at 24h and 48h at room temperature*

The plates were coated with the antibody overnight at 4°C at concentration 1:50 in Antibody coating buffer. After aspirating, 3 x 5 minute washes with 0.05% Tween

were conducted before adding 300 µl Monster Block™ for 24h at room temperature. Dilutions were made immediately before usage and diluted using CRP buffer. 80 µl of CRP buffer was added to each well, and 10 µl of mCRP-biotin at concentrations 0-160 µg/ml. mCRP standards at 0-40 µg/ml were added immediately in triplicate and incubated for 24h or 48h at 4°C or at room temperature to make 4 plates in total. The solution was aspirated and 3 x 5 minute washes with 0.05% Tween were conducted. 0.1 µg/ml avidin-HRP was added and incubated for 30 minutes at room temperature. The solution was aspirated and wells washed as above. TMB and peroxide solutions were added and the reaction stopped in half the wells after 10 minutes and 16 minutes in the other half with 2M sulphuric acid. The plates were read by Synergy HT Microplate reader (BioTek).

#### *2.2.2.14 Use of a prep plate to premix the mCRP-biotin and mCRP before adding to working plate*

Protocol as previous but mCRP-biotin and mCRP were premixed on a prep plate before being added to the working plate. The prep plate was washed and TMB added for 10 minutes to observe any residual mCRP-biotin.



### 2.2.3 Sandwich ELISA development

The project moved onto developing an ELISA protocol, the basics of which are displayed in figure 2.2.3.

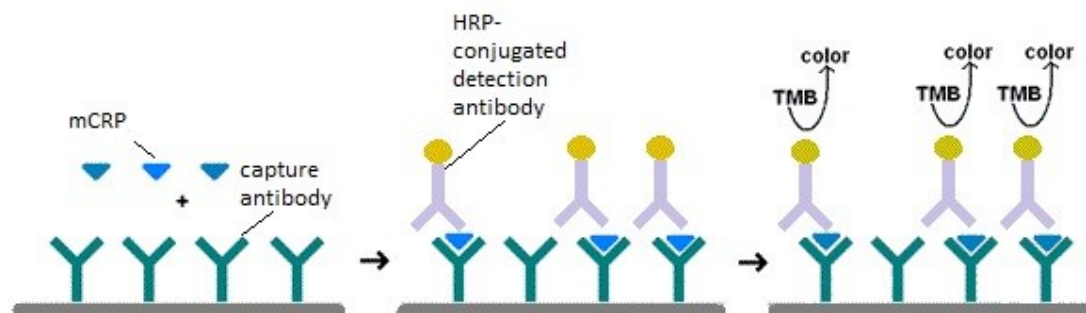


**Figure 2.2.3** Diagram of the mCRP sandwich ELISA. The capture antibody, mCRP antibody clone 8C10, was coated on the wells. The mCRP is added to the wells to bind to the capture antibody, and then the detection antibody is added to bind to the mCRP. TMB is added and the HRP changes the colour of the TMB from colourless to blue. The amount of colour change is measured by absorbance at 450 nm. The mCRP binds directly without competition to available antibodies and therefore a higher mCRP concentration will result in a larger absorbance reading. An array of standards was used per immunoassay to produce standard curves.

#### 2.2.3.1 ELISA with monoclonal detection antibody ab24462

The plates were coated with the antibody overnight at 4°C at concentration 1:50 and 1:200 in Antibody coating buffer. After aspirating, 3 x 5 minute washes with 0.05% Tween were conducted before adding 300 µl Monster Block™ for 24h at room temperature. Dilutions were made immediately before usage and diluted using CRP buffer. 100 µmCRP standards at 0-32 µg/ml were added in triplicate and incubated for 2h at room temperature. The solution was aspirated and 3 x 5 minute washes with 0.05% Tween were conducted. 100 µl of detection antibody (ab24462) at 1:3000 and 1:6000 was added and incubated for 1h at room temperature. The solution was aspirated and wells washed as above. TMB and peroxide solutions were added and the reaction stopped after 10 minutes with 2M sulphuric acid. The plates were read by Synergy HT Microplate reader (BioTek).

#### *2.2.3.2 ELISA with monoclonal detection antibody ab19175*

Protocol as previous but with capture antibody only at 1:50, ab19175 as the detection antibody and mCRP standards at 0-100 µg/ml.

#### 2.2.4 Diagnostic and prognostic analysis of three contemporary assays

As hs-cTn detects cTn in 50% of the population, using any detectable Tn as the rationale for further Tn testing is no longer useful. An alternative is to measure the amount of change observed in patients. The aim of these analyses to identify what change can diagnose AMI.

##### 2.2.4.1 Cohort & Samples

The prospective cohort study recruited patients who presented to the ED with chest pain from 5 sites (Manchester Royal Infirmary, annual ED consensus 145,000) as a part of the BEST study (NHS ethical approval: 14/NW/1344). Patients were over 25 and had chest pain within the last 24h, which the initial treating physician believed was cardiac in nature. Exclusion criteria are as follows: renal failure requiring dialysis, suspected myocardial contusion, another medical condition requiring hospital admission or if they did not consent to have their blood taken for the study.

Blood was drawn at time of ED presentation and at 3h and immediately centrifuged. Plasma was drawn off and frozen at -20°C for up to 48h and -70°C thereafter. The samples were analysed with the high-sensitivity cardiac cTn (hs-cTnT) assay from Roche® Diagnostics by hospital laboratory staff as part of routine diagnostics. The assay had a cTn concentration in the 99<sup>th</sup> percentile of a reference population of 14 pg/ml and CoV of 10% at 5.03 pg/ml. The samples were analysed for hs-cTnI with the ultra-sensitive Singulex Clarity automated analyser (99<sup>th</sup> percentile < 8.67 pg/ml, CV of 10% at 0.53 pg/ml). The assay uses a one-step immunoassay with single molecule counting to measure cTnI very sensitively in 90 minutes (188). The analysis was done at CityLabs 2.0, Manchester, by laboratory staff who were blinded to patient outcomes. Testing for Singulex was completed in

May-June 2017. The handheld point of care device, Abbott iSTAT® cTnI test (99<sup>th</sup> percentile 80 pg/ml, CV of 10% at 100 pg/ml) obtained results within 10 minutes at the patient's bedside. The Abbott iSTAT® system uses single-use cartridges to which a small amount of blood is applied to chemically sensitive biomarkers and inserted into the device for quantification. The device has cartridges for many analytes for different clinical tests but cTnI cartridges were used for these analyses (189).

Follow-up was at 30 days using the National Health Service Strategic Tracing Service database to check for mortality data. Cause of death was retrieved for all deceased patients. The electronic hospital records then were reviewed for every patient, including all subsequent ED attendances, hospital admissions, out-patient clinic appointments and all investigations requested and undertaken. All living patients were contacted by telephone and in the event the patient could not be reached their GP was contacted. Copies of records were retrieved if the patient was hospitalised during the follow-up period.

#### *2.2.4.2 Outcomes*

The primary outcome was AMI; two independent investigators who had all the clinical, laboratory and imaging data available for review but who were blinded to the hs-cTnT levels adjudicated final diagnosis. AMI was diagnosed in accordance with the universal definition of AMI, one of the following symptoms plus a rise of hs-cTnT above the 99<sup>th</sup> percentile of the reference population. Secondary outcome included death and AMI within the next 30 days. Three composite 30-day prognosis endpoints were devised. Composite MACE consisted of all-cause mortality, AMI, revascularisation, PCI, coronary artery bypass graft (CABG), stenosis, tests for heart

disease, cardiac arrest, arrhythmia and acute heart failure. Adverse events 1 (AV1) included all-cause mortality, AMI, revascularisation, PCI, CABG and stenosis and 2 (AV2) included cardiac arrest, arrhythmia and acute heart failure.

#### 2.2.4.3 Statistical analysis

Data was tested for normality using Kolmogorov-Smirnov test and if data was found to be not normally distributed and non-parametric tests were used to analyse the data. Means are presented as mean  $\pm$  SD,  $\pm$  95% confidence intervals (CI) for normally distributed data and median  $\pm$  95% CI for non-normally distributed data. Categorical variables were compared with the  $\chi^2$  test and degrees of change between paired categorical variables were compared with McNemar's test. Receiver operating characteristic (ROC) curves were made for cTn values at 0h, 3h, the maximum value of 0h or 3h (max values), absolute change or delta ( $\Delta_{absolute}$ ), relative to baseline delta ( $\% \Delta_{baseline}$ ) and relative to mean delta ( $\% \Delta_{mean}$ ). Values quoted in the diagnostic tests are absolute to assess magnitude of change instead of direction of change and quoted as 2-tailed significance. The delta values were calculated as Pretorius et al (190):

$$\Delta_{absolute} = 0h - 3h$$

$$\% \Delta_{baseline} = \frac{3h-0h}{0h} \times 100$$

$$\% \Delta_{mean} = \frac{(3h-0h)}{0.5 \times (3h+0h)} \times 100$$

Cut-offs were derived from ROC curve analysis to find the highest sensitivity possible and quoted as pg/ml. If the cut-off found by ROC curve analysis was below the concentration at which the assay exhibits a CV of 10%, the cut-off was set at 10% CV, as specified by the manufacturers. This was done as this is the accepted limit of the functional sensitivity (FS) for assays (146, 191). For the Roche assay, this

concentration was 5.03 pg/ml, for the Singulex assay was 0.53 pg/ml and for the iSTAT assay was 100 pg/ml (details for iSTAT as found in Appendix II). The LoDs for the assays were considered as cut-offs, as explored previously (99), but the confidence in the CV of the Singulex assay at its LoD of 0.08 pg/ml was low as the precision measurements only tested to 1 pg/ml. The precision profile of the assay is shown in figures 2.2.4.3.1 and 2.2.4.3.2 and has been constructed from data provided from Singulex (from raw data in manual found in Appendix I). Sensitivities, specificities, PPVs and NPVs for diagnosis and prognosis were calculated using MedCalc diagnostic test evaluation calculator.

To calculate at which minimum cTn concentration the  $\% \Delta_{\text{baseline}}$  and  $\% \Delta_{\text{mean}}$  cut-offs will surpass the FS in absolute terms, the lowest possible baseline cTn level for effective  $\% \Delta$  ( $\text{cTn}_{\text{low}}$ ) was calculated. The calculation is based on the percentage equation:

$$\% = \frac{FS}{\text{cut-off}} \times 100$$

and was rearranged as:

$$\text{cTn}_{\text{low}} = \frac{100}{\text{cut-off}} \times FS$$

Patients were grouped into rule out, intermediate and rule in groups based on 0h cTn concentration to achieve the greatest sensitivity for the rule out group and the greatest specificity for the rule in group. The intermediate group were patients who were in between these groups. The above analysis was repeated on the individual groups to assess diagnostic accuracy.

Predictor composites were made from 0h cTn values, cTn deltas (all composites including deltas as a variable will be calculated for diagnostic and prognostic accuracy with  $\Delta_{\text{absolute}}$ ,  $\% \Delta_{\text{baseline}}$  and  $\% \Delta_{\text{mean}}$  individually), evidence of ischaemia by

ECG (ECG) and H-FABP. All predictors in composites used the same cut-offs as detailed above and converted to categorical variables. The ECG and H-FABP predictors were provided as categorical variables, ECG as a positive or negative for ischaemia and H-FABP as a semi-qualitative test but quoted as positive or negative for the presence of H-FABP.

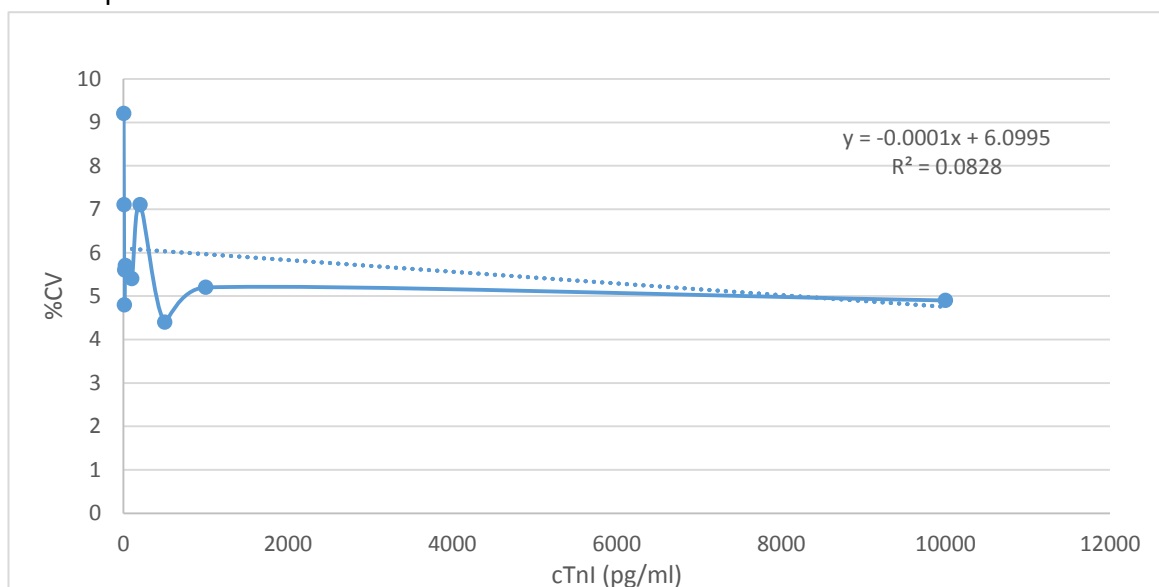


**Figure 2.2.4.3.1 Mean single site repeatability %CV of cTnI Singulex assay.** Repeatability of cTnI measurements over 20 days by 2 operators at one site with a 10-point standard curve, 1-10,000 pg/ml, using 3 lots of reagents. For this graph, the 3 lots were averaged before plotting. Dotted line indicates linear trend line with supporting equation included on chart.

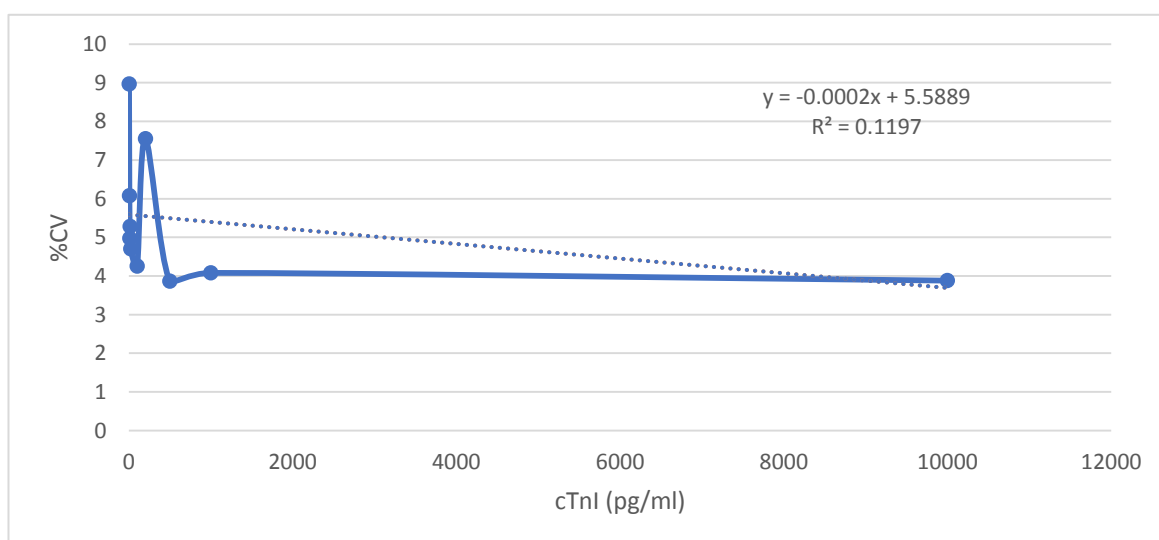


**Figure 2.2.4.3.2 Mean multi-site repeatability %CV of cTnI Singulex assay.** Repeatability of measuring cTnI by two operators at each of the three sites over 5 days using a 10-point standard curve, 1-10,000 pg/ml, in triplicate with a single lot of reagents. The results from the three sites were averaged before plotting.

## **Chapter 3: Immunoassay development**



### 3.1 Competitive immunoassay development

#### 3.1.1 Preliminary competitive immunoassay

The first competitive immunoassays run are shown in figure 3.1.1. mCRP-biotin was used in an array of concentrations to assess which had the best fitting standard curve against the increasing concentrations of competing mCRP. As the signal-producing mCRP-biotin is in competition with biotinylated mCRP, it would be expected for the signal to decrease with increasing mCRP concentration (x-axis). This did not occur and no discernible pattern can be observed from any mCRP-biotin concentration. Values have not been zeroed to show the variability even at 0 concentrations.

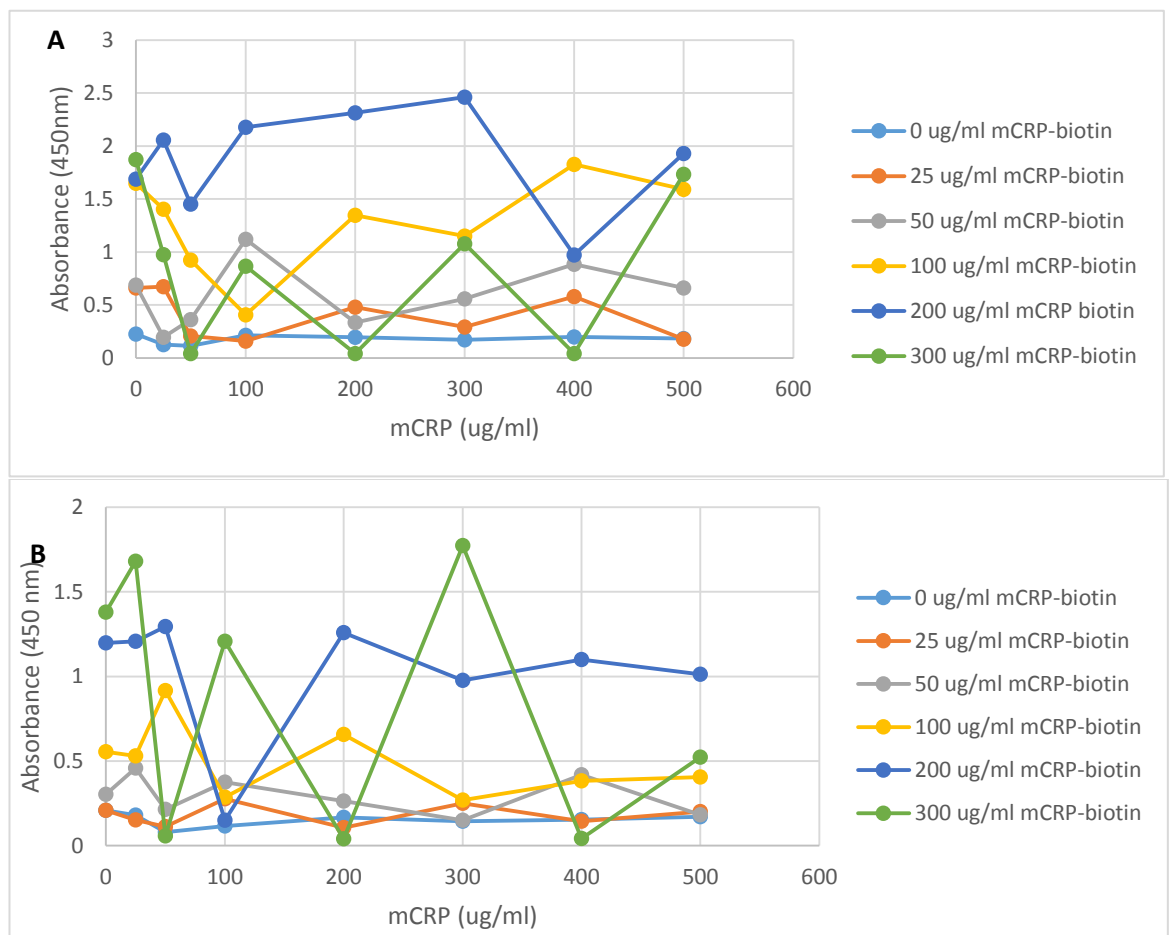


**Figure 3.1.1** Preliminary competitive immunoassay for the determination of mCRP concentration in serum. A) had plates coated with 1:10 8c10 mCRP antibody b) had plates coated with 1:20 8c10 antibody. The standard curve is made of 8 points 0-500 ug/ml. Each data series is one mCRP-biotin concentration.

### 3.1.2 Immunoassay with competition from mCRP removed

As the competition may have caused the large variability within the first assay, as seen in figure 3.1.1, it was decided that competition would be removed to assess which antibody dilution yielded the best fitting standard curve. For figure 3.1.2, the values have been zeroed. This experiment was to determine the correct antibody and mCRP-biotin concentration to use.

There is a general trend of increasing signal with increasing antibody concentration but the stronger signal of the 100 ug/ml mCRP-biotin compared with 200 ug/ml introduces uncertainty. In addition, a high antibody concentration used but resulting absorbance is low.

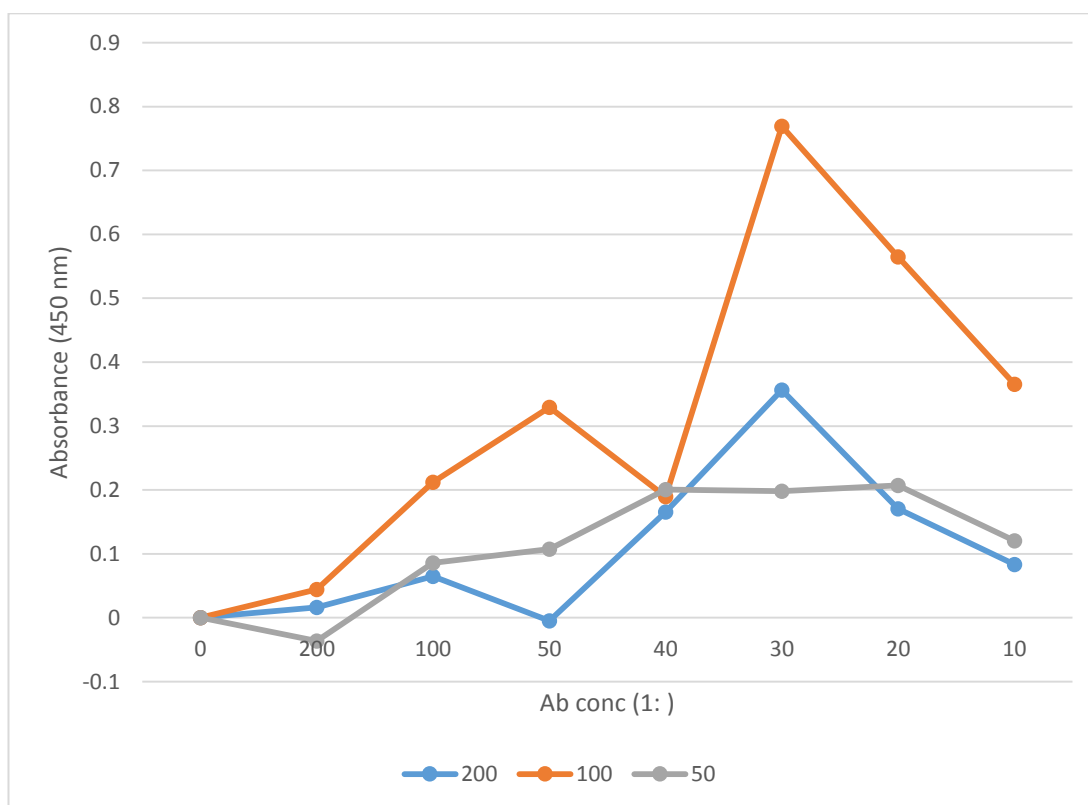


**Figure 3.1.2** Association between antibody concentrations, mCRP-biotin concentrations and absorbance. Antibody concentration is quoted as ratios on the x-axis and the legend denotes the mCRP-biotin concentration in ug/ml.

### 3.1.3 No competition introduced with alternative mCRP-biotin concentrations

Alternative mCRP-biotin concentrations were used to assess their viability as a

possible standard for a standard curve. Figure 3.1.3 below also shows the effort to

try to determine the best antibody concentration to use.

Again, the concentrations have no pattern and the lowest concentrated mCRP-

biotin produced the highest two signal points overall. Also, note how there are no

patterns emerging between any of the assays with respect to variability or

individual antibody titres between assays.

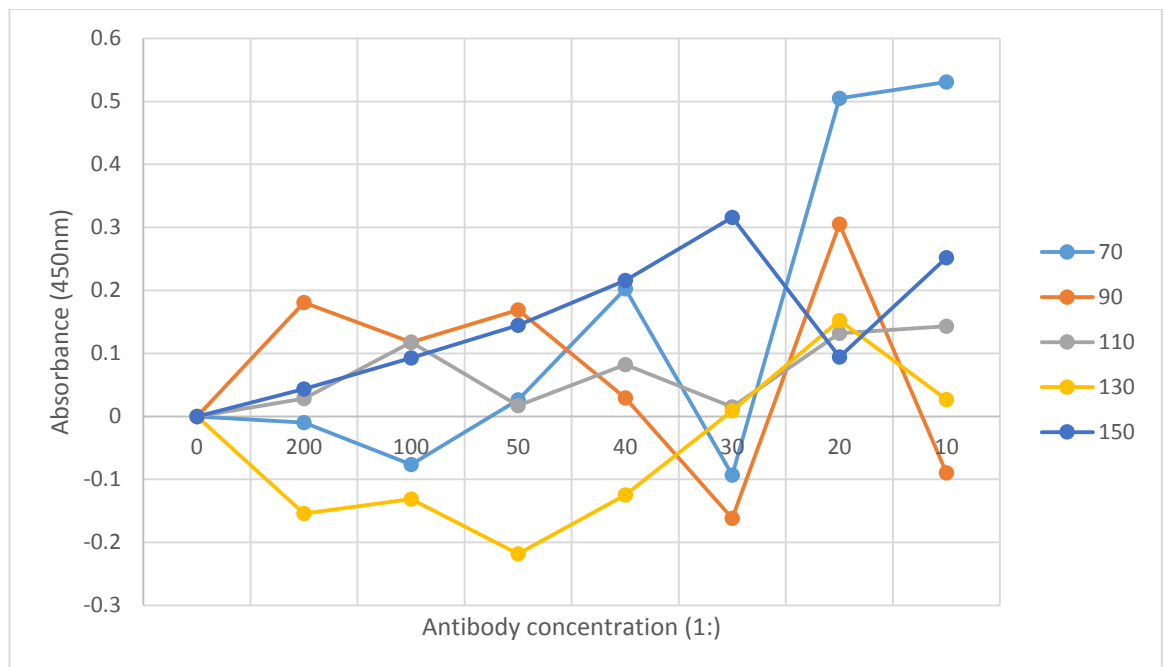


**Figure 3.1.3** Association between antibody concentrations with alternative mCRP-biotin concentrations and absorbance. Antibody concentration (1:200 – 1:10) is quoted as ratios on the x- and the legend denotes the mCRP-biotin concentration in ug/ml.

#### 3.1.4 Addition of 0.05% Tween to wash buffer

The large variation was partly attributed to the wash cycles, which had only contained CRP buffer. Addition of 0.05% Tween would wash away unbound mCRP that could have been causing the variation. Antibody concentration was set at 1:20.

The reduction in overall absorbance shows that the 0.05% Tween did wash away excess mCRP-biotin that was binding non-specifically to the plate. The outliers between 80 – 120  $\mu\text{g/ml}$  can be explained by unusually high background from the 0 antibody negative control wells and slightly low reading from these 1:20 antibody wells. However, the three could be affected by pipetting errors. By discounting the outliers, there appears to be a plateau at around 60  $\mu\text{g/ml}$  suggesting saturation of antibody.

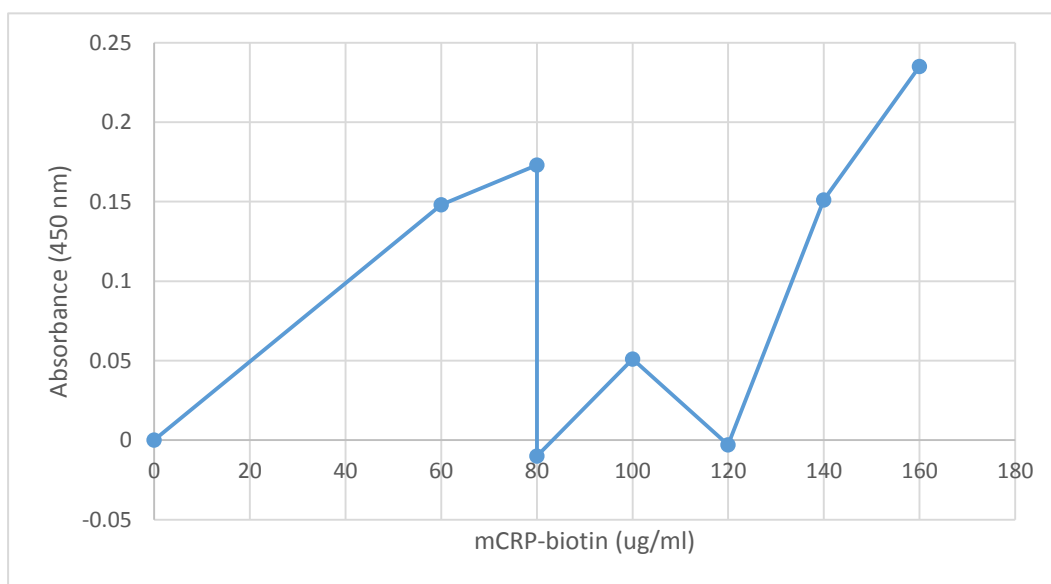


**Figure 3.1.4** The effect of 0.05% Tween in CRP buffer as a wash buffer. Antibody concentration was set at 1:20 and mCRP-biotin standards were 0-160  $\mu\text{g/ml}$ .

### 3.1.5 Reduction in range of mCRP-biotin standards to below 60 $\mu\text{g}/\text{ml}$

As the signal was seen to rise most between 0-40  $\mu\text{g}/\text{ml}$ , the range of standards was reduced. Tween 0.05% in CRP buffer was still used as a wash buffer.

As displayed in figure 3.1.5, there was close agreement between the different antibody concentrations with regards to mCRP-biotin signal strength. However, there remained much variation as the concentrations increased and the antibody concentration has no bearing on signal strength.

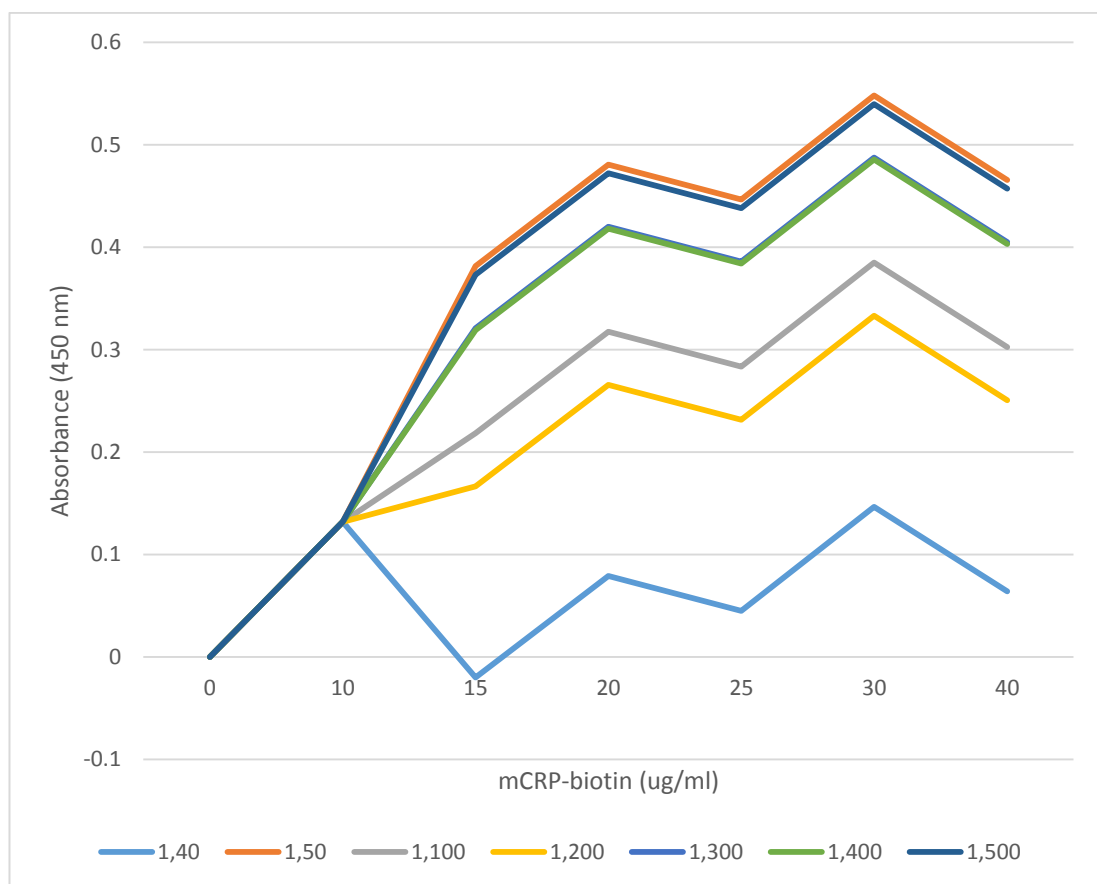


**Figure 3.1.5** Smaller range of mCRP-biotin concentrations in an immunoassay without competition to determine where rises in absorbance occur. Each data series represents a different antibody concentration, expressed as a ratio in the legend. mCRP-biotin standards are 0-40  $\mu\text{g}/\text{ml}$ .

### 3.1.6 Addition of BSA as blocking buffer

Different BSA concentrations were used to assess if there was any impact of the blocking buffer on the variability.

The addition of Tween appeared to limit variability but the standard curves, after an initial rise, are now flat with a slight rise at 160 ug/ml for 2% BSA, displayed in figure 3.1.6. As a blocking buffer, it would be expected that a higher BSA concentration would weaken the signal but this was not observed. Instead, the two BSA concentrations are very similar ( $p = 0.997$ ).

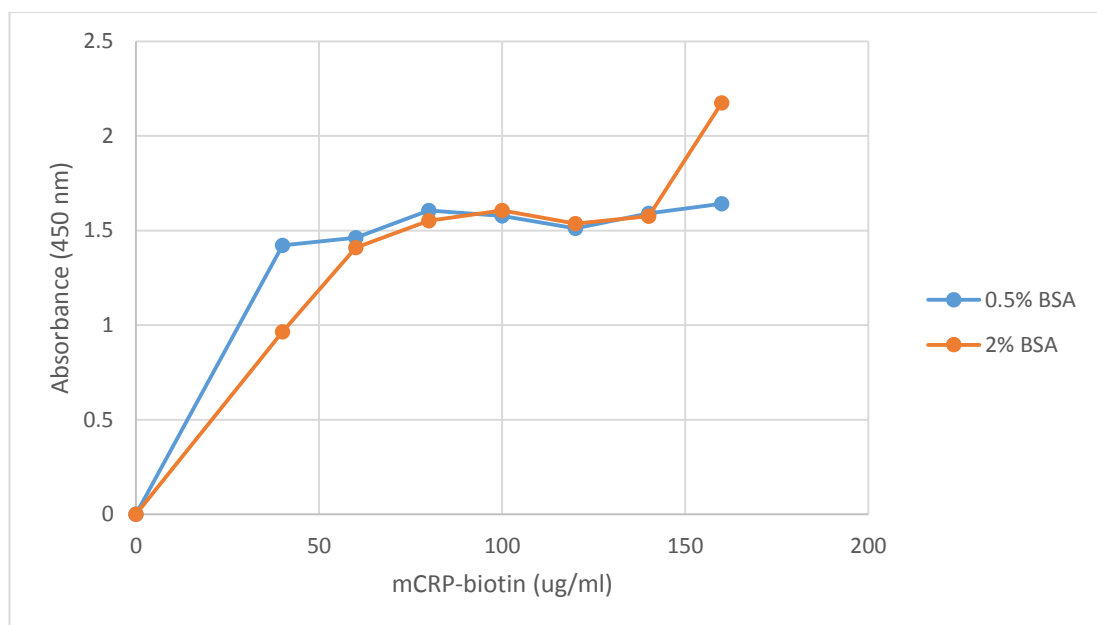


**Figure 3.1.6** Use of 0.05% Tween in CRP buffer for wash cycles and the effect of varying BSA concentrations

### 3.1.7 BSA-mCRP interaction

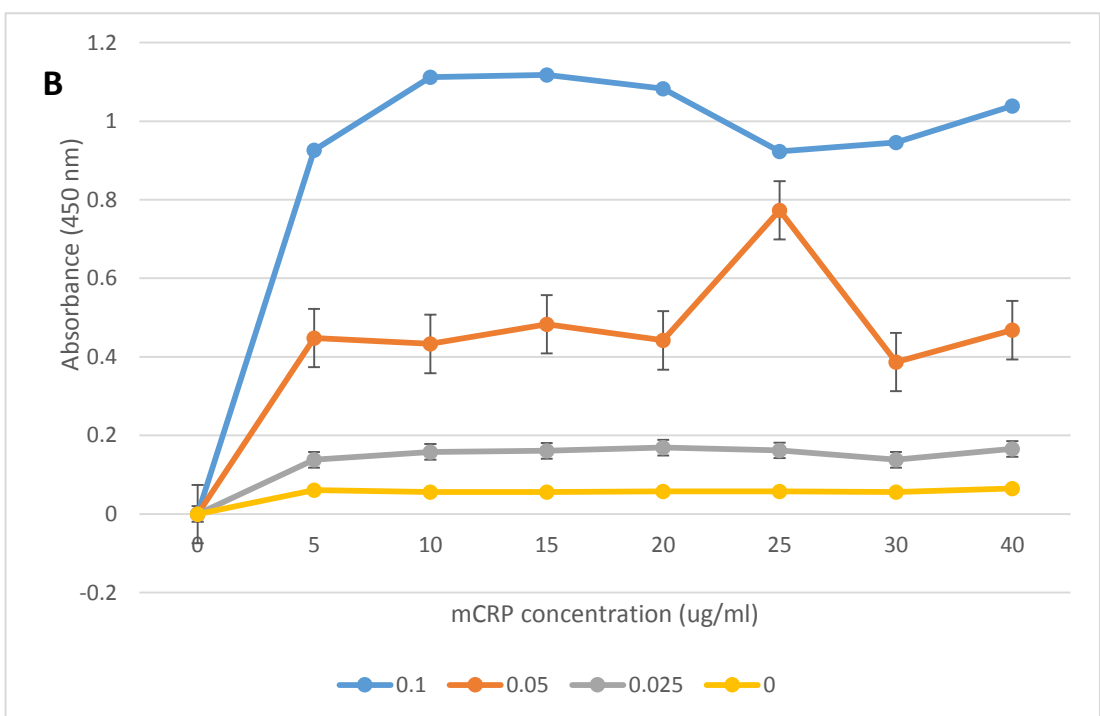
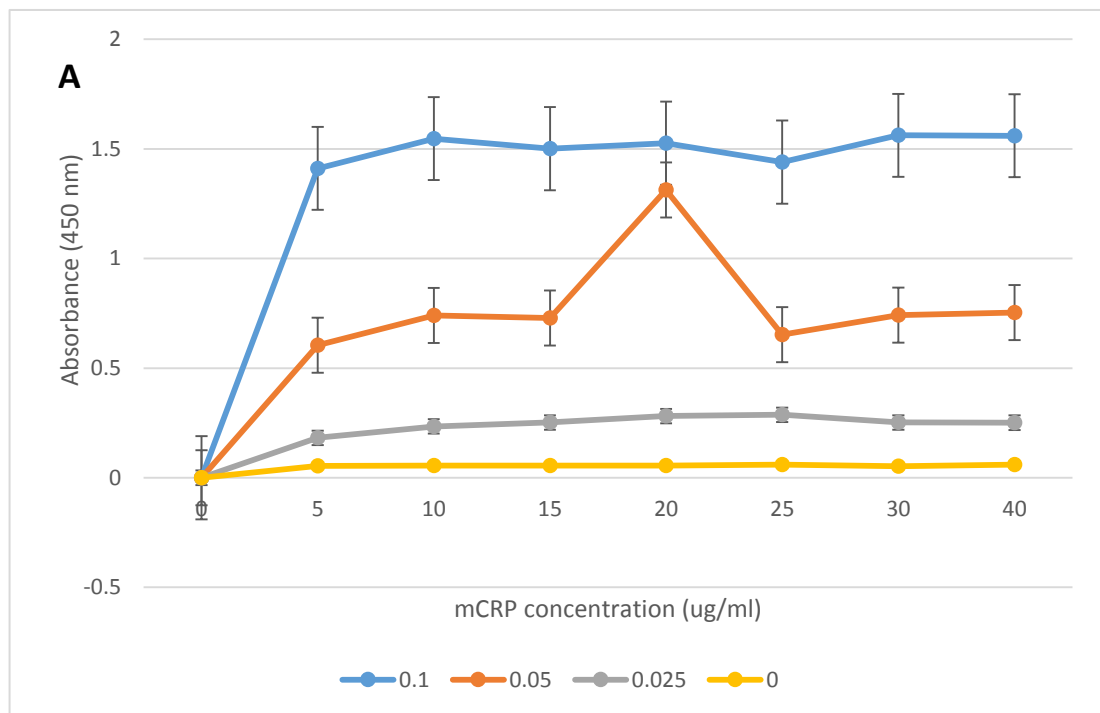
The results of adding BSA as a blocking buffer (figure 3.1.6) was not as expected and therefore its role in the immunoassay and any interactions were explored further.

Figure 3.1.7 shows the effect of different BSA concentrations on signal strength and capture antibody coating with increasing concentrations of biotinylated mCRP. No competition was introduced to the plate in the form of free mCRP in order to assess BSA-mCRP interaction alone.

BSA was first assessed as a potential blocking buffer to reduce non-specific binding.

Figures 3.1.7A-C show that avidin associates to biotinylated mCRP in a dose-dependent manner and there is very little difference in absorbance as biotinylated mCRP concentration increases from 5-40  $\mu\text{g/ml}$ . As it was observed that as BSA concentration increases, absorbance increases as seen in figure 3.1.7D, a graph was plotted to directly compare 0%, 0.5% and 2% BSA and the effect on absorbance.

The absorbance at 0% BSA is only a tenth of that at 2% BSA.





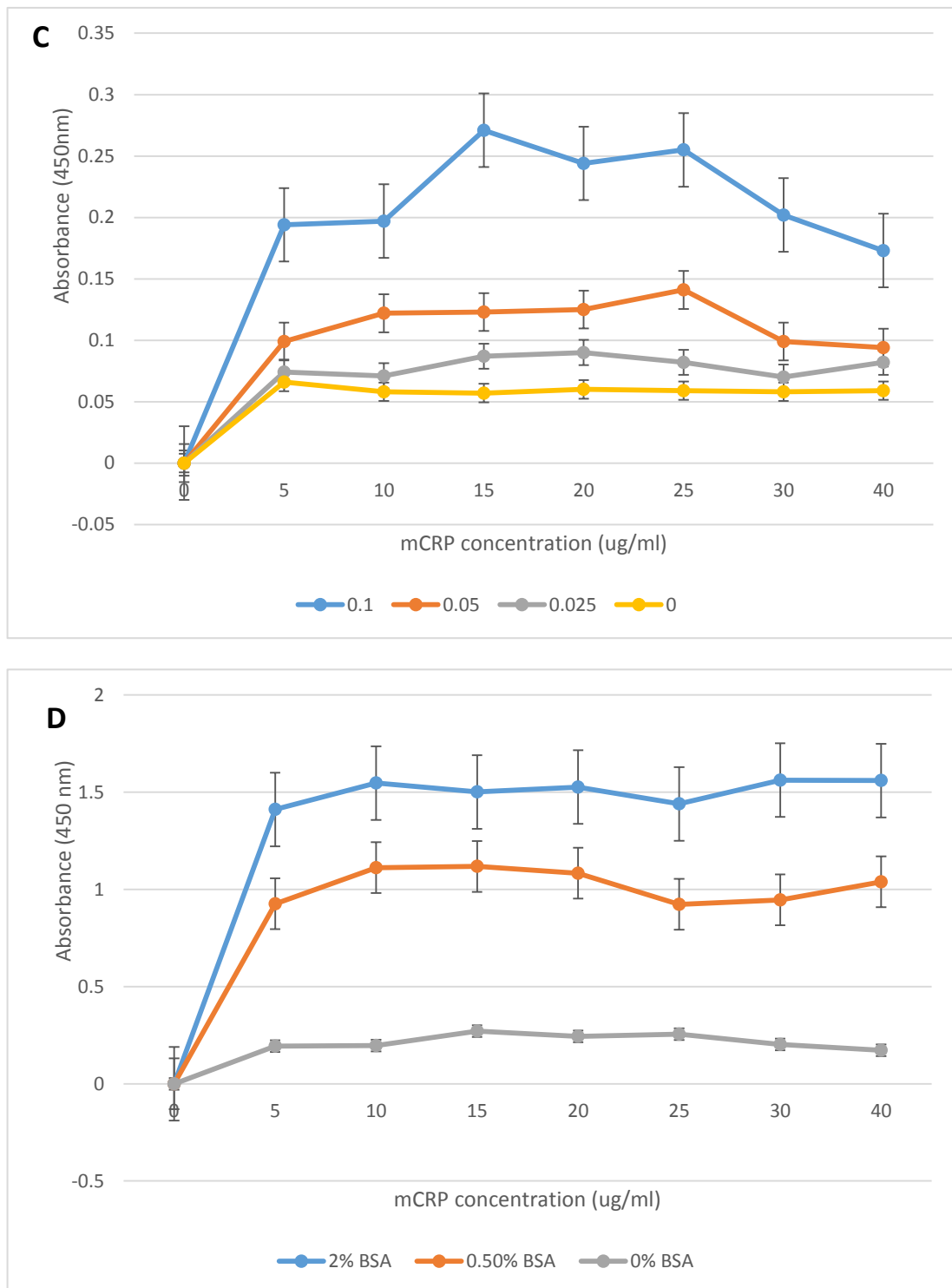
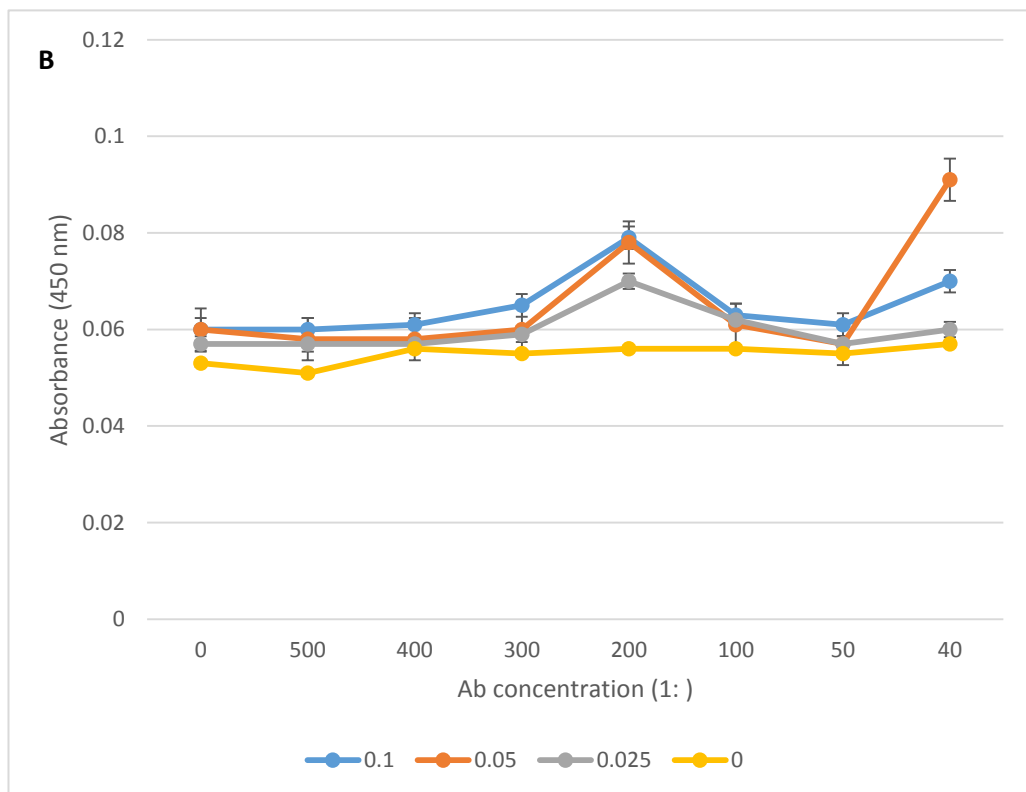
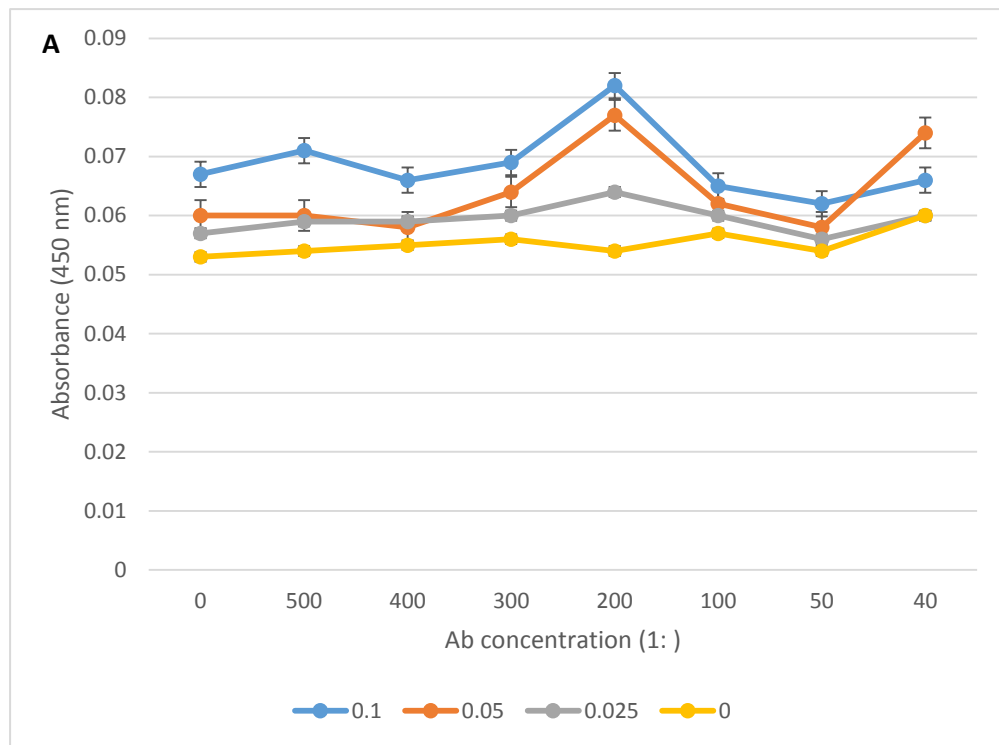


**Figure 3.1.7** Graphs displaying possible BSA-mCRP interaction by using different BSA concentrations. Legends in A-C display avidin concentration ( $\mu\text{g/ml}$ ). In A, BSA concentration is 2%; in B, BSA concentration is 0.5%; in C BSA concentration is 0%. D compares the different BSA concentrations at one avidin concentration – 0.1  $\mu\text{g/ml}$ . Error bars display standard error. There were significant differences between the different BSA concentrations in D ( $p < 0.001$ ).

### 3.1.8 Possible antibody-avidin and plate-avidin non-specific binding

For the analyses presented in figure 3.1.8, antibody was coated on the plate as specified on the x-axes and no mCRP or biotinylated mCRP was added to the plate to assess any avidin-antibody interactions.

In figures 3.1.8A-C, there is no significant difference between absorbance at 1:40 antibody concentration and 0 antibody concentration across all BSA concentration ranges but there are significant differences between different avidin concentrations ( $p > 0.001$ ,  $p = 0.020$  and  $p > 0.001$ , for 2%, 0.5%, 0% BSA, respectively). Figure 3.1.8D compares absorbance at different BSA concentrations at 0.1  $\mu\text{g/ml}$ , there was no significant effect of BSA concentration on absorbance ( $p = 0.50$ ). The absorbance values in figure 3.1.8 is not as great as in figure 3.1.7 and the magnitude of difference between each of the values is also less. In figure 3.1.8.1, there is a slight but not significant association between in plate-avidin binding and increasing avidin concentration ( $p = 0.21$ ). There is an association between BSA concentration and avidin-plate binding ( $p > 0.001$ ).



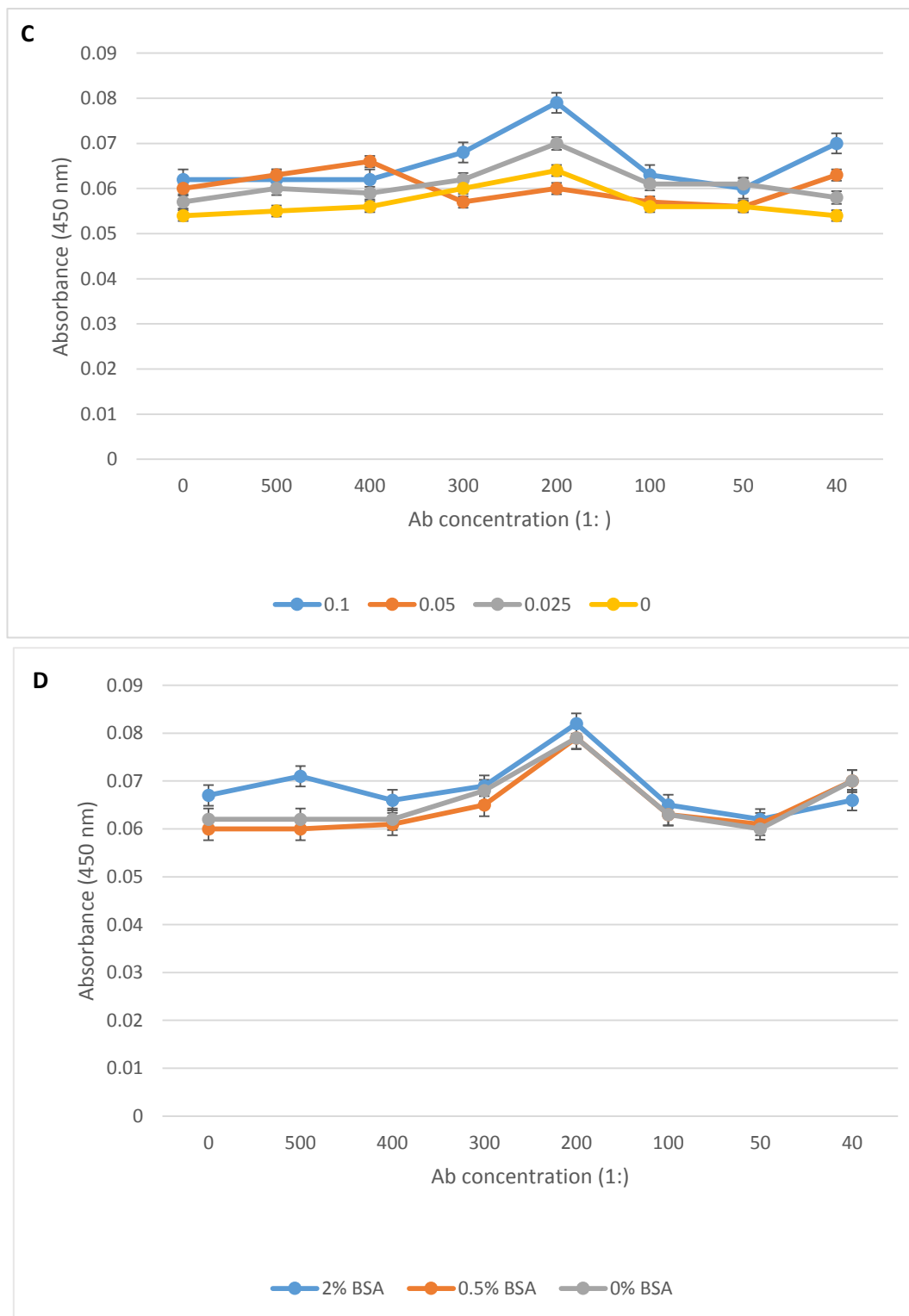


**Figure 5** Assessing possible antibody-avidin non-specific binding. Data from graphs A, B and C were blocked with 2%, 0.5% and 0% BSA, respectively. Legends in A-C display avidin concentration ( $\mu\text{g/ml}$ ). D compares the different BSA concentrations at one avidin concentration – 0.1  $\mu\text{g/ml}$ . Error bars display standard error. Ab: antibody

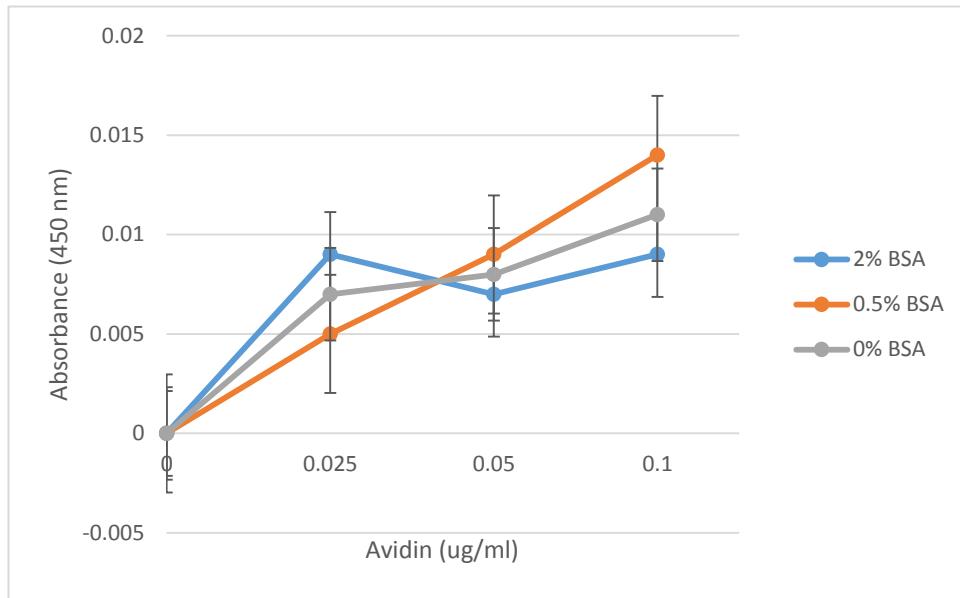


**Figure 3.1.6.1**  
Assessing possible avidin-BSA binding. BSA was made to 0%, 0.5% and 2% concentrations. Error bars represent standard error.

### 3.1.9 Milk protein vs BSA as blocking buffer

The 3.1.7 experiment was repeated by comparing BSA and milk proteins directly over a wider range of mCRP concentrations. This was to assess if milk protein was a more appropriate blocking agent than BSA and if the association between mCRP and BSA was mammalian in nature. The plates were coated with 1:100, 1:200 and 1:400 antibody concentrations. BSA was made to 2% for each experiment, milk protein was made to 5% and 10% concentrations. Each blocking concentration was tested with each mCRP and antibody concentration.

In figure 3.1.9A, the BSA retains a higher signal than milk protein by comparing the same concentration antibodies between the two blocking agents. The distinction between data series and the variability displayed is still poor even when 0.05% Tween washes were used. This demonstrates a problem with repeatability.

When using 10% milk protein to block plates, there is no significant difference between the three antibody concentrations used ( $p = 0.77$ ). In figure 3.1.7B, milk protein concentration has an effect on absorbance. At antibody concentration 1:100, 10% milk produces a significantly higher signal than 5% milk ( $p < 0.01$ ). There are significant differences in absorbance between BSA and milk protein when comparing corresponding antibody concentrations (all  $p > 0.001$ ).

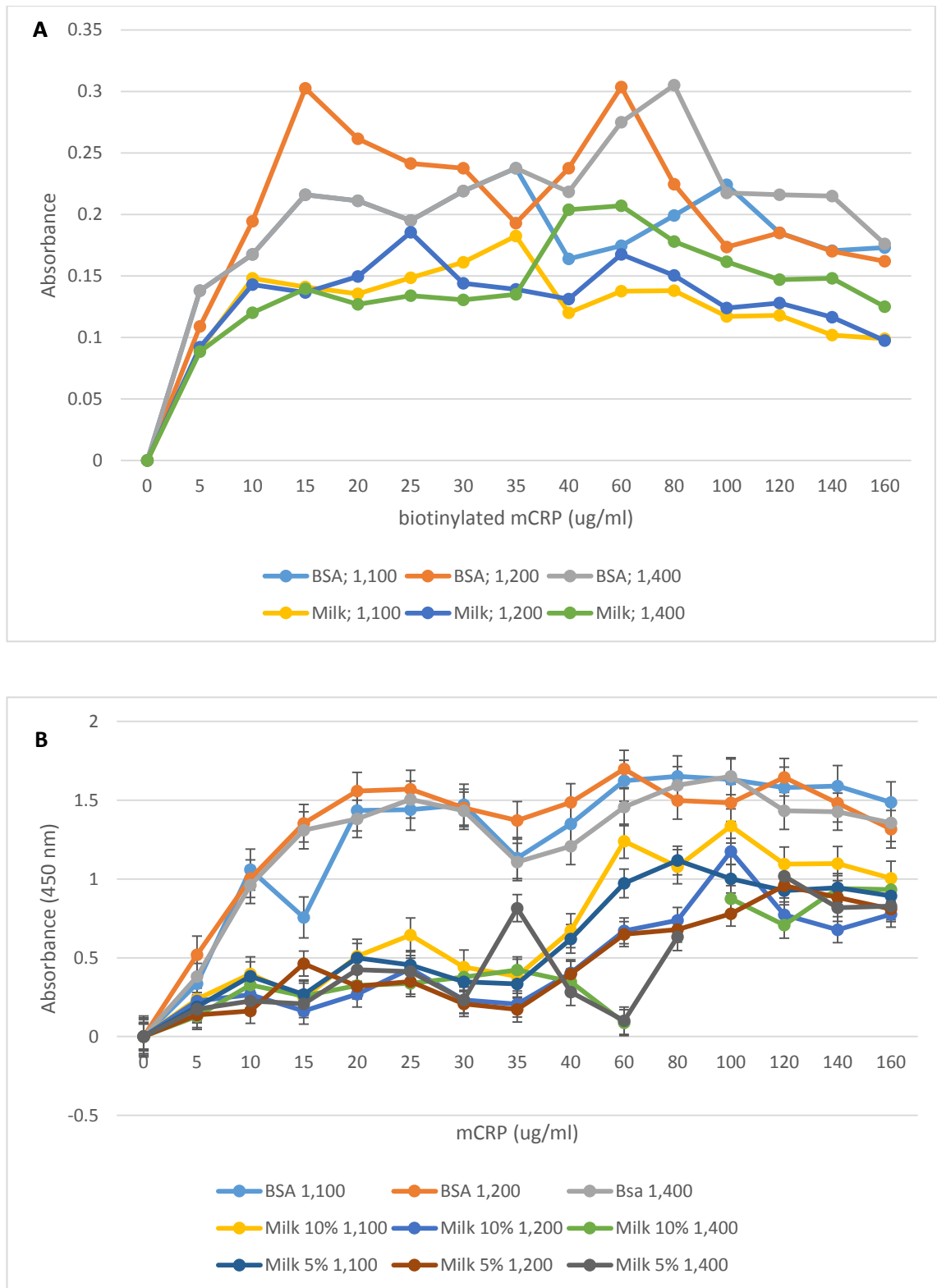


**Figure 3.1.9** Comparing milk protein and BSA as blocking buffers. A) BSA and milk as blocking buffers with antibody concentrations at 1,100, 1,200 and 1,400. B) shows a repeat of the A) but with different concentrations of milk protein and legend shows antibody concentration (1,100; 1,200; 1,400) and BSA, 10% milk and 5% milk. Error bars represent standard error.

### 3.1.10 Antibody coating buffer™ and Monster Block™

Figure 3.1.10 shows the difference in absorbance between using antibody diluted in distilled water to that in Antibody coating buffer™. Antibody coating buffer™ was used as directed by the manufacturer. In figure 3.1.10, a steeper curve is observed between 0-60 µg/ml and a stronger signal overall when using the coating buffer. There is 4 times the signal when using the coating buffer compared to dH<sub>2</sub>O ( $p < 0.001$ ). Figure 3.1.10B shows the correlation between exponential mCRP concentrations and absorbance.  $R^2$  is higher than both  $R^2$  values in figure 3.1.10A.

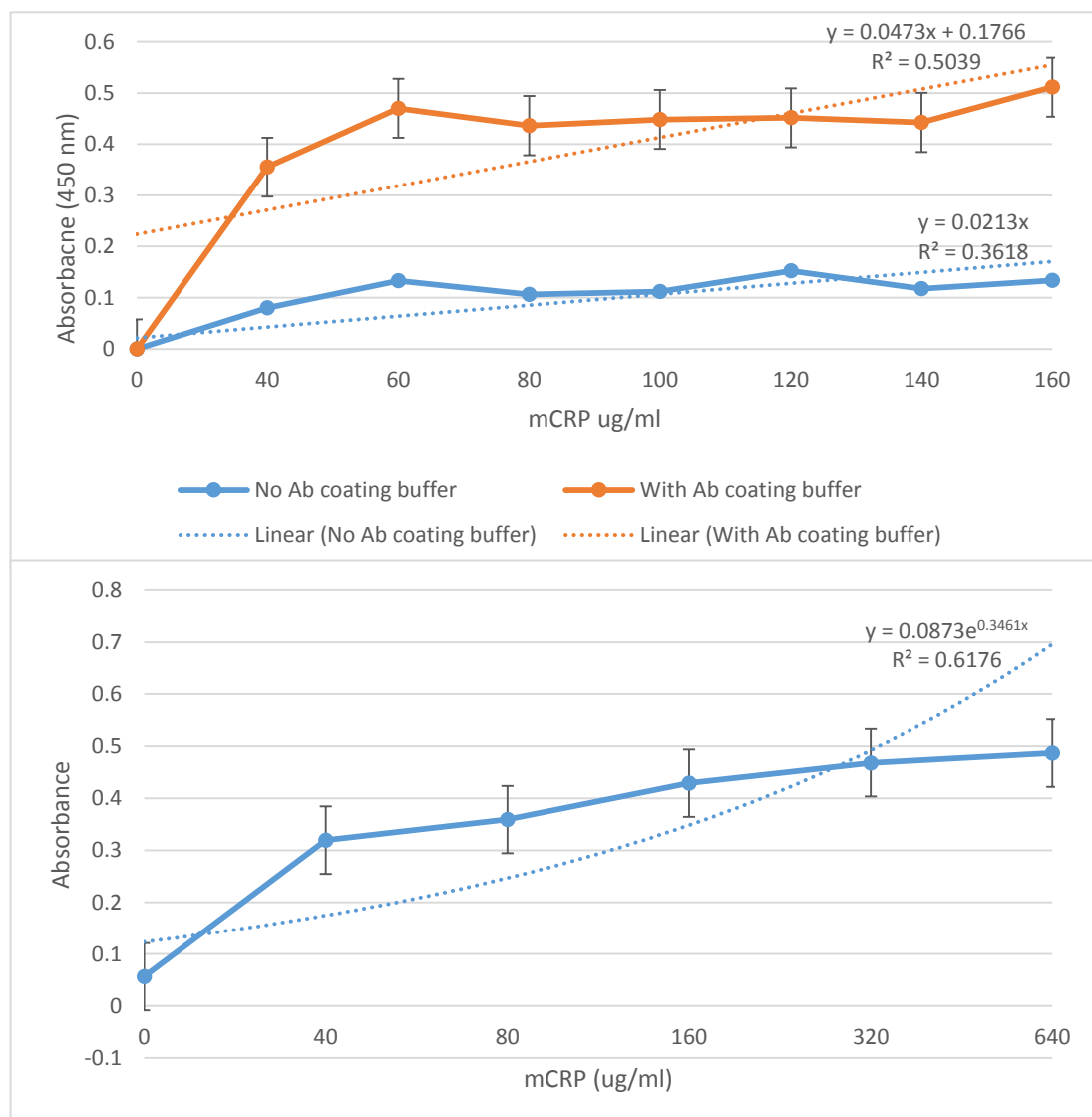


**Figure 3.1.10** Comparison between coating plates with antibody with and without Antibody Coating Buffer™ and possible interaction between mCRP and Monster Block™. (A) is coated with 1:200 antibody and (B) with 1:50 antibody. Error bars represent standard error.



### 3.1.11 Possible interaction between mCRP and Monster Block™

The results from the milk and BSA experiments show a possible affinity between mCRP and mammalian proteins; therefore, a non-mammalian block was found to assess this hypothesis. The same procedure that was done for BSA-mCRP was done for mCRP-Monster Block™ association. However, no antibody was present for these experiments and there was competing mCRP to the mCRP-biotin to make a rudimentary competitive immunoassay. Monster Block™ was used neat (100%) and diluted in dH<sub>2</sub>O to 50% and to 0%. As seen in figure 3.1.11, higher concentration of Monster Block™ produces lower signal. There are significant differences between all Monster Block™ concentrations at 80 µg/ml and 120 µg/ml when competing mCRP standard concentration is 0 µg/ml and across data sets ( $p < 0.001$ ).

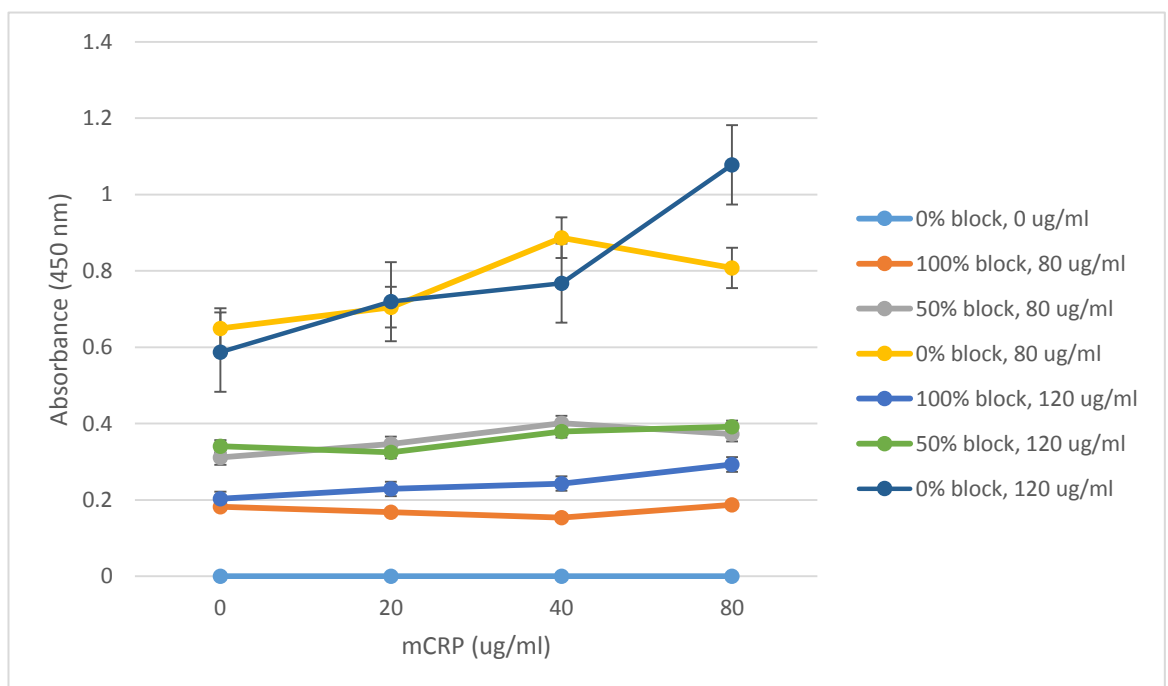


**Figure 3.1.11** Assessing mCRP-Monster Block™ interaction with no antibody present. The different data series represent mCRP-biotin concentration (0, 80, 120 µg/ml) and the different Monster Block concentrations (0%, 50%, 100%). Error bars show standard error.

### 3.1.12 mCRP-biotin conjugate competing with non-labelled mCRP standards

By using the Monster Block, the results looked more linear than with the mammalian blocks and therefore competing mCRP standards were reintroduced to form a competitive assay once more. Figure 3.1.12A shows the use of mCRP from an existing CRP lot and figure 3.1.12B was from a new CRP lot. It was thought that mCRP may degrade even at 4°C and the variation in concentration seen between lots of CRP may also contribute to variation. It was therefore decided to test this hypothesis.

After introducing mCRP standard concentrations, the higher mCRP-biotin concentrations continue yield the highest absorbance values (figure 3.1.12A). There is no trend of decreasing absorbance from 0-70 µg/ml and the intermediate values are not linear.

The same was witnessed for the data in figure 3.1.12B. TMB incubation time was assessed as a potential variable and therefore its incubation time was changed. The longer TMB incubations times did increase signal strength only at higher mCRP-biotin concentrations (both 160 µg/ml and 120 µg/ml 10 mins vs 16 mins  $p < 0.001$ ; 80 µg/ml 10 mins vs 16 mins  $p = 0.840$ ).

The analytical sensitivity under the conditions of figure 3.1.12B was calculated using the theoretical equivalent of two standard deviations above the zero calibrator of 10 replicates of a zero concentration sample and was found to be 0.22 units of absorbance. The within-assay imprecision was too great to estimate to which concentration this refers.

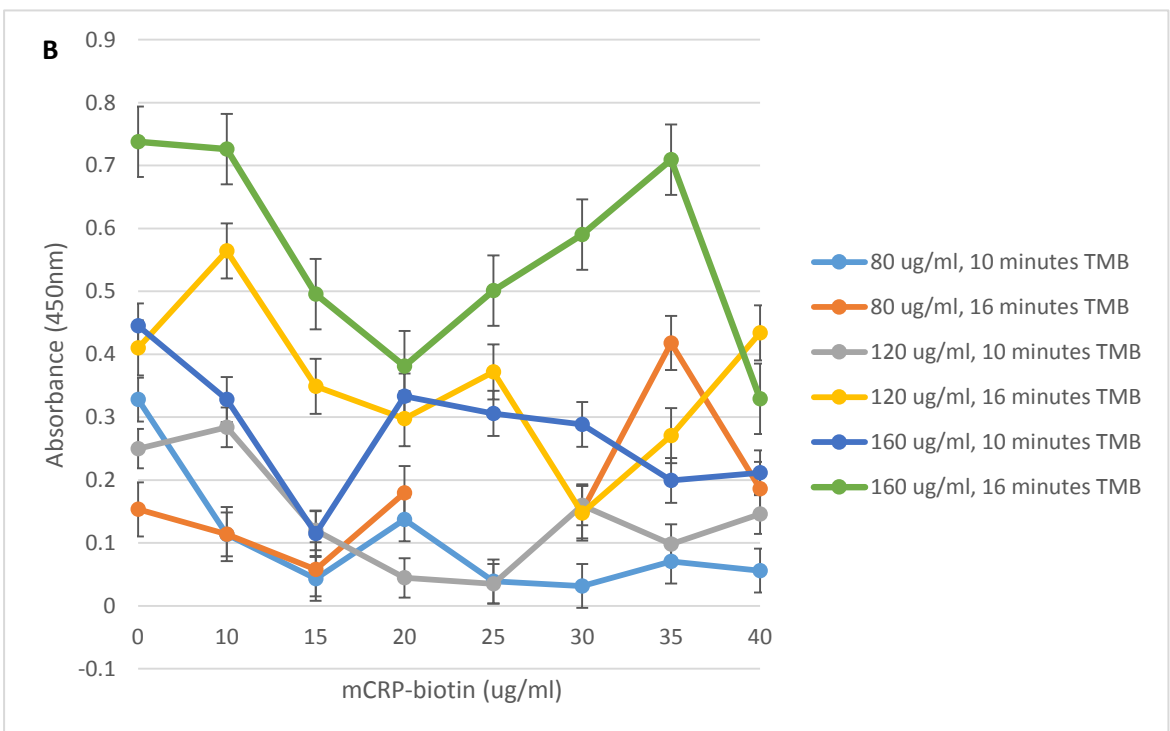
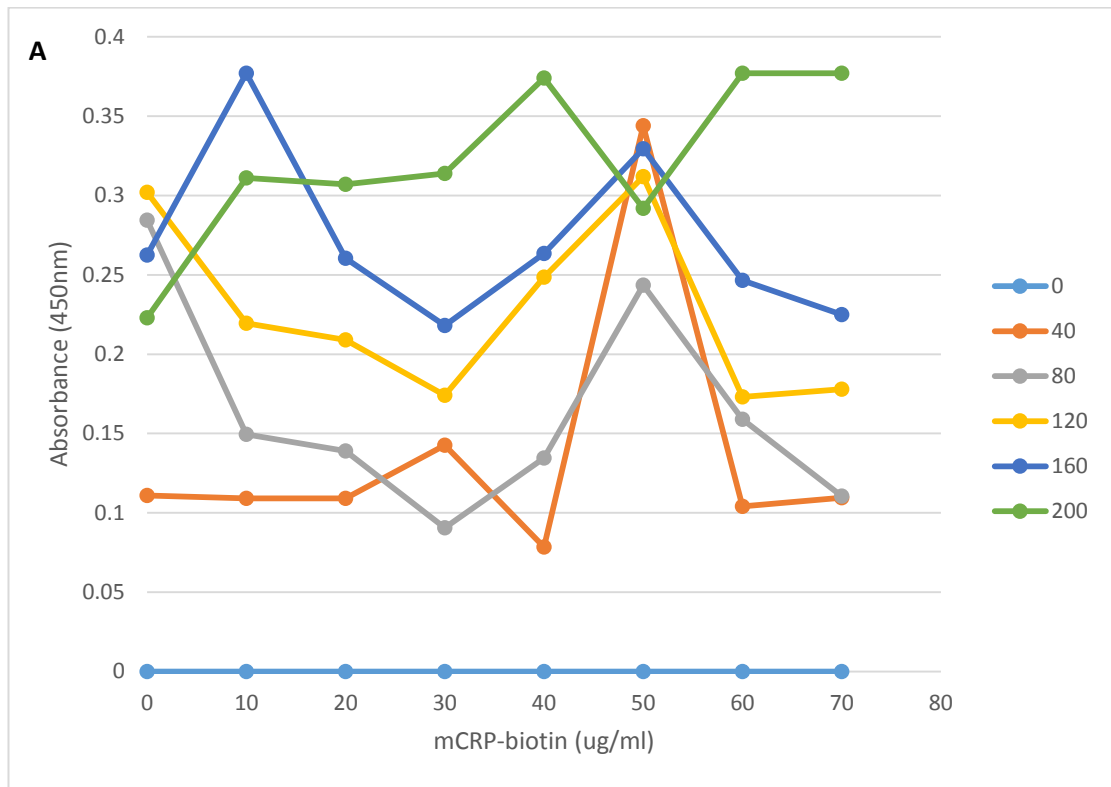


**Figure 3.1.12** Competitive assay between mCRP-biotin and unlabelled mCRP standards. The data series represent mCRP-biotin concentrations and TMB incubation time. Error bars show standard error.

### 3.1.13 Experimentation of mCRP incubation time at 24h and 48h at room temperature

As the difference in TMB incubation made a significant difference to the results of the competitive immunoassay, the incubation times for the competing mCRP were increased to 24h and 48h at room temperature. The hypothesis behind this was to allow the mCRP and the mCRP-biotin to equilibrate to produce a linear, less variable curve. The results in figure 3.1.13 show that the mCRP began to degraded as the signal strength was decreased after 24h and 48h at room temperature.

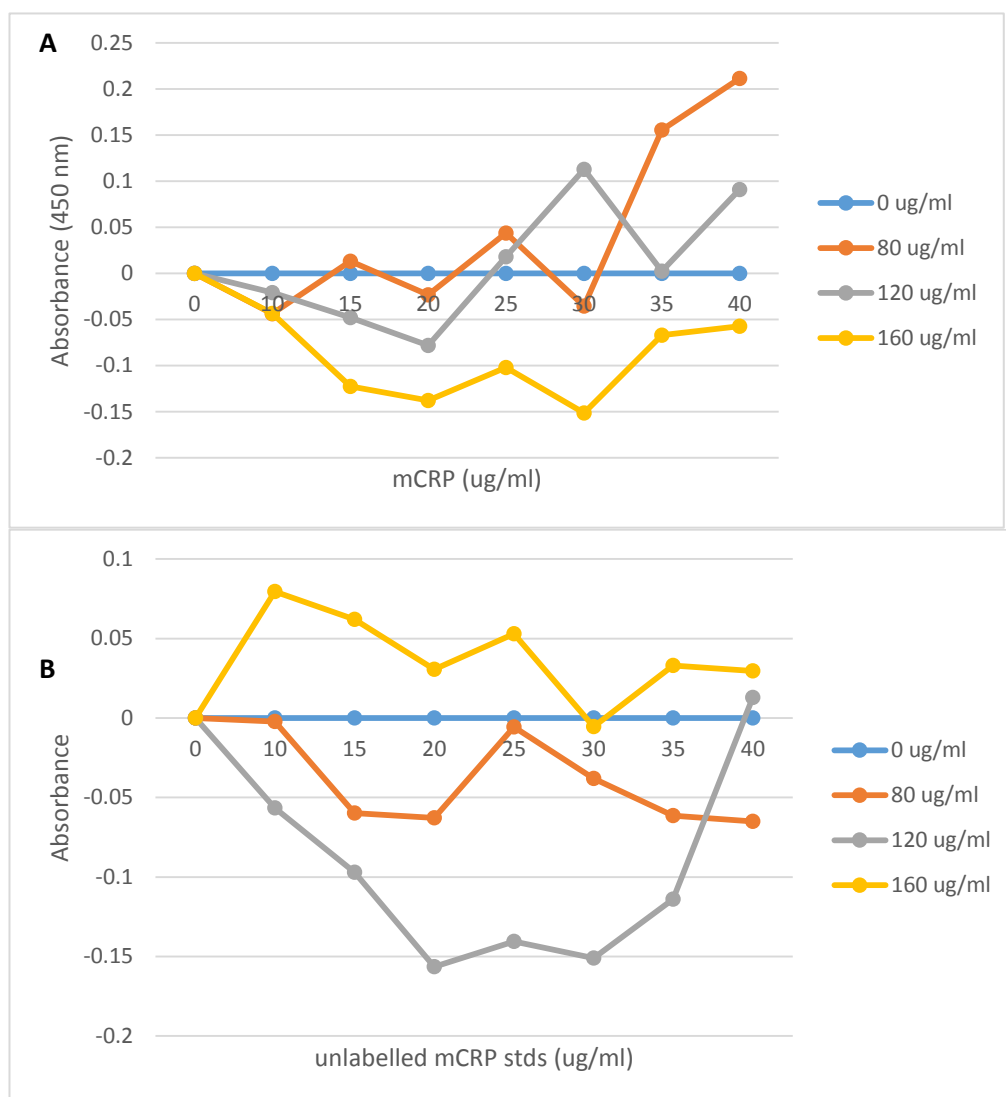


**Figure 3.1.13** Competitive immunoassay with 24h and 48h mCRP incubation time at room temperature. A) shows 24h incubation and B) shows 48h incubation times. mCRP-biotin are shown in the legend and each data series represents one mCRP-biotin concentration.

#### 3.1.14 Experimentation of mCRP incubation time at 24h and 48h at 4°C

It appeared the mCRP was degrading in the immunoassay at room temperature.

Therefore, to allow equilibration to take place but to preserve the integrity of the mCRP, the incubation of the competing mCRP was conducted at 4°C.

At 24h (figure 3.1.14A) the integrity of the mCRP remained somewhat intact.

However, there is a general increasing trend with increasing mCRP concentration, which is opposed to the theory of the assay. It could be that the equilibration stage has allowed the mCRP and mCRP-biotin to associate instead of compete and the unbound mCRP-biotin could associate with antibody-bound unlabelled mCRP. This also could suggest the biotinylation of mCRP may affect its binding properties if unlabelled mCRP is binding to the antibodies and then mCRP-biotin associates to the antibody indirectly through the unlabelled mCRP. The biotinylation kit does quench the biotinylation reaction to prevent further unwanted biotinylation.

Therefore, the error would not come from the kit but this may point to the hydrophobicity of mCRP and its affinity for any species but water.

Figure 3.1.14B shows the result after 48h incubation at 4°C. The pattern of degradation is similar to that of the room temperature incubations (figure 3.1.13). This points to mCRP as not stable outside its specific pH and solute conditions and as the immunoassay would create a different physical chemistry conditions, mCRP is liable to degrade even at low temperatures.

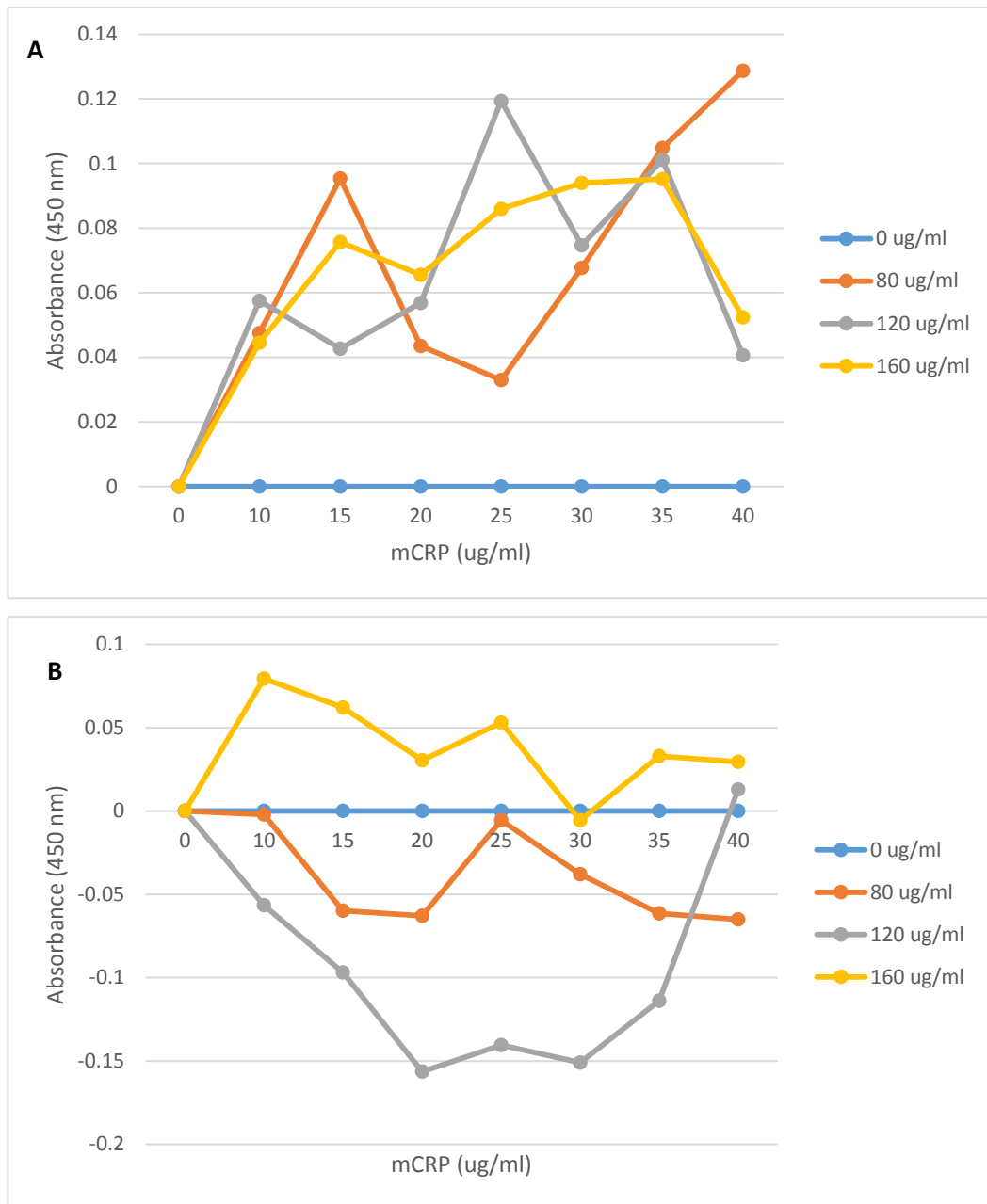


**Figure 3.1.14** Competitive immunoassay with 24h and 48h mCRP incubation time at 4°C. A) shows 24h incubation and B) shows 48h incubation times. mCRP-biotin are shown in the legend and each data series represents one mCRP-biotin concentration.

### 3.1.15 Using a mixing plate to pre-equilibrate the mCRP-biotin and competing mCRP

The equilibration of mCRP-biotin and competing mCRP therefore pre-mixing the

two solutions in an antibody-free prep plate before adding to the experimental

plate was done. TMB of the prep plate was also applied to assess mCRP-plate

binding. The mCRP-biotin would only be present in the plate for a maximum of 5

minutes before application to the experimental plate that had already been coated

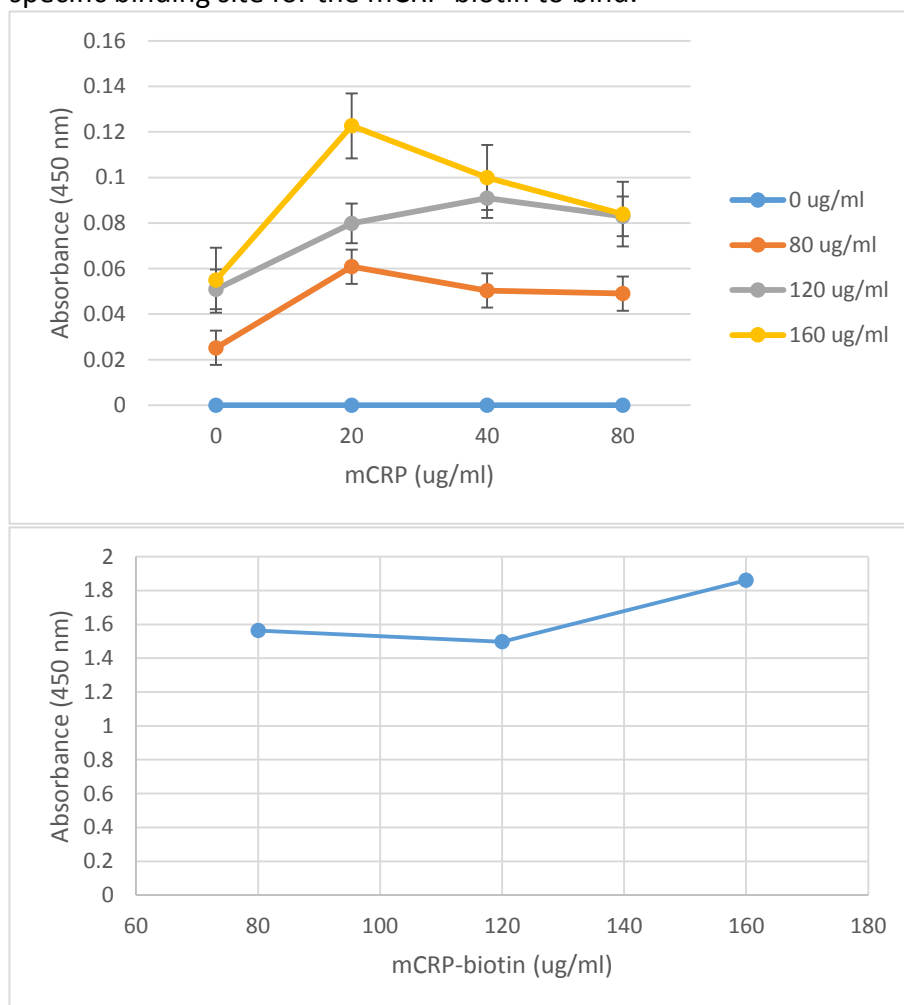
with antibody. Monster Block™ was used as a blocking agent on the experimental

plate.

Similar results (figure 3.1.15) were seen as previously without pre-mixing. The prep

plate had very high absorbance considering there was no antibody and therefore no

specific binding site for the mCRP-biotin to bind.



**Figure 3.1.15** Pre-mixing of mCRP-biotin and mCRP and the effect of absorbance on the mixing plate. A) Legend shows mCRP-biotin concentrations and x-axis shows competing mCRP concentrations. B) mCRP-biotin was in contact with these wells for a maximum of 5 minutes and without antibody. The comparison with antibody without BSA (figure ...) is that the prep plate has over 4 times more signal without antibody than with antibody.

### 3.2 Sandwich ELISA for the determination of mCRP concentration

#### 3.2.1 Monoclonal anti-human CRP antibody ab24462 as detection antibody

A new approach of developing a sandwich ELISA was considered. The 8C10 mCRP antibody was still used, as the lack of sensitivity displayed in previous analyses may be overcome by the addition of a sensitive detection antibody. As Wang et al., (38) showed success with monoclonal antibody ab24462 but a different source of capture antibody, a novel ELISA using the 8C10 clone was proposed for development.

Figure 3.2.1A shows that no signal was achieved by using this antibody pairing as absorbances for all standards (0-32  $\mu\text{g/ml}$ ) fall either side of the zero. The experiment was repeated with a greater range of mCRP standards (0-160  $\mu\text{g/ml}$ ) but still no signal was achieved. It was concluded that the two antibodies shared the same or very close epitopes with the capture antibody, 8C10 hiding the epitope from the detection antibody, ab24462. From this evidence, it was decided that a polyclonal antibody would be a better option because a polyclonal would recognise many different epitopes around the pCRP, and therefore mCRP, molecule and would produce a signal.



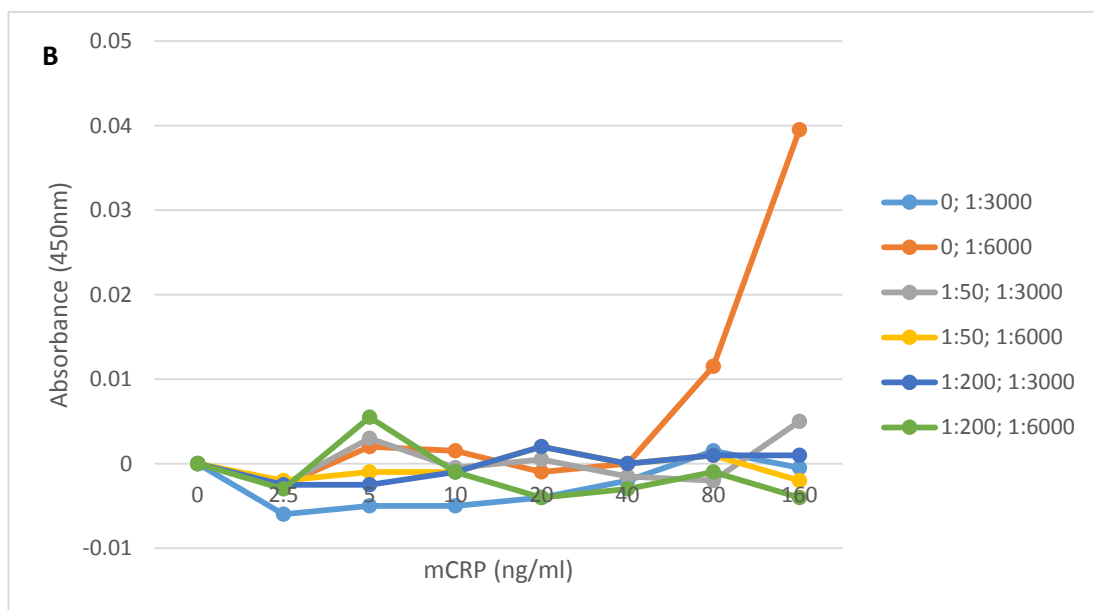
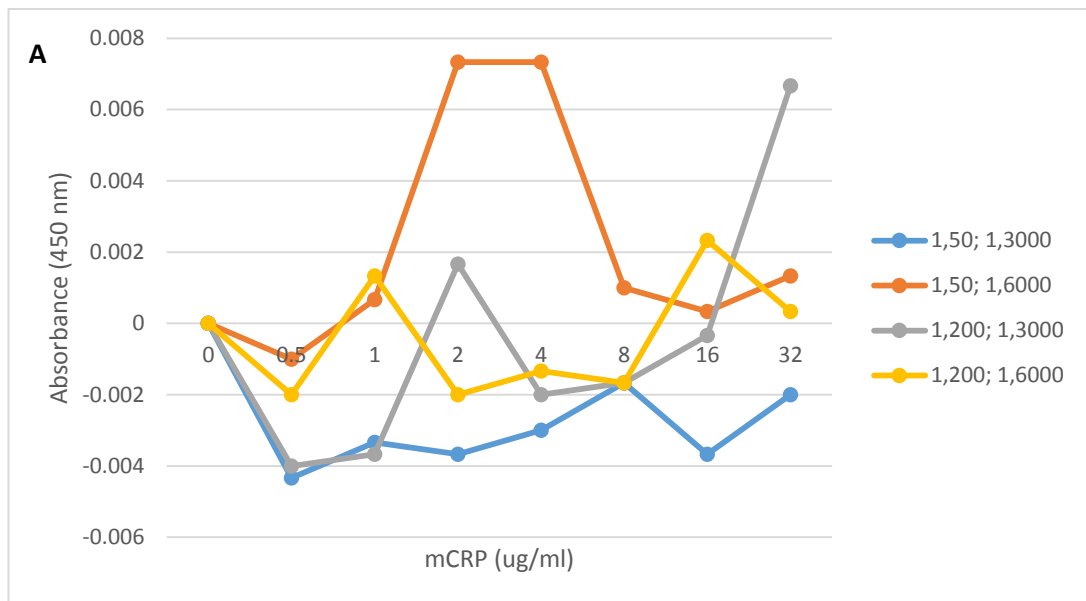


**Figure 3.2.1** Development of sandwich ELISA for mCRP concentration determination using monoclonal antibody ab24462. A) shows the first experiment with a small range of standards (0 – 32 µg/ml) and B) shows a wider range of standards (0 – 160 µg/ml). The legends display the antibody concentrations in the conformation of 8C10; abcam24462. 8C10 was used at concentrations 0, 1:50 and 1:200; abcam24462 was used at 1:3000 and 1:6000. Each concentration was tested with each other to produce 6 data series.

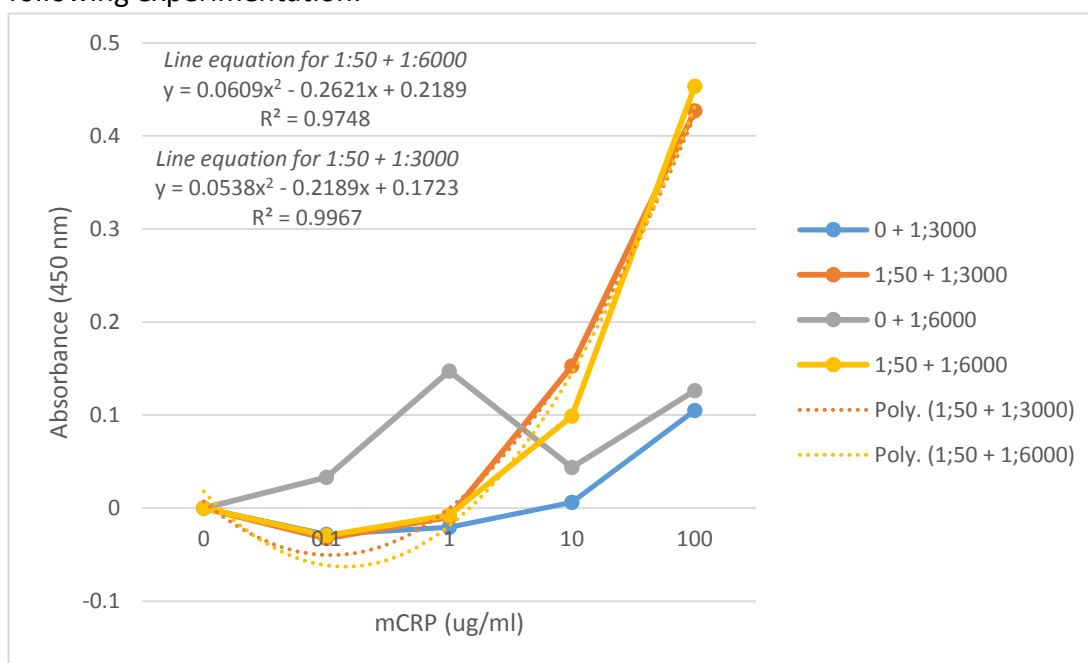
### 3.2.2 Polyclonal anti-human CRP antibody ab19175 as detection antibody

As previously, the assay was conducted with and without capture antibody present.

As seen in figure 3.2.2, the antibody was used at 0 and 1:50 concentration, as

denoted by the first number of each line in the legend. The detection antibody was used at 1:3000, as recommended by the manufacturer, and 1:6000. Concentrations from both antibodies were tested together to produce the data series seen in the figure.

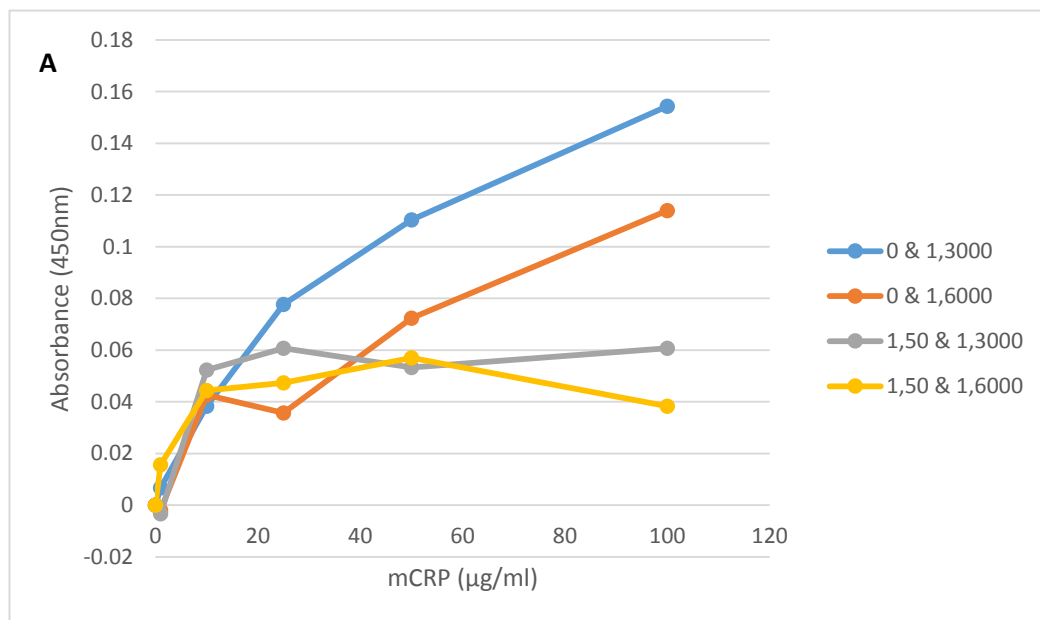
The 1:50 capture antibody concentrations are significantly different from their 0 antibody concentration counterparts (1:3000,  $p < 0.001$ ; 1:6000,  $p < 0.001$ ). There is an outlier at 1  $\mu\text{g/ml}$  for 0 + 1:6000, however due to the apparent random nature of mCRP behaviour, this was not considered representative. However, this curve was not repeatable to the same strength of absorbance nor to the same linearity in following experimentation.

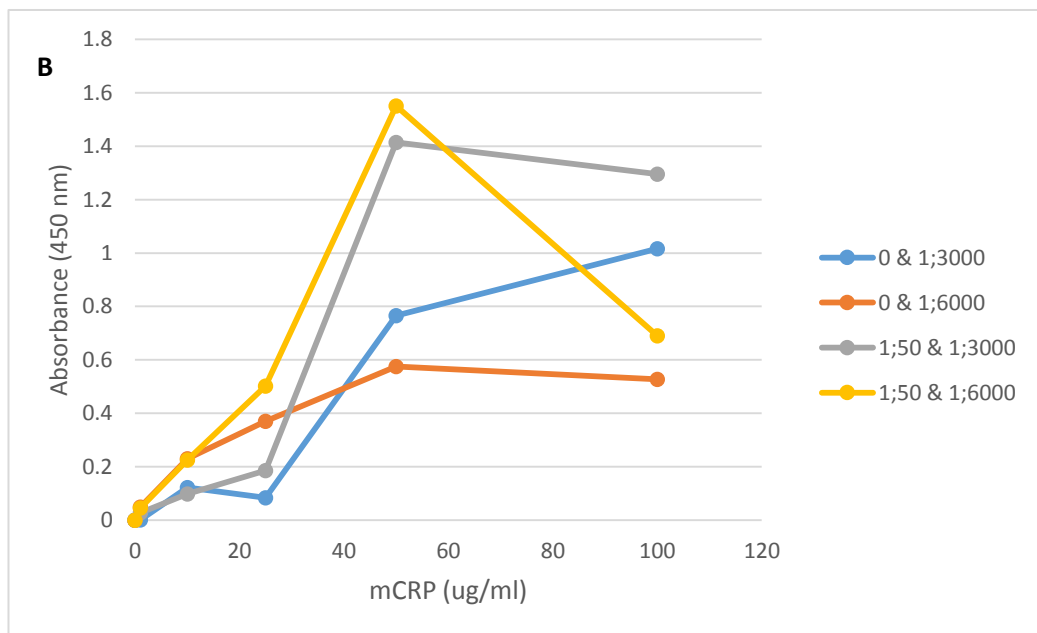


**Figure 3.2.2** Sandwich ELISA for the determination of mCRP concentration. Two concentrations were used for each antibody creating 4 lines in the figure. Capture antibody concentrations were at 0 and 1:50 and detection antibody concentrations were at 1:3000 and 1:6000. Two polynomial trendlines were created for the 1:50 capture antibody for mCRP determination in unknown samples.

### 3.2.3 Non-repeatability of the sandwich ELISA with polyclonal anti-human CRP antibody ab19175

The attempts to repeat the standard curves in figure 3.2.2 are displayed below and in order of when the plates were run. There appeared to be degradation of signal and the strongest signals varied between 0 antibody and antibody presence. pCRP was measured alongside mCRP shown in figure 3.2.3, and no significant differences were found between p/mCRP standard curves (1:50 antibody  $p = 0.535$ ; 0 antibody  $p = 0.092$ ).





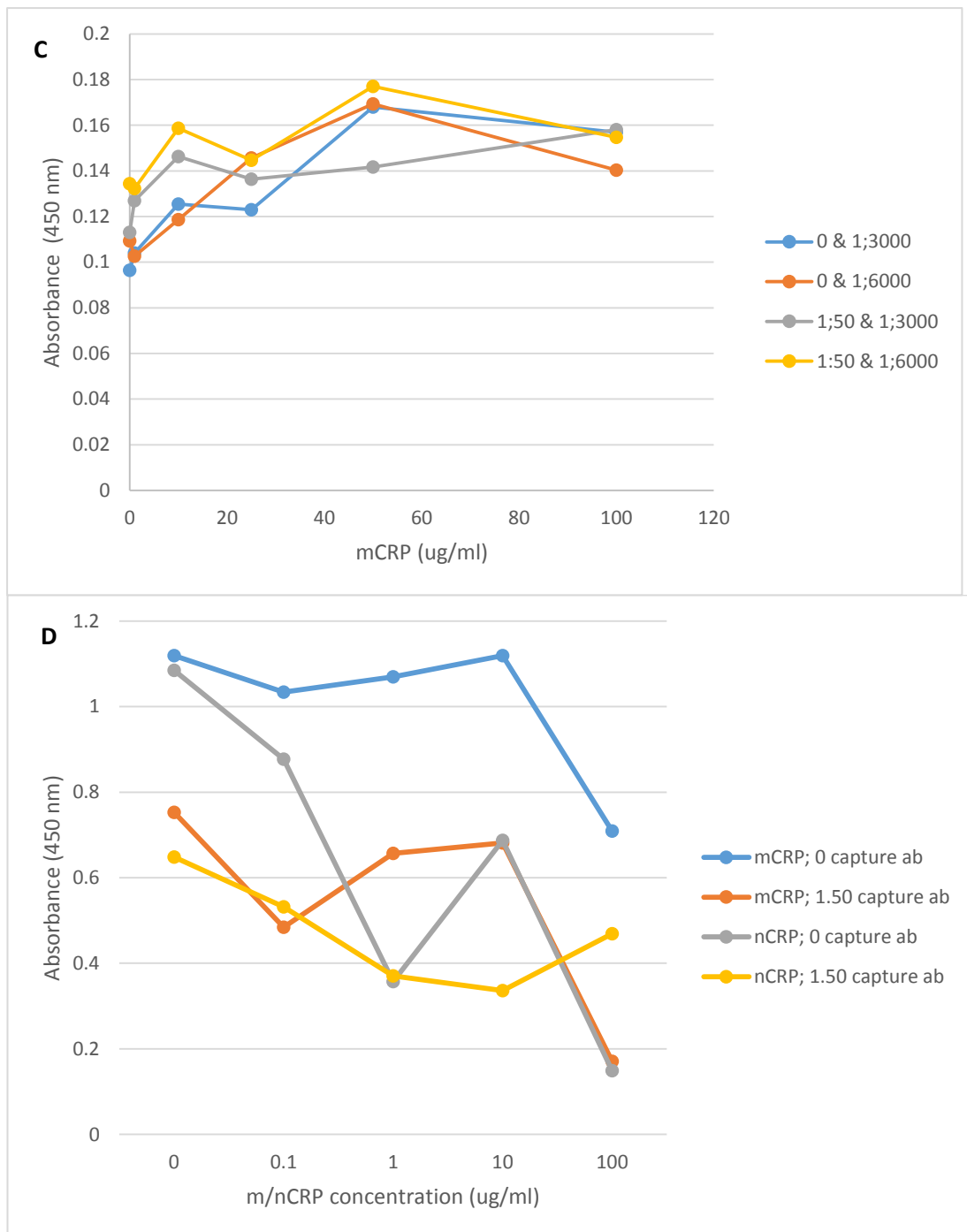


**Figure 3.2.3** Poor repeatability of the mCRP ELISA with ab19175. A), B) and C) all show the same protocol repeated on three separate days in consecutive weeks. Legends denote capture antibody and detection antibody concentrations, respectively. D) shows cross-reactivity between pCRP and the 8C10 mCRP antibody. The curves also have a clear downward trend as the standard concentrations increase. Legend denotes CRP isoform; 8C10 antibody concentration, respectively.

### 3.3 Summary of the immunoassay development

The above analyses show the attempt at immunoassay development for the determination of mCRP in serum. The aim was to create an immunoassay analytically sensitive enough to use in clinical diagnoses. A competitive immunoassay was first developed, which was not sensitive or reliable enough to be used in diagnoses. Therefore, it was decided that an ELISA would be attempted as its design allows higher sensitivity. However, the same problems remained and the major theme for the assay was high intra- and interassay variability that rendered the assay clinically unusable. This is hypothesised to be down to:

- Poor antibody source
- The hydrophobicity and short half-life of mCRP outside of high pH
- mCRP's association with:
  - BSA
  - Milk protein
  - ELISA plate wells
  - Other mCRP monomers

From the evidence shown, the most limiting factor was the poor antibody. The assumed functional sensitivity of 2 µg/ml is far above concentrations found systemically and it became clear that any adaptation to the assay, apart from a more sensitive antibody, would not improve the assay's performance. Therefore, the development was discontinued.

## **Chapter 4: Diagnosis of NSTEMI with non-kinetic cTn values**

#### 4.1 Baseline characteristics of included patients

The baseline characteristics of the 724 patients included in the study are displayed in Table 4.1. AMI was the adjudicated diagnosis in 75 patients (10%). The average time between symptom onset and assessment was 4.5h. After a follow-up period of 42 days there were 6 (0.8%) deaths, 3 (4%) in the group adjudicated with AMI (all 3 of AMI) and 3 (0.4%) in the group who were not adjudicated with AMI (1 of carcinomatosis from the lung, 1 of colon cancer and 1 not recorded).

**Table 4.1 Baseline characteristics of the patients**

Variable	Total (n = 724)	AMI (n = 75)	No AMI (n = 645)	p value
Age (mean, 95% CI)	55.5 (54.4 – 56.7)	62.3 (59.0 – 65.6)	54.7 (53.5 – 55.8)	< 0.001
Sex, male (%)	439 (60.6)	49 (65.3)	388 (645)	0.385
Prior myocardial infarction (%)	175 (24.2)	22 (29.3)	152 (23.6)	0.269
Previous angina (%)	193 (26.7)	22 (29.3)	169 (26.2)	0.561
Prior coronary intervention (%)	141(19.5)	16 (21.3)	124 (19.2)	0.662
Previous hypertension (%)	325 (44.8)	43 (57.3)	281 (43.6)	0.023
Previous hyperlipidaemia (%)	264 (36.5)	42 (56)	222 (34.4)	< 0.001
Current smoker (%)	157 (21.7)	25 (33.3)	132 (20.5)	0.011
ECG ischaemia (%)	58 (8.1)	10 (13.3)	48 (7.4)	0.076
Prior CABG (%)	46 (6.4)	6 (8)	38 (5.9)	0.471
Diabetes mellitus (%)	9 (1.2)	2 (2.7)	7 (1.1)	0.245
Chronic kidney disease (%)	26 (3.6)	9 (12)	16 (2.2)	< 0.001
H-FABP positive (%)	88 (12.2)	12 (16.0)	63 (9.8)	0.291



#### 4.2 Baseline cTn levels of AMI and no AMI groups

Baseline levels of cTn were higher in patients adjudicated with AMI than those who were not as shown in Figure 4.2. In the AMI group, baseline cTn concentrations for the Roche, Singulex and iSTAT assays were 201.92 pg/ml  $\pm$  46.9 (95% CI 121.1 – 305.3), 523.61 pg/ml  $\pm$  206.1 (95% CI 196.4 – 995.9) and 452.4 pg/ml  $\pm$  132.8 (CI 95% 243.8 – 738.6), respectively. Baseline cTn concentrations of patients without AMI for the Roche, iSTAT and Singulex assays were 8.00 pg/ml  $\pm$  10.1 (95% CI 7.2 – 8.8), 38.6 pg/ml  $\pm$  438.4 (95% CI 12.3 – 76.6) and 73.44 pg/ml  $\pm$  1550.4 (95% CI 18.3 – 2680.2), respectively. At baseline, the mean difference between these groups for the Roche assay was 193.92 pg/ml  $\pm$  47.0 (95% CI 100.2 – 287.6;  $p > 0.001$ ) for the Singulex assay was 484.92 pg/ml  $\pm$  215.9 (95% 54.6 – 915.2;  $p = 0.028$ ) and for the iSTAT was 377.4 pg/ml  $\pm$  145.8 (95% CI 88.5 – 666.3;  $p = 0.011$ ).

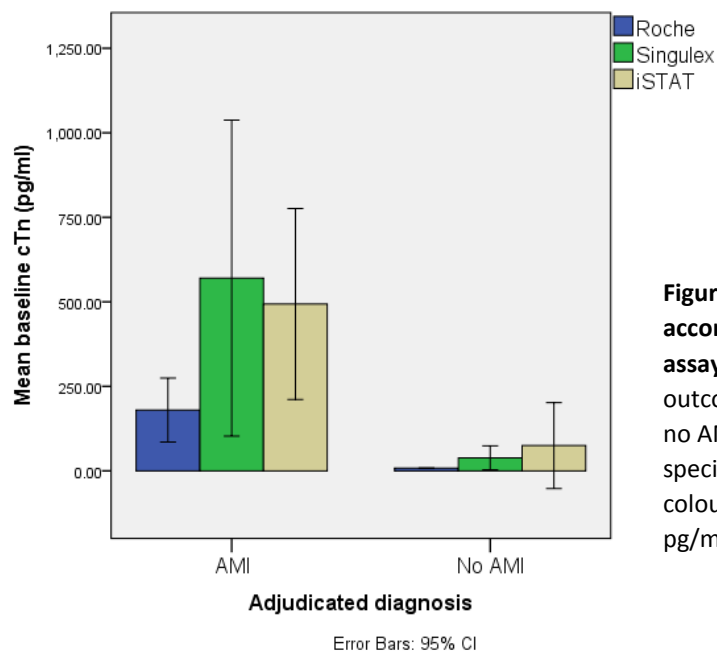


**Figure 4.2 Mean baseline cTn concentrations according to the Roche, Singulex and iSTAT assays.** Bars are clustered by whether an outcome has occurred or not occurred (AMI and no AMI). Bars include results from one assay, as specified by the legends and are assorted by colours. The y-axis shows mean baseline cTn in pg/ml. Error bars indicate 95% CI.

### 4.3 Distribution of cTn 0h and 3h values

For the Roche assay (figure 4.3), the majority of the 0h no AMI samples are to be found between 0 – 100 pg/ml (99.8%) with very little spread across 100 – 1000 pg/ml (0.2% 100 – 200 pg/ml). The majority of the AMI 0h samples are also found in the 0 – 100 pg/ml group but not to the same degree (65.7%) and the frequencies in other groups is higher (19.4% in 100 – 200 pg/ml; 10.4% in 200 – 300 pg/ml; 4.5% at  $\geq 300$  pg/ml). A similar pattern is visible in the 3h samples (0 – 100 pg/ml, 99.8% for no AMI, 67.7% for AMI) but with more spread in the AMI group as more consistent frequencies are seen at higher concentrations (12.3% in 100 – 200 pg/ml; 4.6% 200 – 300 pg/ml; 1.5% for each bin thereafter apart from 800-900 pg/ml, binned every 100 pg/ml).

As with the Roche assay, the majority of the 0h samples according to the Singulex assay (figure 4.3) are found in the lowest concentration bin of 0 – 100 pg/ml (no AMI 98%; AMI 72.1%). There are more consistent frequencies of samples above 100 pg/ml for the 0h AMI samples (7.5% in 100 – 200 pg/ml; 6% in 200 – 300 pg/ml and 3% each in 400 – 500, 500 – 600 and 600 - 700 pg/ml). The 3h no AMI include 99.1% < 100 pg/ml and AMI samples have more patients with higher concentrations, 65.6% at < 100 pg/ml 7.8% in 100 – 200 pg/ml, 3.2% in 200 – 300 pg/ml, 9.4% in 400 – 500 pg/ml and 4.7% in 600 – 700 pg/ml.

The iSTAT assay (figure 4.3) also follows the pattern on the two assays above. For the 0h no AMI and AMI groups there measured 100% and 65.7% < 100 pg/ml .The AMI group showed consistent frequencies from 100 pg/ml onwards (5.9% in 100 – 200 pg/ml; 4.4% in 200 – 300 pg/ml; 2.9% in 300 – 400 pg/ml; 7.3% in 400 – 700

pg/ml and 1.5% in 900 – 1000 pg/ml). This was not seen in the 3h samples where all samples were included < 100 pg/ml.

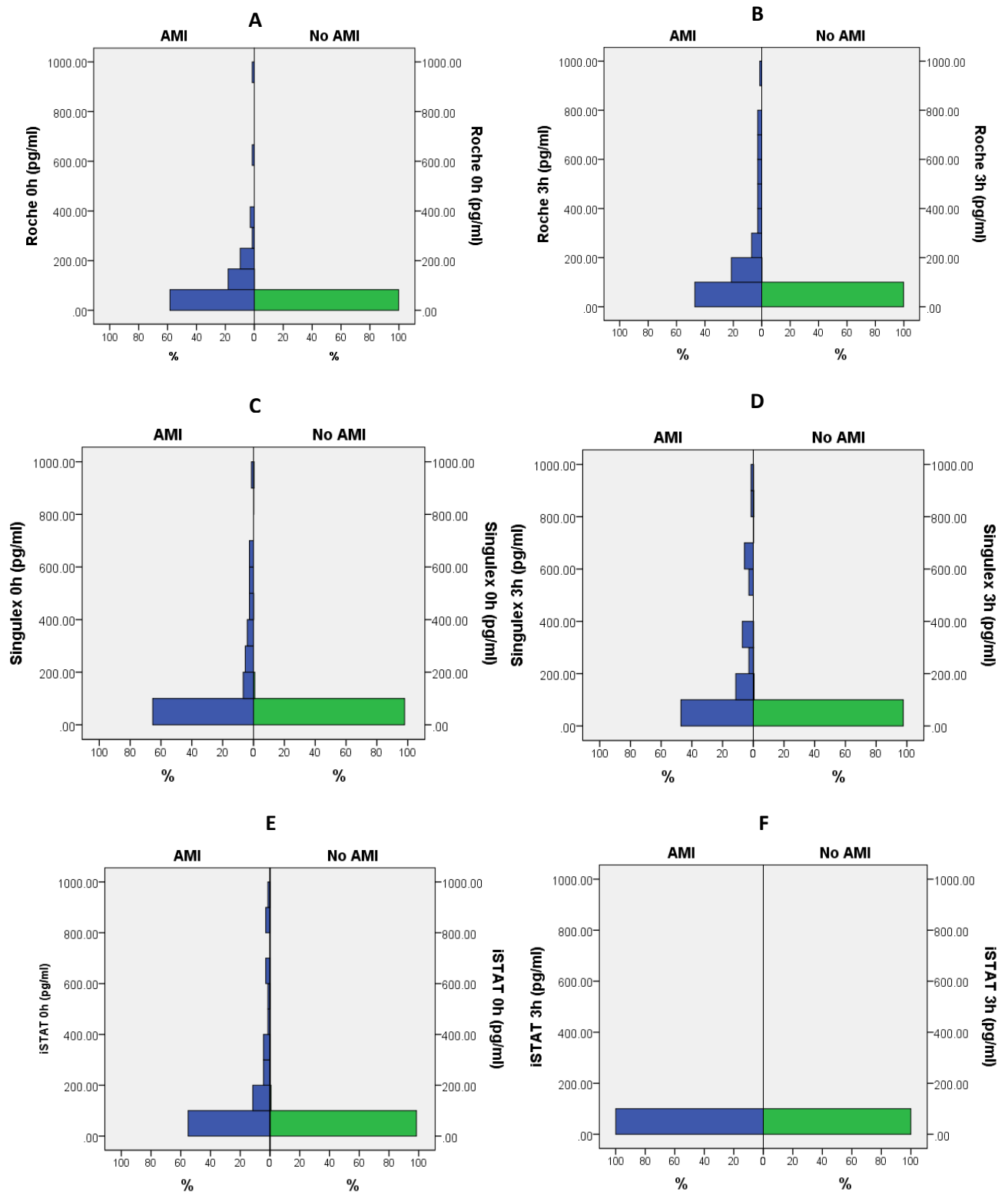


**Figure 4.3** Distribution in histograms of cTn values in AMI and no AMI groups according to the Roche, Singulex and iSTAT assays. A) Roche 0h B) Roche 3h C) Singulex 0h D) Singulex 3h E) iSTAT 0h F) iSTAT 3h. AMI groups (left) are in blue and no AMI groups (right) are shown in green. Distribution is shown as percentage cohort per 100 pg/ml from 0 – 1000 pg/ml.

#### 4.4 Diagnostic accuracy of 0h, 3h and maximum values of cTn for AMI diagnosis

The aim of these analyses was to determine a cut-off that produced 100% sensitivity for rule out diagnoses. The diagnostic accuracy of the iSTAT assay at 0h is higher than that of the Roche and Singulex assays (AUC 0.518, 95% CI 0.444 – 0.592 for Roche assay; AUC 0.84, 95% CI 0.791 – 0.908 for the Singulex assay; AUC 0.890, 95% 0.837 – 0.943 for the iSTAT) (figure 4.4).

As seen in table 4.4, the 0h cut-offs for the Roche, Singulex and iSTAT assays at 5.03, 0.8550 and 10 resulted in sensitivities of 48.5%, 100.0% and 46.0%, of which the Singulex was significantly more clinically sensitive ( $p < 0.001$ ). The number of patients below the cut-off is higher when using the Roche or iSTAT assays but the clinical sensitivities of these assays are significantly lower in comparison to the Singulex assay (48.5%, 47.1%, 51.5%; 100.0%, 97.3%, 100.0%; 46.0%, 65.1%, 57.1%, all assays  $p < 0.001$  for the 0h, 3h and max values of the Roche, Singulex and iSTAT, respectfully).

The Singulex assay produced sensitivities and NPVs for 0h and max values at 100% but the 3h was lower at 97.3% (95% CI 90.6 – 100.0) and 96.4% (95% CI 86.8 – 99.0), respectively (0h vs 3h  $p = 0.542$ ; 3h vs max  $p < 0.001$ ).

The iSTAT assay produced very high specificities (0h: 98.7%, 95% CI 97.2 – 99.5, 3h: 99.2%, 95% CI 98.0 – 99.8, max values: 98.3%, 95% CI 96.7 – 99.2) and with high PPVs (80.6%, 95% CI 65.4 – 90.1, 91.1%, 95% CI 79.2 – 96.5 and 80.0%, 95% CI 66.9 – 88.8, respectively).

Using the max cTn values from the baseline or 3h samples produced a higher cut-off, 1.3450 pg/ml, with 30% of patients below cut-off with 100% sensitivity.

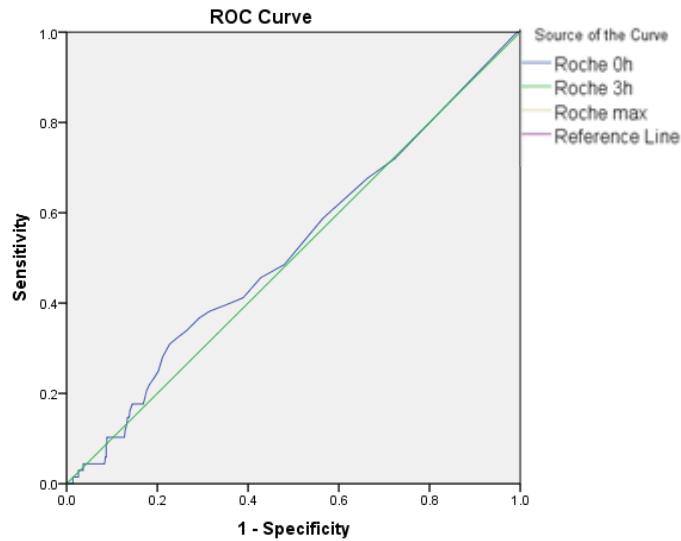


**Figure 4.4 ROC curve of cTn 0h, 3h and max values according to the Roche, Singulex and iSTAT assays for 30-day composite MACE.** Each graph represents the results from one assay. Each line within the graphs represents the ROC curve associated with either 0h, 3h or maximum values, as specified in the legends. A) Roche assay curves; B) Singulex assay curves; C) iSTAT assay curves. 0h: 0h cTn; 3h: 3h cTn; max: maximum value from 0h and 3h cTn samples.

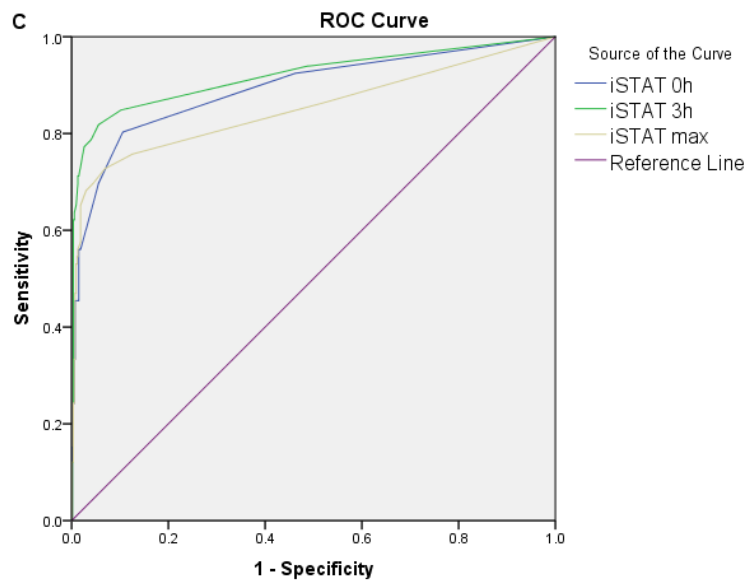
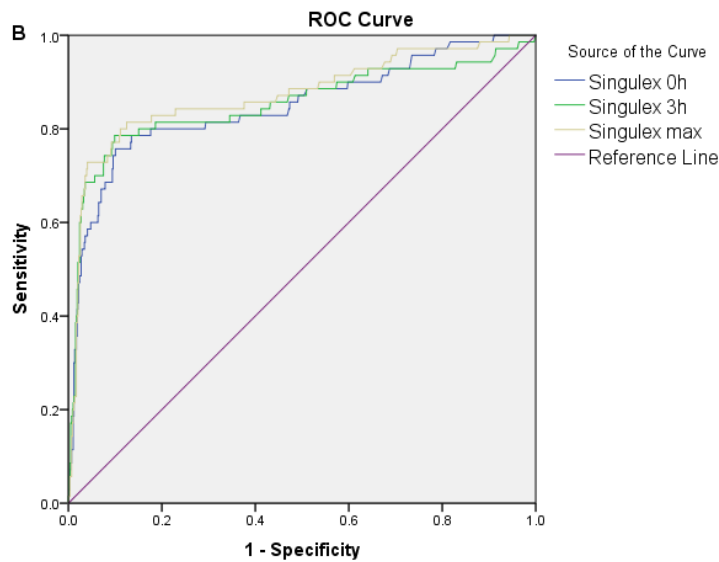


**Table 4.4 Diagnostic accuracy of 0h, 3h and max cTn values for AMI diagnosis**

	AUC (95% CI)	P	Cut-off (pg/ml)	Patients below cut-off (%)	Sensitivity	Specificity	PPV	NPV
<i>Roche</i>								
<b>0h</b>	0.518 (0.444 – 0.592)	< 0.001	5.03	51	48.5 (36.2 – 61.0)	51.9 (47.7 – 56.0)	10.8 (8.5 – 13.5)	89.4 (86.8 – 91.5)
<b>3h</b>	0.480 (0.406 – 0.554)	< 0.001	5.03	52	47.1 (34.8 – 59.6)	49.0 (44.8 – 53.2)	10.0 (7.8 – 12.6)	88.5 (85.9 – 90.8)
<b>Max</b>	0.547 (0.466 – 0.628)	< 0.001	5.03	49	51.5 (39.0 – 63.9)	46.0 (41.9 – 50.2)	10.3 (8.2 – 12.7)	88.9 (85.9 – 91.1)
<i>Singulex</i>								
<b>0h</b>	0.849 (0.791 – 0.908)	< 0.001	0.8550*	21	100.0 (95.3 – 100.0)	23.4 (20.2 – 26.9)	13.5 (13.0 – 14.0)	100.0
<b>3h</b>	0.853 (0.790 – 0.916)	< 0.001	0.53	9	97.3 (90.6 – 100.0)	9.0 (6.9 – 11.7)	11.9 (11.4 – 12.4)	96.4 (86.8 – 99.0)
<b>Max</b>	0.874 (0.819 – 0.928)	< 0.001	1.3450*	30	100.0 (95.1 – 100.0)	5.3 (3.6 – 7.5)	11.8 (11.6 – 12.0)	100.0
<i>iSTAT</i>								
<b>0h</b>	0.890 (0.837 – 0.943)	< 0.001	100*	94	46.0 (33.4 – 59.1)	98.7 (97.2 – 99.5)	80.6 (65.4 – 90.1)	93.8 (92.3 – 95.0)
<b>3h</b>	0.918 (0.868 – 0.968)	< 0.001	100*	92	65.1 (52.0 – 76.7)	99.2 (98.0 – 99.8)	91.1 (79.2 – 96.5)	95.9 (94.4 – 97.0)
<b>Max</b>	0.858 (0.792 – 0.923)	< 0.001	100*	94	57.1 (44.1 – 69.5)	98.3 (96.7 – 99.2)	80.0 (66.9 – 88.8)	95.0 (93.4 – 96.2)

Cut-offs were determined by the concentration the assay exhibits <10% CV. Starred (\*) values are ROC-derived cut-offs.

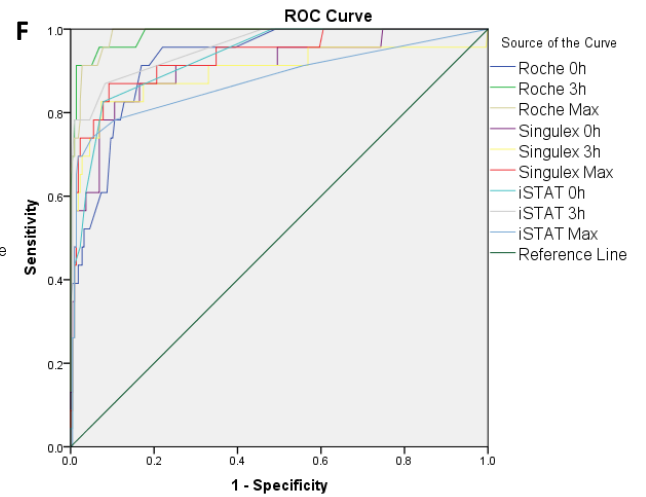
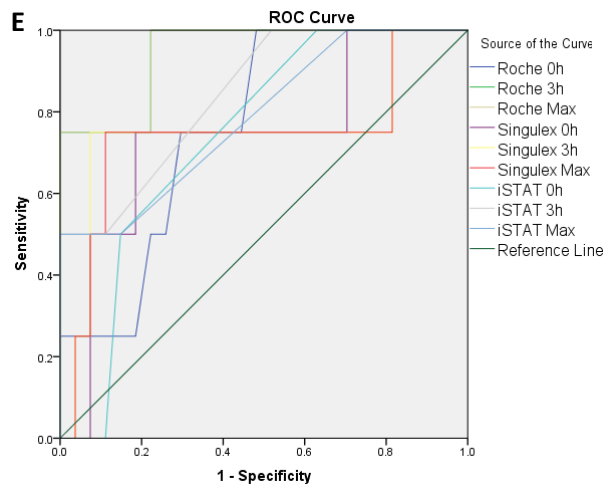
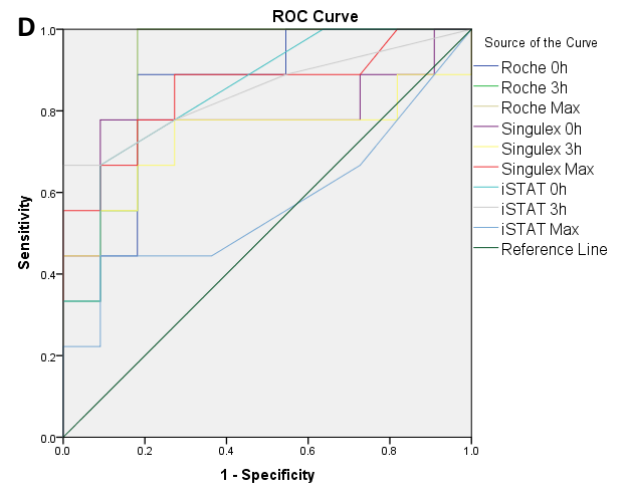
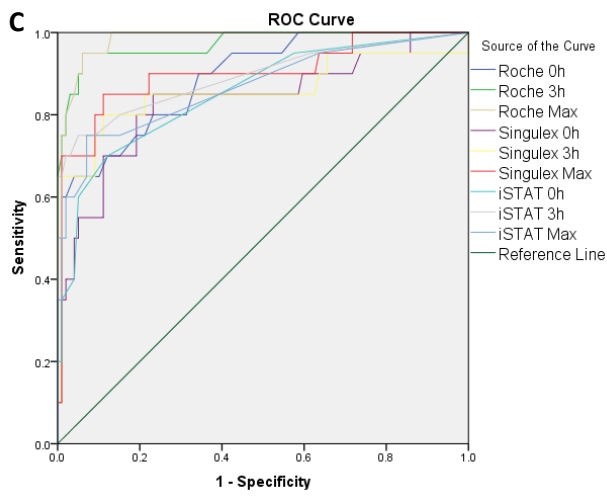
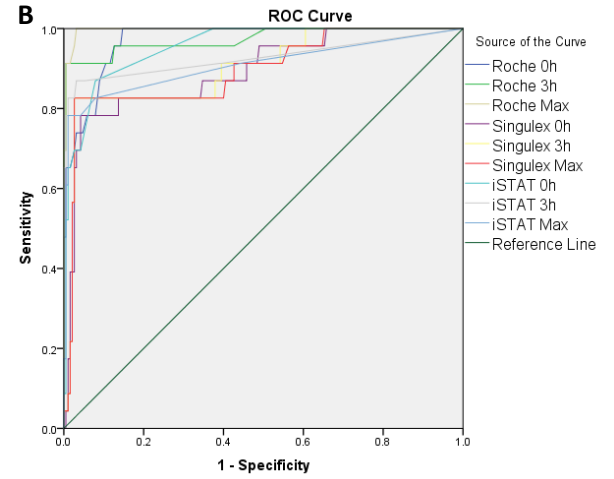
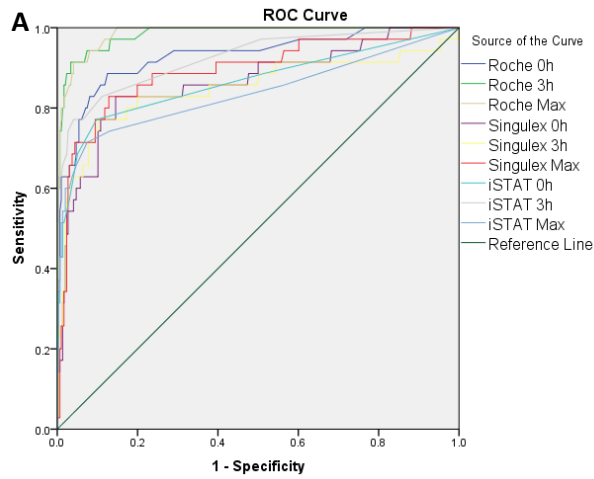
#### 4.5 Diagnostic accuracy of 0h, 3h and max cTn values in important patient subgroups

The results of the overall diagnostic accuracy of the different assays in important patient subgroups are shown in table 4.5 and ROC curves in figure 4.5. Patients with rheumatoid arthritis were also analysed for the diagnostic accuracy of that subgroup according to the three assays but only 2 events were recorded and therefore a reliable ROC curve could not be constructed. The Roche assay had the highest AUC per subgroup across the three assays. There was little difference in AUC between 0h, 3h and max values for each of the assays. The diagnostic accuracy for females was greater than for males across all assays and the max values in female subgroup according to Roche had the highest AUC (0.997). The AUC between the three TSSO groups did not change depending on time elapsed between symptom onset and assessment but max values AUC were higher than 0h and 3h AUC for each TSSO group within assays. The iSTAT assay reported a very low AUC for the 0h TSSO  $\geq$  6h curve with a wide 95% CI (0.564, 95% CI 0.389 – 0.738).

**Table 4.5 Diagnostic accuracy of absolute and relative cTn deltas in patient subgroups using ROC curve analysis**

	n	Roche			Singulex			iSTAT		
		0h	3h	Max	0h	3h	Max	0h	3h	Max
<b>Male</b>	437	0.930	0.984	0.985	0.864	0.848	0.892	0.864	0.924	0.836
<b>Female</b>	285	0.972	0.973	0.997	0.893	0.900	0.895	0.955	0.927	0.908
<b>Elderly (<math>\geq 70</math> y)</b>	151	0.891	0.972	0.985	0.834	0.855	0.901	0.853	0.892	0.867
<b>Renal failure</b>	30	0.848	0.899	0.899	0.788	0.737	0.854	0.848	0.848	0.571
<b>Stroke</b>	40	0.764	0.944	0.944	0.741	0.750	0.741	0.741	0.843	0.787
<b>TSSO &lt; 3h</b>	308	0.927	0.987	0.988	0.906	0.895	0.933	0.932	0.955	0.877
<b>TSSO 3h <math>\leq</math> x &lt; 6h</b>	153	0.988	0.958	0.996	0.804	0.782	0.832	0.930	0.944	0.873
<b>TSSO <math>\geq</math> 6h</b>	164	0.978	0.984	0.991	0.869	0.875	0.867	0.564	0.834	0.906

0h: cTn value at 0h; 3h: cTn value at 3h; Max: maximum cTn value from 0h and 3h samples; TSSO: time since symptom onset





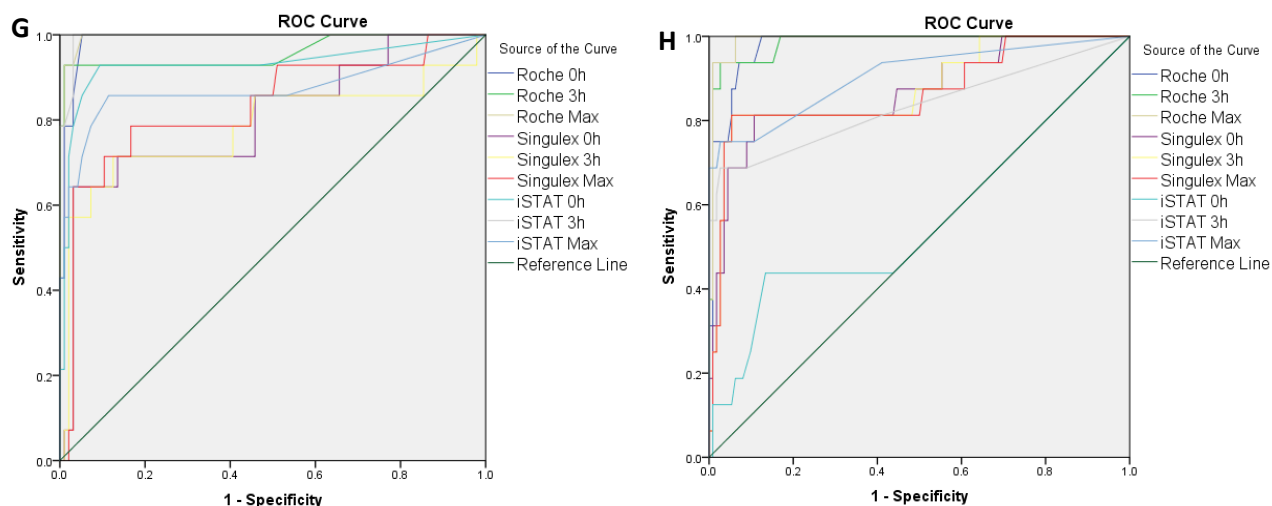


**Figure 4.5 ROC curves for the diagnostic accuracy of 0h, 3h and max values of the Roche, Singulex and iSTAT assays for AMI diagnosis in important patient subgroups. A) male subgroup; B) female subgroup; C) elderly subgroup; D) renal subgroup; E) stroke subgroup; F) < 3h TSSO subgroup; G)  $3h \leq x < 6h$  TSSO subgroup; H) > 6h TSSO subgroup. 0h: 0h cTn sample; 3h: 3h cTn sample; max: maximum value from the 0h and 3h samples.**

#### 4.6 Summary of the diagnosis of NSTEMI with non-kinetic cTn values

The above analyses show an approach for safe cut-off for AMI rule out. hs-cTn

assays can detect cTn in 50% of the healthy population and therefore finding a safe cut-off is necessary. The LoDs of the assays or ROC-derived cut-offs were used as thresholds. The diagnostic accuracy of cTn by the Roche, Singulex and iSTAT assays were observed to assess if patients at low- to no risk of developing AMI could be identified. These showed:

- Singulex assay could rule out AMI from a baseline value with 100% sensitivity
- iSTAT assay has a high specificity and therefore a good candidate for fast rule in, due to its high FS
- Roche assay was an appropriate intermediate and for subgroups
- Higher thresholds will rule out more patients safely and reduce the number of false positives

The different FS of the assays dictated the performance of the assays and showed an important compromise in this cohort:

- A low enough threshold can confidently rule out 100% of patients but will increase the number of false positives
- A higher threshold can rule in patients more confidently but will increase the number of false negatives

## **Chapter 5: Diagnosis of NSTEMI with kinetic cTn deltas**

The baseline characteristics of the cohort are found at the beginning of chapter 2, diagnosis of NSTEMI using cTn values of the Roche, Singulex and iSTAT assays.

### 5.1 Mean $\Delta_{\text{absolute}}$ according to the Roche, Singulex and iSTAT assays

The  $\Delta_{\text{absolute}}$  of cTn between 0h and 3h were significantly different between AMI patients and non-AMI patients across all assays (figure 5.1). The mean  $\Delta_{\text{absolute}}$  in the AMI and no AMI groups for the Roche assay were  $111.06 \text{ pg/ml} \pm 22.0$  (95% CI 71.5 – 157.7) and  $1.1 \pm 0.1$  (95% CI 1.0 – 1.3), respectively. The mean difference between these groups for the Roche assay was  $109.93 \pm 7.5$  (95% CI 95.3 – 124.6;  $p > 0.001$ ). For the Singulex assay, the  $\Delta_{\text{absolute}}$  means were  $649.26 \pm 250.1$  (95% CI 285.2 – 1243.9) and  $51.4 \pm 25.0$  (95% CI 9.7 – 107.7) for the AMI and no AMI groups yielding a mean difference of  $597.8 \pm 243.3$  (95% CI 112.3 – 639.3;  $p = 0.017$ ). The  $\Delta_{\text{absolute}}$  means of the iSTAT results were  $525.97 \pm 172.5$  (95% CI 223.7 – 880.2) for the AMI and no AMI groups, which gave a mean difference of  $513.88 \pm 181.1$  (95% 152.5 – 875.3;  $p = 0.006$ ).

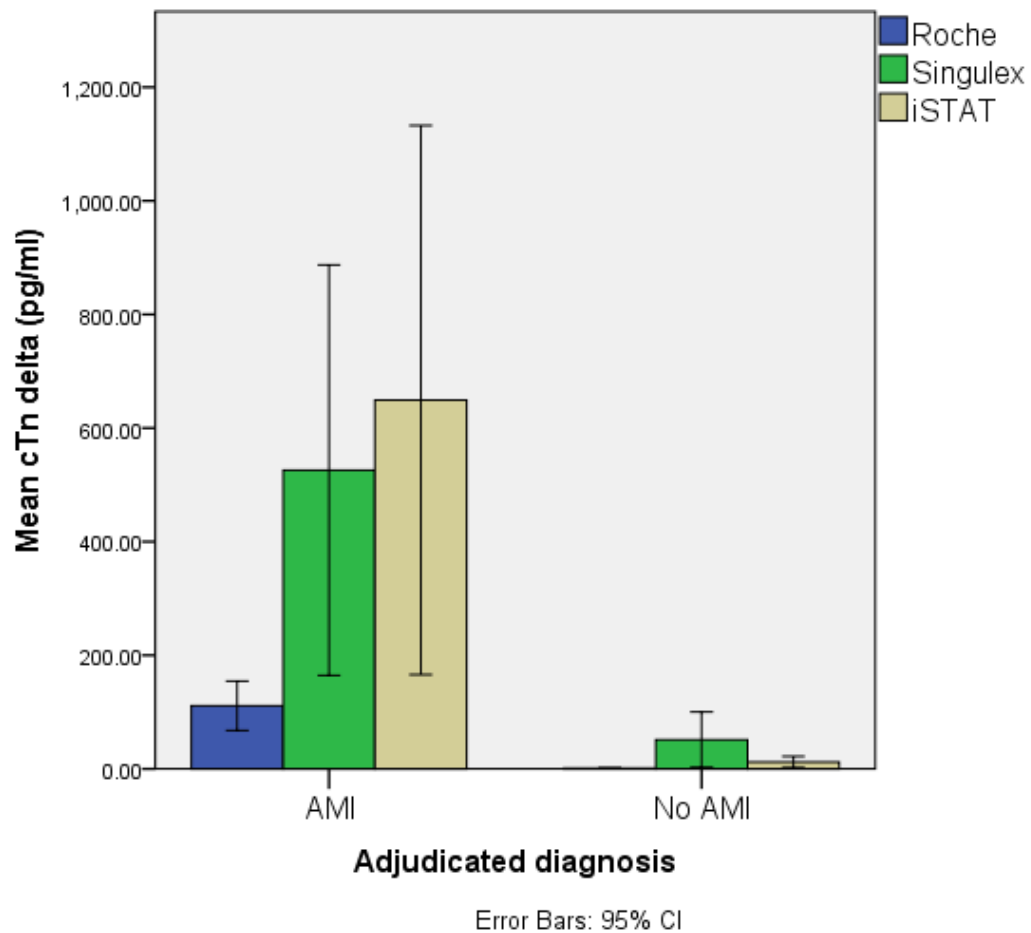


**Figure 5.1 Mean  $\Delta_{\text{absolute}}$  cTn concentrations according to the Roche, Singulex and iSTAT assays.** Bars are clustered by whether an outcome has occurred or not occurred (AMI and no AMI). Bars include results from one assay, as specified by the legends and are assorted by colours. The y-axis shows mean baseline cTn in pg/ml. Error bars indicate 95% CI.

## 5.2 Mean $\% \Delta_{\text{baseline}}$ according to the Roche, Singulex and iSTAT assays

The mean  $\% \Delta_{\text{baseline}}$  according to the different assays are seen in figure 5.2. The absolute relative delta to baseline ( $\% \Delta_{\text{baseline}}$ ) of cTn between AMI and non-AMI groups were significant for the Roche and iSTAT assays but not for the Singulex assay. The mean  $\% \Delta_{\text{baseline}}$  according to the Roche assay for the AMI group is  $320.11\% \pm 194.2$  (95% CI 99.6 – 783.5) and  $19.12\% \pm 2.2$  (95% CI 15.2 – 23.9) in the no AMI group giving a mean difference of  $301.00\% \pm 36.8$  (95% CI 171.7 – 430.3;  $p < 0.001$ ). The means for the AMI and no AMI groups according to the Singulex assay are  $266.1\% \pm 57.6$  (95% CI 164.2 – 391.1) and  $259.7\% \pm 214.7$  (95% CI 54.8 – 735.1), respectively, with a mean difference of  $6.34\% \pm 182.2$  (95% CI -351.6 – 364.3;  $p = 0.972$ ). The iSTAT reported means of  $474.4 \pm 214.7$  (95% CI 175.5 – 943.5) and  $46.8 \pm 13.3$  (95% CI 29.5 – 75.9) for the AMI and no AMI groups, respectively, with a mean difference of  $427.6 \pm 85.5$  (95% CI 259.7 – 595.5;  $p = 0.056$ ).

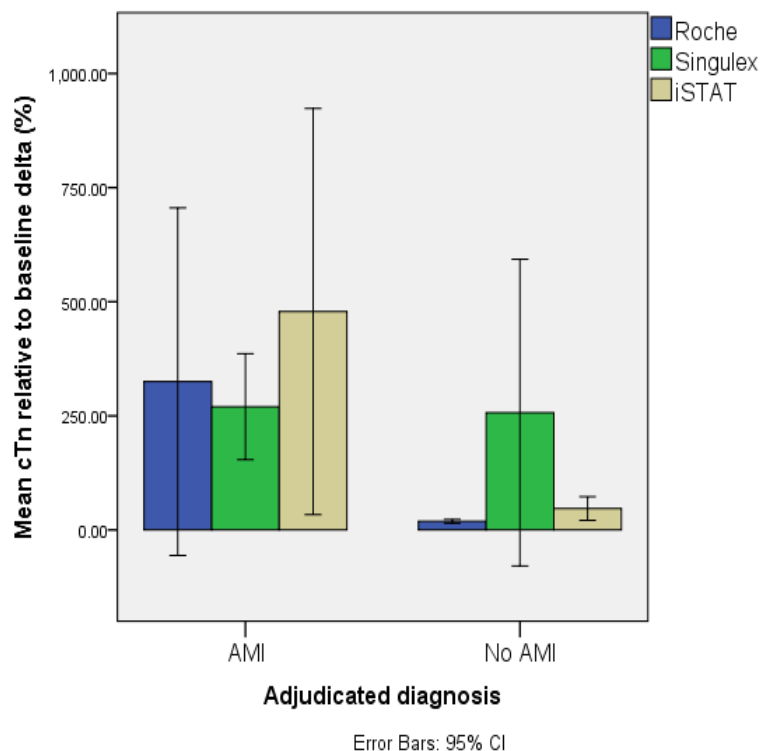


**Figure 5.2 Mean  $\% \Delta_{\text{baseline}}$  cTn concentrations according to the Roche, Singulex and iSTAT assays.** Bars are clustered by whether an outcome has occurred or not occurred (AMI and no AMI). Bars include results from one assay, as specified by the legends and are assorted by colours. The y-axis shows mean  $\% \Delta_{\text{baseline}}$ . Error bars indicate 95% CI.

### 5.3 Mean $\% \Delta_{\text{mean}}$ according to the Roche, Singulex and iSTAT assays

The mean  $\% \Delta_{\text{mean}}$  according to the Roche, Singulex and iSTAT assays are shown in figure 5.3. The absolute relative delta to mean ( $\% \Delta_{\text{mean}}$ ) of cTn between AMI and no AMI groups were significantly different according to the results of each assay. The Roche assay reported means of the AMI and no AMI groups as  $64.5\% \pm 6.5$  (95% CI 52.7 – 77.8) and  $16.9\% \pm 1.3$  (95% CI 14.3 – 19.4), respectively, with a mean difference of  $47.6\% \pm 6.7$  (95% CI 34.2 – 60.9;  $p < 0.001$ ). For the Singulex assay, the means were  $77.6\% \pm 8.3$  (95% CI 62.9 – 96.8) and  $36.5\% \pm 1.9$  (95% CI 32.9 – 40.2) for the AMI and no AMI groups, which yielded a mean difference of  $41.1\% \pm 8.6$  (95% CI 24.0 – 58.2;  $p < 0.001$ ). The iSTAT assay reported means of  $83.3\% \pm 9.0$  (95% CI 67.1 – 101.8) and  $56.9\% \pm 4.1$  (95% CI 48.4 – 64.8) for the AMI and no AMI groups that produced a mean difference of  $26.4\% \pm 9.9$  (95% CI 6.8 – 46.1;  $p = 0.009$ ).

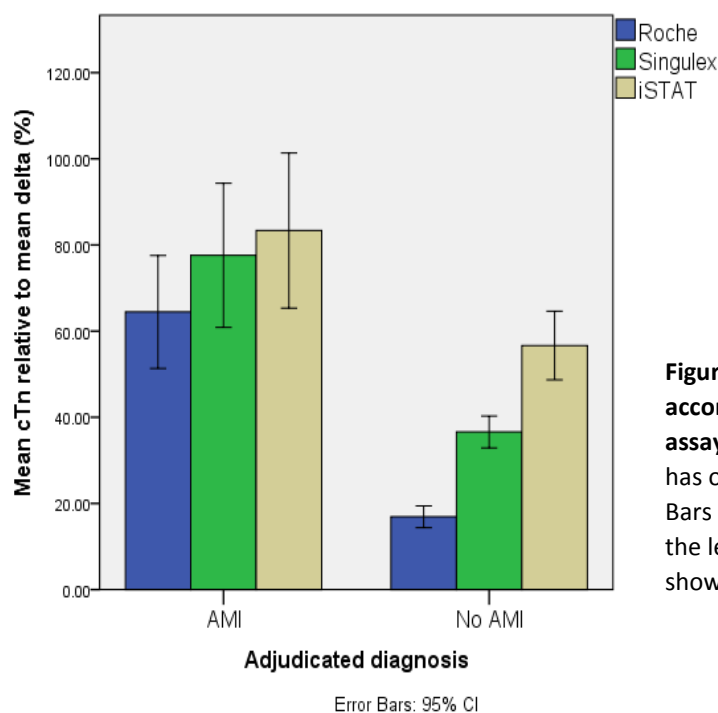


**Figure 5.3 Mean  $\% \Delta_{\text{mean}}$  cTn concentrations according to the Roche, Singulex and iSTAT assays.** Bars are clustered by whether an outcome has occurred or not occurred (AMI and no AMI). Bars include results from one assay, as specified by the legends and are assorted by colours. The y-axis shows mean  $\% \Delta_{\text{mean}}$ . Error bars indicate 95% CI.

#### 5.4 Distribution of cTn $\Delta_{\text{absolute}}$ , $\% \Delta_{\text{baseline}}$ and $\% \Delta_{\text{mean}}$ in AMI and no AMI groups

The distribution of the Roche deltas by AMI and no AMI groups are shown in figure

5.4.1. The vast majority of samples in the no AMI groups for  $\Delta_{\text{absolute}}$ ,  $\% \Delta_{\text{baseline}}$  and  $\% \Delta_{\text{mean}}$  are in the lowest bin of each histogram (100%, 96.1% and 98.1%). The same is true of the AMI group with 73.5%, 55.6% and 75.0% of patients experiencing < 100 pg/ml  $\Delta_{\text{absolute}}$ , < 100%  $\% \Delta_{\text{baseline}}$  and < 20%  $\% \Delta_{\text{mean}}$ , respectively.

The distribution of the Singulex deltas by AMI and no AMI groups are shown in figure 5.4.2. The vast majority of samples in the no AMI groups for  $\Delta_{\text{absolute}}$ ,  $\% \Delta_{\text{baseline}}$  and  $\% \Delta_{\text{mean}}$  are in the lowest bin of each histogram (98.0%, 82.9% and 90.3%). The same is true of the AMI group with 69.1%, 60.9% and 64.3% of patients experiencing < 100 pg/ml  $\Delta_{\text{absolute}}$ , < 100%  $\% \Delta_{\text{baseline}}$  and < 20%  $\% \Delta_{\text{mean}}$ , respectively.

The distribution of the iSTAT deltas by AMI and no AMI groups are shown in figure 5.4.3. The vast majority of samples in the no AMI groups for  $\Delta_{\text{absolute}}$ ,  $\% \Delta_{\text{baseline}}$  and  $\% \Delta_{\text{mean}}$  are in the lowest bin of each histogram (100%, 72.3% and 73.2%). The same is true of the AMI group with 58.8%, 56.5% and 59.1% of patients experiencing < 100 pg/ml  $\Delta_{\text{absolute}}$ , < 100%  $\% \Delta_{\text{baseline}}$  and < 20%  $\% \Delta_{\text{mean}}$ , respectively.



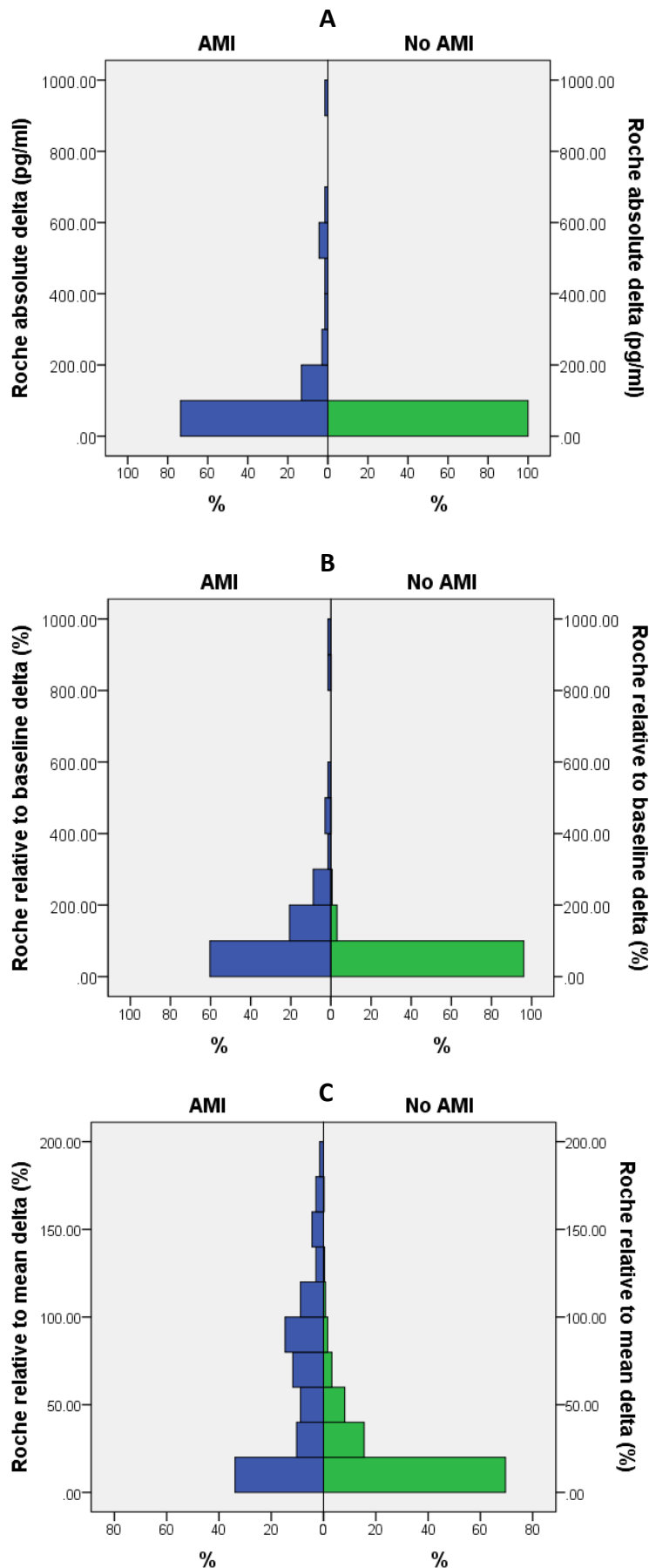


**Figure 5.4.1 Distribution of cTn deltas in AMI and no AMI groups according to the Roche assay.** A) shows the histogram of  $\Delta_{\text{absolute}}$ , B) shows the histogram of  $\% \Delta_{\text{baseline}}$  and C) shows the histogram of  $\% \Delta_{\text{mean}}$ . AMI groups (left) are in blue and no AMI groups (right) are shown in green. Distribution is shown as percentage cohort per 100 pg/ml from 0 – 1000 pg/ml for  $\Delta_{\text{absolute}}$ , 0 – 1000% for  $\% \Delta_{\text{baseline}}$  and 0 – 200% for  $\% \Delta_{\text{mean}}$ .

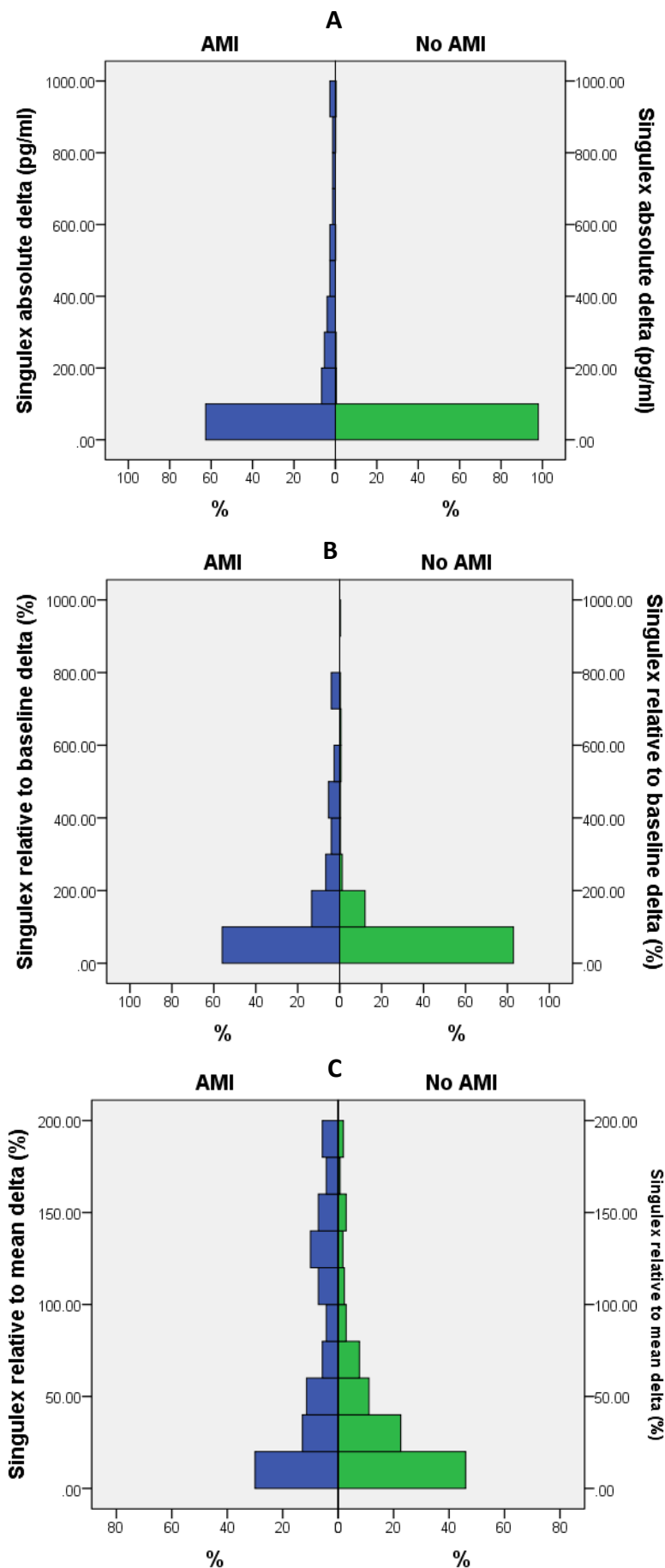


**Figure 5.4.2 Distribution of cTn deltas in AMI and no AMI groups according to the Singulex assay.** A) shows the histogram of  $\Delta_{\text{absolute}}$ , B) shows the histogram of  $\% \Delta_{\text{baseline}}$  and C) shows the histogram of  $\% \Delta_{\text{mean}}$ . AMI groups (left) are in blue and no AMI groups (right) are shown in green. Distribution is shown as percentage cohort per 100 pg/ml for  $\Delta_{\text{absolute}}$ , 0 – 1000% for  $\% \Delta_{\text{baseline}}$  and 0 – 200% for  $\% \Delta_{\text{mean}}$ .

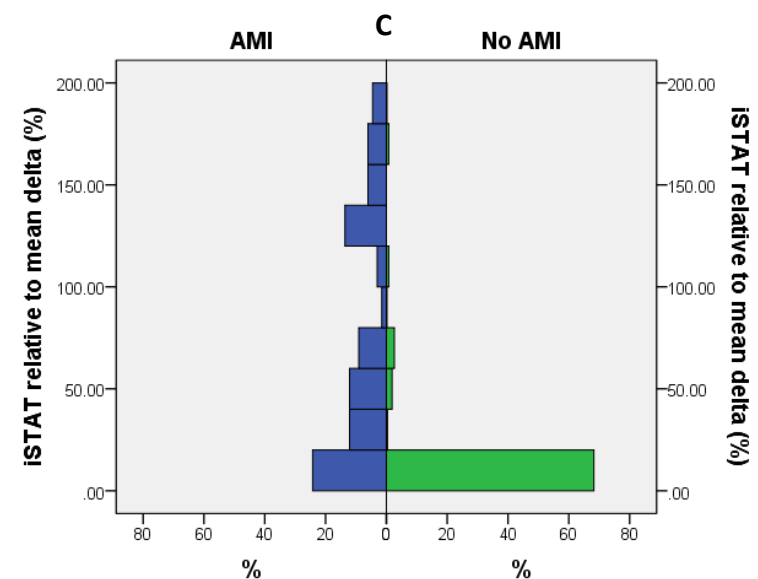
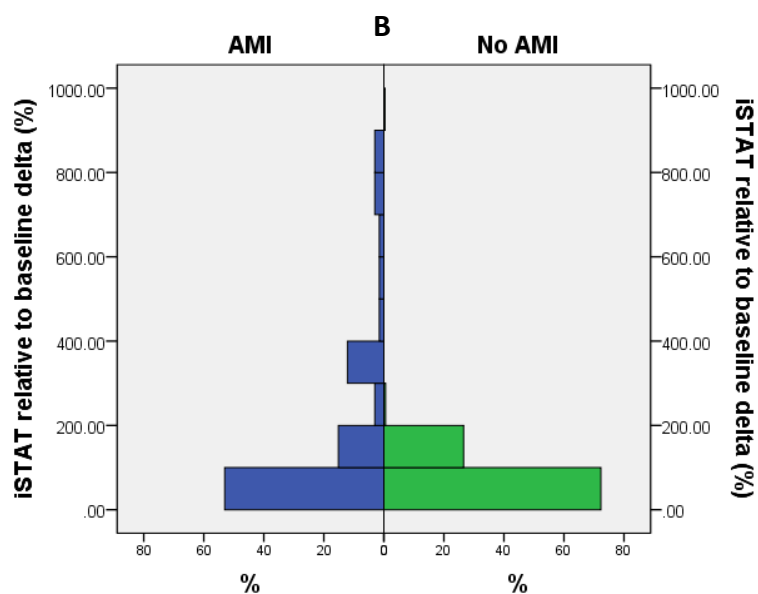
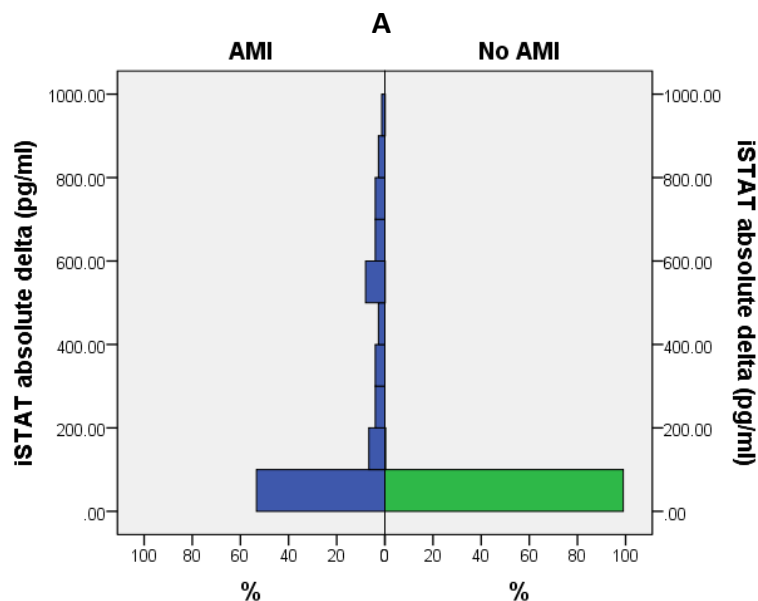


**Figure 5.4.3 Distribution of cTn deltas in AMI and no AMI groups according to the iSTAT assay.** A) shows the histogram of  $\Delta_{\text{absolute}}$ , B) shows the histogram of  $\% \Delta_{\text{baseline}}$  and C) shows the histogram of  $\% \Delta_{\text{mean}}$ . AMI groups (left) are in blue and no AMI groups (right) are shown in green. Distribution is shown as percentage cohort per 100 pg/ml from 0 – 1000 pg/ml for  $\Delta_{\text{absolute}}$ , 0 – 1000% for  $\% \Delta_{\text{baseline}}$  and 0 – 200% for  $\% \Delta_{\text{mean}}$ .

### 5.5 Diagnostic accuracy of cTn $\Delta_{\text{absolute}}$ , $\% \Delta_{\text{baseline}}$ and $\% \Delta_{\text{mean}}$ for AMI diagnosis

The diagnostic accuracy of the three assays for AMI diagnosis is shown in figure 5.5.

The  $\Delta_{\text{absolute}}$  was highest for all assays. For the Roche assay, the AUC for  $\Delta_{\text{absolute}}$ ,  $\% \Delta_{\text{baseline}}$  and  $\% \Delta_{\text{mean}}$  were 0.982 (95% CI, 0.960 – 1.000), 0.824 (95% CI, 0.773 – 0.875) and 0.812 (95% CI, 0.762 – 0.863), respectively. The respective AUC for the Singulex assay were 0.855 (95% CI, 0.795 – 0.915), 0.669 (95% CI, 0.592 – 0.745) and 0.652 (95% CI, 0.577 – 0.727) and for the iSTAT were 0.868 (95% CI, 0.808 – 0.928), 0.763 (95% CI, 0.701 – 0.825) and 0.671 (95% CI, 0.619 – 0.723).

However, the highest sensitivity found for  $\Delta_{\text{absolute}}$  was with the Roche assay at 89.7% (95% CI, 79.9 – 95.8) vs 85.3% (95% CI, 75.3 – 92.4) and 54.0% (95% CI 40.9 – 66.6) for the Singulex and iSTAT assays ( $p < 0.001$ ) (Table 5.5). The highest sensitivity for  $\% \Delta_{\text{baseline}}$  was produced by the Roche assay (98.4%, 95% CI 91.5 – 100.0 for Roche; 97.1%, 95% CI 90.1 – 100.0 for the Singulex; 84.1%, 95% CI 72.7 – 92.1 for the iSTAT,  $p < 0.001$  for all). The sensitivity of the  $\% \Delta_{\text{baseline}}$  and  $\% \Delta_{\text{mean}}$  of the Singulex assay, 97.1% (95% CI 90.1 – 100.0) are significantly different to the  $\Delta_{\text{absolute}}$  sensitivity of 85.3% (95% CI 75.3 – 92.4) at  $p < 0.001$ . The proportion of patients under the cut-offs is lowest in the Singulex assay, 47%, 7% and 7%, respectively, for the  $\Delta_{\text{absolute}}$ ,  $\% \Delta_{\text{baseline}}$  and  $\% \Delta_{\text{mean}}$ , but also has the lowest effective cut-offs at 14%. This is in comparison to 78%, 36% and 41%, and 93%, 62% and 62% of patients under the respective cut-offs of the Roche and iSTAT assays, but the cut-offs must be above 341 pg/ml and 1061 pg/ml, and 66 pg/ml and 67 pg/ml for the  $\% \Delta_{\text{baseline}}$  and  $\% \Delta_{\text{mean}}$  variables, respectfully. The differences in the number of patients ruled out between Roche and the two assays were significant ( $p < 0.001$ ) for all variables.

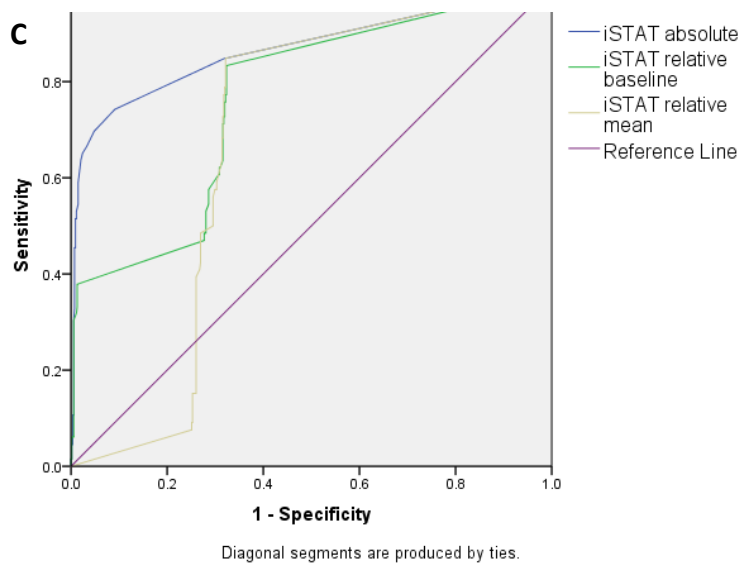
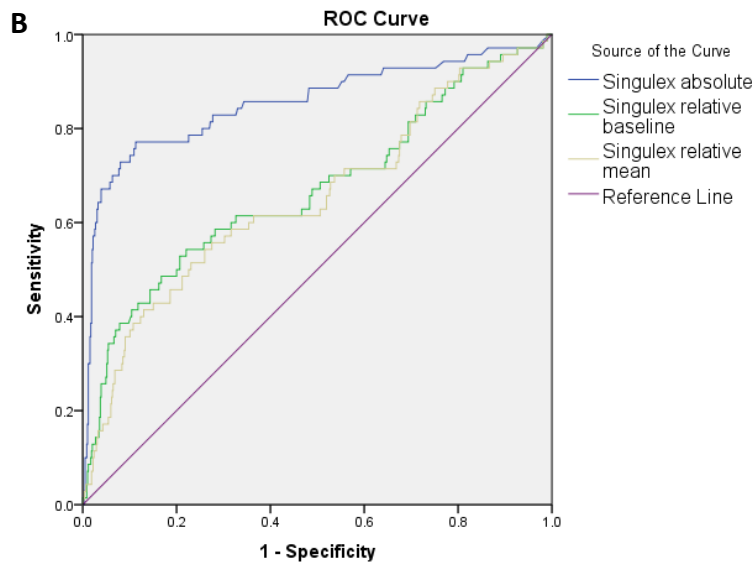
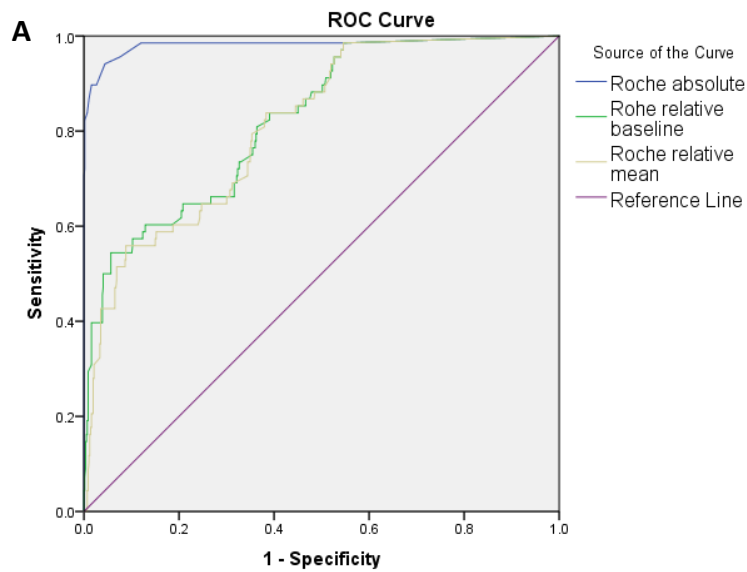


**Figure 5.5 ROC curves of cTn  $\Delta_{\text{absolute}}$ ,  $\% \Delta_{\text{baseline}}$  and  $\% \Delta_{\text{mean}}$  according to the Roche, Singulex and iSTAT assays for AMI diagnosis.** Each graph represents the results from one assay. Each line within the graphs represents the ROC curve associated with either  $\Delta_{\text{absolute}}$ ,  $\% \Delta_{\text{baseline}}$  and  $\% \Delta_{\text{mean}}$ , as specified in the legends. A) Roche assay curves; B) Singulex assay curves; C) iSTAT assay curves. Absolute:  $\Delta_{\text{absolute}}$ ; relative baseline:  $\% \Delta_{\text{baseline}}$ ; relative mean  $\% \Delta_{\text{mean}}$ .

**Table 5.5 AUROC curves for the diagnosis of AMI for cTn  $\Delta_{\text{absolute}}$ ,  $\% \Delta_{\text{baseline}}$  and  $\% \Delta_{\text{mean}}$  after 3 hours from presentation**

	AUC	Cut-off	Patients below cut-off (%)	cTn <sub>low</sub>	Sensitivity	Specificity	PPV	NPV
<i>Roche</i>								
$\Delta_{\text{absolute}}$	0.823 (0.770 – (0.876)	5.03	78	-	89.7 (79.9 – 95.8)	97.4 (95.7 – 98.5)	80.3 (71.0 – 87.1)	98.8 (97.5 – 99.4)
$\% \Delta_{\text{baseline}}$	0.823 (0.770 – 0.876)	1.4774*	36	341	98.4 (91.5 – 100.0)	46.2 (41.8 – 50.6)	18.1 (16.9 – 19.4)	99.6 (97.2 – 99.9)
$\% \Delta_{\text{mean}}$	0.812 (0.759 – 0.865)	0.4739*	41	1061	98.4 (91.4 – 100.0)	45.7 (41.3 – 50.1)	18.0 (16.8 – 19.3)	99.6 (97.1 – 99.9)
<i>Singulex</i>								
$\Delta_{\text{absolute}}$	0.855 (0.795 – 0.915)	0.53	47	-	85.3 (75.3 – 92.4)	50.9 (46.9 – 54.8)	16.8 (15.2 – 18.6)	96.8 (94.5 – 98.1)
$\% \Delta_{\text{baseline}}$	0.669 (0.592 – 0.745)	3.6901*	7	14	97.1 (90.1 – 100.0)	7.4 (5.4 – 10.0)	11.2 (10.7 – 11.6)	95.6 (84.2 – 98.9)
$\% \Delta_{\text{mean}}$	0.652 (0.577 – 0.727)	3.7050*	7	14	97.1 (90.1 – 100.0)	7.4 (5.4 – 10.0)	11.2 (10.7 – 11.6)	95.6 (84.2 – 98.9)
<i>iSTAT</i>								
$\Delta_{\text{absolute}}$	0.873 (0.813 – 0.933)	10	93	-	54.0 (40.9 – 66.6)	99.0 (97.8 – 99.7)	87.2 (73.4 – 94.4)	94.7 (93.1 – 95.9)
$\% \Delta_{\text{baseline}}$	0.769 (0.706 – 0.832)	1.5150*	62	6600	84.1 (72.7 – 92.1)	67.2 (63.0 – 71.3)	23.8 (20.9 – 26.9)	97.2 (95.2 – 98.4)
$\% \Delta_{\text{mean}}$	0.672 (0.619 – 0.724)	1.4950*	62	6700	85.7 (74.6 – 93.3)	67.4 (63.2 – 71.5)	24.2 (21.4 – 27.3)	97.5 (95.5 – 98.6)

Cut-offs were determined by the concentration the assay exhibits <10% CV. Starred (\*) values are ROC-derived cut-offs. All AUC were  $p < 0.001$

## 5.6 AMI diagnosis with $\% \Delta_{\text{baseline}}$ and $\% \Delta_{\text{mean}}$ with fixed cut-offs

The 10% cut-off was chosen as it is the universally agreed maximum amount of variation in a clinically used assay. Therefore it can be said that when measuring above the concentration at which the CV <10% variation outside of this bracket can be attributed to cTn fluctuations in patients and not attributed to the assay's variation. By using this method, as seen in table 5.6, the sensitivities are similar with the Singulex  $\% \Delta_{\text{baseline}}$  sensitivity being significantly higher, 86.7% (95% CI 76.8 – 93.4) in comparison to the Roche, 76.0% (95% CI 64.8 – 85.1,  $p < 0.001$ ), and iSTAT, 68.0% (95% CI 56.2 – 78.3,  $p < 0.001$ ) assays. The Singulex assay yielded the greatest  $\% \Delta_{\text{mean}}$  sensitivity at 82.7% (95% CI 72.2 – 90.4) while the Roche and iSTAT assays produce 77.3% (95% CI 66.2 – 86.2  $p < 0.001$ ) and 70.7% (95% CI 59.0 – 80.6  $p < 0.001$ ), respectfully. The number of missed diagnoses for Roche would be 18 and 17, for Singulex would be 10 + 13 and for the iSTAT would be 24 and 22, all respectively.

**Table 5.6 Diagnostic accuracy of absolute relative deltas with cut-offs at 10% for AMI diagnosis**

Variable	Assay	Cut-off (%)	Sensitivity (95% CI)	Specificity (95% CI)	PPV (95% CI)	NPV(95% CI)
$\% \Delta_{\text{baseline}}$	Roche	10	76.0 (64.8 – 85.1)	60.5 (56.6 – 64.3)	18.3 (16.0 – 20.8)	95.6 (93.5 – 97.0)
	Singulex	10	86.7 (76.8 – 93.4)	22.8 (19.6 – 26.2)	11.6 (10.6 – 12.6)	93.6 (89.0 – 96.4)
	iSTAT	10	68.0 (56.2 – 78.3)	73.0 (69.4 – 76.4)	22.7 (19.3 – 26.4)	95.2 (93.4 – 96.5)
$\% \Delta_{\text{mean}}$	Roche	10	77.3 (66.2 – 86.2)	60.9 (57.0 – 64.7)	18.7 (16.5 – 21.2)	95.6 (93.8 – 97.2)
	Singulex	10	82.7 (72.2 – 90.4)	12.2 (9.5 – 15.3)	12.2 (11.1 – 13.4)	82.7 (73.4 – 89.2)
	iSTAT	10	70.7 (59.0 – 80.6)	73.2 (69.6 – 76.6)	23.5 (20.2 – 27.1)	95.6 (93.8 – 96.8)

### 5.7 Diagnostic accuracy of $\Delta_{\text{absolute}}$ , $\% \Delta_{\text{baseline}}$ and $\% \Delta_{\text{mean}}$ cTn deltas based on baseline cTn

Two groups were omitted, the rule out group for the Singulex assay ( $< 0.53$  pg/ml;  $n=50$ , none with AMI) as there were no patients with cTnI below the cut-off of 0.53, and the rule in group for the iSTAT assay ( $\geq 5460$  pg/ml;  $n=2$ , 1 with AMI) as there were too few patients included.

As displayed in table 5.7.1, the rule out group ( $< 5.03$  pg/ml) for the Roche assay included 322 patients, 4 of whom had AMI. The AUCs for this group were 0.998 (95% CI, 0.994 – 1.000), 0.998 (95% CI, 0.992 – 1.000) and 0.985 (95% CI, 0.971 – 0.998) for  $\Delta_{\text{absolute}}$ ,  $\% \Delta_{\text{baseline}}$  and  $\% \Delta_{\text{mean}}$  and were the highest out of all the groups for Roche. The respective AUC for the intermediate group ( $n = 291$ , 41 with AMI) were 0.983 (95% CI, 0.968 – 0.997), 0.861 (95% CI, 0.790 – 0.932) and 0.850 (95% CI, 0.779 – 0.921) and for the rule in group ( $n = 27$ , 25 with AMI) were 0.960 (95% CI, 0.883 – 1.000) for all variables.

The sensitivities in the Roche intermediate group were all 100.0% (95% CI, 91.4 – 100.0) and NPVs all 100.0%, both higher than the rule out counterparts. The specificities for  $\Delta_{\text{absolute}}$  and both  $\% \Delta$  were 79.5% (95% CI, 73.9 – 84.3) and 26.1% (95% CI, 20.8 – 32.0) with PPVs at 44.1% (95% CI, 38.2 – 50.1) and 18.0% (95% CI, 16.9 – 19.1), all respectively. The Roche rule in group presented a specificity and PPV of 100.0% for all variables, and a sensitivity of 96.0% (95% CI 79.6 – 99.9) and NPV of 50.0% (95% CI, 12.8 – 87.2).

The sensitivities in the Roche rule out group were all 50.0% (95% CI, 6.8 – 93.2) and the specificities were 99.7% (95% CI, 98.3 – 100.0) and 62.3% (95% CI, 56.8 – 67.7) for  $\Delta_{\text{absolute}}$  and  $\% \Delta$ , respectively, and the PPVs were 66.7% (95% CI, 18.3 – 94.7) and



1.7% (95% CI, 0.6 – 4.3), respectively. The respective NPVs were 99.4% (95% CI, 98.3 – 99.8) and 99.0% (95% CI, 97.4 – 99.6).

<b>Table 5.7.1 Diagnostic accuracy of cTn <math>\Delta_{\text{absolute}}</math>, <math>\% \Delta_{\text{baseline}}</math> and <math>\% \Delta_{\text{mean}}</math> after 3h grouped by baseline levels for AMI diagnosis according to the Roche assay</b>								
Cut-offs were determined by the concentration the assay exhibits <10% CV. Starred (*) values are ROC-derived cut-offs.								
	AUC (95% CI)	P	ROC cutoff	Sensitivity	Specificity	PPV	NPV	$\chi^2$ p value
<i>Roche</i>								
<b>&lt; 5.03 pg/ml</b>								
<b>n=322, 4 with AMI</b>								
$\Delta_{\text{absolute}}$	0.998 (0.994 – 1.000)	0.015	10.5	50.0 (6.8 – 93.2)	99.7 (98.3 – 100.0)	66.7 (18.3 – 94.7)	99.4 (98.3 – 99.8)	<0.001
$\% \Delta_{\text{baseline}}$	0.998 (0.992 – 1.000)	0.015	10	50.0 (6.8 – 93.2)	62.3 (56.8 – 67.7)	1.7 (0.6 – 4.3)	99.0 (97.4 – 99.6)	0.487
$\% \Delta_{\text{mean}}$	0.985 (0.971 – 0.998)	0.018	9	50.0 (6.8 – 93.2)	62.3 (56.8 – 67.7)	1.7 (0.6 – 4.3)	99.0 (97.4 – 99.6)	0.487
<b>5.03 &lt; x &lt; 10 pg/ml</b>								
<b>n=295, 41 with AMI</b>								
$\Delta_{\text{absolute}}$	0.983 (0.968 – 0.997)	< 0.001	2.5	100.0 (91.4 – 100.0)	79.5 (73.9 – 84.3)	44.1 (38.2 – 50.1)	100.0	<0.001
$\% \Delta_{\text{baseline}}$	0.861 (0.790 – 0.932)	< 0.001	2.8	100.0 (91.4 – 100.0)	26.1 (20.8 – 32.0)	18.0 (16.9 – 19.1)	100.0	<0.001
$\% \Delta_{\text{mean}}$	0.850 (0.779 – 0.921)	< 0.001	2.8	100.0 (91.4 – 100.0)	26.1 (20.8 – 32.0)	18.0 (16.9 – 19.1)	100.0	<0.001
<b><math>\geq 105</math> pg/ml</b>								
<b>n= 27, 25 with AMI</b>								
$\Delta_{\text{absolute}}$	0.960 (0.883 – 1.000)	0.125	6.0	96.0 (79.6 – 99.9)	100.0	100.0	50.0 (12.8 – 87.2)	0.077
$\% \Delta_{\text{baseline}}$	0.960 (0.883 – 1.000)	0.125	1.5	96.0 (79.6 – 99.9)	100.0	100.0	50.0 (12.8 – 87.2)	0.077
$\% \Delta_{\text{mean}}$	0.960 (0.883 – 1.000)	0.125	1.5	96.0 (79.6 – 99.9)	100.0	100.0	50.0 (12.8 – 87.2)	0.077

The diagnostic accuracy of the Singulex assay  $\Delta_{\text{absolute}}$ ,  $\% \Delta_{\text{baseline}}$  and  $\% \Delta_{\text{mean}}$  with patients grouped by baseline cTn are shown in table 5.7.2. In the intermediate group, the  $\% \Delta_{\text{baseline}}$  and  $\% \Delta_{\text{mean}}$  showed good rule out capability with sensitivities of 100.0 (95% CI, 94.5 – 100.0) and NPVs of 100.0 but very low specificities (1.8%, 95% CI 0.2 – 1.9) and PPVs (10.9%, 95% CI 10.9 – 11.0). The NPV of  $\Delta_{\text{absolute}}$  was lower at 96.4% (95% CI, 93.7 – 98.0) with a sensitivity of 85.5% (95% CI, 75.0 – 92.8) and the specificity and PPV were low (46.6%, 95% CI 42.5 – 50.8; 16.2%, 95% CI 14.6 – 17.9, respectively). The rule out group had low patient numbers (n = 8, 5 with AMI) to attain the highest rule in diagnostic utility. The  $\Delta_{\text{absolute}}$ ,  $\% \Delta_{\text{baseline}}$  and  $\% \Delta_{\text{mean}}$  all displayed the same sensitivity and PPV at 80.0% (95% CI, 28.4 – 99.5) and 57.1% (95% CI, 46.2 – 67.4), respectively, and 0% specificity and NPV.

**Table 5.7.2 Diagnostic accuracy of cTn  $\Delta_{\text{absolute}}$ ,  $\% \Delta_{\text{baseline}}$  and  $\% \Delta_{\text{mean}}$  after 3h grouped by baseline levels for AMI diagnosis according to the Singulex assay**

Cut-offs were determined by the concentration the assay exhibits <10% CV. Starred (\*) values are ROC-derived cut-offs.

	AUC (95% CI)	P	Cut-off	Sensitivity	Specificity	PPV	NPV	$\chi^2$ p value
<i>Singulex</i>								
<b>0.53 &lt; x &lt; 1620 pg/ml</b>								
<b>n=646, 69 with AMI</b>								
$\Delta_{\text{absolute}}$	0.827 (0.765 – 0.892)	<0.001	0.53	85.5 (75.0 – 92.8)	46.6 (42.5 – 50.8)	16.2 (14.6 – 17.9)	96.4 (93.7 – 98.0)	<0.001
$\% \Delta_{\text{baseline}}$	0.680 (0.600 – 0.760)	<0.001	0.66	100.0 (94.5 – 100.0)	1.8 (0.2 – 1.9)	10.9 (10.9 – 11.0)	100.0	0.630
$\% \Delta_{\text{mean}}$	0.665 (0.586 – 0.744)	<0.001	0.65	100.0 (94.5 – 100.0)	1.8 (0.2 – 1.9)	10.9 (10.9 – 11.0)	100.0	0.630
<b>≥ 1620 pg/ml</b>								
<b>n=8, 5 with AMI</b>								
$\Delta_{\text{absolute}}$	0.200 (0.000 – 0.570)	0.180	513	80.0 (28.4 – 99.5)	0.0 (0.0 – 70.8)	57.1 (46.2 – 67.4)	0	0.625
$\% \Delta_{\text{baseline}}$	0.200 (0.000 – 0.570)	0.180	12	80.0 (28.4 – 99.5)	0.0 (0.0 – 70.8)	57.1 (46.2 – 67.4)	0	0.625
$\% \Delta_{\text{mean}}$	0.200 (0.000 – 0.570)	0.180	12	80.0 (28.4 – 99.5)	0.0 (0.0 – 70.8)	57.1 (46.2 – 67.4)	0	0.625

The diagnostic accuracy of the iSTAT assay  $\Delta_{\text{absolute}}$ ,  $\% \Delta_{\text{baseline}}$  and  $\% \Delta_{\text{mean}}$  with patients grouped by baseline cTn are shown in table 5.7.3. In the rule out group, the sensitivity and NPV was found to be 60.0% (95% CI, 14.7 – 94.7) and 99.2% (95% CI, 97.6 – 99.7), respectively, for all deltas. The specificity and PPVs for  $\Delta_{\text{absolute}}$  and  $\% \Delta_{\text{mean}}$  were 76.4% (95% CI, 71.4 – 81.0) and 3.9% (95% CI, 1.9 – 7.8), respectively, and for  $\% \Delta_{\text{baseline}}$  were 76.1% (95% CI, 71.0 – 80.7) and 3.8% (95% CI, 1.8 – 7.7), respectively.

The intermediate iSTAT group also displayed similarities between the performance of  $\Delta_{\text{absolute}}$  and  $\% \Delta_{\text{mean}}$ . Sensitivity, PPV and NPV were the same for  $\Delta_{\text{absolute}}$  and  $\% \Delta_{\text{mean}}$  at 82.5% (95% CI, 70.9 – 91.0), 34.9% (95% CI, 30.6 – 39.5) and 94.4% (95% CI, 90.7 – 96.7), respectively. Whereas the respective results for  $\% \Delta_{\text{baseline}}$  were 81.0% (95% CI, 69.1 – 89.8), 34.5% (95% CI, 30.1 – 39.1) and 93.9% (95% CI, 90.2 – 96.3). All deltas reported the same specificity at 65.6% (95% CI, 59.7 – 71.1).

**Table 5.7.3 AUROC for AMI diagnosis by absolute and relative cTn deltas between baseline and 3h grouped by baseline levels according to the iSTAT assay**

Cut-offs were determined by the concentration the assay exhibits <10% CV. Starred (\*) values are ROC-derived cut-offs.

	AUC (95% CI)	P	Cut-off	Sensitivity	Specificity	PPV	NPV	$\chi^2$ p value
<b>iSTAT</b>								
<b>&lt; 5 pg/ml</b>								
<b>n=324, 11 with AMI</b>								
<b><math>\Delta_{\text{absolute}}</math></b>	0.717 (0.435 – 0.998)	0.097	5	60.0 (14.7 – 94.7)	76.4 (71.4 – 81.0)	3.9 (1.9 – 7.8)	99.2 (97.6 – 99.7)	0.093
<b><math>\% \Delta_{\text{baseline}}</math></b>	0.668 (0.416 – 0.921)	0.198	50	60.0 (14.7 – 94.7)	76.1 (71.0 – 80.7)	3.8 (1.8 – 7.7)	99.2 (97.6 – 99.7)	0.096
<b><math>\% \Delta_{\text{mean}}</math></b>	0.670 (0.417 – 0.922)	0.193	100	60.0 (14.7 – 94.7)	76.4 (71.4 – 81.0)	3.9 (1.9 – 7.8)	99.2 (97.6 – 99.7)	0.093
<b>5 &lt; x &lt; 5460 pg/ml</b>								
<b>n=348, 56 with AMI</b>								
<b><math>\Delta_{\text{absolute}}</math></b>	0.865 (0.802 – 0.928)	< 0.001	4.5	82.5 (70.9 – 91.0)	65.6 (59.7 – 71.1)	34.9 (30.6 – 39.5)	94.4 (90.7 – 96.7)	< 0.001
<b><math>\% \Delta_{\text{baseline}}</math></b>	0.747 (0.676 – 0.817)	< 0.001	1.5150	81.0 (69.1 – 89.8)	65.6 (59.7 – 71.1)	34.5 (30.1 – 39.1)	93.9 (90.2 – 96.3)	< 0.001
<b><math>\% \Delta_{\text{mean}}</math></b>	0.645 (0.581 – 0.708)	0.001	1.4950	82.5 (70.9 – 91.0)	65.6 (59.7 – 71.1)	34.9 (30.6 – 39.5)	94.4 (90.7 – 96.7)	< 0.001

### 5.8 Diagnostic accuracy of baseline cTn in predictor composites with cTn deltas, acute ischaemia, and H-FABP diagnosis for AMI diagnosis for cardiac-associated conditions

The diagnostic accuracy of composite predictors of 0h cTn plus cardiac ischaemia, cTn deltas and H-FABP test results are shown below. The results of the Roche assay are shown in table 5.8.1. The cTn + ECG composite produced sensitivity and NPV of 94.7% (95% CI, 86.9 – 98.5) and 98.9% (95% CI, 97.1 – 100.0), respectively. The specificity and PPV of cTn + ECG were 54.8% (95% CI, 50.6 – 58.5) and 19.5% (95% CI, 18.0 – 21.1). By making the composite of cTn +  $\Delta_{\text{absolute}}$ ,  $\% \Delta_{\text{baseline}}$  or  $\% \Delta_{\text{mean}}$  instead of ECG ischaemia, the sensitivity is 100.0% (95% CI, 95.0 – 100.0) and NPVs are 100%. However, specificities are low at 56.3% (95% CI, 52.4 – 60.2), 0.3% (95% CI, 0.0 – 1.1) and 38.2% (95% CI, 34.0 – 42.1), respectively, as well as PPVs (20.5%, 95% CI 19.1 – 22.0; 10.2%, 95% CI 10.1 – 1.2; 15.4%, 95% CI 14.6 – 16.2, respectively). Diagnostic accuracy of the tests were significantly different to each other,  $\Delta_{\text{absolute}}$ ,  $\% \Delta_{\text{baseline}}$  and  $\% \Delta_{\text{mean}}$  at  $p = 0.041$ ,  $< 0.001$  and  $< 0.001$ , respectively. The addition of both ECG ischaemia and  $\Delta_{\text{absolute}}$ ,  $\% \Delta_{\text{baseline}}$  or  $\% \Delta_{\text{mean}}$  to cTn produced the same sensitivities at 97.3% (95% CI, 90.7 – 100.0), which were lower than the deltas alone, and NPVs at 100%. The respective specificities were 56.3% (95% CI, 52.4 – 60.2), 0.9% (95% CI, 0.3 – 2.0) and 37.2% (95% CI, 33.5 – 41.1) and the PPVs were similar than cTn + deltas or + ECG alone at 19.8% (95% CI, 18.4 – 21.3), 10.3% (95% CI, 9.9 – 10.6) and 15.3% (95% CI, 14.4 – 16.2). This composite was significantly different to cTn +  $\Delta_{\text{absolute}}$  and  $\% \Delta_{\text{mean}}$  alone ( $p < 0.001$  and  $= 0.008$ ), respectively, but not for  $\% \Delta_{\text{baseline}}$  ( $p = 1.000$ ). The addition of H-FABP improves sensitivity across all deltas once more to 100.0% (95% CI, 95.2 – 100.0) and NPV to 100.0%. Specificities are similar to the composite without the addition of H-FABP

analysis at 52.3% (95% CI, 48.3 – 56.2), 0.9% (95% CI, 0.3 – 2.0) and 35.8% (95% CI, 32.1 – 39.7), respectively. The same occurs with the PPVs at 19.8% (95% CI, 18.4 – 21.3), 10.3% (95% CI, 9.9 – 10.6) and 15.3% (95% CI, 14.6 – 16.1), respectively.

Diagnostic accuracy of the predictors +  $\Delta_{\text{absolute}}$  and +  $\% \Delta_{\text{mean}}$  were significantly different to each other, at  $p < 0.001$  and  $< 0.001$ , respectively, but +  $\% \Delta_{\text{baseline}}$  was not ( $p = 0.500$ ).

**Table 5.8.1 Diagnostic accuracy of baseline cTn in predictor composites with cTn deltas, acute ischaemia, and H-FABP for AMI diagnosis according to the Roche assay**

		Sensitivity (95% CI)	Specificity (95% CI)	PPV (95% CI)	NPV (95% CI)	$\chi^2$ p value
<b>Roche, n = 719</b>						
<b>cTn + ECG</b>		94.7 (86.9 – 98.5)	54.8 (50.6 – 58.5)	19.5 (18.0 – 21.1)	98.9 (97.1 – 100.0)	<0.001
<b>cTn + delta</b>	$\Delta_{\text{absolute}}$ pg/ml	100.0 (95.0 – 100.0)	56.3 (52.4 – 60.2)	20.5 (19.1 – 22.0)	100.0	<0.001
	$\% \Delta_{\text{baseline}}$	100.0 (95.0 – 100.0)	0.3 (0.0 – 1.1)	10.2 (10.1 – 1.2)	100.0	1.000
	$\% \Delta_{\text{mean}}$	100.0 (95.0 – 100.0)	38.2 (34.0 – 42.1)	15.4 (14.6 – 16.2)	100.0	<0.001
<b>cTn + ECG + delta</b>	$\Delta_{\text{absolute}}$ pg/ml	97.3 (90.7 – 100.0)	54.1 (50.2 – 58.0)	19.8 (18.4 – 21.3)	99.4 (97.8 – 99.9)	<0.001
	$\% \Delta_{\text{baseline}}$	97.3 (90.7 – 100.0)	0.9 (0.3 – 2.0)	10.3 (9.9 – 10.6)	75.0 (38.1 – 93.6)	0.199
	$\% \Delta_{\text{mean}}$	97.3 (90.7 – 100.0)	37.2 (33.5 – 41.1)	15.3 (14.4 – 16.2)	99.2 (96.8 – 99.8)	<0.001
<b>cTn + ECG + delta + H-FABP</b>	$\Delta_{\text{absolute}}$ pg/ml	100.0 (95.2 – 100.0)	52.3 (48.3 – 56.2)	19.6 (18.3 – 20.9)	100.0	<0.001
	$\% \Delta_{\text{baseline}}$	100.0 (95.2 – 100.0)	0.9 (0.3 – 2.0)	10.5 (10.4 – 10.6)	100.0	0.516
	$\% \Delta_{\text{mean}}$	100.0 (95.2 – 100.0)	35.8 (32.1 – 39.7)	15.3 (14.6 – 16.1)	100.0	<0.001

cTn = baseline cTn; ECG = evidence of ischaemia by ECG; H-FABP = positive or negative test for H-FABP; n = number of patients positive for variable in question, in the case of cut-offs a positive result is above the cut-off.

The results of the diagnostic accuracy of the predictor composites for the Singulex assay are shown in table 5.8.2. The cTn + ECG composite produced high sensitivity and NPV of 98.7 (95% CI, 2.8 – 100.0) and 98.5% (95% CI, 90.0 – 99.8), respectively and a specificity and PPV of 9.9% (95% CI, 7.7 – 12.5) and 11.3% (95% CI, 10.9 – 11.7), respectively. The cTn +  $\Delta_{\text{absolute}}$  and +  $\% \Delta_{\text{mean}}$  did not increase the sensitivity from cTn + ECG (98.6%, 95% CI, 92.5 – 100.0 vs 98.7%, 95% CI 92.8 – 100.0) but  $\% \Delta_{\text{baseline}}$  did (100.0%, 95% CI 95.0 – 100.0) and its NPV also increased to 100%. The NPVs of cTn +  $\Delta_{\text{absolute}}$  and +  $\% \Delta_{\text{mean}}$  did not increase (98.3%, 95% CI 88.9 – 100.0 and 95.0%, 95% CI 72.1 – 99.3, respectively) nor did the specificities (8.9%, 95% CI 6.8 – 11.4 and 3.0%, 95% CI 0.0 – 10.0, respectively). The specificity of cTn +  $\Delta_{\text{absolute}}$  did decrease to 1.9% (95% CI, 1.0 – 3.3) and the PPVs across cTn +  $\Delta_{\text{absolute}}$ , +  $\% \Delta_{\text{baseline}}$  and +  $\% \Delta_{\text{mean}}$  were 10.9% (95% CI, 10.5 – 11.2), 10.3% (95% CI, 10.2 – 10.4) and 10.3% (95% CI, 10.0 – 10.6), respectively. The difference seen was not significant for +  $\Delta_{\text{absolute}}$  ( $p = 0.180$ ) but were found to be significant for +  $\% \Delta_{\text{baseline}}$  or +  $\% \Delta_{\text{mean}}$  (both  $p < 0.001$ ).

The combination of cTn + ECG +  $\Delta_{\text{absolute}}$ , +  $\% \Delta_{\text{baseline}}$  or +  $\% \Delta_{\text{mean}}$  did not improve diagnostic accuracy from cTn +  $\Delta_{\text{absolute}}$ , +  $\% \Delta_{\text{baseline}}$  or +  $\% \Delta_{\text{mean}}$  ( $p = 0.500$ ,  $p = 1.000$  and  $p = 1.000$ ). The cTn + ECG +  $\Delta_{\text{absolute}}$  was similar to cTn +  $\Delta_{\text{absolute}}$  with only sensitivity and PPV changing to 98.7% (95% CI, 92.8 – 100.0) and 11.2% (95% CI, 10.8 – 11.5), respectively. The cTn + ECG +  $\% \Delta_{\text{mean}}$  had small changes to sensitivity, specificity, PPV and NPV at 98.7% (95% CI, 92.8 – 100.0), 3.1 (95% CI, 1.9 – 4.8), 10.6% (95% CI, 10.3 – 10.9) and 95.2% (95% CI, 73.1 – 99.3). The results for cTn + ECG +  $\% \Delta_{\text{baseline}}$  were also similar to cTn +  $\% \Delta_{\text{baseline}}$  with only specificity and PPV increasing slightly (2.0%, 95% CI 1.1 – 3.4; 10.6% (95% CI, 10.5 – 10.7, respectively,

p = ... vs cTn + % $\Delta_{\text{baseline}}$ ). The addition of H-FABP to cTn + ECG + % $\Delta_{\text{baseline}}$  or + % $\Delta_{\text{mean}}$  did not improve diagnostic accuracy for any parameter but did produce smaller specificity and PPV for cTn + ECG +  $\Delta_{\text{absolute}}$  + H-FABP (8.5%, 95% CI 6.5 – 11.0 and 11.1%, 95% CI 10.8 – 11.5, respectively). The differences seen were not significant for +  $\Delta_{\text{absolute}}$ , + % $\Delta_{\text{baseline}}$  or + % $\Delta_{\text{mean}}$  (p = 0.500, = 1.000 and 1.000, respectively). The similarities between the diagnostic accuracy of the cTn + ECG +  $\Delta_{\text{absolute}}$ /% $\Delta_{\text{baseline}}$ /% $\Delta_{\text{mean}}$  + H-FABP and without the addition of H-FABP resulted in non-significant differences (p = 0.500, = 1.000 and = 1.000, respectively).

**Table 5.8.2 Diagnostic accuracy of baseline cTn in predictor composites with cTn deltas, acute ischaemia, and H-FABP for AMI diagnosis according to the Singulex assay**

		Sensitivity (95% CI)	Specificity (95% CI)	PPV (95% CI)	NPV (95% CI)	$\chi^2$ p value
<b><i>Singulex, n = 715</i></b>						
<b>cTn + ECG</b>		98.7 (92.8 – 100.0)	9.9 (7.7 – 12.5)	11.3 (10.9 – 11.7)	98.5 (90.0 – 99.8)	0.009
<b>cTn + delta</b>	$\Delta_{\text{absolute}}$ pg/ml	98.6 (92.5 – 100.0)	8.9 (6.8 – 11.4)	10.9 (10.5 – 11.2)	98.3 (88.9 – 100.0)	0.022
	% $\Delta_{\text{baseline}}$	100.0 (95.0 – 100.0)	1.9 (1.0 – 3.3)	10.3 (10.2 – 10.4)	100.0	0.622
	% $\Delta_{\text{mean}}$	98.6 (92.5 – 100.0)	3.0 (2.5 – 100.0)	10.3 (10.0 – 10.6)	95.0 (72.1 – 99.3)	0.711
<b>cTn + ECG + delta</b>	$\Delta_{\text{absolute}}$ pg/ml	98.7 (92.8 – 100.0)	8.9 (6.8 – 11.3)	11.2 (10.8 – 11.5)	98.3 (88.9 – 99.8)	0.022
	% $\Delta_{\text{baseline}}$	100.0 (95.2 – 100.0)	2.0 (1.1 – 3.4)	10.6 (10.5 – 10.7)	100.0	0.381
	% $\Delta_{\text{mean}}$	98.7 (92.8 – 100.0)	3.1 (1.9 – 4.8)	10.6 (10.3 – 10.9)	95.2 (73.1 – 99.3)	0.338
<b>cTn + ECG + delta + H-FABP</b>	$\Delta_{\text{absolute}}$ pg/ml	98.7 (92.8 – 100.0)	8.5 (6.5 – 11.0)	11.1 (10.8 – 11.5)	98.2 (88.5 – 99.8)	0.022
	% $\Delta_{\text{baseline}}$	100.0 (95.2 – 100.0)	2.0 (1.1 – 3.4)	10.6 (10.5 – 10.7)	100.0	0.236
	% $\Delta_{\text{mean}}$	98.7 (92.8 – 100.0)	3.1 (1.9 – 4.8)	10.6 (10.3 – 10.9)	95.2 (73.1 – 99.3)	0.338

cTn = baseline cTn; ECG = evidence of ischaemia by ECG; H-FABP = positive or negative test for H-FABP; n = number of patients positive for variable in question, in the case of cut-offs a positive result is above the cut-off.

The results of the diagnostic accuracy of the predictor composites for the iSTAT assay are shown in table 5.8.3. The specificity and PPV for cTn + ECG were 92.4% (95% CI, 89.9 – 94.3) and 95.0% (95% CI, 93.6 – 96.2), respectively, and sensitivity and PPV were 58.0% (95% CI, 45.5 – 69.8) and 46.5% (95% CI, 38.2 – 55.1), respectively. The cTn +  $\Delta_{\text{absolute}}$  was greater than cTn + ECG across sensitivity, specificity, PPV and NPV at 62.3% (95% CI, 49.8 – 73.7), 98.3% (95% CI, 97.0 – 99.2), 81.1% (95% CI, 69.4 – 89.1) and 95.8% (95% CI, 94.4 – 96.9), respectively,  $p < 0.001$  vs equivalents of cTn + ECG. For cTn +  $\% \Delta_{\text{baseline}}$  and  $\% \Delta_{\text{mean}}$  the sensitivities (81.2%, 95% CI 69.9 – 89.6 and 82.6%, 95% CI 71.6 – 90.7, respectively) and NPVs (97.0%, 95% CI 95.2 – 98.2 and 97.4%, 95% CI 95.8 – 98.5, respectively) were higher but specificities (70.9%, 95% CI 67.1 – 74.5 and 72.4%, 95% CI 68.8 – 75.9, respectively) and NPVs (24.2%, 95% CI 21.3 – 27.5 and 24.7%, 95% CI 21.7 – 27.9, respectively) were lower ( $p < 0.001$  for all).

For the cTn + ECG +  $\Delta_{\text{absolute}}$  only sensitivity increased (71.0%, 95% CI 58.8 – 81.3) compared to cTn +  $\Delta_{\text{absolute}}$ , specificity, PPV and NPV decreased to 92.2% (95% CI, 89.7 – 94.2), 51.0% (95% CI, 43.3 – 58.8) and 96.5% (95% CI, 95.0 – 97.6), respectively. For cTn + ECG +  $\% \Delta_{\text{baseline}}$  and  $\% \Delta_{\text{mean}}$ , sensitivities increased to 85.5% (95% CI, 75.0 – 92.8 and 87.0% (95% CI, 76.7 – 93.9), respectively, and NPVs increased to 97.6% (95% CI, 95.8 – 98.6) and 97.9% (95% CI, 96.1 – 98.8), respectively. The specificities of the respective predictors decreased to 68.1% (95% CI, 64.2 – 71.8) and 68.2% (95% CI, 64.3 – 71.9) and PPVs to 23.5% (95% CI, 20.9 – 26.3) and 23.9% (95% CI, 21.3 – 26.7) The differences seen resulted in  $p < 0.001$  for the three deltas. The cTn + ECG +  $\% \Delta_{\text{baseline}}/\% \Delta_{\text{mean}}$  + H-FABP had increased sensitivity to 92.8% (95% CI, 83.9 – 97.6) for both deltas but specificities (60.1%,



95% CI 56.0 – 64.0 and 60.2%, 95% CI, 56.2 – 64.2, respectively), PPVs (both at 21.1%, 95% CI 19.2 – 23.1) and NPVs (both at 98.6%, 95% CI 96.9 – 99.4) decreased when H-FABP was added to the composite. For The cTn + ECG +  $\Delta_{\text{absolute}}$  + H-FABP composite, sensitivity, specificity and PPV decreased (76.8%, 95% CI 65.1 – 86.1; 81.5%, 95% CI 78.2 – 84.6; 32.3%, 95% CI 27.8 – 37.1, respectively) and only NPV increased (96.8%, 95% CI 95.2 – 97.9, all  $p < 0.001$ ).

**Table 5.8.3 Diagnostic accuracy of baseline cTn in predictor composites with cTn deltas, acute ischaemia, and H-FABP for AMI diagnosis according to the iSTAT assay**

		Sensitivity (95% CI)	Specificity (95% CI)	PPV (95% CI)	NPV(95% CI)	$\chi^2$ p value
<i>iSTAT, n = 670</i>						
<b>cTn + ECG</b>		58.0 (45.5 – 69.8)	92.4 (89.9 – 94.3)	46.5 (38.2 – 55.1)	95.0 (93.6 – 96.2)	< 0.001
<b>cTn + delta</b>	$\Delta_{\text{absolute}}$	62.3 (49.8 – 73.7)	98.3 (97.0 – 99.2)	81.1 (69.4 – 89.1)	95.8 (94.4 – 96.9)	< 0.001
	% $\Delta_{\text{baseline}}$	81.2 (69.9 – 89.6)	70.9 (67.1 – 74.5)	24.2 (21.3 – 27.5)	97.0 (95.2 – 98.2)	< 0.001
	% $\Delta_{\text{mean}}$	82.6 (71.6 – 90.7)	72.4 (68.8 – 75.9)	24.7 (21.7 – 27.9)	97.4 (95.8 – 98.5)	< 0.001
<b>cTn + ECG + delta</b>	$\Delta_{\text{absolute}}$	71.0 (58.8 – 81.3)	92.2 (89.7 – 94.2)	51.0 (43.3 – 58.8)	96.5 (95.0 – 97.6)	< 0.001
	% $\Delta_{\text{baseline}}$	85.5 (75.0 – 92.8)	68.1 (64.2 – 71.8)	23.5 (20.9 – 26.3)	97.6 (95.8 – 98.6)	< 0.001
	% $\Delta_{\text{mean}}$	87.0 (76.7 – 93.9)	68.2 (64.3 – 71.9)	23.9 (21.3 – 26.7)	97.9 (96.1 – 98.8)	< 0.001
<b>cTn + ECG + delta + H-FABP</b>	$\Delta_{\text{absolute}}$	76.8 (65.1 – 86.1)	81.5 (78.2 – 84.6)	32.3 (27.8 – 37.1)	96.8 (95.2 – 97.9)	< 0.001
	% $\Delta_{\text{baseline}}$	92.8 (83.9 – 97.6)	60.1 (56.0 – 64.0)	21.1 (19.2 – 23.1)	98.6 (96.9 – 99.4)	< 0.001
	% $\Delta_{\text{mean}}$	92.8 (83.9 – 97.6)	60.2 (56.2 – 64.2)	21.1 (19.2 – 23.2)	98.6 (96.9 – 99.4)	< 0.001

cTn = baseline cTn; ECG = evidence of ischaemia by ECG; H-FABP = positive or negative test for H-FABP; n = number of patients positive for variable in question, in the case of cut-offs a positive result is above the cut-off.

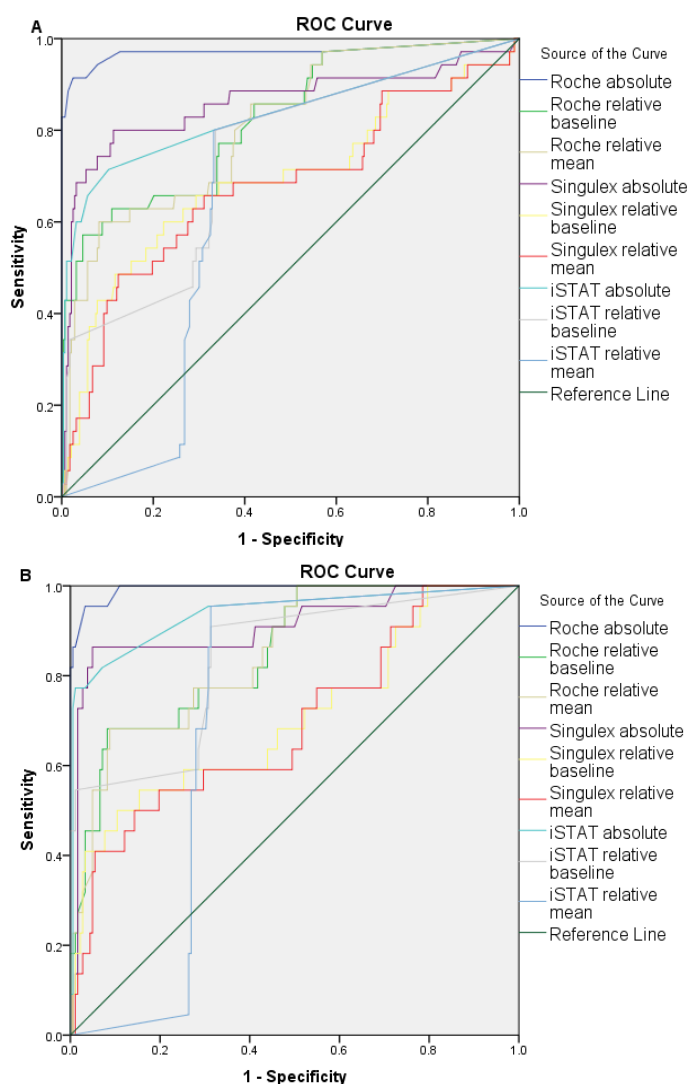
### 5.9 Diagnostic accuracy of absolute and relative cTn deltas in important patient subgroups

The results of overall diagnostic accuracy of the different assays in important patient subgroups are shown in table 5.9 and ROC curves in figure 5.9. The diagnostic accuracy of  $\Delta_{\text{absolute}}$  was higher than  $\% \Delta_{\text{baseline}}$  and  $\% \Delta_{\text{mean}}$  in all assays across the subgroups but most prominent in the elderly and patients with renal failure. In the elderly subgroup, the Roche assay reported 0.979, 0.773 and 0.771, the Singulex assay reported 0.901, 0.764 and 0.760 and the iSTAT assay reported 0.826, 0.724 and 0.619, all respectively. For the renal failure subgroup, the Roche assay reported 0.911, 0.778 and 0.778, the Singulex assay reported 0.878, 0.789 and 0.789 and the iSTAT assay reported 0.833, 0.644 and 0.606, all respectively. The diagnostic accuracy in females was greater than in males and by using the Roche assay for  $\Delta_{\text{absolute}}$  a nearly perfect AUC was found (0.993) but was lower for the Singulex and iSTAT assays (0.9110 and 0.938, respectively). The rheumatoid arthritis subgroup had perfect diagnostically accurate AUC for  $\Delta_{\text{absolute}}$  of all assays and  $\% \Delta_{\text{baseline}}$  of the iSTAT assay but due to the low patient number with rheumatoid arthritis ( $n = 22$ ), these results are not reliable and a study focused on rheumatoid arthritis with a larger cohort would be needed to validate these results.

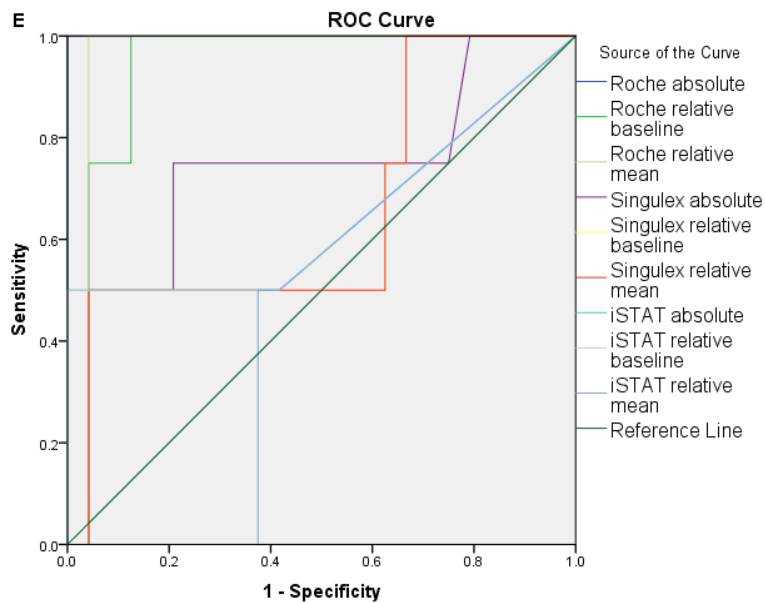
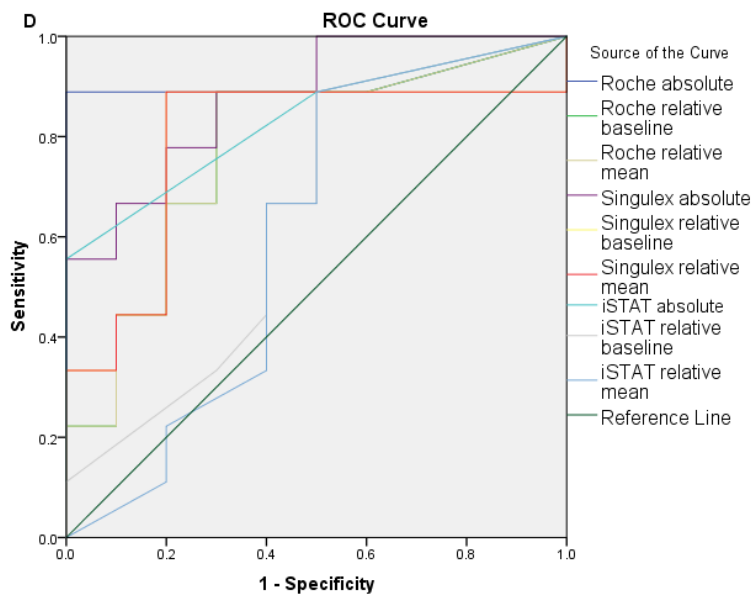
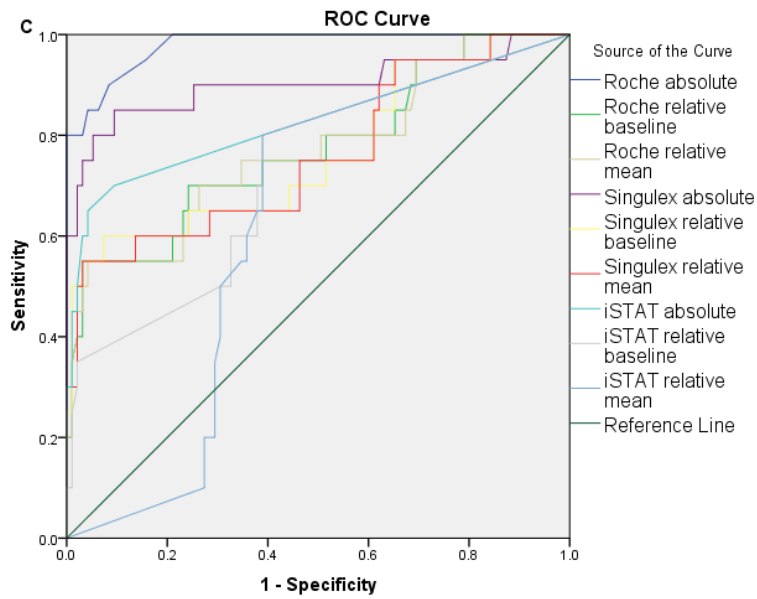
**Table 5.9 Diagnostic accuracy of absolute and relative cTn deltas in patient subgroups using ROC curve analysis**

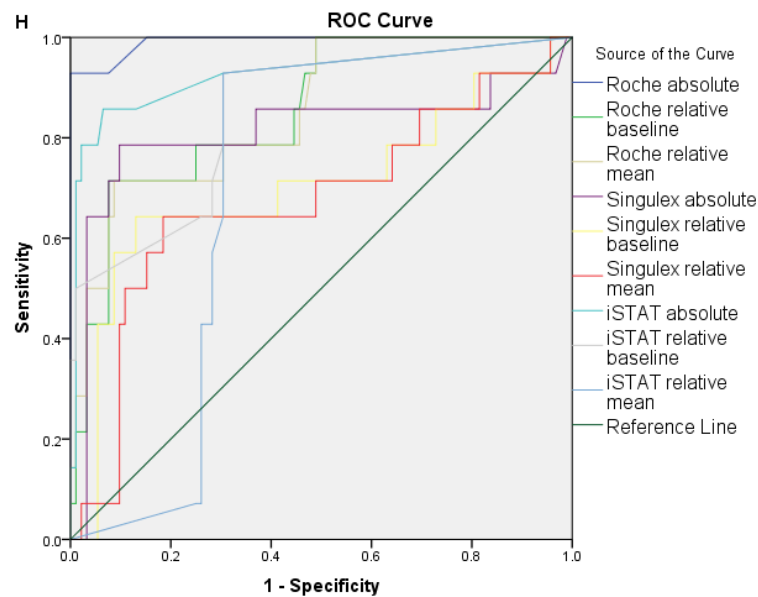
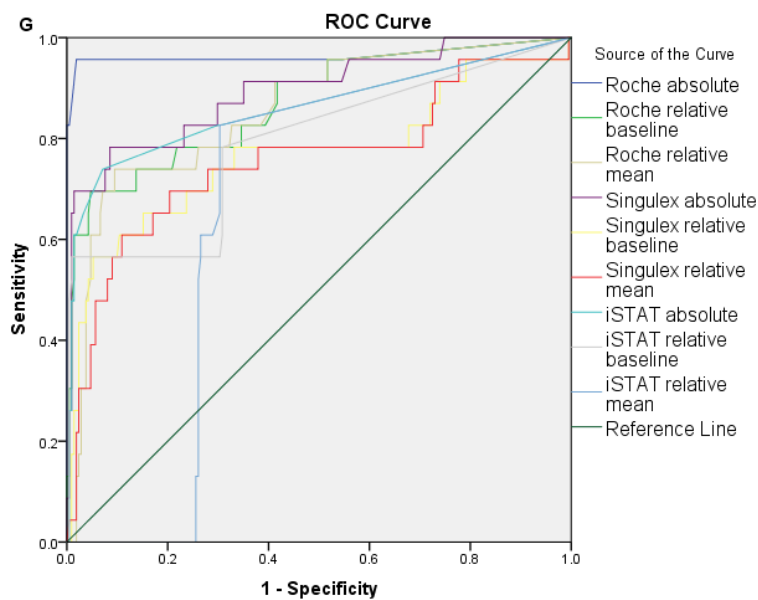
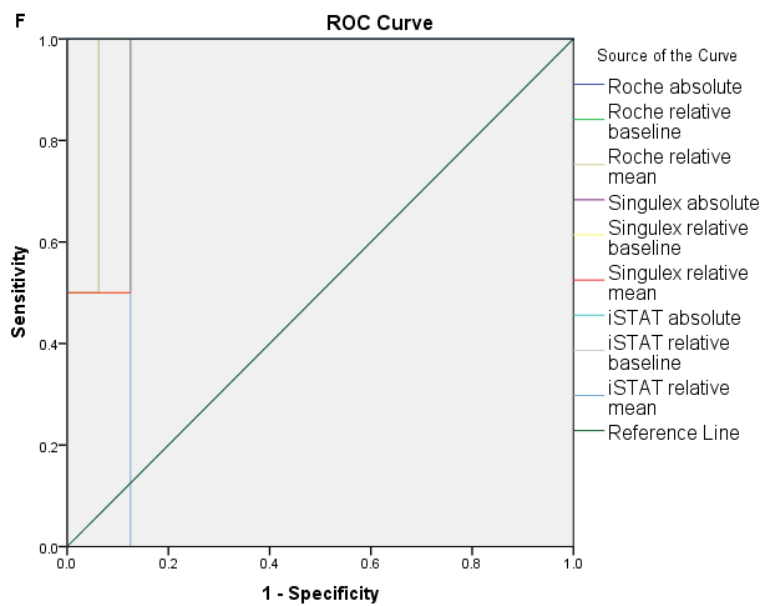
		Roche			Singulex			iSTAT		
	n	$\Delta$	% $\Delta_b$	% $\Delta_m$	$\Delta$	% $\Delta_b$	% $\Delta_m$	$\Delta$	% $\Delta_b$	% $\Delta_m$
<b>Male</b>	437	0.972	0.823	0.809	0.860	0.692	0.677	0.836	0.736	0.645
<b>Female</b>	285	0.993	0.849	0.847	0.910	0.705	0.691	0.938	0.837	0.708
<b>Elderly (<math>\geq 70</math> y)</b>	151	0.979	0.773	0.771	0.901	0.764	0.760	0.826	0.724	0.619
<b>Renal failure</b>	30	0.911	0.778	0.778	0.878	0.789	0.789	0.833	0.644	0.606
<b>Stroke</b>	40	1.000	0.937	0.958	0.734	0.656	0.656	0.646	0.646	0.458
<b>Rheumatoid arthritis</b>	22	1.000	0.969	0.969	1.000	0.938	0.938	1.000	1.000	0.875
<b>TSSO &lt; 3h</b>	308	0.965	0.870	0.854	0.893	0.768	0.757	0.860	0.788	0.663
<b>TSSO 3h <math>\leq</math> x &lt; 6h</b>	153	0.992	0.852	0.851	0.811	0.703	0.675	0.926	0.848	0.703
<b>TSSO <math>\geq</math> 6h</b>	164	0.991	0.810	0.800	0.884	0.641	0.626	0.850	0.701	0.633

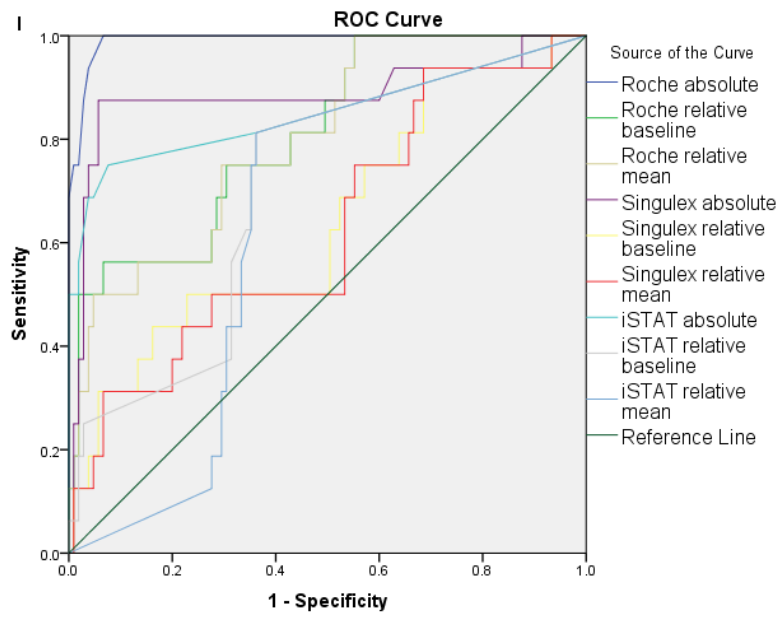
$\Delta$ :  $\Delta_{\text{absolute}}$ ; % $\Delta_b$ : % $\Delta_{\text{baseline}}$ ; % $\Delta_m$ : % $\Delta_{\text{mean}}$ ; TSSO: time since symptom onset



**Figure 5.9 ROC curves for the diagnostic accuracy of  $\Delta_{\text{absolute}}$ , % $\Delta_{\text{baseline}}$  and % $\Delta_{\text{mean}}$  according to the Roche, Singulex and iSTAT assays for AMI diagnosis in important patient subgroups. A) male subgroup; B) female subgroup; C) elderly subgroup; D) renal subgroup; E) stroke subgroup; F) rheumatoid arthritis subgroup; G) < 3h TSSO subgroup; H) 3h  $\leq$  x < 6h TSSO subgroup; I) > 6h TSSO subgroup. Absolute:  $\Delta_{\text{absolute}}$ ; relative baseline: % $\Delta_{\text{baseline}}$ ; relative mean: % $\Delta_{\text{mean}}$ .**







### 5.10 Summary of the diagnosis of NSTEMI with kinetic cTn deltas

The three assays were assessed for the capability of rapid rule out for NSTEMI based on cTn deltas. Absolute and relative deltas were based on the FS of the assays for maximum sensitivity and therefore only cTn above a calculated level were deemed reliable for the relative deltas. The analyses showed:

- Relative deltas outcome performed absolute deltas
- Lower thresholds for Singuex cTn<sub>low</sub> allowed more of the cohort to be ruled out with 100% sensitivity and NPV
- Tailoring rule in/rule out deltas based on baseline cTn can aid diagnostic accuracy
- $\Delta_{\text{absolute}}$  is more accurate at lower concentrations and  $\% \Delta$  is more accurate at higher concentrations
- For Singuex, the early rise in H-FABP in AMI pathology does not improve accuracy as its very low FS detects cTn rise, and therefore AMI, earlier regardless
- For iSTAT, its poor FS does not detect cTn rises early and therefore the addition of an early biomarker such as H-FABP increases its NPV
- Combining biomarkers that cover more AMI physiology will improve diagnostic accuracy

## **Chapter 6: Does non-kinetic cTn predict 30-day outcome?**



### 6.1 Baseline characteristics of the 30-day MACE and 30-day no MACE patients

The baseline characteristics of the patients are presented in Table 6.1. In total, 10 conditions were highlighted to assess the prognostic strength of the deltas. The 10 conditions were all-cause mortality, AMI, revascularisation, PCI, CABG, stenosis, tests for heart disease, cardiac arrest, arrhythmia and acute heart failure. 40 patients (5.5%) of the 724 cohort experienced MACE within 30 days from presentation. There were three (0.2%) deaths in the MACE group, one of AMI and two of non-cardiac related diseases (1 of carcinomatosis from the lung and 1 of colon cancer). The cause of death for the only death of the no MACE group (0.5%) was not recorded.

There were 40 composite MACE events (5.5%) within 30 days including 11 instances of PCI, 8 of stenosis, 6 of acute heart failure, 2 patients who experienced cardiac arrest and 4 of CABG. There were no patients who had diabetes mellitus and experienced 30-day composite MACE and therefore the variable was removed from the analyses.

The average age of the MACE patients was 57.2 years and the majority were male (56.3%) but the frequency was less than in the total cohort (60.6%). Patients with ischaemia present on ECG had higher than expected incidences of MACE (16.2%,  $p < 0.001$ ). Hyperlipidaemia was found in 43.0% of MACE patients and hypertension found in 47.9% of the MACE group.

**Table 6.1 Baseline characteristics of 30-day MACE positive and 30-day MACE negative patients**

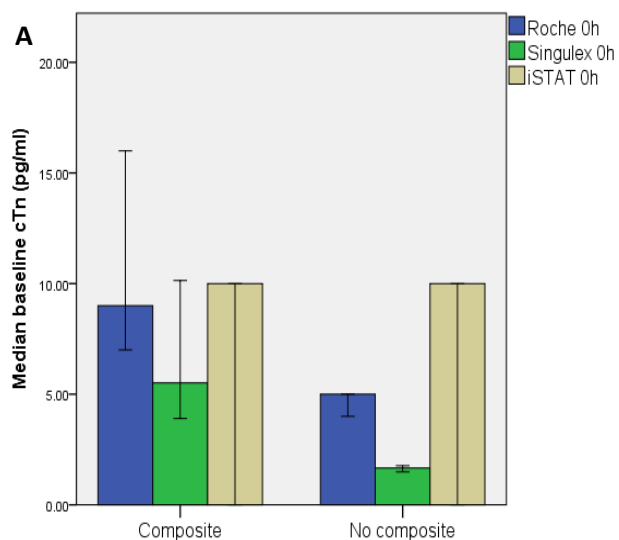
Variable	Total (n = 724)	MACE (n = 142)	No MACE (n = 582)	p value
Age (mean, 95% CI)	55.5 (54.4 – 56.7)	57.2 (54.8 – 59.6)	55.1 (53.8 – 56.3)	0.144
Sex, male (%)	439 (60.6)	80 (56.3)	359 (61.7)	0.242
Prior myocardial infarction (%)	175 (24.2)	36 (25.4)	139 (23.9)	0.714
Previous angina (%)	193 (26.7)	37 (26.1)	156 (26.8)	0.857
Prior coronary intervention (%)	141(19.5)	28 (19.7)	113 (19.4)	0.935
Previous hypertension (%)	325 (44.8)	68 (47.9)	257 (44.2)	0.433
Previous hyperlipidaemia (%)	264 (36.5)	61 (43.0)	203 (35.0)	0.075
Current smoker (%)	157 (21.7)	33 (23.6)	124 (21.6)	0.614
ECG ischaemia (%)	58 (8.1)	23 (16.2)	35 (6.0)	< 0.001
Prior CABG (%)	46 (6.4)	8 (5.6)	38 (6.5)	0.695
Diabetes mellitus (%)	9 (1.2)	2 (1.4)	7 (1.2)	0.838
Chronic kidney disease (%)	26 (3.6)	9 (6.4)	21 (3.6)	0.142
H-FABP positive (%)	88 (12.2)	22 (15.5)	66 (11.3)	0.175

MACE: major adverse cardiac events as described in the text within 30 days

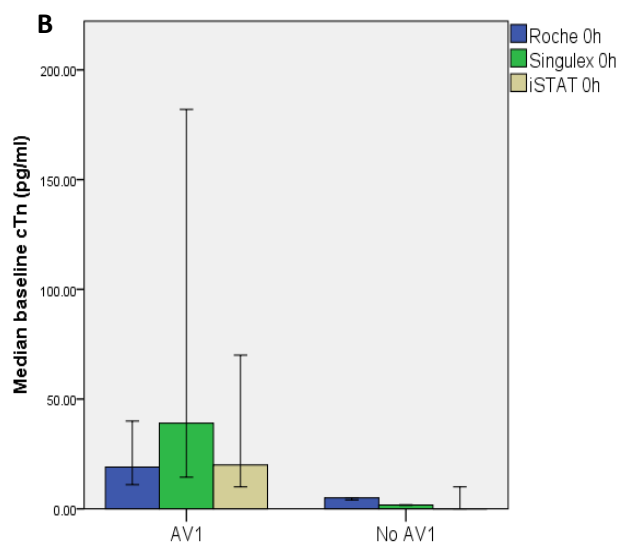
## 6.2 Baseline cTn concentrations of different 30-day composite outcomes

The composite MACE group included all outcomes; AV1 included all-cause mortality, AMI, revascularisation, PCI, CABG and stenosis; adverse events 2 included cardiac arrest, arrhythmia and acute heart failure. All outcomes included events that occurred 30 days post-presentation.

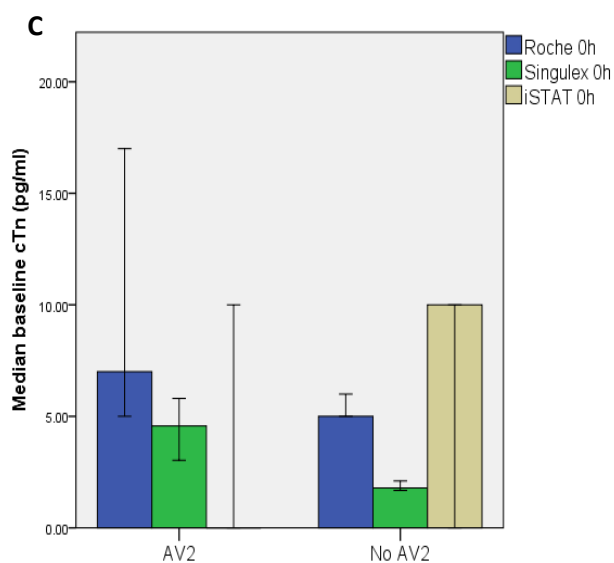
The differences between cTn levels at baseline are shown in figure 6.2. According to independent-samples median tests, the differences in median baseline cTn in the composite MACE and adverse events 1 were all  $p < 0.001$  for all assays. For adverse events 2, only the Singulex showed a significant difference between positive and negative groups ( $p = 0.019$ ) whereas the Roche and iSTAT assays did not ( $p = 0.621$  and  $p = 0.870$ , respectively).



Error Bars: 95% CI



Error Bars: 95% CI



Error Bars: 95% CI

**Figure 6.2 Median cTn values at baseline by different 30-day prognoses according to the Roche, Singulex and iSTAT assays.**

Bars are clustered by whether an outcome has occurred or not occurred. Bars include results from one assay, as specified by the legends and are colour coded. Error bars indicate 95% CI. Composite: composite MACE; AV1 – adverse events 1; AV2 – adverse events 2.

### 6.3 30-day composite MACE prediction by cTn 0h, 3h and max values according to the Roche, Singulex and iSTAT assays

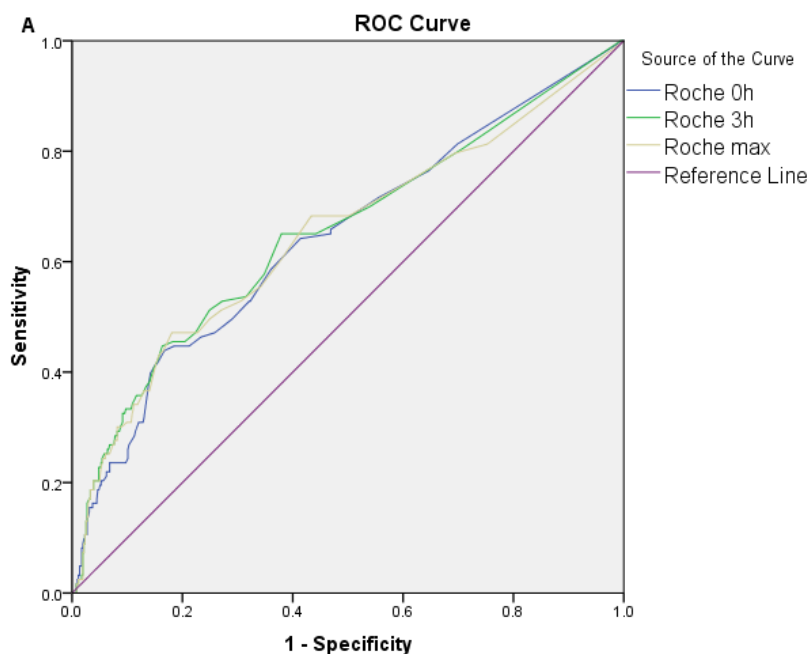
The ROC curves corresponding to the cTn values of the different assays are displayed in figure 6.3 and the AUCs are available in table 6.3. The Roche assay produced AUROC of 0.656 (95% CI, 0.594 – 0.717), 0.664 (95% CI, 0.601 – 0.726) and 0.661 (95% CI, 0.598 – 0.724) for the 0h, 3h and max values variables, respectively all  $p < 0.001$ . The Singulex assay had AUROCs for 0h, 3h and max values of 0.726 (95% CI, 0.664 – 0.788), 0.741 (95% CI, 0.682 – 0.800) and 0.736 (95% CI, 0.677 – 0.796), respectively. The iSTAT produced AUROCs for 0h, 3h and max values of 0.606 (95% CI, 0.539 – 0.673), 0.652 (95% CI, 0.587 – 0.716) and 0.601 (95% CI, 0.533 – 0.669), respectively.

The prognostic accuracy of the Roche, Singulex and iSTAT assays are displayed in table 6.3. For Roche, the sensitivity for the 0h, 3h and max values were 65.0% (95% CI, 55.9 – 73.4), 65.9% (95% CI, 56.8 – 74.2) and 68.3% (95% CI, 59.3 – 76.4), respectively. All of which were greater than the respective specificities at 55.8% (95% CI, 51.4 – 60.2), 53.1% (95% CI, 48.7 – 57.5) and 49.8% (95% CI, 45.4 – 54.2). NPVs were 87.0% (95% CI 83.8 – 89.6) for 0h, 86.7% (95% CI 83.4 – 89.4) for 3h and 86.8% (95% CI 83.3 -89.6). The PPVs were much lower at 26.1% (95% CI, 23.1 – 29.3), 86.7% (95% CI, 83.4 – 89.4) and 86.8% (95% CI, 83.3 -89.6), for the 0h, 3h and max value variables, respectively.

For the 0h, 3h and max values of the Singulex assay, the sensitivities (96.3%, 95% CI 91.6 – 98.8; 97.8%, 95% CI 93.6 – 100.0; 98.5%, 95% CI 94.7 – 99.8, respectively) and NPVs (8.6%, 95% CI 7.8 – 9.4; 94.6%, 95% CI 84.6 – 98.2; 93.6%, 95% CI 77.8 – 98.4, respectively) were both high with the exception of the 0h NPV. Specificities

were low for 0h (21.4%, 95% CI 91.8 – 98.4), 3h (21.9%, 95% CI 21.2 – 22.5) and max values 21.2% (95% CI, 20.7 – 21.7). The lowest performance was found with the respective specificities at 8.6% (95% CI, 6.3 – 11.3), 9.9% (95% CI, 7.5 – 12.8) and 5.5% (95% CI 3.7 – 7.9).

Conversely, the iSTAT specificities were the highest at 97.1% (95% Ci, 95.2 – 98.4), 95.8% (95% CI, 93.7 – 97.4) and 95.4% (95% CI, 93.2 – 97.1) for 0h, 3h, max values, respectively. The NPVs were high but not as high as the specificities (82.5%, 95% CI 81.2 – 83.8; 82.9%, 95% CI 81.5 – 84.3; 82.6%, 95% CI 81.1 – 83.9). PPVs for the 0h, 3h and max values were 64.1% (95% CI, 48.9 – 76.9), 59.2% (95% CI, 45.9 – 71.2) and 55.1% (95% CI, 42.0 – 67.5), respectively, and the lowest values were found in the sensitivities (20.2%, 95% CI 13.5 – 28.3; 23.4% (95% CI, 16.3 – 31.8; 21.8%, 95% CI 14.9 – 30.1, respectively).



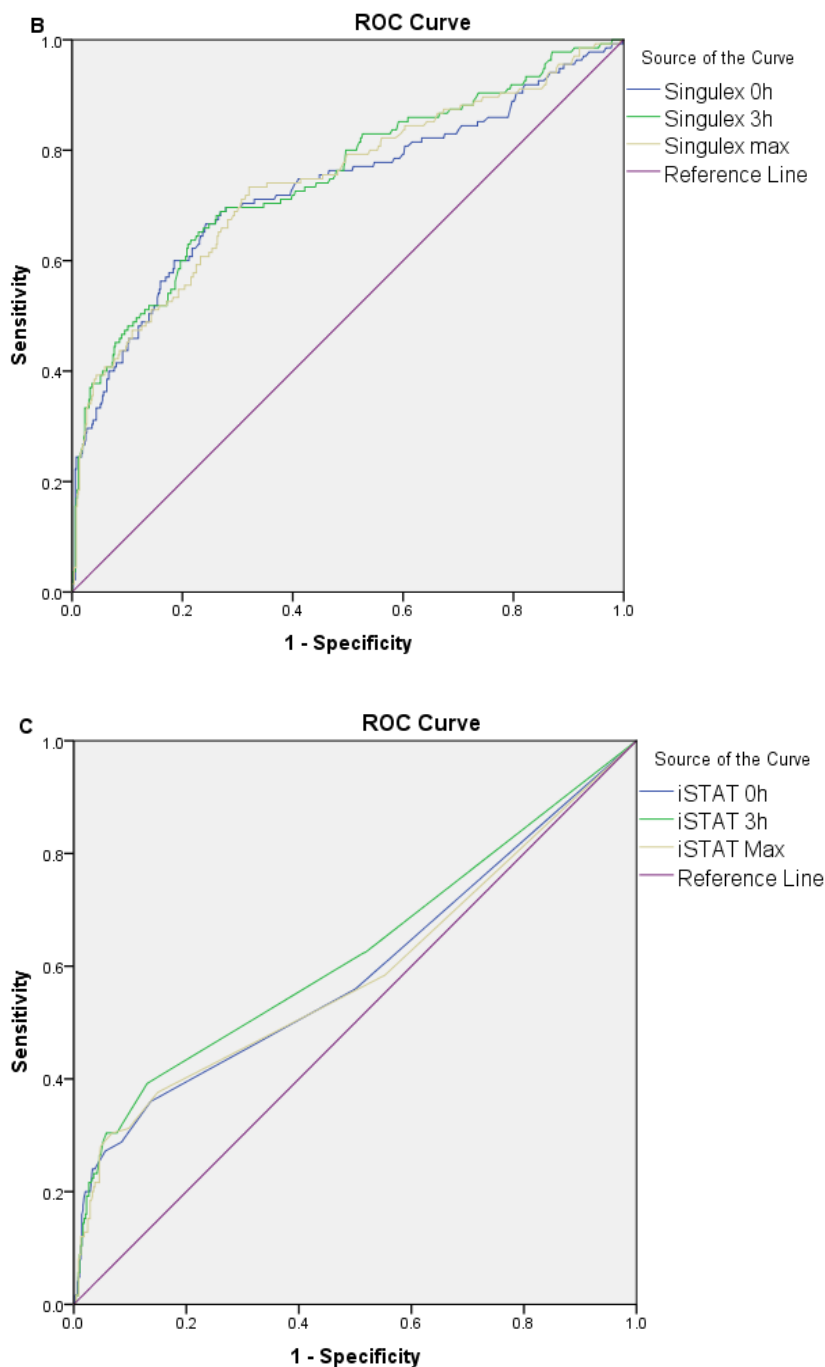


**Figure 6.3 ROC curve of cTn 0h, 3h and maximum values according to the Roche, Singulex and iSTAT assays for 30-day composite MACE** Each graph represents the results from one assay. Each line within the graphs represents the ROC curve associated with either 0h, 3h or maximum values, as specified in the legends. A) Roche assay curves; B) Singulex assay curves; C) iSTAT assay curves. 0h: 0h cTn sample; 3h: 3h cTn sample; max: maximum cTn value of the 0h or 3h samples. The composite MACE group included all outcomes: all-cause mortality, AMI, revascularisation, PCI, CABG, stenosis, tests for heart disease, cardiac arrest, arrhythmia and acute heart failure.

**Table 6.3 30-day composite MACE prediction by cTn 0h, 3h and max values according to the Roche, Singulex and iSTAT assays**

	AUC (95% CI)	P	Cut-off (pg/ml)	Sensitivity	Specificity	PPV	NPV
<i>Roche</i>							
<b>0h</b>	0.656 (0.594 – 0.717)	< 0.001	5.03	65.0 (55.9 – 73.4)	55.8 (51.4 – 60.2)	26.1 (23.1 – 29.3)	87.0 (83.8 – 89.6)
<b>3h</b>	0.664 (0.601 – 0.726)	< 0.001	5.03	65.9 (56.8 – 74.2)	53.1 (48.7 – 57.5)	25.2 (22.3 – 28.2)	86.7 (83.4 – 89.4)
<b>Max</b>	0.661 (0.598 – 0.724)	< 0.001	5.03	68.3 (59.3 – 76.4)	49.8 (45.4 – 54.2)	24.6 (21.9 – 29.6)	86.8 (83.3 – 89.6)
<i>Singulex</i>							
<b>0h</b>	0.726 (0.664 – 0.788)	< 0.001	0.53	96.3 (91.6 – 98.8)	8.6 (6.3 – 11.3)	21.4 (91.8 – 98.4)	8.6 (7.8 – 9.4)
<b>3h</b>	0.741 (0.682 – 0.800)	< 0.001	0.53	97.8 (93.6 – 100.0)	9.9 (7.5 – 12.8)	21.9 (21.2 – 22.5)	94.6 (84.6 – 98.2)
<b>Max</b>	0.736 (0.677 – 0.796)	< 0.001	0.53	98.5 (94.7 – 99.8)	5.5 (3.7 – 7.9)	21.2 (20.7 – 21.7)	93.6 (77.8 – 98.4)
<i>iSTAT</i>							
<b>0h</b>	0.606 (0.539 – 0.673)	< 0.001	100	20.2 (13.5 – 28.3)	97.1 (95.2 – 98.4)	64.1 (48.9 – 76.9)	82.5 (81.2 – 83.8)
<b>3h</b>	0.652 (0.587 – 0.716)	< 0.001	100	23.4 (16.3 – 31.8)	95.8 (93.7 – 97.4)	59.2 (45.9 – 71.2)	82.9 (81.5 – 84.3)
<b>Max</b>	0.601 (0.533 – 0.669)	< 0.001	100	21.8 (14.9 – 30.1)	95.4 (93.2 – 97.1)	55.1 (42.0 – 67.5)	82.6 (81.1 – 83.9)

Cut-offs were determined by the concentration the assay exhibits <10% CV. Starred (\*) values are ROC-derived cut-offs.



#### 6.4 30-day AV1 prediction by cTn 0h, 3h and max values according to the Roche, Singulex and iSTAT assays

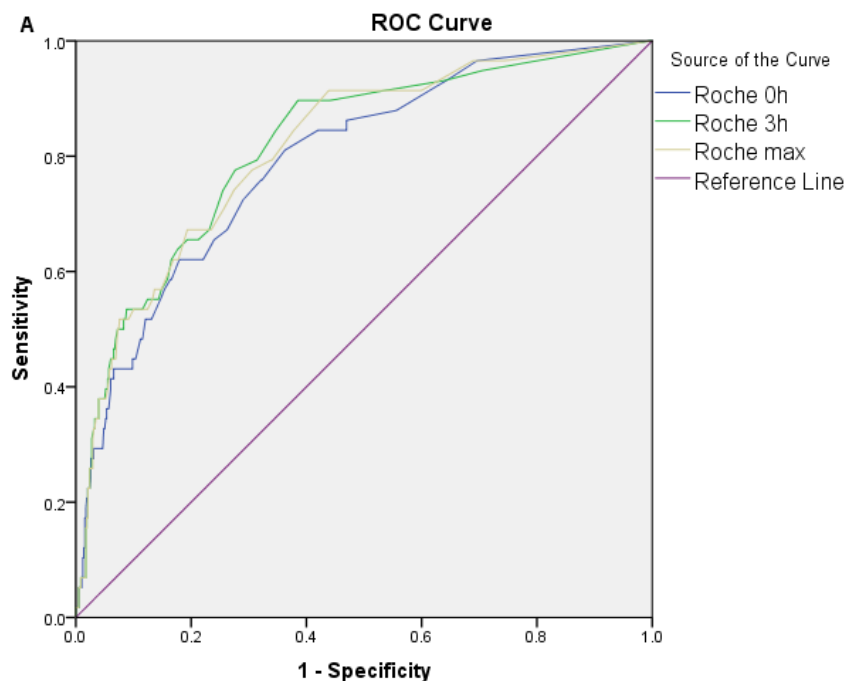
The prognostic accuracy of the Roche, Singulex and iSTAT assays for 30-day AV1 prediction are shown as ROC curves in figure 6.4. The AUC for the 0h, 3h and max values for the Roche assay are 0.814 (95% CI, 0.756 – 0.872), 0.837 (95% CI, 0.780 – 0.893) and 0.837 (95% CI, 0.783 – 0.891), respectively. The respective AUC for the Singulex assay are 0.867 (95% CI, 0.804 – 0.931), 0.861 (95% CI, 0.795 – 0.927) and 0.872 (95% CI, 0.812 – 0.931), respectively and for the iSTAT assay are 0.867 (95% CI, 0.804 – 0.931), 0.784 (95% CI, 0.712 – 0.855) and 0.707 (95% CI, 0.619 – 0.795), respectively.

The prediction accuracy of the three assays for 0h, 3h and max values for 30-day AV1 prognosis are shown in table 6.4. The sensitivities of the Roche assay for 0h, 3h and max values are 89.3% (95% CI, 78.1 – 96.0), 83.3% (95% CI, 71.5 – 91.7) and 86.9% (95% CI, 75.8 – 94.2), respectively and NPVs of 98.2% (95% CI, 96.2 – 99.1), 97.2% (95% CI, 95.2 – 98.4) and 97.7% (95% CI, 95.6 – 98.8), respectively. The respective specificities were 56.0% (95% CI, 51.8 – 60.1), 54.3% (95% CI, 50.3 – 58.2) and 51.7% (95% CI, 47.8 – 55.6) and the PPVs were low for 0h, 3h and max values at 16.5% (95% CI, 14.8 – 18.4), 14.6% (95% CI, 12.9 – 16.4) and 14.5% (95% CI, 13.0 – 16.1).

The Singulex assay produced the highest sensitivity for the AV1 composite out of the three assays and were 98.1% (95% CI, 89.9 – 100.0), 96.2% (95% CI, 86.8 – 99.5) and 100.0% (95% CI, 94.0 – 100.0) for 0h, 3h and max values. The respective NPV are also high at 98.2% (95% CI, 96.2 – 99.1), 97.2% (95% CI, 95.2 – 98.4) and 100.0%. The specificities for 0h, 3h and max values are low at 7.7% (95% CI, 5.6 –

10.3), 8.7% (95% CI, 6.4 – 11.5) and 5.1% (95% CI, 3.5 – 7.2), respectively and were also low for the PPVs at 16.5% (95% CI, 14.8 – 18.4), 10.0% (95% CI, 9.4 – 10.5) and 9.8% (95% CI, 9.6 – 9.9), respectively.

As with previous analyses, the iSTAT assay had much higher cut-offs that lead to the differences between the iSTAT and the other assays, especially when considering sensitivity and specificity. For the iSTAT sensitivities for 0h, 3h and max values were 20.2% (95% CI, 13.5 – 28.3), 23.4% (95% CI, 16.3 – 31.8) and 21.8% (95% CI, 14.9 – 30.1), respectively (all  $p < 0.001$  vs equivalents of Roche and Singulex assays). The respective specificities were higher at 97.1% (95% CI, 95.2 – 98.4), 95.8% (95% CI, 93.7 – 97.4) and 95.4% (95% CI, 93.2 – 97.1) and the PPVs were the highest of all assays (64.1%, 95% CI 48.9 – 76.9; 59.2%, 95% CI 45.9 – 71.2; 55.1%, 95% CI 42.0 – 67.5, all  $p < 0.001$  vs equivalents of Roche and Singulex). The NPVs for 0h, 3h and max values were 82.5% (95% CI, 81.2 – 83.8), 82.9% (95% CI, 81.5 – 84.3) and 82.6% (95% CI, 81.1 – 83.9), respectively.



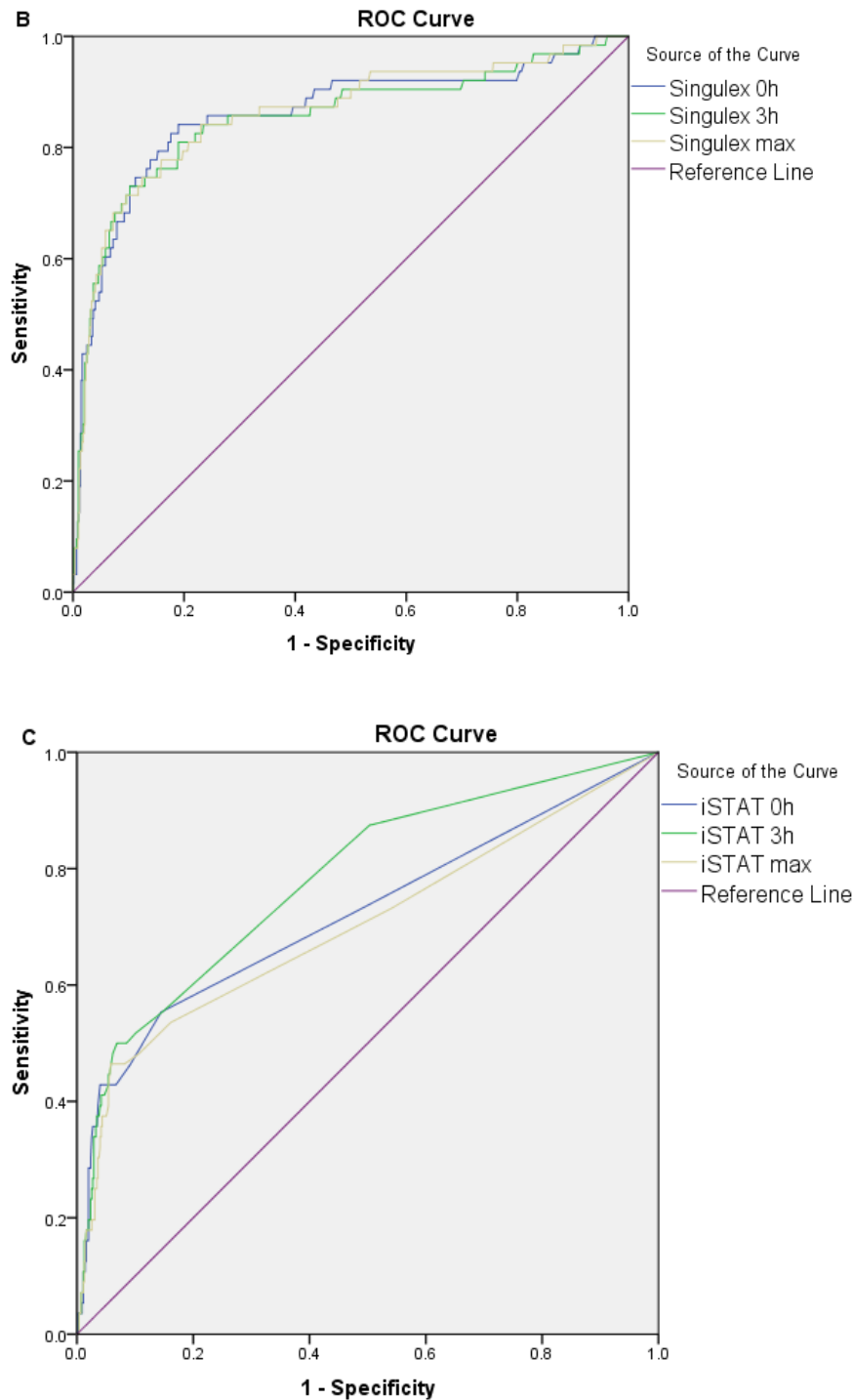


**Figure 6.4 ROC curve of cTn 0h, 3h and maximum values according to the Roche, Singulex and iSTAT assays for 30-day adverse events 1 prognosis.** Each graph represents the results from one assay. Each line within the graphs represents the ROC curve associated with either 0h, 3h or maximum values, as specified in the legends. A) Roche assay curves; B) Singulex assay curves; C) iSTAT assay curves. 0h: 0h cTn sample; 3h: 3h cTn sample; max: maximum cTn value of the 0h or 3h samples. Adverse events 1 included all-cause mortality, AMI, revascularisation, PCI, CABG and stenosis.

**Table 6.4 30-day adverse events 1 prediction by cTn 0h, 3h and max values according to the Roche, Singulex and iSTAT assays**

	AUC (95% CI)	P	Cut-off (pg/ml)	Sensitivity	Specificity	PPV	NPV
<i>Roche</i>							
<b>0h</b>	0.814 (0.756 – 0.872)	< 0.001	5.03	89.3 (78.1 – 96.0)	56.0 (51.8 – 60.1)	16.5 (14.8 – 18.4)	98.2 (96.2 – 99.1)
<b>3h</b>	0.837 (0.780 – 0.893)	< 0.001	5.03	83.3 (71.5 – 91.7)	54.3 (50.3 – 58.2)	14.6 (12.9 – 16.4)	97.2 (95.2 – 98.4)
<b>Max</b>	0.837 (0.783 – 0.891)	< 0.001	5.03	86.9 (75.8 – 94.2)	51.7 (47.8 – 55.6)	14.5 (13.0 – 16.1)	97.7 (95.6 – 98.8)
<i>Singulex</i>							
<b>0h</b>	0.867 (0.804 – 0.931)	< 0.001	0.53	98.1 (89.9 – 100.0)	7.7 (5.6 – 10.3)	9.6 (9.2 – 10.0)	97.6 (85.2 – 100.0)
<b>3h</b>	0.861 (0.795 – 0.927)	< 0.001	0.53	96.2 (86.8 – 99.5)	8.7 (6.4 – 11.5)	10.0 (9.4 – 10.5)	95.6 (84.3 – 98.6)
<b>Max</b>	0.872 (0.812 – 0.931)	< 0.001	0.53	100.0 (94.0 – 100)	5.1 (3.5 – 7.2)	9.8 (9.6 – 9.9)	100.0
<i>iSTAT</i>							
<b>0h</b>	0.728 (0.642 – 0.814)	< 0.001	100	20.2 (13.5 – 28.3)	97.1 (95.2 – 98.4)	64.1 (48.9 – 76.9)	82.5 (81.2 – 83.8)
<b>3h</b>	0.784 (0.712 – 0.855)	< 0.001	100	23.4 (16.3 – 31.8)	95.8 (93.7 – 97.4)	59.2 (45.9 – 71.2)	82.9 (81.5 – 84.3)
<b>Max</b>	0.707 (0.619 – 0.795)	< 0.001	100	21.8 (14.9 – 30.1)	95.4 (93.2 – 97.1)	55.1 (42.0 – 67.5)	82.6 (81.1 – 83.9)

Cut-offs were determined by the concentration the assay exhibits <10% CV. Starred (\*) values are ROC-derived cut-offs.

### 6.5 30-day AV2 prediction by cTn 0h, 3h and max values according to the Roche, Singulex and iSTAT assays

The predictive accuracy for AV2 by the cTn values is shown as ROC curves in figure

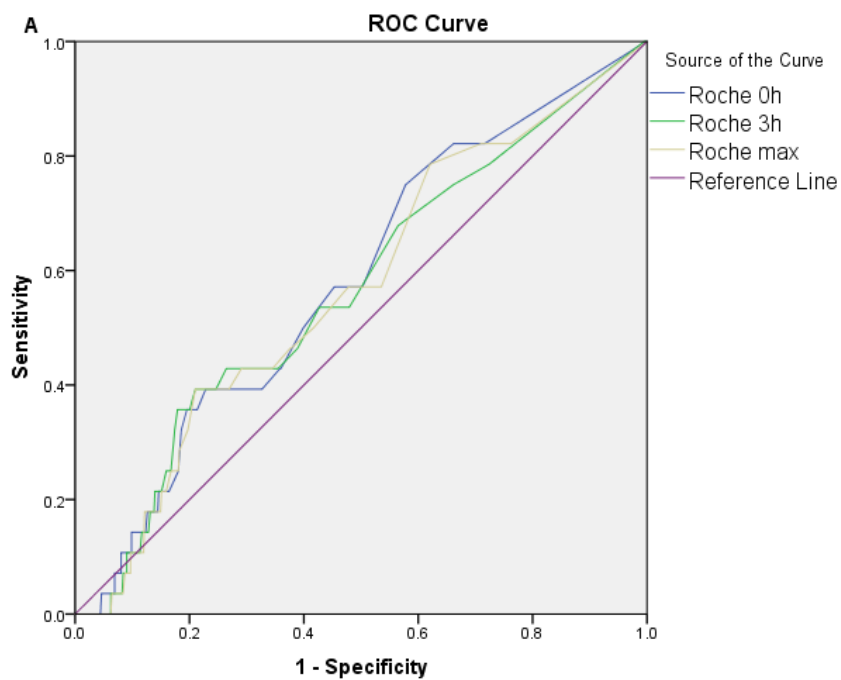
6.5. The Roche AUC are 0.582 (95% CI 0.479 – 0.686), 0.568 (95% CI 0.458 – 0.677) and 0.570 (95% CI 0.463 – 0.676) for 0h, 3h and max values, respectively. The respective AUC for the Singulex assay is 0.611 (95% CI, 0.510 – 0.712), 0.642 (95% CI, 0.546 – 0.737) and 0.621 (95% CI, 0.524 – 0.719) and for the iSTAT assay are 0.526 (95% CI, 0.410 – 0.641), 0.559 (95% CI, 0.438 – 0.680) and 0.597 (95% CI, 0.478 – 0.716).

The predictive accuracy of cTn values for composite endpoint AV2 prognosis according to the three assays is shown in table 6.5. The Roche assay had intermediate but consistent results for 0h, 3h and max values when concerning sensitivity (59.3%, 95% CI 38.8 – 77.6; 52.2%, 95% CI 48.0 – 56.5; 59.3%, 95% CI 38.8 – 77.6, respectively) and specificity (50.3%, 95% CI 46.0 – 54.5; 52.2%, 95% CI 48.0 – 56.5; 46.9%, 95% CI 42.7 – 51.1, respectively). The PPVs for 0h, 3h and max values were low but also consistent at 5.4% (95% CI 4.00 – 7.4), 5.3% (95% CI, 3.8 – 7.4) and 5.1% (95% CI, 3.8 – 6.9), respectively, and the NPVs were high at 96.2% (95% CI, 94.2 – 97.6), 96.1% (95% CI, 94.1 – 97.4) and 96.0% (95% CI, 93.7 – 97.4), respectively.

The Singulex assay showed promising rule out capabilities with sensitivities of 96.3 (95% CI, 81.0 – 99.9) for 0h, 3h and max values and NPVs of 97.9% (95% CI, 86.8 – 99.7), 98.0% (95% CI, 87.8 – 99.7) and 96.6% (95% CI, 79.8 – 99.5), respectively. This had a significant effect on the respective specificities at 8.2% (95% CI, 6.1 – 10.8),

8.9% (95% CI, 6.7 – 11.6) and 5.0% (95% CI, 3.4 – 7.2) and the PPVs at 4.8% (95% CI, 4.5 – 5.2), 4.8% (95% CI, 4.5 – 5.2) and 4.7% (95% CI, 4.3 – 5.0).

The iSTAT assay had high specificities for 0h, 3h and max values at 93.6% (95% CI, 91.2 – 95.5), 92.1% (95% CI, 89.6 – 94.2) and 92.1% (95% CI, 89.6 – 94.2), respectively, and high NPVs at 95.6% (95% CI, 95.3 – 96.0), 95.7% (95% CI, 95.2 – 96.2) and 92.1% (95% CI, 89.6 – 94.2), respectively. The respective sensitivities are low at 4.0% (95% CI 0.1 – 20.4), 8.0% (95% CI, 1.0 – 26.0) and 8.0% (95% CI, 1.0 – 26.0), as are the PPVs at 2.7% (95% CI, 0.4 – 16.3), 4.4% (95% CI 1.2 – 15.0) and 4.4% (95% CI 1.2 – 15.0) for 0h, 3h and max values, respectively.



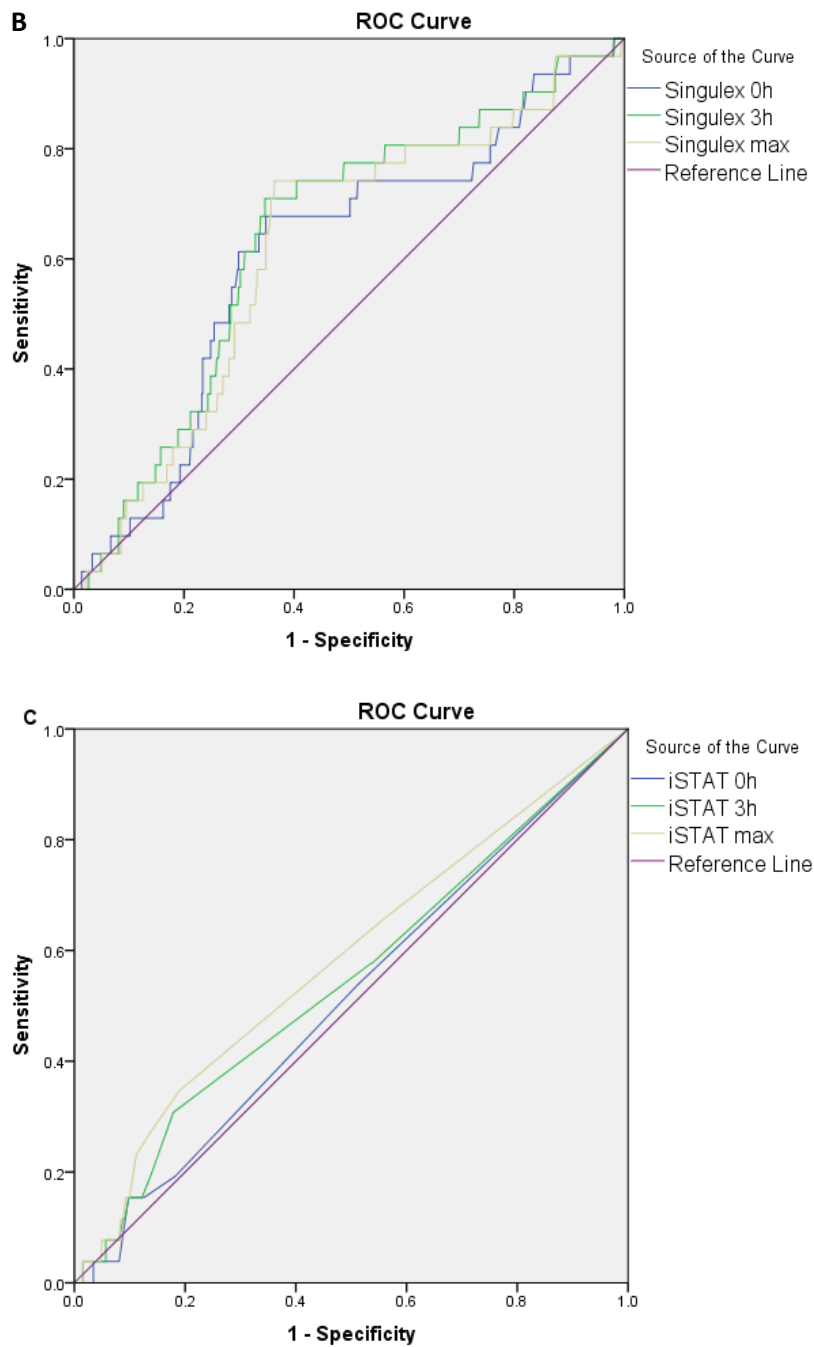


**Figure 6.5 ROC curve of cTn 0h, 3h and maximum values according to the Roche, Singulex and iSTAT assays for 30-day adverse events 2 prognosis.** Each graph represents the results from one assay. Each line within the graphs represents the ROC curve associated with either 0h, 3h or maximum values, as specified in the legends. A) Roche assay curves; B) Singulex assay curves; C) iSTAT assay curves. 0h: 0h cTn sample; 3h: 3h cTn sample; max: maximum cTn value of the 0h or 3h samples. Adverse events 2 included cardiac arrest, arrhythmia and acute heart failure.

**Table 6.5 30-day AV2 prediction by cTn 0h, 3h and max values according to the Roche, Singulex and iSTAT assays**

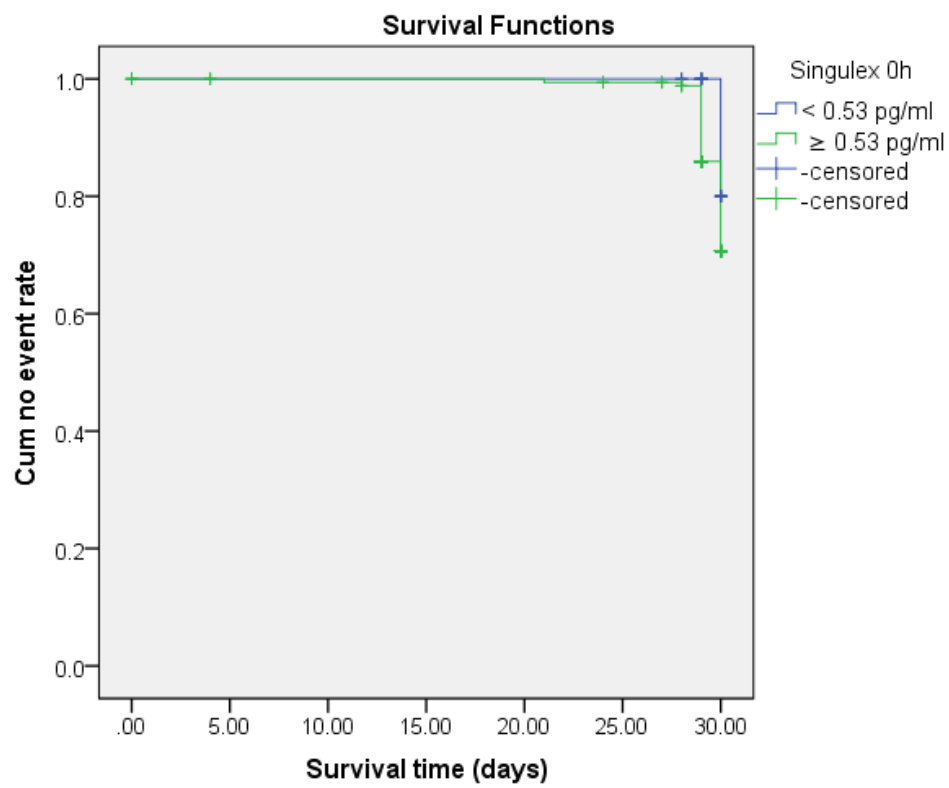
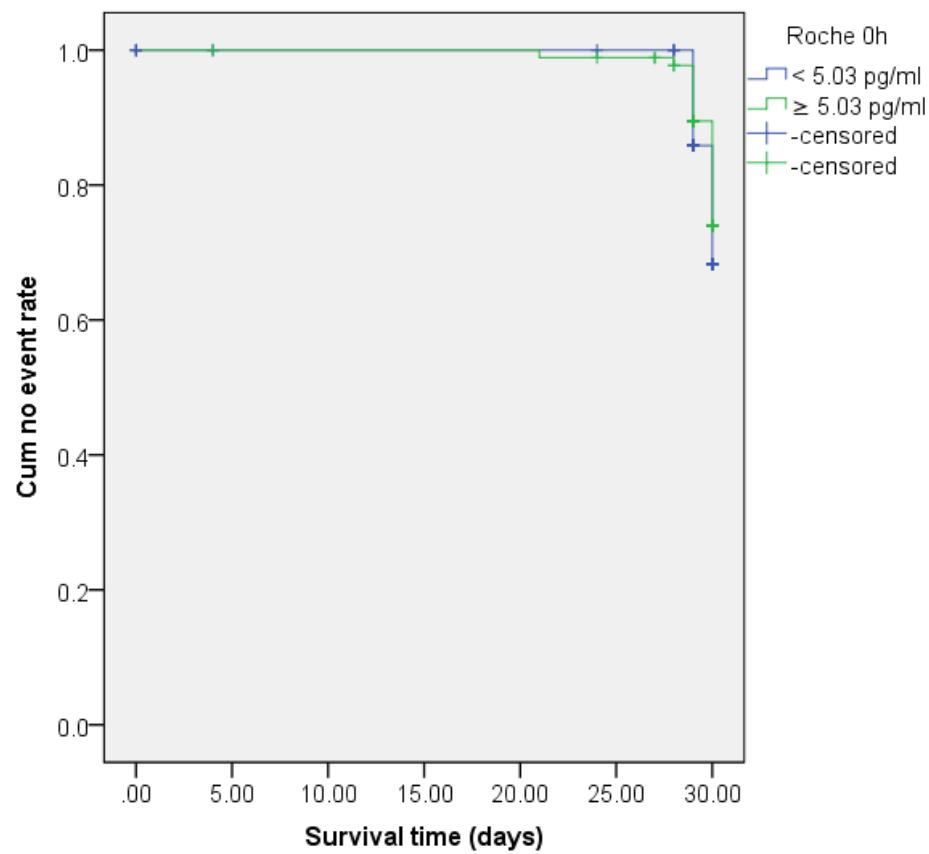
	AUC (95% CI)	P	Cut-off (pg/ml)	Sensitivity	Specificity	PPV	NPV
<i>Roche</i>							
<b>0h</b>	0.582 (0.479 – 0.686)	0.140	5.03	59.3 (38.8 – 77.6)	50.3 (46.0 – 54.5)	5.4 (4.00 – 7.4)	96.2 (94.2 – 97.6)
<b>3h</b>	0.568 (0.458 – 0.677)	0.226	5.03	55.6 (35.3 – 74.5)	52.2 (48.0 – 56.5)	5.3 (3.8 – 7.4)	96.1 (94.1 – 97.4)
<b>Max</b>	0.570 (0.463 – 0.676)	0.212	5.03	59.3 (38.8 – 77.6)	46.9 (42.7 – 51.1)	5.1 (3.8 – 6.9)	96.0 (93.7 – 97.4)
<i>Singulex</i>							
<b>0h</b>	0.611 (0.510 – 0.712)	0.037	0.53	96.3 (81.0 – 99.9)	8.2 (6.1 – 10.8)	4.8 (4.5 – 5.2)	97.9 (86.8 – 99.7)
<b>3h</b>	0.642 (0.546 – 0.737)	0.008	0.53	96.3 (81.0 – 99.9)	8.9 (6.7 – 11.6)	4.8 (4.5 – 5.24)	98.0 (87.8 – 99.7)
<b>Max</b>	0.621 (0.524 – 0.719)	0.022	0.53	96.3 (81.0 – 99.9)	5.0 (3.4 – 7.2)	4.7 (4.3 – 5.0)	96.6 (79.8 – 99.5)
<i>iSTAT</i>							
<b>0h</b>	0.526 (0.410 – 0.641)	0.661	100	4.0 (0.1 – 20.4)	93.6 (91.2 – 95.5)	2.7 (0.4 – 16.3)	95.6 (95.3 – 96.0)
<b>3h</b>	0.559 (0.438 – 0.680)	0.317	100	8.0 (1.0 – 26.0)	92.1 (89.6 – 94.2)	4.4 (1.2 – 15.0)	95.7 (95.2 – 96.2)
<b>Max</b>	0.597 (0.478 – 0.716)	0.100	100	8.0 (1.0 – 26.0)	92.1 (89.6 – 94.2)	4.4 (1.2 – 15.0)	95.7 (95.2 – 96.2)

Cut-offs were determined by the concentration the assay exhibits <10% CV. Starred (\*) values are ROC-derived cut-offs.



## 6.6 Comparison of the 0h cut-offs of the Roche, Singulex and iSTAT assays as event predictors

Survival analysis was done using the cut-offs used previously in the analyses (Roche: 5.03 pg/ml; Singulex 0.53 pg/ml; iSTAT 100 pg/ml) and presented as Kaplan-Meier curves (figure 6.6). Events are defined as a composite MACE event within 30-days. Differences in survival were assessed for significance using the log rank test. For the Roche assay, the mean time to event for the low cTn group was 29.86 days (95% CI, 29.79 – 29.93) and for the high cTn group was 29.80 days (95% CI, 29.58 – 30.01). The difference was not significant ( $p = 0.449$ ). The mean time to events for the low cTn and high cTn group according to the Singulex assay were 30.00 days (95% CI, 30.00 – 30.00) and 29.81 days (95% CI, 29.69 – 29.92;  $p = 0.170$ ). According to the iSTAT assay, the mean time to event in the low and high cTn groups were 29.88 days (95% CI, 29.82 – 29.93) and 28.88 days (95% CI, 26.35 – 31.40;  $p = 0.300$ ), respectively.



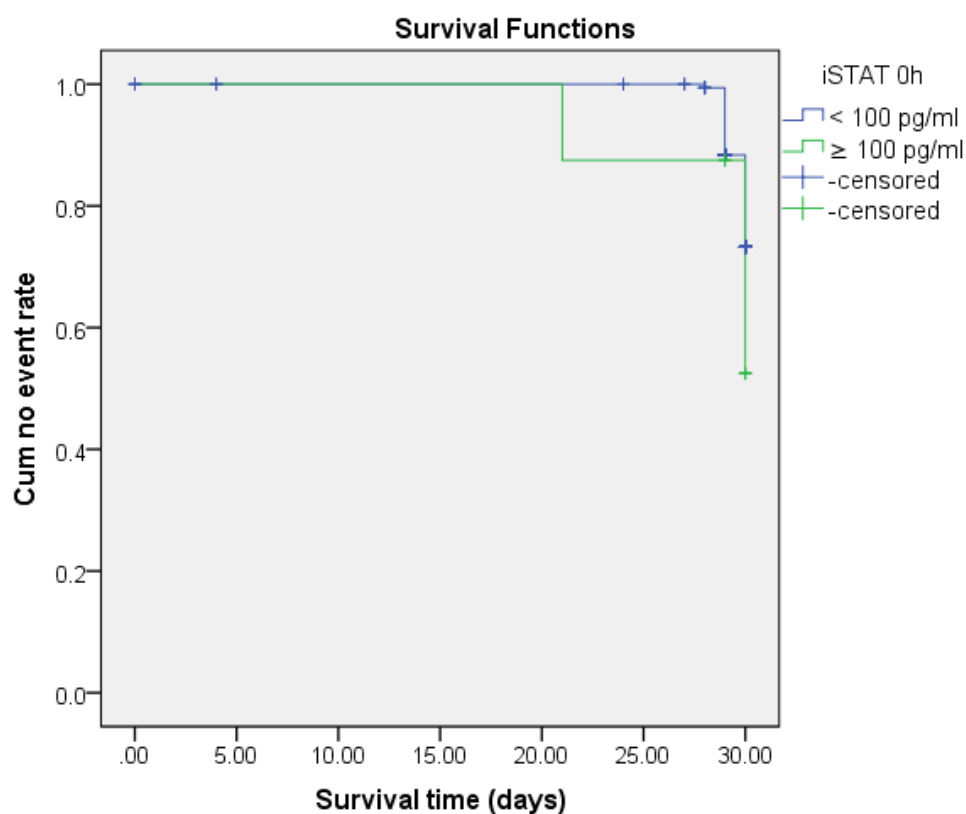


**Figure 6.6 Kaplan-Meier curves for the prognostic value of the 0h cTn sample values for composite MACE prediction between high and low cTn groups according to the Roche, Singulex and iSTAT assays.** A) Roche assay high and low cTn groups; B) Singulex high and low cTn groups; C) iSTAT high and low cTn groups. High cTn groups are in green and low cTn groups in blue. Events occurred within 30-days of presentation to the ED and time to event is counted in days. All curves use the cut-offs of 5.03 pg/ml for the Roche assay, 0.53 pg/ml for the Singulex assay and 100 pg/ml for the iSTAT assay.

### 6.7 Summary of predicting 30 day MACE outcome with cTn values

These analyses assessed if cTn at 0h or 3h could be used to predict 30 day outcome for ACS-related and HF-related conditions. They showed:

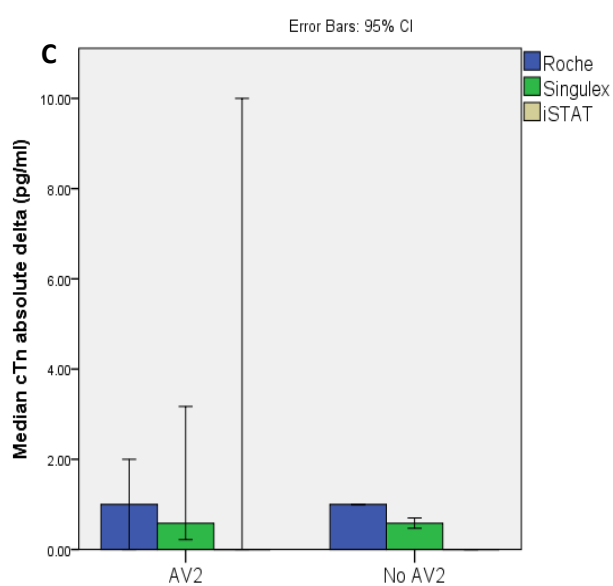
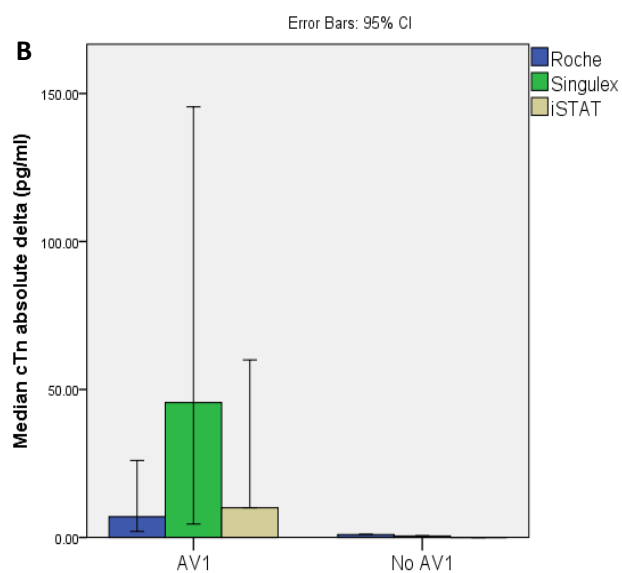
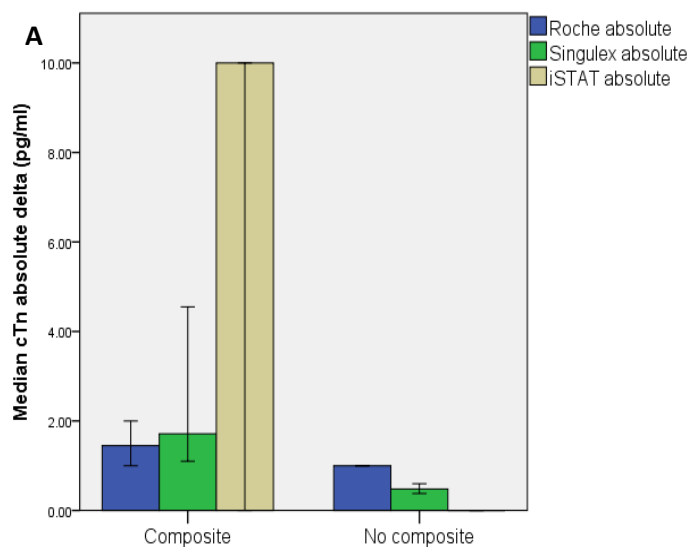
- Only small differences between 0h, 3h and max values occurred and only small differences between assays for same outcome were also similar
- Roche had better accuracy for predicting ACS-related outcomes (AV1) than HF-related outcomes (AV2)
- iSTAT had high specificity for predicting a MACE event within 30 days

## **Chapter 7: Does kinetic cTn predict 30-day outcome?**

The baseline characteristics of the cohort are found in at the beginning of chapter 4, prediction of 30-day MACE using cTn values of the Roche, Singulex and iSTAT assays. As previously, 10 cardiac-related conditions were grouped into three composites to assess the prognostic strength of the deltas. The 10 conditions were all-cause mortality, AMI, revascularisation, PCI, CABG, stenosis, tests for heart disease, cardiac arrest, arrhythmia and acute heart failure. The composite MACE group included all outcomes; AV1 included all-cause mortality, AMI, revascularisation, PCI, CABG and stenosis; adverse events 2 included cardiac arrest, arrhythmia and acute heart failure. All outcomes included events that occurred 30 days post-presentation.

#### 7.1 $\Delta_{\text{absolute}}$ of different 30-day composite outcomes

The  $\Delta_{\text{absolute}}$  of the different assays according to 30-day diagnosis of the aforementioned conditions are shown in figure 7.1. Independent samples Mann-Whitney U tests showed that there were significant differences in the distributions between positive and negative composite MACE groups and AV1 across all assays,  $p < 0.001$ . In the case of AV2, Roche, Singulex and iSTAT reported no difference in the distribution between the positive and negative patients ( $p = 0.742, 0.630$  and  $0.183$ , respectively).



Error Bars: 95% CI

**Figure 7.1 Median cTn  $\Delta_{\text{absolute}}$  by different 30-day prognoses according to the Roche, Singulex and iSTAT assays** Bars are clustered by whether an outcome has occurred or not occurred. Bars include results from one assay, as specified by the legends and are colour coded. Error bars indicate 95% CI. Composite: composite MACE; AV1 – adverse events 1; AV2 – adverse events 2.

## 7.2 % $\Delta_{\text{baseline}}$ of different 30-day composite outcomes

The % $\Delta_{\text{baseline}}$  of the different composite outcomes according to the three different assays are shown in figure 7.2. The difference in distribution was measured via Mann Whitney U test for independent samples for all % $\Delta_{\text{baseline}}$ . For composite MACE outcomes, distributions between positive and negative groups were considered different according to the Roche and iSTAT assays ( $p = 0.026$  and  $p < 0.001$ , respectively) but not for the Singulex assay ( $p = 0.849$ ). The same occurred for the AV1 composite with  $p < 0.001$  for Roche and iSTAT and  $p = 0.174$  for the Singulex assay. For the AV2, no significant difference for the Roche, Singulex and iSTAT assays were found ( $p = 0.712$ ,  $0.055$  and  $0.086$ ).



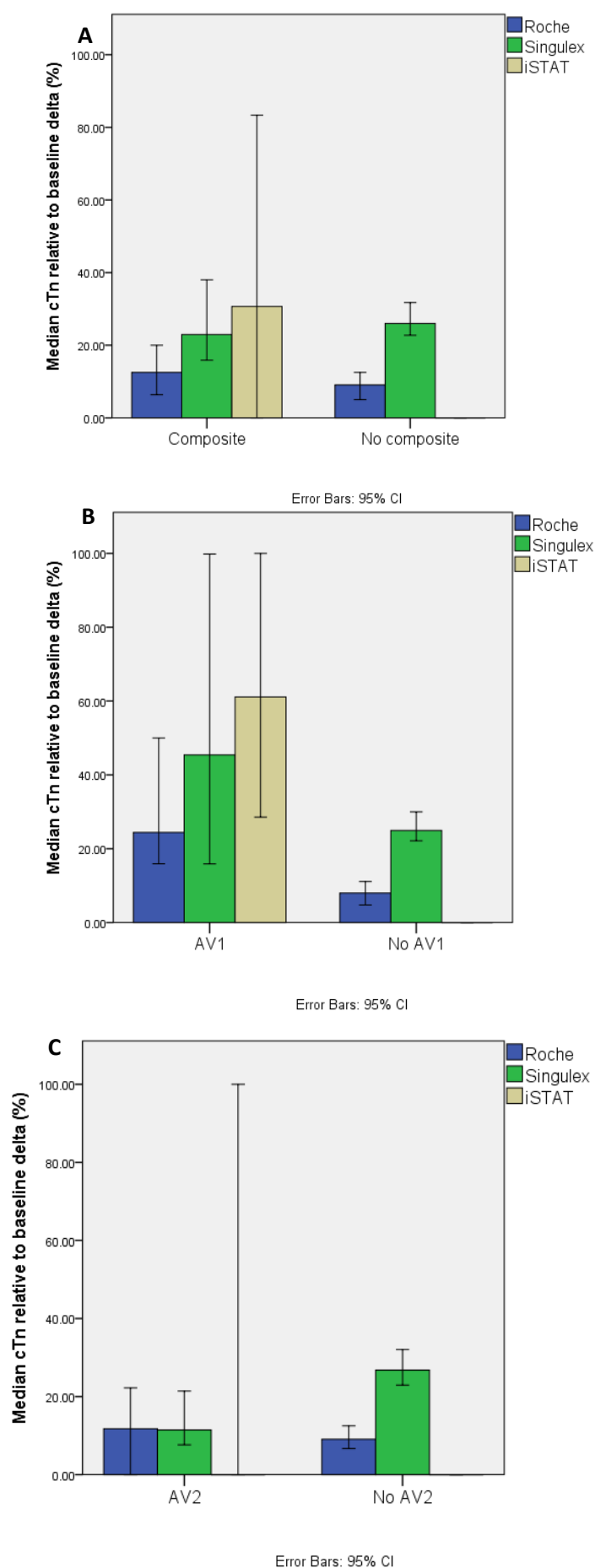
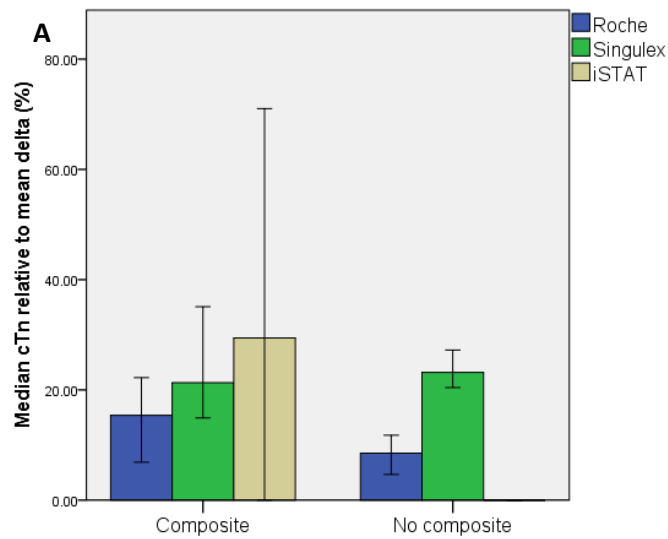


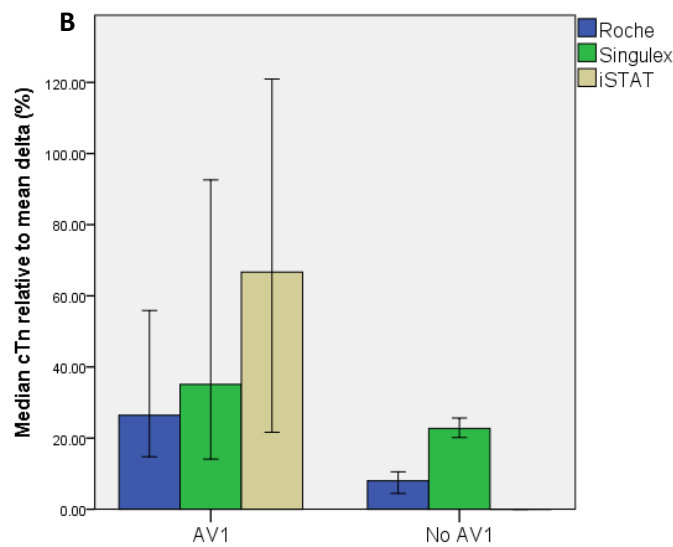
**Figure 7.2 Median cTn  $\Delta$ baseline by different 30-day prognoses according to the Roche, Singulex and iSTAT assays.** Bars are clustered by whether an outcome has occurred or not occurred. Bars include results from one assay, as specified by the legends and are colour coded. Error bars indicate 95% CI. Composite: composite MACE; AV1 – adverse events 1; AV2 – adverse events 2.

### 7.3 % $\Delta_{\text{mean}}$ of different 30-day composite outcomes

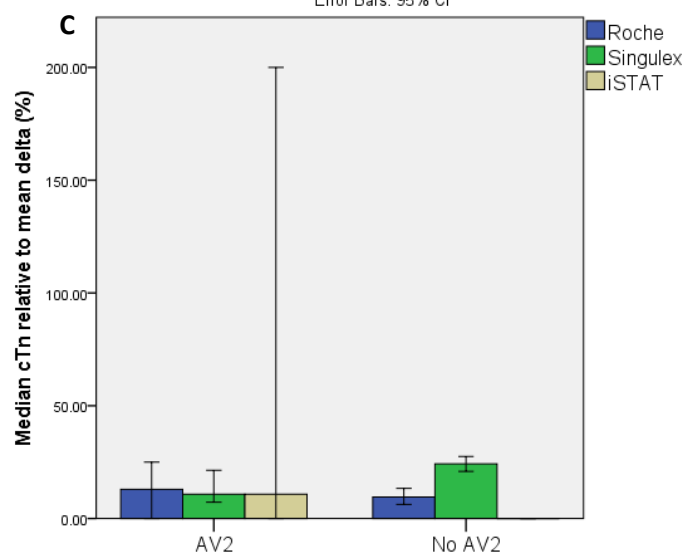
The different medians of % $\Delta_{\text{mean}}$  of the positive and negative patients of different 30-day composite outcomes are shown in figure 7.3. The Singulex assay did not show any significant difference between the positive and negative groups for the composite MACE, AV1 and AV2 ( $p = 0.702, 0.181, 0.053$ ). The Roche assay reported significant differences between the positive and negative groups of the composite MACE and AV1 outcomes ( $p = 0.047$ , and  $< 0.001$ , respectively) but not in the AV2 outcomes group ( $p = 0.727$ ). The iSTAT assay showed a significant difference between positive and negative groups in the composite MACE and AV1 outcomes (both  $p < 0.001$ ) but not in the AV2 group ( $p = 0.164$ ).



Error Bars: 95% CI



Error Bars: 95% CI



Error Bars: 95% CI

**Figure 7.3 Median cTn % $\Delta_{\text{mean}}$  by different 30-day prognoses according to the Roche, Singulex and iSTAT assays.** Bars are clustered by whether an outcome has occurred or not occurred. Bars include results from one assay, as specified by the legends and are colour coded. Error bars indicate 95% CI. Composite: composite MACE; AV1 – adverse events 1; AV2 – adverse events 2.

#### 7.4 30-day composite MACE prediction by cTn $\Delta_{\text{absolute}}$ , $\% \Delta_{\text{baseline}}$ and $\% \Delta_{\text{mean}}$ according to the Roche, Singulex and iSTAT assays

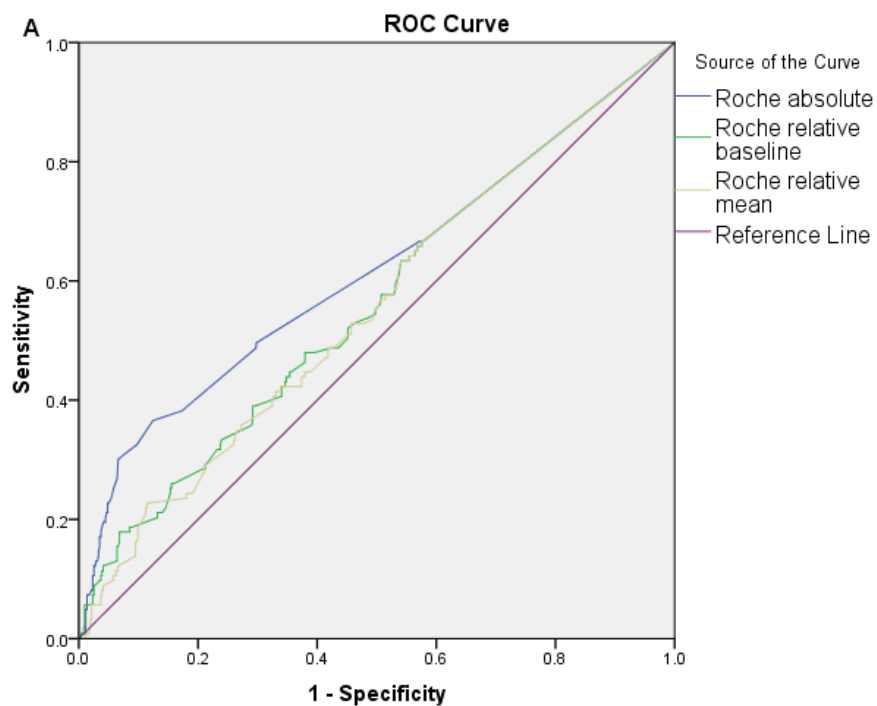
The ROC curve analysis is available in figure 7.4 and the AUROC available in table

7.4. The Roche assay produced AUROCs for the  $\Delta_{\text{absolute}}$ ,  $\% \Delta_{\text{baseline}}$  and  $\% \Delta_{\text{mean}}$  of 0.638 (95% CI, 0.572 – 0.703), 0.581 (95% CI, 0.519 – 0.643) and 0.575 (95% CI, 0.513 – 0.636), respectively. The respective AUROCs for the Singulex assay show higher overall diagnostic accuracy at for  $\Delta_{\text{absolute}}$  0.690 (95% CI, 0.628 – 0.752) but not for,  $\% \Delta_{\text{baseline}}$  and  $\% \Delta_{\text{mean}}$  (0.533, 95% CI 0.468 – 0.599; 0.524, 95% CI 0.460 – 0.589, respectively). The iSTAT assay had the highest overall prognostic accuracy for the respective variables at 0.657 (95% CI, 0.593 – 0.720), 0.614 (95% CI, 0.553 – 0.675) and 0.587 (95% CI, 0.529 – 0.645).

The prognostic accuracy of cTn deltas for adverse events 1 within 30 days according to the Roche, Singulex and iSTAT assays are shown in table 7.4. For the Roche assay, the  $\Delta_{\text{absolute}}$  sensitivity is lower than the  $\% \Delta_{\text{baseline}}$  and  $\% \Delta_{\text{mean}}$  (30.7%, 95% 22.7 – 39.6; 41.3%, 95% CI 31.9 – 51.1; 65.1%, 95% CI 55.4 – 74.0, respectively) but the opposite is true with the PPV (48.7%, 95% CI 38.9 – 58.6; 31.7%, 95% CI 25.9 – 38.1; 23.4%, 95% CI 20.7 – 26.5). The specificity for  $\Delta_{\text{absolute}}$  was higher at 92.3% (95% CI, 89.7 – 94.4) than the  $\% \Delta_{\text{baseline}}$  and  $\% \Delta_{\text{mean}}$  (76.7%, 95% CI 72.3 – 80.7 and 44.2% 95% CI 39.4 – 49.2, respectively).

The Singulex assay showed a 100% NPV for all deltas and a sensitivity of 100% (95% CI, 96.7 – 100.0) for all deltas meaning all patients below the cut-off could be successfully ruled out of 30-day composite MACE prognosis. The low cut-off means there is very low specificity across all deltas (0.7%, 95% CI 0.2 – 2.1) and low PPV (all 20.9%, 95% CI 20.8 – 21.0).

The higher  $\Delta_{\text{absolute}}$  cut-off for the iSTAT produced a lower sensitivity (19.4%, 95% CI 12.8 – 27.4) than the other two assays and sensitivities of 56.0% (95% CI, 46.1 – 65.5) and 56.8% (95% CI, 47.1 – 66.3) for  $\% \Delta_{\text{baseline}}$  and  $\% \Delta_{\text{mean}}$ , respectively. Specificities for  $\Delta_{\text{absolute}}$ ,  $\% \Delta_{\text{baseline}}$  and  $\% \Delta_{\text{mean}}$  were higher at 96.5% (95% CI, 94.4 – 97.9), 66.6% (95% CI, 61.8 – 71.1) and 66.8% (95% CI, 62.1 – 71.3), respectively. The NPVs are consistent across the  $\Delta_{\text{absolute}}$ ,  $\% \Delta_{\text{baseline}}$  and  $\% \Delta_{\text{mean}}$  at 82.3% (95% CI, 81.0 – 83.5), 85.2% (95% CI, 82.2 – 87.8) and 85.5% (95% CI, 82.5 – 88.1) but there were discrepancies between the PPVs (58.5%, 95% CI 43.9 – 71.8; 30.5%, 95% CI 26.2 – 35.2; 31.0%, 95% CI 26.6 – 35.7, respectively).



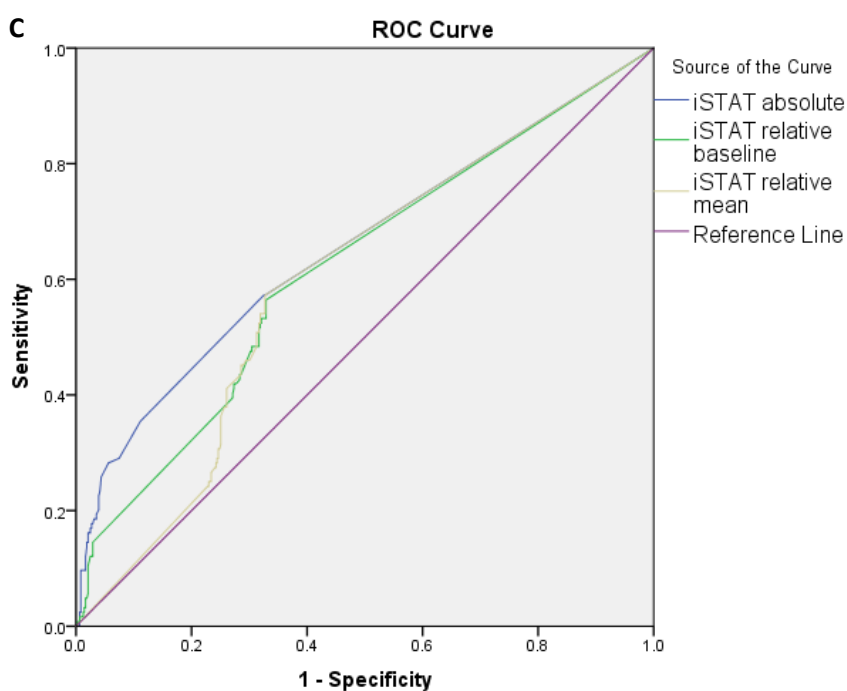
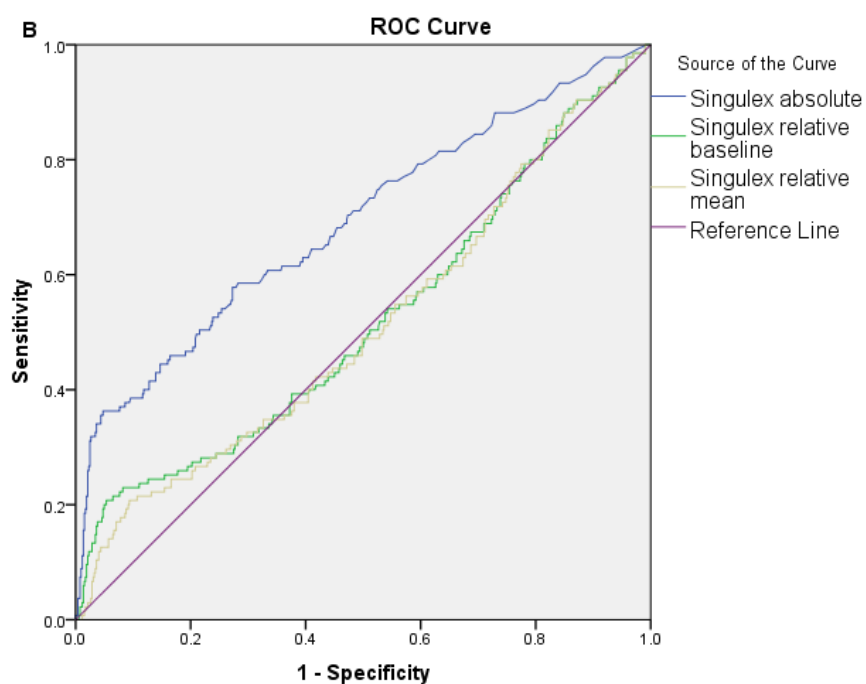


**Figure 7.4 ROC curve of cTn  $\Delta_{\text{absolute}}$ ,  $\% \Delta_{\text{baseline}}$  and  $\% \Delta_{\text{mean}}$  according to the Roche, Singulex and iSTAT assays for 30-day composite MACE.** Each graph represents the results from one assay. Each line within the graphs represents the ROC curve associated with either  $\Delta_{\text{absolute}}$ ,  $\% \Delta_{\text{baseline}}$  and  $\% \Delta_{\text{mean}}$ , as specified in the legends. A) Roche assay curves; B) Singulex assay curves; C) iSTAT assay curves. Absolute:  $\Delta_{\text{absolute}}$ ; relative baseline:  $\% \Delta_{\text{baseline}}$ ; relative mean  $\% \Delta_{\text{mean}}$ . The composite MACE group included all outcomes: all-cause mortality, AMI, revascularisation, PCI, CABG, stenosis, tests for heart disease, cardiac arrest, arrhythmia and acute heart failure.

**Table 7.4 30-day composite MACE prediction by cTn  $\Delta_{\text{absolute}}$ ,  $\% \Delta_{\text{baseline}}$  and  $\% \Delta_{\text{mean}}$  according to the Roche, Singulex and iSTAT assays**

	AUC (95% CI)	P	Cut-off	Sensitivity	Specificity	PPV	NPV
<i>Roche</i>							
$\Delta_{\text{absolute}}$	0.638 (0.572 – 0.703)	< 0.001	5.03	30.7 (22.7 – 39.6)	92.3 (89.7 – 94.4)	48.7 (38.9 – 58.6)	84.7 (83.2 – 86.3)
$\% \Delta_{\text{baseline}}$	0.581 (0.519 – 0.643)	0.009	0.4762*	41.3 (31.9 – 51.1)	76.7 (72.3 – 80.7)	31.7 (25.9 – 38.1)	83.3 (80.9 – 85.5)
$\% \Delta_{\text{mean}}$	0.575 (0.513 – 0.636)	0.017	3.8476*	65.1 (55.4 – 74.0)	44.2 (39.4 – 49.2)	23.4 (20.7 – 26.5)	82.9 (78.6 – 86.5)
<i>Singulex</i>							
$\Delta_{\text{absolute}}$	0.690 (0.628 – 0.752)	< 0.001	0.53	100.0 (96.7 – 100.0)	0.7 (0.2 – 2.1)	20.9 (20.8 – 21.0)	100.0
$\% \Delta_{\text{baseline}}$	0.533 (0.468 – 0.599)	0.282	0.2901*	100.0 (96.7 – 100.0)	0.7 (0.2 – 2.1)	20.9 (20.8 – 21.0)	100.0
$\% \Delta_{\text{mean}}$	0.524 (0.460 – 0.589)	0.432	0.2915*	100.0 (96.7 – 100.0)	0.7 (0.2 – 2.1)	20.9 (20.8 – 21.0)	100.0
<i>iSTAT</i>							
$\Delta_{\text{absolute}}$	0.657 (0.593 – 0.720)	< 0.001	100	19.4 (12.8 – 27.4)	96.5 (94.4 – 97.9)	58.5 (43.9 – 71.8)	82.3 (81.0 – 83.5)
$\% \Delta_{\text{baseline}}$	0.614 (0.553 – 0.675)	< 0.001	1.5150*	56.0 (46.1 – 65.5)	66.6 (61.8 – 71.1)	30.5 (26.2 – 35.2)	85.2 (82.2 – 87.8)
$\% \Delta_{\text{mean}}$	0.587 (0.529 – 0.645)	0.005	1.4950*	56.8 (47.1 – 66.3)	66.8 (62.1 – 71.3)	31.0 (26.6 – 35.7)	85.5 (82.5 – 88.1)

Cut-offs were determined by the concentration the assay exhibits <10% CV. Starred (\*) values are ROC-derived cut-offs.

### 7.5 30-day AV1 prediction cTn $\Delta_{\text{absolute}}$ , $\% \Delta_{\text{baseline}}$ and $\% \Delta_{\text{mean}}$ according to the Roche, Singulex and iSTAT assays

The prognostic accuracy of the three assays for prognosis of AV1 within 30 days is shown in figure 7.5. For the Roche assay, the AUC for  $\Delta_{\text{absolute}}$ ,  $\% \Delta_{\text{baseline}}$  and  $\% \Delta_{\text{mean}}$  were 0.776 (95% CI, 0.700 – 0.853), 0.692 (95% CI, 0.615 – 0.768) and 0.682 (95% CI, 0.607 – 0.757), respectively. The respective AUC for the Singulex assay were 0.827 (95% CI, 0.757 – 0.897), 0.595 (95% CI, 0.492 – 0.677) and 0.585 (95% CI, 0.492 – 0.677) and for the iSTAT were 0.747 (95% CI, 0.666 – 0.828), 0.686 (95% CI, 0.609 – 0.763) and 0.628 (95% CI, 0.560 – 0.696).

The prediction accuracy of the three assays for AV1 prognosis are shown in table 7.5. The Roche assay showed differences in sensitivity between the  $\Delta_{\text{absolute}}$  (19.0%, 95% CI 9.9 - 31.4) and  $\% \Delta_{\text{baseline}}$  and  $\% \Delta_{\text{mean}}$  (59.8%, 95% CI, 50.4 – 68.8; 60.5%, 95% CI 51.1 – 69.3, respectively, both  $p < 0.001$  vs  $\Delta_{\text{absolute}}$ ). The specificity showed an opposite pattern between the higher  $\Delta_{\text{absolute}}$  result (88.5%, 95% CI 85.6 – 91.0) and  $\% \Delta_{\text{baseline}}$  and  $\% \Delta_{\text{mean}}$  at 43.1% (95% CI, 38.5 – 47.7) and 43.1% (95% CI, 38.5 – 47.7), respectively (both  $p < 0.001$  vs  $\Delta_{\text{absolute}}$ ). The PPVs for  $\Delta_{\text{absolute}}$ ,  $\% \Delta_{\text{baseline}}$  and  $\% \Delta_{\text{mean}}$  are low at 14.3% (95% CI, 8.6 – 22.9), 20.8% (95% CI, 18.1 – 23.7) and 21.2% (95% CI, 18.6 – 24.1), respectively, but NPVs are higher at 91.5% (95% CI, 90.5 – 92.4), 81.1% (95% CI, 77.1 – 84.6) and 81.1% (95% CI, 77.1 – 84.6), respectively.

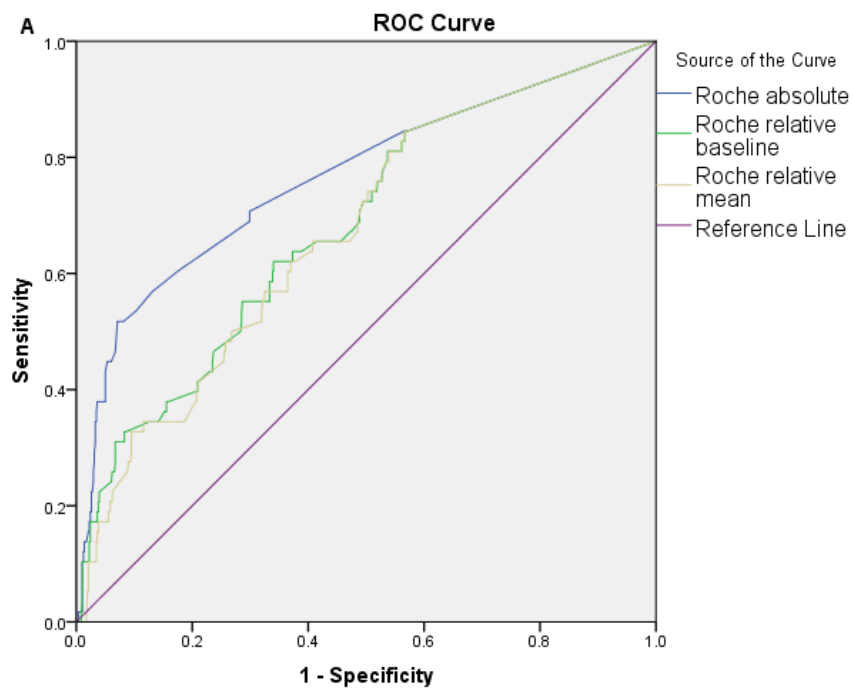
The Singulex assay had sensitivities of 100.0% (95% CI, 94.3 – 100.0) for both  $\% \Delta$  and 100% NPV for the same parameter but the  $\Delta_{\text{absolute}}$  sensitivity was 60.0% (95% CI, 46.5 – 72.4) and its NPV was 92.7% (95% CI, 90.2 – 94.6). However, the specificities for  $\% \Delta_{\text{baseline}}$  and  $\% \Delta_{\text{mean}}$  are 0.8% (95% CI, 0.3 – 2.0) and 0.5% (95% CI, 0.1 – 1.5) and 50.6% (95% CI, 46.5 – 54.7) for  $\Delta_{\text{absolute}}$ . The PPVs for  $\Delta_{\text{absolute}}$ ,  $\% \Delta_{\text{baseline}}$



and  $\Delta_{\text{mean}}$  are 10.8% (95% CI, 8.9 – 13.2), 9.6% (95% CI, 9.6 – 9.7) and 9.6% (95% CI, 9.6 – 9.7), respectively.

The sensitivities of the iSTAT assay for  $\Delta_{\text{absolute}}$ ,  $\Delta_{\text{baseline}}$  and  $\Delta_{\text{mean}}$  were 37.5% (95% CI, 23.4 – 49.6), 55.4% (95% CI 41.5 – 68.7) and 71.4% (95% CI, 57.8 – 82.7).

The specificity of  $\Delta_{\text{absolute}}$  is higher than the  $\Delta_{\text{baseline}}$  and  $\Delta_{\text{mean}}$  (78.2%, 95% CI, 74.5 – 81.6; 66.4%, 95% CI 62.3 – 70.4) and the PPVs follow the same pattern (48.8%, 95% CI 35.5 – 62.2; 20.5%, 95% CI 16.3 – 25.5; 17.9%, 95% CI 15.1 – 21.1, respectively). The NPVs of the iSTAT for  $\Delta_{\text{absolute}}$ ,  $\Delta_{\text{baseline}}$  and  $\Delta_{\text{mean}}$  are similar (93.6%, 95% CI 92.4 – 94.7; 94.5%, 95% CI 92.8 – 95.9; 95.7%, 95% CI 93.7 – 97.2, respectively).



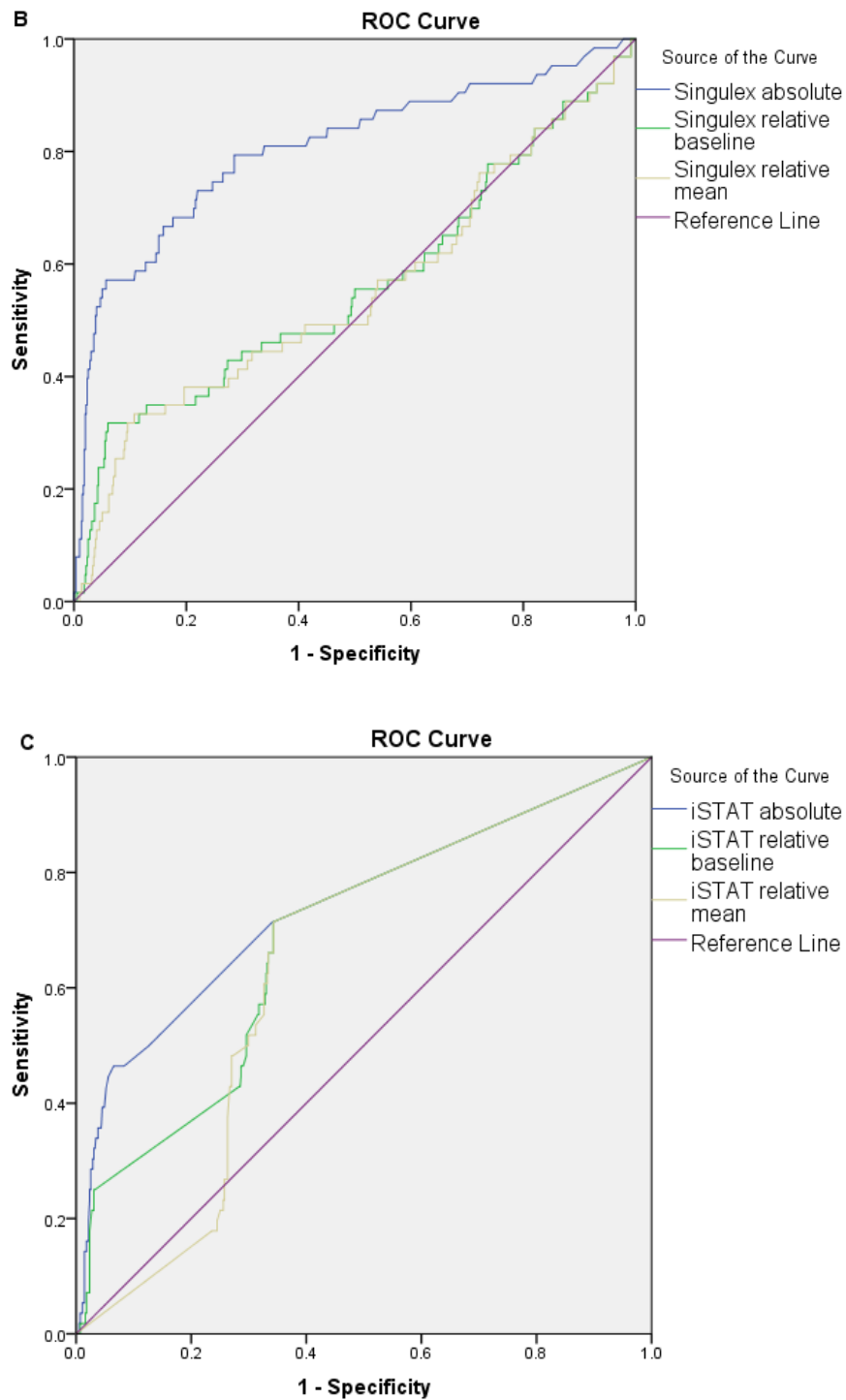


**Figure 7.5 ROC curves of cTn  $\Delta_{\text{absolute}}$ ,  $\% \Delta_{\text{baseline}}$  and  $\% \Delta_{\text{mean}}$  according to the Roche, Singulex and iSTAT assays for 30-day AV1.** Each graph represents the results from one assay. Each line within the graphs represents the ROC curve associated with either  $\Delta_{\text{absolute}}$ ,  $\% \Delta_{\text{baseline}}$  and  $\% \Delta_{\text{mean}}$ , as specified in the legends. A) Roche assay curves; B) Singulex assay curves; C) iSTAT assay curves. Absolute:  $\Delta_{\text{absolute}}$ ; relative baseline:  $\% \Delta_{\text{baseline}}$ ; relative mean  $\% \Delta_{\text{mean}}$ . AV1 included all-cause mortality, AMI, revascularisation, PCI, CABG and stenosis.

**Table 7.5 30-day AV1 prediction cTn  $\Delta_{\text{absolute}}$ ,  $\% \Delta_{\text{baseline}}$  and  $\% \Delta_{\text{mean}}$  according to the Roche, Singulex and iSTAT assays**

	AUC	P	Cut-off	Sensitivity	Specificity	PPV	NPV
<i>Roche</i>							
$\Delta_{\text{absolute}}$	0.776 (0.700 – 0.853)	< 0.001	5.03	19.0 (9.9 – 31.4)	88.5 (85.6 – 91.0)	14.3 (8.6 – 22.9)	91.5 (90.5 – 92.4)
$\% \Delta_{\text{baseline}}$	0.692 (0.615 – 0.768)	< 0.001	0.4762	59.8 (50.4 – 68.8)	43.1 (38.5 – 47.7)	20.8 (18.1 – 23.7)	81.1 (77.1 – 84.6)
$\% \Delta_{\text{mean}}$	0.682 (0.607 – 0.757)	< 0.001	0.4739	60.5 (51.1 – 69.3)	43.1 (38.5 – 47.7)	21.2 (18.6 – 24.1)	81.1 (77.1 – 84.6)
<i>Singulex</i>							
$\Delta_{\text{absolute}}$	0.827 (0.757 – 0.897)	< 0.001	0.53	60.0 (46.5 – 72.4)	50.6 (46.5 – 54.7)	10.8 (8.9 – 13.2)	92.7 (90.2 – 94.6)
$\% \Delta_{\text{baseline}}$	0.595 (0.492 – 0.677)	0.110	0.6074	100.0 (94.3 – 100.0)	0.8 (0.3 – 2.0)	9.6 (9.6 – 9.7)	100.0
$\% \Delta_{\text{mean}}$	0.585 (0.492 – 0.677)	0.181	0.2915	100.0 (94.3 – 100.0)	0.5 (0.1 – 1.5)	9.6 (9.6 – 9.7)	100.0
<i>iSTAT</i>							
$\Delta_{\text{absolute}}$	0.747 (0.666 – 0.828)	< 0.001	100	37.5 (23.4 – 49.6)	96.2 (94.2 – 97.6)	48.8 (35.5 – 62.2)	93.6 (92.4 – 94.7)
$\% \Delta_{\text{baseline}}$	0.686 (0.609 – 0.763)	< 0.001	1.5150	55.4 (41.5 – 68.7)	78.2 (74.5 – 81.6)	20.5 (16.3 – 25.5)	94.5 (92.8 – 95.9)
$\% \Delta_{\text{mean}}$	0.628 (0.560 – 0.696)	0.001	1.4950	71.4 (57.8 – 82.7)	66.4 (62.3 – 70.4)	17.9 (15.1 – 21.1)	95.7 (93.7 – 97.2)

Cut-offs were determined by the concentration the assay exhibits <10% CV. Starred (\*) values are ROC-derived cut-offs.

## 7.6 30-day AV2 prediction cTn $\Delta_{\text{absolute}}$ , $\% \Delta_{\text{baseline}}$ and $\% \Delta_{\text{mean}}$ according to the Roche, Singulex and iSTAT assays

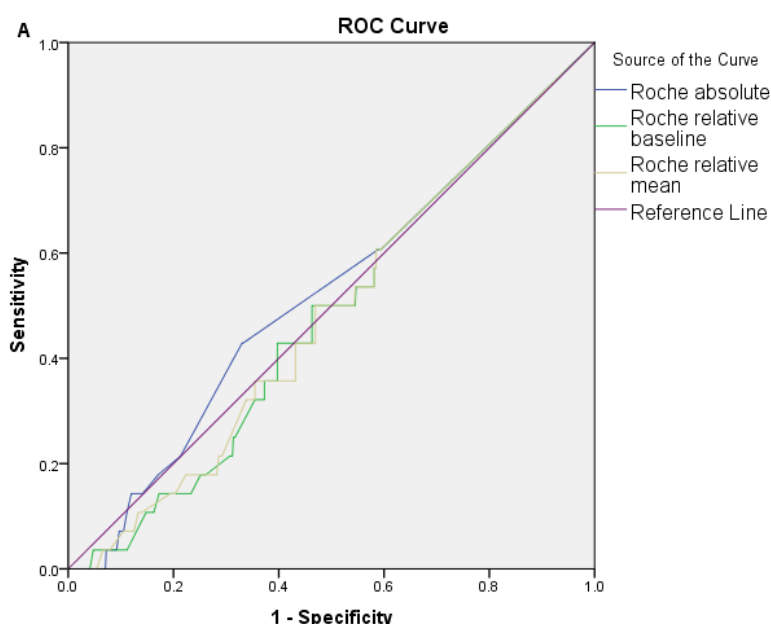
30-day MACE prediction of AV2 by the cTn deltas is shown as ROC curves in figure 7.6. The Roche AUC are 0.536 (95% CI, 0.415 – 0.658), 0.511 (95% CI, 0.394 – 0.628) and 0.514 (95% CI, 0.377 – 0.618) for 0h, 3h and max values, respectively. The respective AUC for the Singulex assay is 0.497 (95% CI, 0.377 – 0.618), 0.342 (95% CI, 0.225 – 0.460) and 0.344 (95% CI, 0.228 – 0.459) and for the iSTAT assay are 0.580 (95% CI, 0.450 – 0.709), 0.574 (95% CI, 0.445 – 0.703) and 0.558 (95% CI, 0.436 – 0.681).

The predictive accuracy of cTn deltas for composite endpoint AV2 prognosis by the different assays is shown in table 7.6. For the Roche assay, there were differences between the  $\Delta_{\text{absolute}}$  and  $\% \Delta$  sensitivities and specificities. The sensitivity of the  $\Delta_{\text{absolute}}$  was 14.8% (95% CI, 4.2 – 33.7) whereas the  $\% \Delta_{\text{baseline}}$  and  $\% \Delta_{\text{mean}}$  were higher at 63.0% (95% CI, 42.4 – 80.6) and 63.0% (95% CI, 42.4 – 80.6). The opposite was true for the respective the specificities at 88.4% (95% CI, 85.4 – 90.9), 41.1% (95% CI, 37.0 – 45.4) and 41.1% (95% CI, 37.0 – 45.4). The NPVs were consistently high at 95.6% (95% CI, 94.8 – 96.2), 95.8% (95% CI, 93.3 – 97.4) and 95.8% (95% CI, 93.3 – 97.4) and NPVs consistently low for PPVs at 5.8% (95% CI, 2.4 – 13.5), 4.9% (95% CI, 3.7 – 6.5) and 4.9% (95% CI, 3.7 – 6.5) for  $\Delta_{\text{absolute}}$ ,  $\% \Delta_{\text{baseline}}$  and  $\% \Delta_{\text{mean}}$ , respectively.

The differences between  $\Delta_{\text{absolute}}$  and  $\% \Delta$  sensitivities and specificities was also seen in the Singulex assay. The sensitivities were lower for  $\Delta_{\text{absolute}}$  than  $\% \Delta_{\text{baseline}}$  and  $\% \Delta_{\text{mean}}$  48.2% (95% CI, 28.7 – 68.1), 100.0% (95% CI, 87.2 – 100.0) and 100.0% (95% CI, 87.2 – 100.0), respectively. The respective specificities showed the opposite

pattern displaying 49.7% (95% CI, 45.5 – 54.0), 5.7% (95% CI, 4.0 – 8.0) and 5.2% (95% CI, 3.5 – 7.4). PPVs were low cut consistent at 4.4 (3.0 – 6.5) and 4.9 (4.8 – 5.0) for the  $\Delta_{\text{absolute}}$  and the two  $\% \Delta$ , and the NPVs were consistently high at 95.2% (95% CI, 93.2 – 96.7) and 100.0%, respectively.

The iSTAT assay displayed a similar pattern to the Roche assay with respect to sensitivities and specificities. However, the sensitivities were lower at 4.0% (95% CI, 0.1 – 20.4) and 52.0% (95% CI, 31.3 – 72.2) for the  $\Delta_{\text{absolute}}$  and the two  $\% \Delta$  but the respective specificities were higher than that of the Roche assay at 93.2% (95% CI, 90.8 – 95.2) and 62.5% (95% CI, 58.3 – 66.5). As with the Roche and Singulex assays, the PPVs were low at 2.6 (0.4 – 15.5) and 5.8 (4.0 – 8.4) for the  $\Delta_{\text{absolute}}$  and the two  $\% \Delta$ , respectively, and the NPVs were high at 95.6% (95% CI, 95.2 – 95.9) and 96.7% (95% CI, 95.1 – 97.8), respectively.



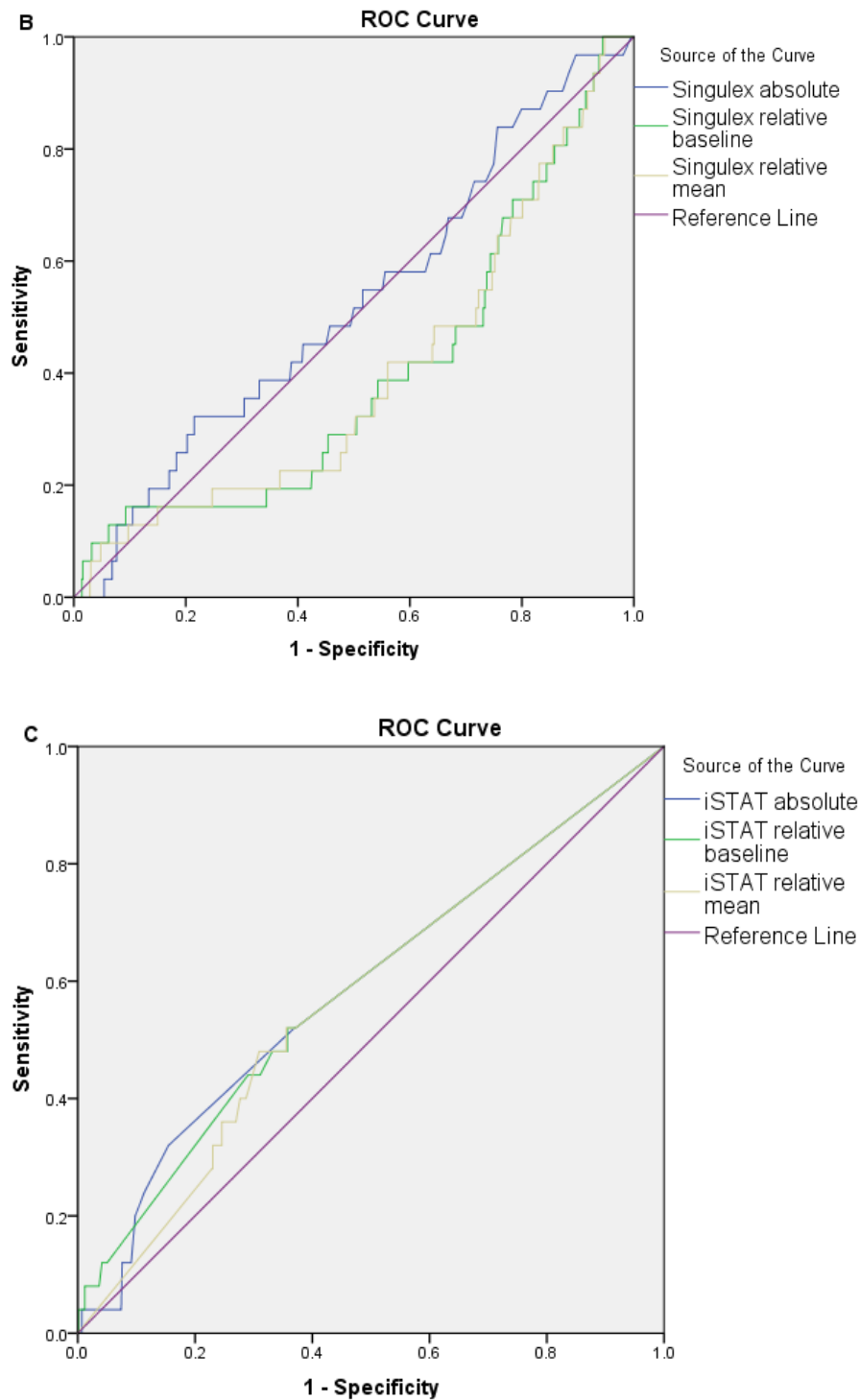


**Figure 7.6 ROC curves of cTn  $\Delta_{\text{absolute}}$ ,  $\% \Delta_{\text{baseline}}$  and  $\% \Delta_{\text{mean}}$  according to the Roche, Singulex and iSTAT assays for 30-day AV2.** Each graph represents the results from one assay. Each line within the graphs represents the ROC curve associated with either  $\Delta_{\text{absolute}}$ ,  $\% \Delta_{\text{baseline}}$  and  $\% \Delta_{\text{mean}}$ , as specified in the legends. A) Roche assay curves; B) Singulex assay curves; C) iSTAT assay curves. Absolute:  $\Delta_{\text{absolute}}$ ; relative baseline:  $\% \Delta_{\text{baseline}}$ ; relative mean  $\% \Delta_{\text{mean}}$ . AV2 included cardiac arrest, arrhythmia and acute heart failure.

**Table 7.6 30-day AV2 prediction cTn  $\Delta_{\text{absolute}}$ ,  $\% \Delta_{\text{baseline}}$  and  $\% \Delta_{\text{mean}}$  according to the Roche, Singulex and iSTAT assays**

	AUC (95% CI)	P	Cut-off (pg/ml)	Sensitivity	Specificity	PPV	NPV
<i>Roche</i>							
$\Delta_{\text{absolute}}$	0.520 (0.411 – 0.629)	0.721	5.03	14.8 (4.2 – 33.7)	88.4 (85.4 – 90.9)	5.8 (2.4 – 13.5)	95.6 (94.8 – 96.2)
$\% \Delta_{\text{baseline}}$	0.480 (0.379 – 0.581)	0.722	0.4762	63.0 (42.4 – 80.6)	41.1 (37.0 – 45.4)	4.9 (3.7 – 6.5)	95.8 (93.3 – 97.4)
$\% \Delta_{\text{mean}}$	0.481 (0.379 – 0.583)	0.736	0.4739	63.0 (42.4 – 80.6)	41.1 (37.0 – 45.4)	4.9 (3.7 – 6.5)	95.8 (93.3 – 97.4)
<i>Singulex</i>							
$\Delta_{\text{absolute}}$	0.525 (0.421 – 0.628)	0.644	0.53	48.2 (28.7 – 68.1)	49.7 (45.5 – 54.0)	4.4 (3.0 – 6.5)	95.2 (93.2 – 96.7)
$\% \Delta_{\text{baseline}}$	0.342 (0.225 – 0.460)	0.052	3.0077	100.0 (87.2 – 100.0)	5.7 (4.0 – 8.0)	4.9 (4.8 – 5.0)	100.0
$\% \Delta_{\text{mean}}$	0.344 (0.228 – 0.459)	0.053	2.8870	100.0 (87.2 – 100.0)	5.2 (3.5 – 7.4)	4.9 (4.8 – 5.0)	100.0
<i>iSTAT</i>							
$\Delta_{\text{absolute}}$	0.580 (0.450 – 0.709)	0.134	100	4.0 (0.1 – 20.4)	93.2 (90.8 – 95.2)	2.6 (0.4 – 15.5)	95.6 (95.2 – 95.9)
$\% \Delta_{\text{baseline}}$	0.574 (0.445 – 0.703)	0.152	1.5150	52.0 (31.3 – 72.2)	62.5 (58.3 – 66.5)	5.8 (4.0 – 8.4)	96.7 (95.1 – 97.8)
$\% \Delta_{\text{mean}}$	0.558 (0.436 – 0.681)	0.248	1.4950	52.0 (31.3 – 72.2)	62.5 (58.3 – 66.5)	5.8 (4.0 – 8.4)	96.7 (95.1 – 97.8)

Cut-offs were determined by the concentration the assay exhibits <10% CV. Starred (\*) values are ROC-derived cut-offs.

## 7.7 Prediction of 30-day composite MACE with baseline cTn in predictor

composites with cTn  $\Delta_{\text{absolute}}$ ,  $\% \Delta_{\text{mean}}$  or  $\% \Delta_{\text{baseline}}$ , acute ischaemia, and H-FABP

The results for the Roche assay are reported in table 7.7.1. Sensitivity and specificity of 64.1% (95% CI 55.6 – 72.0) and 52.8% (95% CI, 48.6 – 56.9), respectively, for the cTn + ECG composite. Both parameters improved with cTn +  $\% \Delta_{\text{baseline}}$  (100.0%, 95% CI 97.4 – 100.0,  $p < 0.001$ ) and cTn +  $\% \Delta_{\text{mean}}$  (72.1%, 95% CI 63.9 – 79.4) but only cTn +  $\% \Delta_{\text{baseline}}$  was accompanied by 100% NPV. Improvement did not occur for cTn +  $\Delta_{\text{absolute}}$  (63.6, CI 95% 55.0 – 71.6 and 54.0%, 95% CI 49.8 – 58.1, respectively). The addition of ECG improved prognosis for  $\Delta_{\text{absolute}}$  and  $\% \Delta_{\text{mean}}$  (both 100.0%, 95% CI 93.8 – 100.0,  $p < 0.001$ ) but the cTn + ECG +  $\% \Delta_{\text{baseline}}$  was not different and had a much lower specificity (1.5%, 95% CI 0.7 – 2.7) than  $\Delta_{\text{absolute}}$  (54.0%, 95% CI 49.8 – 58.1) and  $\% \Delta_{\text{mean}}$  (35.9% (95% CI 32.0 – 40.0). However, all cTn + ECG + deltas had 100%. Adding H-FABP reduced sensitivity for  $\Delta_{\text{absolute}}$ ,  $\% \Delta_{\text{mean}}$  or  $\% \Delta_{\text{baseline}}$  (68.3%, 95% CI 60.0 – 75.9; 99.3%, 95% CI 96.1 – 100.0; 75.4%, 95% CI 67.4 – 82.2, respectively). The specificities were consistent with other composites at 50.5% (95% CI, 46.4 – 54.7), 1.0% (95% CI, 0.4 – 2.2) and 34.0% (95% CI, 30.2 – 38.0), respectively but the NPVs reduced to 86.7% (95% CI, 83.5 – 89.4), 85.7% (95% CI 42.1 – 98.0) and 85.0% (95% CI, 80.9 – 88.5), respectively.



**Table 7.7.1 Prediction of 30-day composite MACE with baseline cTn in predictor composites with cTn  $\Delta_{\text{absolute}}$ ,  $\% \Delta_{\text{mean}}$  or  $\% \Delta_{\text{baseline}}$ , acute ischaemia, and H-FABP with cTn according to the Roche assay**

		Sensitivity (95% CI)	Specificity (95% CI)	PPV (95% CI)	NPV (95% CI)	$\chi^2$ p value
<b>Roche, n = 719</b>						
<b>cTn + ECG</b>		64.1 (55.6 – 72.0)	52.8 (48.6 – 56.9)	24.9 (22.2 – 27.8)	85.8 (82.7 – 88.3)	<0.001
<b>cTn + delta</b>	$\Delta_{\text{absolute}}$ pg/ml	63.6 (55.0 – 71.6)	54.0 (49.8 – 58.1)	25.2 (22.4 – 28.2)	85.9 (82.8 – 88.5)	<0.001
	$\% \Delta_{\text{baseline}}$	100.0 (97.4 – 100.0)	0.4 (0.0 – 1.3)	19.7 (19.6 – 19.7)	100.0	0.646
	$\% \Delta_{\text{mean}}$	72.1 (63.9 – 79.4)	35.9 (32.0 – 40.0)	21.5 (19.6 – 23.6)	84.1 (79.8 – 87.6)	0.044
<b>cTn + ECG + delta</b>	$\Delta_{\text{absolute}}$ pg/ml	100.0 (93.8 – 100.0)	53.1 (49.2 – 56.9)	15.6 (14.6 – 16.7)	100.0	<0.001
	$\% \Delta_{\text{baseline}}$	100.0 (93.8 – 100.0)	1.5 (0.7 – 2.7)	8.1 (8.0 – 8.2)	100.0	0.432
	$\% \Delta_{\text{mean}}$	100.0 (93.8 – 100.0)	36.7 (33.1 – 40.5)	12.1 (11.5 – 12.7)	100.0	<0.001
<b>cTn + ECG + delta + H-FABP</b>	$\Delta_{\text{absolute}}$ pg/ml	68.3 (60.0 – 75.9)	50.5 (46.4 – 54.7)	25.2 (22.7 – 27.9)	86.7 (83.5 – 89.4)	<0.001
	$\% \Delta_{\text{baseline}}$	99.3 (96.1 – 100.0)	1.0 (0.4 – 2.2)	19.7 (19.4 – 19.9)	85.7 (82.1 – 98.0)	0.587
	$\% \Delta_{\text{mean}}$	75.4 (67.4 – 82.2)	34.0 (30.2 – 38.0)	21.8 (20.0 – 23.7)	85.0 (80.9 – 88.5)	0.019

cTn = baseline cTn; ECG = evidence of ischaemia by ECG; H-FABP = positive or negative test for H-FABP; n = number of patients positive for variable in question, in the case of cut-offs a positive result is above the cut-off.

The results for the Singulex assay are reported in table 7.7.2. The sensitivities of the Singulex assay are consistent across all composites and deltas with consistently low specificities. In the cTn + ECG composite, the sensitivity was 95.8% (95% CI, 91.0 – 98.4) with a specificity of 10.3% (95% CI 8.0 – 13.1) and PPV and NPV of 20.7% (95% CI, 20.0 – 21.4) and 90.9% (95% CI, 81.5 – 95.8), respectively. The addition of  $\Delta_{\text{absolute}}$ ,  $\% \Delta_{\text{baseline}}$  and  $\% \Delta_{\text{mean}}$  to cTn instead of ECG did not have an effect on the sensitivities (96.4%, 95% CI 91.9 – 98.8; 97.9%, 95% CI 93.9 – 99.6; 97.9%, 95% CI, 93.9 – 99.6, respectively), the PPVs (20.6%, 95% CI, 19.9 – 21.3; 19.5%, 95% CI 19.1 – 19.9; 19.7%, 95% CI 19.3 – 20.2, respectively) or the  $\Delta_{\text{absolute}}$  NPV at 91.5 (95% CI, 81.5 – 96.4) and  $\Delta_{\text{absolute}}$  specificity at 9.4% (95% CI, 7.2 – 12.1). The NPVs of  $\% \Delta_{\text{baseline}}$  and  $\% \Delta_{\text{mean}}$  were lower at 75.0% (95% CI, 45.1 – 91.6) and 85.0% (95% CI, 62.7 – 95.0) and respective specificities were lower at 1.6% (95% CI, 0.7 – 3.0) and 3.0% (95% CI, 1.7 – 4.7).

The cTn + ECG + delta composite had sensitivities of 100.0% (95% CI, 93.8 – 100.0) and 100.0% NPVs for all deltas. The specificities for  $\Delta_{\text{absolute}}$ ,  $\% \Delta_{\text{baseline}}$  and  $\% \Delta_{\text{mean}}$  were low at 9.0 (6.9 – 11.4), 2.1 (1.2 – 3.5) and 3.3% (95% CI, 2.1 – 5.0) and low PPVs at 8.7% (95% CI, 8.5 – 8.9), 8.2% (95% CI, 8.1 – 8.2) and 8.3% (95% CI, 8.1 – 8.4), all respectively.

The addition of H-FABP into the composite reduced sensitivity to 97.2% (95% CI 92.9 – 99.2) and 98.6% (95% CI 95.0 – 99.8) for  $\Delta_{\text{absolute}}$  and both  $\% \Delta$ , respectively. The NPVs remained high but are still lower than without the addition of H-FABP at 93.0% (95% CI, 83.0 – 97.3), 84.6% (95% CI, 55.2 – 96.1) and 90.5% (95% CI, 69.1 –

97.6) for  $\Delta_{\text{absolute}}$ ,  $\% \Delta_{\text{baseline}}$  and  $\% \Delta_{\text{mean}}$ , respectively. Specificities remained low at 9.1% (95% CI, 6.9 – 11.7), 1.9% (95% CI, 1.0 – 3.4) and 3.3% (95% CI, 2.0 – 5.1) and PPVs were 20.7% (95% CI, 20.1 – 21.3), 19.7% (95% CI, 19.3 – 20.1) and 19.9% (95% CI, 19.5 – 20.3), all respectively.

**Table 7.7.2 Prediction of 30-day composite MACE with baseline cTn in predictor composites with cTn  $\Delta_{\text{absolute}}$ ,  $\% \Delta_{\text{mean}}$  or  $\% \Delta_{\text{baseline}}$ , acute ischaemia, and H-FABP with cTn according to the Singulex assay**

		Sensitivity (95% CI)	Specificity (95% CI)	PPV (95% CI)	NPV(95% CI)	$\chi^2$ p value
<b><i>Singulex, n = 715</i></b>						
<b>cTn + ECG</b>		95.8 (91.0 – 98.4)	10.3 (8.0 – 13.1)	20.7 (20.0 – 21.4)	90.9 (81.5 – 95.8)	0.013
<b>cTn + delta</b>	$\Delta_{\text{absolute}}$ pg/ml	96.4 (91.9 – 98.8)	9.4 (7.2 – 12.1)	20.6 (19.9 – 21.3)	91.5 (81.5 – 96.4)	0.013
	$\% \Delta_{\text{baseline}}$	97.9 (93.9 – 99.6)	1.6 (0.7 – 3.0)	19.5 (19.1 – 19.9)	75.0 (45.1 – 91.6)	0.428
	$\% \Delta_{\text{mean}}$	97.9 (93.9 – 99.6)	3.0 (1.7 – 4.7)	19.7 (19.3 – 20.2)	85.0 (62.7 – 95.0)	0.426
<b>cTn + ECG + delta</b>	$\Delta_{\text{absolute}}$ pg/ml	100.0 (93.8 – 100.0)	9.0 (6.9 – 11.4)	8.7 (8.5 – 8.9)	100.0	0.005
	$\% \Delta_{\text{baseline}}$	100.0 (93.8 – 100.0)	2.1 (1.2 – 3.5)	8.2 (8.1 – 8.2)	100.0	0.308
	$\% \Delta_{\text{mean}}$	100.0 (93.8 – 100.0)	3.3 (2.1 – 5.0)	8.3 (8.1 – 8.4)	100.0	0.155
<b>cTn + ECG + delta + H-FABP</b>	$\Delta_{\text{absolute}}$ pg/ml	97.2 (92.9 – 99.2)	9.1 (6.9 – 11.7)	20.7 (20.1 – 21.3)	93.0 (83.0 – 97.3)	0.006
	$\% \Delta_{\text{baseline}}$	98.6 (95.0 – 99.8)	1.9 (1.0 – 3.4)	19.7 (19.3 – 20.1)	84.6 (55.2 – 96.1)	0.515
	$\% \Delta_{\text{mean}}$	98.6 (95.0 – 99.8)	3.3 (2.0 – 5.1)	19.9 (19.5 – 20.3)	90.5 (69.1 – 97.6)	0.186

cTn = baseline cTn; ECG = evidence of ischaemia by ECG; H-FABP = positive or negative test for H-FABP; n = number of patients positive for variable in question, in the case of cut-offs a positive result is above the cut-off.

The prognostic accuracy of baseline cTn in predictor composites with cTn deltas, acute ischaemia, and H-FABP for MACE prognosis at 30 days according to the iSTAT assay is shown in table 7.7.3. For the cTn + ECG composite, the specificity was 90.9% (95% CI, 88.2 – 93.2) and the NPV was 83.5% (95% CI, 81.9 – 84.9). The sensitivity and PPV for this composite were 28.2% (95% CI, 20.8 – 36.5) and 43.7% (95% CI, 34.7 – 53.1), respectively. In regards to cTn + delta, there were differences between  $\Delta_{\text{absolute}}$ , and  $\% \Delta_{\text{baseline/mean}}$  in sensitivity (23.0%, 95% CI, 16.2 – 31.0; 52.6%, 95% CI 43.8 – 61.3; 53.3%, 95% CI 44.6, – 62.0, respectively), specificity (95.7%, 95% CI 93.7 – 97.3; 70.1%, 95% CI 66.1 – 74.0; 70.3%, 95% CI 66.3 – 74.1, respectively) and PPVs (57.4%, 95% CI 44.9 – 69.1; 30.6%, 95% CI 26.4 – 35.1; 31.0%, 95% CI 26.8 – 35.6, respectively). The cTn +  $\Delta_{\text{absolute}}$ , +  $\% \Delta_{\text{baseline}}$  and +  $\% \Delta_{\text{mean}}$  were similar at 83.2% (95% CI, 81.9 – 84.5), 85.5% (95% CI, 83.1 – 87.7) and 85.8% (95% CI, 83.3 – 87.9), respectively. The cTn + ECG +  $\Delta_{\text{absolute}}$ , +  $\% \Delta_{\text{baseline}}$  and +  $\% \Delta_{\text{mean}}$  show differences between the  $\Delta_{\text{absolute}}$  and  $\% \Delta$  once more, but the values are greater than cTn + delta for the sensitivities (32.6%, 95% CI 24.8 – 41.2; 55.6%, 95% CI 46.8 – 64.1; 56.3%, 95% CI 47.5 – 64.8, respectively) and specificities (90.2%, 95% CI 87.3 – 92.6; 67.2%, 95% CI 63.0 – 71.1; 67.4%, 95% CI 63.2 – 71.3, respectively). The PPVs are lower than the cTn + delta (45.4%, 95% CI 36.9 – 54.2; 29.8%, 95% CI 25.9 – 34.0; 30.2%, 95% CI 26.3 – 34.4, respectively) and the NPVs are similar (84.2%, 95% CI 82.6 – 85.8; 85.8%, 95% CI 83.2 – 88.0; 86.0%, 95% CI 83.4 – 88.3, respectively).

**Table 7.7.3 Prediction of 30-day composite MACE with baseline cTn in predictor composites with cTn  $\Delta_{\text{absolute}}$ ,  $\% \Delta_{\text{mean}}$  or  $\% \Delta_{\text{baseline}}$ , acute ischaemia, and H-FABP with cTn according to the iSTAT assay**

		Sensitivity (95% CI)	Specificity (95% CI)	PPV (95% CI)	NPV(95% CI)	$\chi^2$ p value
<b>iSTAT, n = 670</b>						
<b>cTn + ECG</b>		28.2 (20.8 – 36.5)	90.9 (88.2 – 93.2)	43.7 (34.7 – 53.1)	83.5 (81.9 – 84.9)	< 0.001
<b>cTn + delta</b>	$\Delta_{\text{absolute}}$ pg/ml	23.0 (16.2 – 31.0)	95.7 (93.7 – 97.3)	57.4 (44.9 – 69.1)	83.2 (81.9 – 84.5)	< 0.001
	$\% \Delta_{\text{baseline}}$	52.6 (43.8 – 61.3)	70.1 (66.1 – 74.0)	30.6 (26.4 – 35.1)	85.5 (83.1 – 87.7)	< 0.001
	$\% \Delta_{\text{mean}}$	53.3 (44.6 – 62.0)	70.3 (66.3 – 74.1)	31.0 (26.8 – 35.6)	85.8 (83.3 – 87.9)	< 0.001
<b>cTn + ECG + delta</b>	$\Delta_{\text{absolute}}$ pg/ml	32.6 (24.8 – 41.2)	90.2 (87.3 – 92.6)	45.4 (36.9 – 54.2)	84.2 (82.6 – 85.8)	< 0.001
	$\% \Delta_{\text{baseline}}$	55.6 (46.8 – 64.1)	67.2 (63.0 – 71.1)	29.8 (25.9 – 34.0)	85.8 (83.2 – 88.0)	< 0.001
	$\% \Delta_{\text{mean}}$	56.3 (47.5 – 64.8)	67.4 (63.2 – 71.3)	30.2 (26.3 – 34.4)	86.0 (83.4 – 88.3)	< 0.001
<b>cTn + ECG + delta + H-FABP</b>	$\Delta_{\text{absolute}}$ pg/ml	41.5 (33.1 – 50.3)	79.8 (76.1 – 83.1)	33.9 (28.4 – 40.0)	84.5 (82.4 – 86.3)	< 0.001
	$\% \Delta_{\text{baseline}}$	63.7 (55.0 – 71.8)	59.4 (55.1 – 63.6)	28.2 (25.0 – 31.6)	86.7 (83.8 – 89.2)	< 0.001
	$\% \Delta_{\text{mean}}$	63.7 (55.0 – 71.8)	59.6 (55.3 – 63.7)	28.3 (25.1 – 31.7)	86.8 (83.8 – 89.2)	< 0.001

cTn = baseline cTn; ECG = evidence of ischaemia by ECG; H-FABP = positive or negative test for H-FABP; n = number of patients positive for variable in question, in the case of cut-offs a positive result is above the cut-off.

### 7.8 Univariate and multivariate analysis for cTn as measured by the Roche, Singulex and iSTAT assays and of cardiovascular risk factors for composite MACE at 30 days

There were 40 composite MACE events (5.5%) within 30 days including 11 instances of PCI, 8 of stenosis, 6 of acute heart failure, 2 patients who experienced cardiac arrest and 4 of CABG. There were no patients who had diabetes mellitus and experienced 30-day composite MACE and therefore the variable was removed from the analyses.

The results of the univariate Cox regression proportional hazards analyses for 30-day composite MACE are shown in tables 7.8.1, 7.8.2, 7.8.3 and 7.8.4. Only patients with prior angina showed a significant association with 30-day MACE risk with a hazard ratio of 0.462 (95% CI, 0.238 – 0.896,  $p = 0.022$ ) and Singulex  $\Delta_{\text{absolute}}$  with a hazard ratio of 2.466 (95% CI, 1.288 – 4.723,  $p = 0.006$ ). The two variables were entered into a multivariate Cox regression proportional hazards model where both were shown to be independent predictors for 30-day MACE, as displayed in table 7.8.5. Patients with prior angina had a hazard ratio of 0.463 (95% CI, 0.238 – 0.901,  $p = 0.023$ ) suggesting a statistically and possibly clinically significant decrease in risk of MACE at 30 days for this group. On the other hand, patients with  $\Delta_{\text{absolute}} \geq 0.53$  pg/ml according to the Singulex were associated with an increased risk of 30 day MACE yielding a hazard ratio of 2.425 (95% CI, 1.266 – 4.646,  $p = 0.008$ ).

**Table 7.8.1 Univariate Cox proportional hazard analyses of predicting 30-day composite MACE**

Variables	Hazard ratio	95% CI	p value
Age (per year increase)	0.990	0.974 – 1.013	0.498
Sex (male vs female)	0.634	0.340 – 1.183	0.152
Prior MI	0.616	0.313 – 1.211	0.160
Prior angina	0.462	0.238 – 0.896	0.022
Prior PCI	0.696	0.340 – 1.423	0.321
Prior CABG	0.455	0.178 – 1.161	0.099
Hypertension	1.085	0.578 – 2.035	0.800
Hyperlipidaemia	0.817	0.436 – 1.532	0.529
Chronic kidney disease	0.473	0.145 – 1.536	0.213
Smoker	0.781	0.371 – 1.647	0.517

**Table 7.8.2 Roche univariate Cox proportional hazard analyses of predicting 30-day composite MACE**

Variables	Hazard ratio	95% CI	p value
$\geq 5.03$ pg/ml	0.798	0.427 – 1.495	0.482
$\Delta_{\text{absolute}}$	1.636	0.679 – 3.943	0.272
$\%\Delta_{\text{baseline}}$	0.841	0.451 – 1.568	0.585
$\%\Delta_{\text{mean}}$	0.841	0.451 – 1.568	0.586

**Table 7.8.3 Singulex univariate Cox proportional hazard analyses of predicting 30-day composite MACE**

Variables	Hazard ratio	95% CI	p value
$\geq 0.53$ pg/ml	2.458	0.592 – 10.198	0.215
$\Delta_{\text{absolute}}$	2.466	1.288 – 4.723	0.006
$\%\Delta_{\text{baseline}}$	1.116	0.396 – 3.148	0.835
$\%\Delta_{\text{mean}}$	1.250	0.553 – 2.828	0.592

**Table 7.8.4 iSTAT univariate Cox proportional hazard analyses of predicting 30-day composite MACE**

Variables	Hazard ratio	95% CI	p value
$\geq 100$ pg/ml	1.777	0.543 – 5.816	0.342
$\Delta_{\text{absolute}}$	0.476	0.065 – 3.501	0.466
$\%\Delta_{\text{baseline}}$	1.478	0.720 – 3.031	0.287
$\%\Delta_{\text{mean}}$	1.478	0.720 – 3.031	0.287

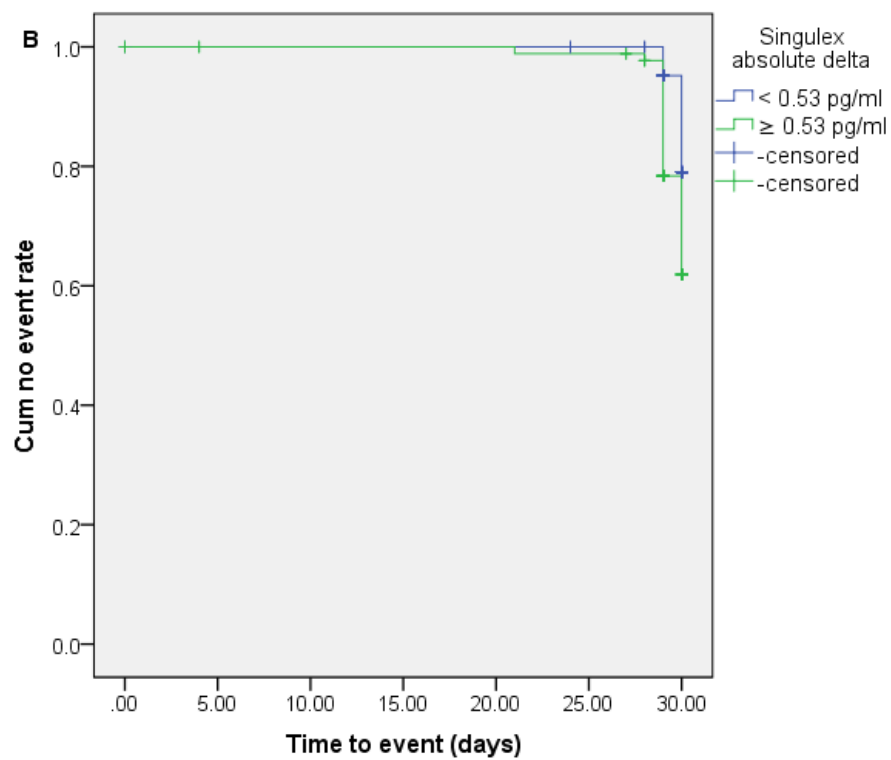
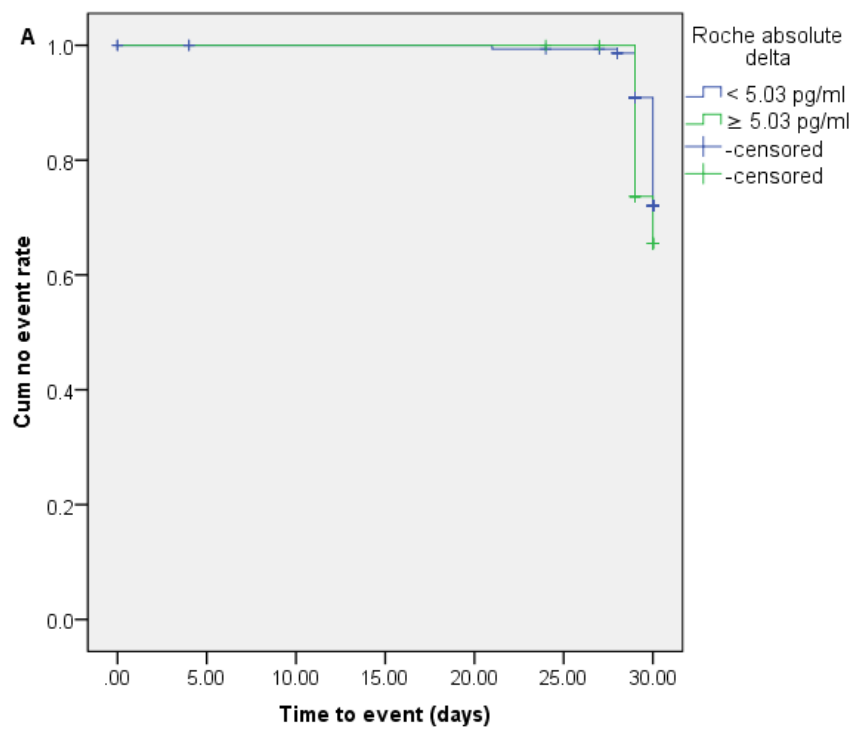
**Table 7.8.5 Multivariate Cox proportional hazard analyses of predicting 30-day composite MACE**

Variables	Hazard ratio	95% CI	p value
Prior angina	0.463	0.238 – 0.901	0.023
Singulex $\Delta_{\text{absolute}}$	2.425	1.266 – 4.646	0.008

### 7.9 Comparison of the $\Delta_{\text{absolute}}$ cut-offs of the Roche, Singulex and iSTAT assays as event predictors

Survival analysis was done using the cut-offs used previously in the analyses (Roche: 5.03 pg/ml; Singulex 0.53 pg/ml; iSTAT 100 pg/ml) and presented as Kaplan-Meier curves (figure 7.9). Events are defined as a composite MACE event within 30-days. Differences in survival were assessed for significance using the log rank test. For the Roche assay, the mean time to event for the low cTn group was 29.85 days (95% CI, 29.72 – 29.98) and for the high cTn group was 29.74 days (95% CI, 29.52 – 29.95). The difference was not significant ( $p = 0.234$ ). The mean time to events for the low cTn and high cTn group according to the Singulex assay were 29.95 days (95% CI, 29.91 – 30.00) and 29.68 days (95% CI, 29.46 – 29.90;  $p = 0.003$ ) producing a statistically significant result, although possibly limited in clinical utility. According to the iSTAT assay, the mean time to event in the low and high cTn groups were 29.83 days (95% CI, 29.70 – 29.96) and 30.00 days (95% CI, 30.00 – 30.00;  $p = 0.421$ ), respectively.





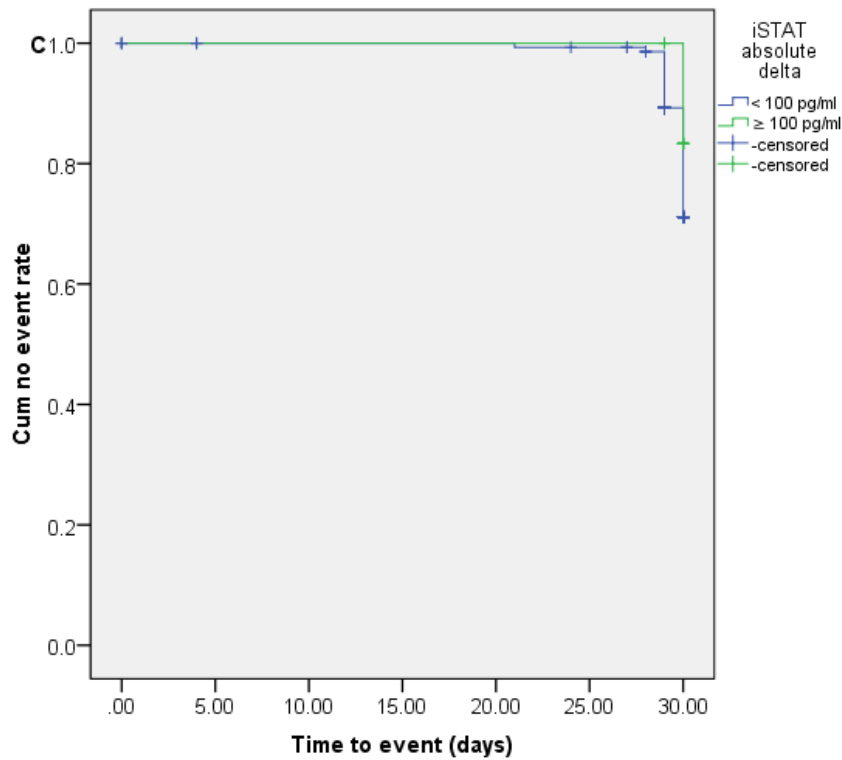


**Figure 7.9 Kaplan-Meier curves for the prognostic value of the  $\Delta_{\text{absolute}}$  for 30-day composite MACE prediction between high and low cTn groups according to the Roche, Singulex and iSTAT assays.** A) Roche assay high and low cTn groups; B) Singulex high and low cTn groups; C) iSTAT high and low cTn groups. High cTn groups are in green and low cTn groups in blue. Events occurred within 30-days of presentation to the ED and time to event is counted in days. All curves use the cut-offs of 5.03 pg/ml for the Roche assay, 0.53 pg/ml for the Singulex assay and 100 pg/ml for the iSTAT assay.

### 7.10 Summary of predicting 30 day MACE outcome with cTn deltas

For these results, cTn deltas were assessed for MACE rule in and rule out prediction and survival at 30 days. Risk factors for AMI and CVD were chosen to assess which factors are associated with poor short-term outcome.

- $\Delta_{\text{absolute}}$  values are not as specific for AV1/2 as  $\% \Delta$
- iSTAT had high specificity but low PPV reducing the possibility that it will be a good short-term AMI predictor due to the large number of false positives this would yield
- Singulex had many patients with 0h cTn values below that of  $\text{cTn}_{\text{low}}$ , which could allow more patients at risk to be identified useful for 30 day AMI prediction
- Prior angina was a negative predictor of all composite MACE at 30 days and Singulex  $\Delta_{\text{absolute}}$  was a positive predictor for the same outcome

## **Chapter 8: Discussion**

## 8.1 mCRP immunoassay development

The original proposal was to create a competitive immunoassay for use on clinical samples to measure mCRP concentration of chest pain patients. The competitive immunoassay was very variable in intra-assay and inter-assay precision. It was then decided that an ELISA would be developed with a commercial detection antibody that would compensate the low analytical sensitivity of the non-commercial 8C10 antibody. The high variability was hypothesised to originate from three main sources: 1) a non-commercial antibody that had to be used at very high concentrations; 2) the association between mCRP and mammalian blocking buffers; 3) the hydrophobicity of mCRP.

### 8.1.1 8c10 mCRP antibody clone

Although the mCRP antibody clone 8C10 has been used elsewhere (47-49, 67), its use is limited to immunohistochemistry or as a blocking antibody to abolish mCRP signalling. For these methods, the high working concentration needed is less of a problem than when using the clone for molecular purposes, such as in an immunoassay. The precision of the antibody to identify mCRP molecules selectively and specifically is paramount to accurately report the concentration of mCRP and to form a reliable standard curve from which to calculate the mCRP concentrations.

By changing protocols to develop a sandwich ELISA, the lack of sensitivity of the mCRP 8C10 antibody was to be overcome by the high sensitivity of the ab24462 and ab19175 antibodies. The ab24462 antibody did not produce a signal and it was assumed that the monoclonal ab24462 and 8C10 were both binding to epitopes that were in close proximity on mCRP. Therefore a polyclonal anti-CRP antibody was used to prevent this occurring again. However, by using this antibody another

problem arose, the inaccuracy of the 8C10 antibody was enhanced by the sensitivity and scaling-up effect of the polyclonal ab19175 antibody. As a polyclonal antibody, ab19175 binds to many different CRP epitopes allowing one mCRP molecule to bind multiple detection antibodies enhancing the signal. In addition, the added sensitivity of ab19175 enhanced any inaccuracies arising from the 8C10 mCRP antibody and was seen as unworkable. There was only one standard curve that was usable for mCRP concentration determination that could not be repeated. Furthermore, the hypothesised functional sensitivity of the ELISA was at 2 µg/ml, which is far above what has been found in human serum (38) and therefore would not be clinically useful.

#### 8.1.2 mCRP and mammalian blocking buffers association

The initial poor resolution was due to interaction between mCRP and BSA leading to non-specific binding. BSA was assessed as a potential blocking agent to reduce non-specific binding. The results show a difference between different BSA concentrations and absorbance at fixed avidin concentrations. The higher the BSA concentration, the higher the absorbance. Further to these results, it was necessary to clarify whether the mCRP or the avidin-HRP complex was binding to the plate and/or BSA. In addition, how much the plate-avidin-HRP was contributing to the non-specific binding. The differences between each mCRP concentration within one BSA concentration and avidin concentration is negligible. This increase is not of the same magnitude as in figure 3.1.7 and therefore avidin-HRP-antibody and avidin-HRP-plate association, seen in figure 3.1.8, does not account for the signal change between BSA concentrations. This means that the mCRP is interacting with the BSA and not the avidin or the plate.

As this also occurred with milk protein, it was deduced that interactions between mCRP and mammalian proteins are potentially ubiquitous. There is far too much interaction between BSA and milk protein with mCRP for them to be part of a coherent, reproducible and reliable assay. This meant a change to a non-mammalian blocking agent (Monster Block™). This shown to be an effective block to non-specific binding and did show the same pattern to binding mCRP as BSA and milk protein. Higher concentration of Monster Block™ lowered signal suggesting it is effective blocking non-specific mCRP binding. Also, by using antibody coating buffer, signal strength was increased that suggests increased stability of the antibody and more effective coating of antibody to the plate.

As the non-specific binding was abundant when using BSA and milk protein, the signal became saturated very quickly and therefore TMB incubation periods were reduced to try to resolve separate concentrations. However, when using the new blocking agent, it appears that the TMB incubation time must now be increased to resolve the different concentrations to increase sensitivity and accuracy of the assay. Dilutional recovery improved by using the antibody coating buffer and the Monster Block™ but decreased again upon adding the mCRP standards.

#### 8.1.3 Hydrophobicity of mCRP

Through the dissociation from pCRP to mCRP, the solubility of mCRP is greatly reduced (192-194). The poor solubility of mCRP could affect its variability and recovery as the identification of stock mCRP concentration proves difficult when the protein does not fully solubilise leading to inaccurate stock concentrations. This could be overcome by changes to the pH of the buffers but this would impact on other reagents and the binding affinity between mCRP and its antibodies.

Furthermore, the lack of solubility may force mCRP from the solution and this may increase or be the cause of the high non-specific binding seen for mCRP. This may also explain the association between mCRP and the blocking buffers of BSA and milk proteins. The affinity between mCRP and the blocking buffers was greater than between mCRP and the CRP buffer indicating it is more energetically favourable for mCRP to associate with BSA and milk protein than to remain in the CRP buffer.

The lack of solubility of mCRP has been overcome when using recombinant mCRP ( $r_m$ CRP) expressed in *E. coli* (193). The group used anhydride reagents to solubilise  $r_m$ CRP and purification to remove interfering endotoxins. This was considered for the current study but the source of CRP for the immunoassay was purification from human plasma and not from a recombinant source, which is necessary when creating a standard curve for human mCRP determination. Secondly, the solubilisation of mCRP in an anhydrous manner creates an effective solution but its use in wet laboratory protocols would return the mCRP to an effective precipitate.

#### 8.1.4 Future work for mCRP immunoassays

The dilutional recovery may be improved by first incubating the mCRP standards overnight at 4°C and then adding the labelled mCRP after a defined period of time.. By allowing the standards to equilibrate with the antibody before adding the labelled mCRP, this should provide greater linearity in the assay.

When adding competition, there appeared to be conflicting results between the different mCRP concentrations. Lower concentrations appear to compete correctly with labelled mCRP but higher concentrations appear to aid labelled mCRP binding. The readiness of CRP monomers forming dimers would mean that any competing



mCRP bound to the antibody would not adversely affect labelled mCRP binding enough for a valid assay. If unlabelled and labelled bind to produce a higher signal, this could suggest that CRP dimers have more affinity for the antibody than mCRP. The competing unlabelled mCRP would not be in competition with the labelled mCRP and therefore the competitive format may be abandoned. Further test must be done to assess this hypothesis. One such test would be to isolate dimeric CRP and mCRP and use a dot blot format to observe to which isoform the antibody shows the greatest affinity.

One group have developed an ELISA for mCRP that was then used for measuring the amount of mCRP in human serum (38). This ELISA produced a measuring range of 1 – 160 ng/ml and day-to-day CV was 10.6%. Although, the group claimed that the capture antibody that was used was developed by the group themselves but characterisation of the antibody was not included in the analyses. Furthermore, the protocol explains that BSA was used and the results above show that this is not an appropriate blocking agent for BSA and would have an effect on appropriate binding of mCRP.

A possible route would be to use a pCRP kit and amend the protocol to include an mCRP antibody as the detection antibody. However, how the biotinylated antibody and mCRP interact after biotinylation is unknown. As mCRP is a molecule that has many unknown qualities, it would be difficult to create an assay for the determination of its concentration in serum. The shelf-life of the protein, interactions with other proteins and lipids and its hydrophobicity are all relatively

unknown to researchers, all of which cause barriers to create a clinically useful immunoassay.

Another route would be to use flow cytometry to measure mCRP on MPs. This method is very sensitive and could provide the required analytical sensitivity for use in clinical diagnosis. It has been shown that measuring mCRP by flow cytometry is possible (46, 195) and by using this method the source of the MPs can also be measured, which may glean more information about the type of ACS the patient is experiencing. This was considered as an alternative to the immunoassay for this current study but the antibody was not sensitive enough to produce any useful data for measuring even high concentrations of mCRP (50 µg/ml) via flow cytometry. However, as flow cytometers are becoming more common in hospital laboratories and mCRP concentration is higher in AMI patients (46), this could be an avenue to pursue to include mCRP in ACS diagnosis.

## 8.2 cTn in the diagnosis of NSTEMI and prediction of 30-day MACE

These analyses assessed the diagnostic and prognostic efficacy of three immunoassays that measure cTn that were the fifth-generation Elecsys, Roche Diagnostics hs-cTnT assay, the Singulex Clarity™ cTnI assay and the Abbott Point of Care iSTAT cTnI assay. To evaluate the diagnostic effectiveness of the assays, the two samples at 0h and 3h and the resulting  $\Delta_{\text{absolute}}$ ,  $\% \Delta_{\text{baseline}}$  and  $\% \Delta_{\text{mean}}$  were assessed with ROC-derived cut-offs and within certain patient subgroups.  $\Delta_{\text{absolute}}$ ,  $\% \Delta_{\text{baseline}}$  and  $\% \Delta_{\text{mean}}$  were also assessed by setting  $\% \Delta$  cut-offs set at 10%, utility of  $\Delta_{\text{absolute}}$ ,  $\% \Delta_{\text{baseline}}$  and  $\% \Delta_{\text{mean}}$  after patients were grouped by 0h cTn concentration and within predictor composites with cardiac ischaemia and H-FABP. The prognostic accuracy of the assays for 3 composite endpoint groups were assessed by 0h and 3h cTn concentration,  $\Delta_{\text{absolute}}$ ,  $\% \Delta_{\text{baseline}}$  and  $\% \Delta_{\text{mean}}$  and with composite predictor groups. This was done as the assays have different analytical characteristics and through treating the data by various methods, the different strengths of the assays were shown. In most of the analyses, the purpose was to achieve maximum sensitivity with the aim of producing quick, successful rule out.

### 8.2.1 AMI diagnosis by cTn values at 0h and 3h

As more and more sensitive cTn assays were produced allowing lower cut-offs, novel ways of determining cut-offs were proposed (196) and with the advent of ultra-sensitive assays detecting cTn at much lower levels (LoD 0.2 pg/mL) (197), the need for a categorisation of a safe cTn level was necessary. This also meant that at risk patients could be identified quicker and the need to wait for 6h for a detectable cTn in NSTEMI was no longer necessary (156-158, 198-200). Moreover, at the low end of the measuring range of the less sensitive assays, the concentration of cTn at

the 10% CV level would be above the 99<sup>th</sup> percentile, which is evaluated as not clinically usable (146, 191). Although some argue that 20% CV is acceptable as it does not result in false positives (201) and would include other assays that would otherwise not be acceptable (202). As a result, the European Society of Cardiology has recommended reducing the minimal time between sampling from 6h to 3h (163).

Comparing assays that measure hs-cTnT and hs-cTnI may cause concern but as has been shown previously (203) that it can be done as the comparison lies not between the analytical parameters of the individual assays but the diagnostic accuracy of the resulting cut-offs. Indeed, the different analytical parameters of the assays impacts on the diagnostic accuracy, differences also lie between assays that measure the same cTn isoform, such as the Singulex and iSTAT assays.

The Roche assay is the standard assay used in the MRI hospital laboratories and has mostly effective sensitivity and specificity, least interpatient variation and high rule out cut-offs. As with all the assays, the cut-offs were set according to their respective FS or higher, where appropriate. The relatively high FS of the Roche assay at 5.03 pg/ml means by using the 0h and 3h values, 51% and 52% of patients are below the cut-off resulting in sensitivities of 48.5% and 47.1% and cannot be stratified accurately within 3h. Using the patients' maximum cTn value only increased the sensitivity marginally to 52%.

Whereas the Singulex assay analysis showed its lower FS cut-off could produce 100% sensitivity and NPV at 0h, meaning 21% of the cohort could be ruled out from AMI diagnosis. In fact, the 0h cut-off that produced this sensitivity was at 0.8550

pg/ml, which is higher than the reported FS of 0.53 pg/ml allowing more patients to be ruled out confidently. When taking the max value of the two samples, a cut-off of 1.3450 pg/ml also yielded 100% sensitivity and NPV with 30% of patients below the cut-off. The higher concentration would mean smaller %CV and more confidence in the result according to the Singulex precision profiles, as seen in the methodology. Although, for patients, a longer wait for the 3h sample is needed for the max values variable to be utilised, its superiority to the 3h alone means that both 0h and 3h could be considered as one but further studies must be done to assess its validity in other settings.

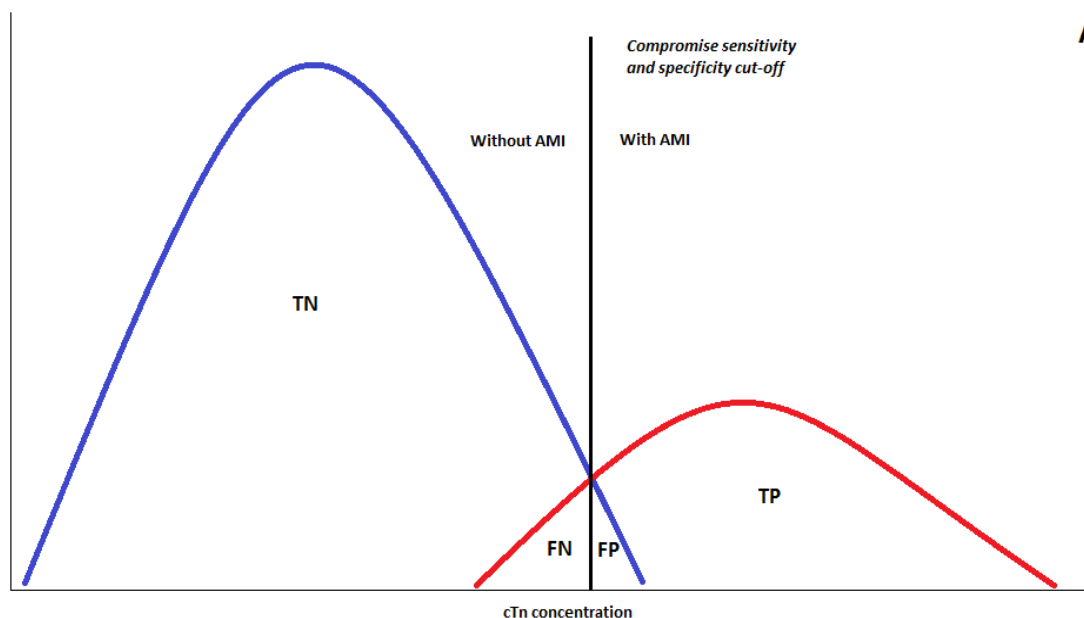
By using these cut-offs, the effect on the specificity of the Singulex assay was marked. The specificity was compromised and was found to be 23.4%, 9.0% and 5.3% for 0h, 3h and max values and PPVs of 10.8%, 10.0% and 10.3%, respectively, 90% of patients will be initially incorrectly ruled in. However, the aim of the analyses was to use the higher analytical sensitivity of the Singulex assay to achieve the highest sensitivity and NPV for rule out. As NSTEMI patients present with lower cTn concentrations, the lower FS of the Singulex assay would be even more useful in this cohort, which it has shown by excluding 30% of the cohort. However, the precision profiles of the Singulex assay produced from the data provided cast doubt on whether the assay is reliable enough to be clinically useful.

The low specificity can be attributed to a low cut-off but also can be down to high variability of the assay in the lower concentrations especially surrounding the chosen cut-off, which was chosen as it was reported the assay showed 10% CV at this level. A significantly greater CV at the reported FS would cause more random

assignment of patients, whose true cTn concentrations lie close to the cut-off, into rule in and rule out groups.

In contrast, the higher FS of the iSTAT assay produced much higher specificities for rule in diagnoses. At 0h, 6% of patients could be ruled in for AMI diagnosis with a specificity of 98.7% and 8% of patients ruled in at 3h with 99.2% specificity. The PPVs were not as high (80.6% at 0h) indicating that even though 98.7% of patients who have AMI are correctly identified at baseline, there remains 20% who are incorrectly ruled in for AMI. However, as the iSTAT is a point of care device, the higher specificities are an important tool to provide clinicians with immediate data of patients who are at high risk and therefore treatments are provided as quickly as possible. The risk of this approach is a high false negative rate, a phenomenon which is shown in figure 8.2.1C. The high cut-off produces high specificity with few false positives and more confidence that patients above the cut-off will be correctly identified as having AMI and for treatments to be given. A lower cut-off, as seen with the Singulex assay and in figure 8.2.1A, will produce high sensitivities, which will reduce the probability of a missed diagnosis and is possibly a safer option when concerning uncertainty of diagnosis in ACS and in the confidence in a rule out diagnosis.

These findings of early rule out within 3h are supported by previous studies (131, 156-161). Macrae et al questioned the American Heart Association's (AHA) definition of AMI calling for a 6h interval between sampling and explored if 3h would be sufficient to rule out. The recorded prevalence of AMI did not significantly decrease when sampling occurred at a 3h interval instead of a 6h interval (33.7% vs

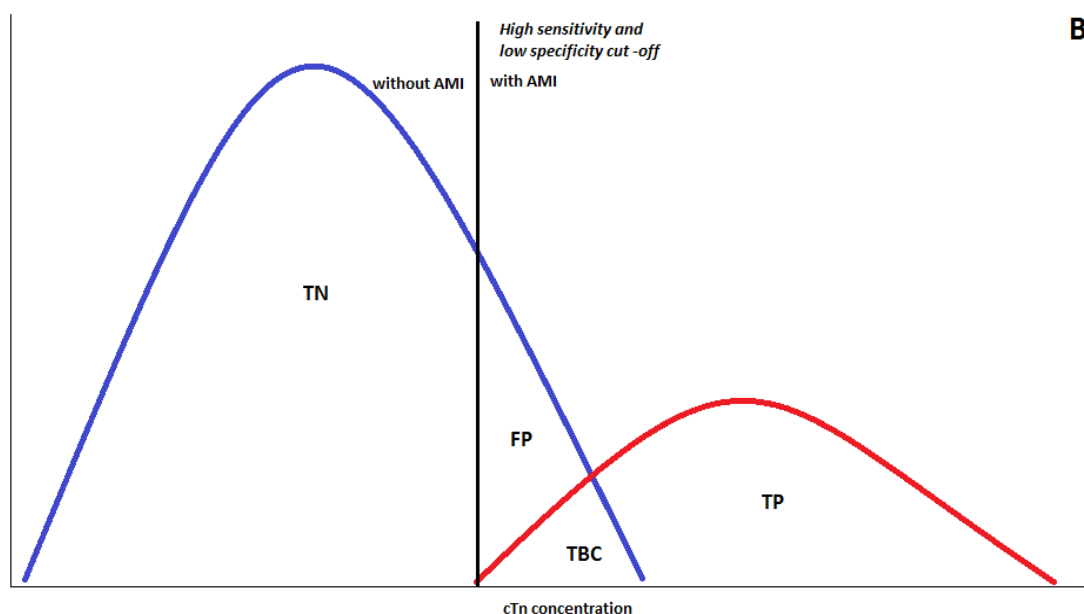


**A** Figure 8.2.1 The effect of adjusting diagnostic cut-offs on diagnostic sensitivity and specificity. The

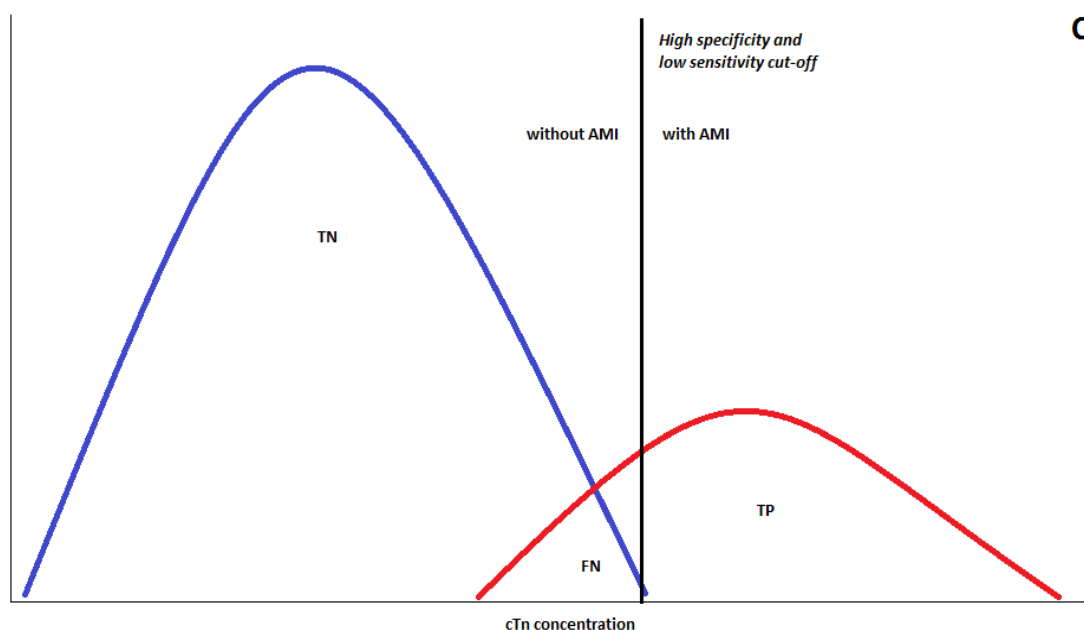
blue curve includes all patients who truly do not have the disease; the red curve includes all patients who truly have the disease. The black lines indicate the cut-offs. TN – true negative; FN – false negative; FP – false positive; TP – true positive; TBC – to be confirmed.

The patients to the left of the cut-off line will be considered as without AMI and the patients to the right of the cut-off will be considered as with AMI. A) shows a cut-off with a compromise for sensitivity and specificity, B) shows a low cut-off with high sensitivity and low specificity, and C) shows a high cut-off with high specificity and low sensitivity.

**B**



**C**



35.7%, respectively,  $p > 0.05$ ;  $n = 258$ ). As was seen by Eggers et al (131), using a

lower cut-off corresponding to 10% CV increased sensitivity and retained high specificity at 93% and 81% at 2h, respectively. Keller et al (157) found no significant difference in the diagnostic accuracy of sampling at baseline and the serial samples and that with patients presenting 3h after symptom onset, a NPV of 84.1% and a PPV of 86.7% was reported with baseline samples.

With further advances in assay sensitivity, the smaller cTn concentration differences between baseline and 3h samples are proving to provide significantly greater sensitivities and NPVs at 3h. By using a hs-cTnI assay on a cohort of 1818 across multiple centres, Keller et al (161) found that at baseline, the assay yielded a sensitivity of 82.3% and a NPV of 94.7%, which rose to 98.2% and 99.4% at 3h, respectively. Interestingly, the sensitivity and NPV for the hs-TnI and the cTnI were exactly the same at 3h but the 99<sup>th</sup> percentile cut-off for the respective assays were 30 pg/ml and 32 pg/ml. The differences in LoD may not mean a better diagnostic test, necessarily, as if the 99<sup>th</sup> percentile is used as a universal cut-off, higher analytical sensitivity will not result in a higher diagnostic sensitivity.

In a change to the recognised procedure of using the 99<sup>th</sup> percentile as a diagnostic cut-off, Body et al (99) investigated using the LoB as a cut-off for a novel rule out strategy. The assay used was the Roche Diagnostics Elecsys hs-cTnT 5<sup>th</sup> Gen assay and a cohort of 703, of whom 13 had AMI. No patient who experienced AMI had detectable hs-cTnT leading to a sensitivity and NPV of 100%. By using this strategy, 27.7% of patients would be ruled out of AMI, 2 of whom had negative outcomes in the following 6 months. In a validation study leading on from this research (same paper), one patient (from a cohort of 915) had a cTnT rise and AMI producing a NPV



of 99.4%. In a slight amendment, the LoD of was used as a cut-off to assess if more patients could be safely ruled out this way. Of the 463 patients, 96 had hs-cTnT concentrations below the LoD and only one had an AMI. This produced a sensitivity of 98.7% and a NPV of 99.0% and increased to 100% for both in patients who were under the LoD and did not indicate ECG ischaemia. As expected, by using the 99<sup>th</sup> percentile as a cut-off, the sensitivity was reported as 94.9% and the NPV at 93.9%, which is similar to the results found in the literature for hs-cTn assays using 99<sup>th</sup> percentile cut-offs (7, 161, 162).

A multicentre, international cohort from Australia, New Zealand and the UK (100) also used the LoD (1.2 ng/L) as a cut-off at presentation with sensitivity of 99.0% and NPV of 99.5%, which is very similar to Body et al. (99). However, due to its lower cut-off, fewer of the cohort would be ruled out, 18.8% in comparison to 27.7%. This paper also address the importance of using decimals with hs-cTnI assays by using rounded cut-off values from 1.2 ng/L up to and including 5 ng/L. Rounded cut-offs did not have sensitivities of more than 98%, which is below the acceptable limit of missed diagnoses (204). Although the rounded cut-offs displayed results of more than 99%, NPVs are dependent on disease prevalence within a population and it was recommended that each site should produce its own NPV for its population (100).

#### 8.2.2 Diagnostic accuracy of cTn $\Delta_{\text{absolute}}$ , $\% \Delta_{\text{baseline}}$ and $\% \Delta_{\text{mean}}$ for AMI diagnosis

The problem with using a single measurement of cTn is that it does not allow for the rise and fall pattern to be traced, as is called for in the universally accepted definition of AMI (164). The introduction of hs-cTn assays allowed more sensitive but less specific diagnoses and more unnecessary hospitalisations. This

phenomenon may not matter in early rule out, only that small changes or low concentrations are detected to distinguish between different sources of cTn rises. Chronic rises in cTn such as in chronic heart failure, left ventricular hypertrophy and coronary artery disease do not have a rise and fall pattern and can be distinguished from ACS (205). However, very small increases could be wrongly attributed to AMI when they are caused by non-ischaemic conditions such as myocarditis, pericarditis, cardiac contusion, or the damage caused by shocks from pacemakers, or non-cardiac-related cTn release, such as in renal failure (206, 207). Higher specificity with more analytically sensitive assays have been shown using deltas. The aim of these analyses was to produce maximum sensitivity to find the optimum magnitude of cTn change that would confidently rule out 100% of patients below the cut-off.

The clinical sensitivity of  $\Delta_{\text{absolute}}$  was lower than the sensitivities of the  $\% \Delta_{\text{baseline}}$  and  $\% \Delta_{\text{mean}}$  for each assay. By using  $\Delta_{\text{absolute}}$ ,  $\% \Delta_{\text{baseline}}$  and  $\% \Delta_{\text{mean}}$ , the clinical sensitivity of the Roche assay was higher than using the 0h and 3h values alone. The Roche assay reported sensitivities of 89.7%, 98.4% and 98.4%, respectively. The increase in sensitivity did not have the effect of decreasing the specificities and in the case of  $\Delta_{\text{absolute}}$  the specificity was higher at 97.4%. This may be due to the  $\Delta_{\text{absolute}}$  cut-off was set by the analytical limits of the assays but the  $\% \Delta_{\text{baseline}}$  and  $\% \Delta_{\text{mean}}$  were ROC-derived cut-offs.

The Singulex assay had similar sensitivity results for  $\Delta_{\text{absolute}}$ ,  $\% \Delta_{\text{baseline}}$  and  $\% \Delta_{\text{mean}}$  but its cut-offs were higher allowing more patients to be included in a possible rule out diagnosis. Also, as it is more sensitive than the Roche assay, the lowest possible baseline cTn concentration for an effective  $\% \Delta$  is much lower, both at 14 pg/ml. In

the cohort, 93 patients were below 14 pg/ml according to the Singulex assay, of whom 7 had  $\% \Delta_{\text{baseline}}$  of less than 3.6901%.

For the iSTAT assay, the  $\% \Delta_{\text{baseline}}$  and  $\% \Delta_{\text{mean}}$  sensitivities also outperformed the  $\Delta_{\text{absolute}}$  sensitivity but the opposite occurred with specificity. By using the 100 pg/ml cut-off, specificity was 99.0% with 7% of the cohort above the threshold. The  $\% \Delta_{\text{baseline}}$  and  $\% \Delta_{\text{mean}}$  specificities (67.2% and 67.4%, respectively) were lower than their sensitivities at 84.1% and 85.7%, respectively but only one patient fulfilled both criteria of lowest possible baseline cTn level for an effective  $\% \Delta$  and the  $\% \Delta$  cut-off. This may limit its clinical utility.

Distinction between ACS-related rises in cTn and other causes is important as only a third of cTn rises are attributed to ACS (208). Mueller et al (209) investigated the basis of the rationale to use serial cTn testing to observe what magnitude of change can define an AMI and a non-ACS-related condition. The NSTEMI ACS was also analysed separately (STEMI exclusion of the same cohort) to distinguish between MI ACS and non-MI ACS. Absolute changes performed better than relative changes according to AUC of ROC curve analysis (AUC = 0.898 and 0.752, respectfully,  $p > 0.0001$ ).

62.4% of patients with non-ACS conditions still had a rise of hs-cTnT of 20% compared with 75.2% of NSTEMI. 24.8% of NSTEMI did not experience this change during the first 6h but did during a 24h period. There is a large trade off in using absolute changes in this model, the high sensitivities seen is met with lower specificities, unlike Apple et al (210) who used a delta of  $>30\%$  produced a sensitivity of 75% and a specificity of 91%. The retention of specificity in the Apple

analyses does make the diagnostic accuracy more robust overall but when looking at rule out, the strength of specificity could be seen as not as much of a concern. Moreover, the more sensitive an assay and higher its clinical sensitivity, the more it negatively affects the specificity (211, 212) as was seen with the Singulex assay. However, by optimising the cut-off via ROC curve analysis for rule in, specificity can also be high for hs-cTnI assays (213).

In a study with shorter times between sampling than the current analysis, a cTnI ultra assay was compared with a hs-cTnT assay for deltas of 1h, 2h and 6h (160). The  $\Delta$  was outperformed at every time point with each assay by  $\Delta_{\text{absolute}}$ . The hs-cTnT assay showed the strongest AUC with  $\Delta_{\text{absolute}}$  at 2h and the cTnI ultra assay demonstrated the strongest AUC with  $\Delta_{\text{absolute}}$  at 2h. This is more evidence that early sampling is as effective as 6h sampling and that early rule out with the newer more analytically sensitive assays could aid the busy, contemporary EDs.

However, the benefit of  $\Delta_{\text{absolute}}$  and  $\Delta$  may be redundant when observing patients with abnormally high baseline cTn. From a cohort of 1282, a group with hs-cTnT > 60 ng/L had PPV of 87.2%, which was unchanged when the cut-off was increased to > 80 ng/L and > 100 ng/L (214). Furthermore, the addition of  $\Delta$  at 20% did not improve PPV for quick rule in (1h  $\Delta$  84% and 2h  $\Delta$  88.9%) and was only increased slightly when the interval was extended to 4-14h (91.2% for > 80 ng/L and 90.4% for 100 ng/L). Although the PPVs are not 100% and therefore there will be false positives, crucially the PPV does not increase with the addition of  $\Delta$ . The  $\Delta$  cut-off could be increased but this would lead to fewer positive diagnoses and an increased risk of false negatives. It is also important to assess any conditions the

patients that would cause chronic rises in cTn as this could lead to unnecessary and potential damaging treatment to the patient.

### 8.2.3 Diagnostic accuracy of $\Delta_{\text{absolute}}$ , $\% \Delta_{\text{baseline}}$ and $\% \Delta_{\text{mean}}$ cTn deltas based on baseline cTn

If the cTn deltas were only used independently, the lack of specificity would be a problem. However, diagnoses are rarely based on one piece of evidence and clinical judgement will always remain an important part of diagnostics (215). In addition, by stratifying patients into different risk groups and assessing the optimal cut-offs for each group, diagnostic accuracy would be assumed to increase. The aim of these analyses was to stratify patients into rule out, intermediate and rule in groups based on ROC curve analysis and treat each group as its own cohort with further ROC curve analysis providing group-specific cut-offs for  $\Delta_{\text{absolute}}$ ,  $\% \Delta_{\text{baseline}}$  and  $\% \Delta_{\text{mean}}$  for highest possible clinical sensitivity.

For the Roche rule out group, sensitivity was low at 50.0% (95% CI, 6.8 – 93.2) for all deltas but specificity was higher for  $\Delta_{\text{absolute}}$  (99.7%, 95% CI 98.3 – 100.0) than  $\% \Delta_{\text{baseline}}$  and  $\% \Delta_{\text{mean}}$  62.3% (95% CI, 56.8 – 67.7), which agrees with the phenomenon of  $\Delta_{\text{absolute}}$  having better diagnostic accuracy at lower baseline cTn values than  $\% \Delta$ . The lower PPVs for  $\% \Delta$  (1.7%, 95% CI, 0.6 – 4.3) than  $\Delta_{\text{absolute}}$  (66.7%, 95% CI 18.3 – 94.7) suggesting  $\% \Delta$  has less rule in power in the low-risk group. The intermediate group produced 100% sensitivity and NPV for all deltas suggesting all patients within this group will be identified as successfully ruled out if under the cut-off. The high-risk group showed 100% specificity and PPV implying that all patients below the cut-off could be successfully ruled out and all patients adjudicated with AMI by the Roche assay are correctly diagnosed. The reported

diagnostic accuracy of the high-risk group may be affected by the low number of patients ( $n = 27$ ) and the high proportion patients who experienced AMI (with AMI = 25).

The Singulex assay did not have any patients in the rule out group due to the 0h cTn having 100% sensitivity and NPV. According to the Singulex assay, the  $\% \Delta$  had 100% sensitivity and NPV, whereas the  $\Delta_{\text{absolute}}$  reported 85.5% (95% CI, 75.0 – 92.8) and 96.4% (95% CI, 93.7 – 98.0), respectively. This is in opposition to the idea that  $\Delta_{\text{absolute}}$  is more clinically useful at lower cTn concentrations. This could be down to the wide range of cTn concentrations in this group leading to slightly poorer diagnoses and the possible variation seen in the Singulex assay could be mitigated by conversion to percentages. The rule in group presented very poor ROC curve analysis when combined with any of the deltas (0.200, 95% CI, 0.000 – 0.570) but this is due to low patient numbers in the group ( $n = 8$ , with AMI = 5) and the test unable to identify any patients without AMI correctly.

For the iSTAT assay, the NPVs were all 99.2% (95% CI, 97.6 – 99.7) and 94.4% (95% CI, 90.7 – 96.7) for the rule out group, and in the intermediate group 93.9% (95% CI, 90.2 – 96.3) and 94.4% (95% CI, 90.7 – 96.7) for  $\Delta_{\text{absolute}}$ ,  $\% \Delta_{\text{baseline}}$  and  $\% \Delta_{\text{mean}}$ , respectively, suggesting a good diagnostic accuracy of the iSTAT for rule out. However, the poorer specificity and sensitivity (60.0%, 95% CI 14.7 – 94.7 and 76.4%, 95% CI 71.4 – 81.0 for  $\Delta_{\text{absolute}}$  in rule out group) would suggest a large portion of the cohort would be yet to be either ruled in or out. As a point of care device, the iSTAT assay is best at providing almost immediate results for the benefit of identifying those most at risk. By waiting 3h for a second sample and creating

either  $\Delta_{\text{absolute}}$ ,  $\% \Delta_{\text{baseline}}$  or  $\% \Delta_{\text{mean}}$ , the point of care device no longer delivers its purpose of quick stratification. For this reason, the lower diagnostic accuracy is not as much of a concern.

In a similar idea, combining cTn levels at presentation and deltas, an attempt to triage patients more quickly was made by a study aimed to use hs-cTnT at 0h and 1h to rule in and rule out AMI (216). It is a prospective validation study of 1282 patients that uses absolute changes in hs-cTnT concentration between 0h and 1h to triage patients to rule out status, observational zone or rule in. CoV was 10% at 13ng/L, 99<sup>th</sup> percentile at 14ng/L for hs-cTnT (Roche) and s-c-TnI-ultra has LoD of 6ng/L, 99<sup>th</sup> percentile cut-off of 40ng/L and CoV of <10% at 30ng/L. By using the 1h algorithm, 63.5% were ruled out with a miss rate of 0.9%, 14.4% were ruled in and 22.2% were triaged. Of those triaged, 22.5% experienced AMI and this observational group allows the diagnostic performance in the rule in and out groups to be much higher. However, the algorithm allows rule in stratification of patients to be done at presentation (criteria: 0h  $\geq 52$  ng/L or delta 1h  $\geq 5$  ng/L), which permits urgent care to patients most at risk at presentation with a PPV and specificity of 77.2% and 96.1%, respectively. The rule out criteria (0h < 12 ng/L and delta 1h < 3) reported a sensitivity and NPV of 96.7% and 99.1%, respectively.

This algorithm produces better NPV and sensitivity than the Roche and Singulex  $\Delta_{\text{absolute}}$  alone but the Singulex did provide a 100% NPV by using 0h values at a cut-off above its 10% CV. In the stratification of this current research, the Roche assay achieved a sensitivity and NPV of 100% for all deltas for the intermediate group ( $5.03 < x < 10$  pg/ml; n=295, 41 with AMI) by using low delta cut-offs. The Roche

assay produced the same results when using a composite predictor of 0h cTnT and delta values (cut-offs of 5.03 pg/ml for 0h and  $\Delta_{\text{absolute}}$ , 1.4774% for  $\% \Delta_{\text{baseline}}$ , 0.4739% for  $\% \Delta_{\text{mean}}$ ) but as the deltas are over 3h instead of 1h more patients may be at risk by waiting longer for a correct diagnosis.

The approach of assessing rule in and rule out patients differently, with respect to diagnosis, was used by Sandoval et al. (217). Patients were ruled out by the 99<sup>th</sup> percentile of the hs-cTnI and a normal ECG with 100% sensitivity and NPV at 0h and 3h. Whereas patients were ruled in by delta values alone and produced a specificity of 89.3% with an absolute delta of > 5 ng/L. With regard to rule out, this is comparable to the sensitivity and NPVs of the Roche assay, 94.7% and 98.9%, and the Singulex assay, 98.7% and 98.5%. This paper also observed the possible need for differing deltas for different baseline hs-cTnI as patients presenting with negative hs-cTnI who had an absolute delta of > 5 ng/L provided a specificity of 94.2% but with those presenting with a positive hs-cTnI and a delta of > 5 ng/L, the specificity dropped to 54.2%. The absolute delta would have to be raised to > 100 ng/L to obtain a specificity of 94.1% highlighting that certain tools may be better suited to different risk groups of NSTEMI.

Not only could the application of rule in and rule out differ in the magnitude of cTn change but different deltas could be used.  $\Delta_{\text{absolute}}$  cut-offs are more diagnostically useful at lower concentrations but will not be as useful as higher concentrations. The reasons for this are two-fold – the same  $\Delta_{\text{absolute}}$  at a higher concentration means less pathophysiologically and at very high concentrations other ischaemic cardiac conditions are more likely to be the cause of a cTn rise and mask  $\Delta_{\text{absolute}}$ .



For these reasons, it may be more clinically useful to reserve  $\Delta_{\text{absolute}}$  analysis to the low-risk ACS group.

On the other hand, concerning  $\% \Delta_{\text{baseline}}$  and  $\% \Delta_{\text{mean}}$  are more clinically useful at higher cTn concentrations. Not only does the effect of biological and analytical variation lessen at higher concentrations but to surpass the FS in absolute terms, the baseline or mean concentrations have to be at a minimum concentration for the  $\% \Delta$  to be effective. For the Roche assay, the lowest concentration for  $\% \Delta_{\text{mean}}$  would have to be 1061 pg/ml for the cut-off of 0.4739% to exceed 5.03 pg/ml in absolute terms.

With regards to the high Roche  $\% \Delta_{\text{baseline}}$  and  $\% \Delta_{\text{mean}}$  clinical sensitivities, there were no patients who had a  $\% \Delta$  lower than the quoted cut-offs (1.4774 and 0.4739, respectively) and whose baseline level was greater than what was needed for the  $\% \Delta$  to be greater than the analytical sensitivity of the assay (341 pg/ml and 1061 pg/ml, respectively). The high clinical sensitivities are not clinically useful and therefore the use of Roche  $\% \Delta$  for rule out may not be appropriate. However, the Singulex assay has much lower analytical sensitivity allowing for lower baseline cTn required (14 pg/ml) for the  $\% \Delta_{\text{baseline}}$  and  $\% \Delta_{\text{mean}}$  cut-offs of 3.6901% and 3.7050% to be effective. The baseline values required for the iSTAT assay are very high at 6,660 pg/ml and 6,700 pg/ml, which only two patients in the cohort exceeded but also exceeded the  $\% \Delta$  cut-offs.

Considering the universal definition of AMI requires a rise and fall pattern of cTn for a positive diagnosis, the quantification of this threshold for the greatest PPV and specificity should be elucidated. The use of the deltas have shown to be not as

clinically useful in rule out as using 0h and 3h sample concentrations. However, the use of concentrations from single samples is dependent on the assay that is used and each assay must be assessed for its clinical utility based on its analytical parameters.

#### 8.2.4 Absolute relative deltas with fixed cut-offs based on %CV

The 10% CV level was explored further by using it as a cut-off for  $\% \Delta_{\text{baseline}}$  and  $\% \Delta_{\text{mean}}$  for the reasons described above. As the cut-offs are higher than the ROC-derived cut-offs for  $\% \Delta_{\text{baseline}}$  and  $\% \Delta_{\text{mean}}$ , the sensitivity and NPVs are not as high. By using this cut-off alone, the Roche assay would miss 2% of AMI diagnoses in comparison to the  $\% \Delta_{\text{baseline}}$  and  $\% \Delta_{\text{mean}}$  ROC-derived cut-offs (1.4774% and 0.4739%, respectively) that would miss 1% of diagnoses. The ROC-derived cut-off for  $\% \Delta_{\text{baseline}}$  Singulex allow only 0.3% of patients to be missed instead of 3% if the cut-off is raised to 10% and for the iSTAT assay 2% of patients would be diagnosed by using the  $\% \Delta_{\text{mean}}$  cut-off of 1.4950% instead of 9% when using the 10% cut-off. The precision profiles of the individual assays would have to be consulted to assess at which concentrations the %CV is lower than the ROC-derived cut-offs and may be very high and not clinically useful. However, as stated above, there are problems with using the lower ROC-derived cut-offs in that they are only effective above certain baseline cTn concentrations, which may supersede the concentration needed to overcome the %CV.

By using ROC curve analysis, the maximum sensitivity can be set but with  $\Delta_{\text{absolute}}$  the assay is the limiting factor. However, the  $\Delta_{\text{absolute}}$  must be set by the assay's own analytics otherwise - by using a lower ROC-derived cut-off for an absolute value - a true change cannot be confidently observed. However, this is an important factor

that cannot be ignored to keep consistent analytical accuracy and to the universally accepted 10% CV level.

#### 8.2.5 Diagnostic value of baseline cTn in predictor composites with cTn deltas, acute ischaemia, and H-FABP diagnosis for AMI diagnosis according to the 3 assays

The addition of other associated factors into possible AMI diagnosis allows a broader range of causes for the AMI instead of focusing on cTn and cTn deltas arising from cTn sampling. As seen above, and across the literature, cTn has high diagnostic value in ACS and can be used more quickly with assays that are more sensitive. However, the diagnoses remain problematic in certain patients. The use of novel cardiac biomarker H-FABP could allow for even faster diagnosis as it has been shown to be a sensitive marker for AMI. Ischaemia as evidenced on ECG was also used as ischaemia is a prerequisite of AMI and could provide a more informative diagnosis. The cut-offs used for the quantifiable variables, cTn and deltas, are as quoted in tables 4.4 and 5.5 in chapters 4 and 5, respectively. H-FABP and ECG ischaemia were categorical and as adjudicated by hospital staff as positive or negative.

The sensitivities and NPVs of the Roche assay were high for all composites. The sensitivity of cTn + ECG was 94.7% (95% CI, 86.9 – 98.5) but the cTn + deltas were all 100.0% (95% CI, 95.0 – 100.0). By combining both to produce cTn + ECG + delta, the sensitivity decreased to 97.3% (95% CI, 90.7 – 100.0) for all deltas. The addition of H-FABP again increased the sensitivity to 100.0 (95% CI, 95.2 – 100.0). Overall, the significant differences between the composites do have a significant effect on potential future diagnostic practises as the accepted level of sensitivity required for

rule out is 99% and especially for cTn + delta and cTn + ECG + delta + H-FABP as they had 100% NPV suggesting all rule out diagnoses would be correct.

The Singulex assay did not see significant differences by adding factors to the composites but the  $\% \Delta_{\text{baseline}}$  did produce 100% sensitivity and NPV for all composites. The composites with  $\Delta_{\text{absolute}}$  and  $\% \Delta_{\text{mean}}$  did not reach 99% and therefore would not be clinically useful for rule out. However, a bigger validation cohort may provide a higher sensitivity and better clinical utility for rule out.

The higher PPVs of the iSTAT assay (98.6%, 95% CI 96.9 – 99.4 for both cTn + ECG +  $\% \Delta$  + H-FABP) can be put down to its higher cTn baseline cut-off and therefore the lower number of false positives that occurs with the lower cut-offs observed with the Singulex and Roche assays. However, the iSTAT assay reported lower PPVs with cTn +  $\% \Delta$  (cTn+  $\% \Delta_{\text{baseline}}$  at 97.0%, 95% CI 95.2 – 98.2) as the  $\%$  cut-offs were very low and would also result in a high number of false positives. Conversely, this has resulted in sensitivities of  $\Delta_{\text{absolute}}$  to be lower than the specificity (62.3%, 95% CI 49.8 – 73.7 and 98.3%, 95% CI, 97.0 – 99.2 for cTn +  $\Delta_{\text{absolute}}$ , respectively) and lower than its  $\% \Delta$  counterparts (81.2%, 95% CI 69.9 – 89.6 and 82.6%, 95% CI 71.6 – 90.7 for  $\% \Delta_{\text{baseline}}$  and  $\% \Delta_{\text{mean}}$  sensitivities, respectively).

The significant rise of sensitivity and NPV was seen with each addition of a variable to the composite but as the cut-offs were already set at the limit of the assay's reportable range, the iSTAT may be more suitable to be used as a rule in device in combination with ECG, deltas and H-FABP. As a point of care device, this use is preferable as it will alert clinicians to high-risk patients quicker. However, by combining the iSTAT results with other variables, the decision would have to wait

until H-FABP assay results return from the lab. Instead, the device could alert clinicians to medium risk patients to which the H-FABP results could produce a rule in diagnosis. In addition, the  $\% \Delta$  would be better suited to higher baseline cTn, as previously discussed, which would present in patients of medium risk. The high sensitivity would allow more accurate positive diagnosis of patients who are above the cut-off. The low PPV of these relative delta results mean that this may not be possible.

This is the first time H-FABP has been used in this specific combination with cTn deltas. Previously, H-FABP has been shown to be a better exclusion marker than cTnI for early NSTEMI diagnosis (180-183) and the early rise of h-FABP allows high diagnostic accuracy < 3h with AUC of 0.841 (181). However, multivariate analysis showed complete exclusion was only possible with cTnI and H-FABP combination with a sensitivity of 96.9% and NPV of 98.8% (180). This allowed AMI to be excluded immediately in 44.7% of the cohort (n = 705) with a miss-rate of 0.6%. This study shows the added benefit of H-FABP but also that H-FABP alone will not be diagnostically accurate enough to confidently exclude patients from AMI. This may be because H-FABP does not have specific cardiac expression (218, 219) and the cause of the rise may be non-ACS, such as in chronic heart failure (220), or non-cardiac, such as in pulmonary embolism (221) or even possibly in neurodegenerative diseases (222).

Due to the rapid increase of systemic h-FABP concentration, its rise may precede that of cTn, especially if patients present < 1h from symptom onset and could be cTn negative at presentation. In fact, 55% of AMI patients were h-FABP positive at

presentation in comparison to 34.6% of AMI who were hs-TnI positive ( $p = 0.015$ ) (184). The diagnostic accuracy of h-FABP in early presenters negative for cTn has been found to be AUC = 0.946 with a relative risk of 9.042 of later developing AMI (185). These studies are small scale ( $n = 56$  and  $n = 55$ , respectively) but they do show that h-FABP could have an added benefit at very early presentation and should be included in clinical diagnosis algorithms.

However, not all studies show the added benefit of h-FABP to cTn negative patients. A cohort of 317 patients from France showed that there was no significant increase in NPV from 95% or cTnI alone to 96% when h-FABP was included in the diagnosis (223). The analysis was split into high and low-risk groups depending on pretest probability of AMI and there was no difference between cTnI alone or when combined with h-FABP (99% vs 100%) in the low-risk group. This study was conducted on STEMI and NSTEMI patients, however, and could influence the results. The study ROC curve analysis was conducted with 2 different assays, which could lead to imprecisions and a semi-qualitative assay was used, from which quantitative data was used.

The POCT iSTAT assay was commented on being limited when used in conjunction with other biomarkers that require lab-based results as other results would take longer to return. This may be overcome by using h-FABP POCT also, such as the Cardio Detect med that was shown to have higher sensitivity than cTnT < 3h at 79% vs 32% (183) and a qualitative approach that had a sensitivity of 93.0% for patients presenting within 12h (186). This study was carried out on a STEMI cohort ( $n = 52$ ) but it still demonstrates the usefulness of the POCT devices and that by combining

the results from two devices the exclusion could be quicker and more accurate (180, 183). However, the use of these devices may require training to use properly, may take up time of frontline healthcare staff and therefore might not be the solution to quick rule out.

With regards to using ECG ischaemia, creating a composite predictor algorithm including ECG ischaemia and cTn  $\Delta_{\text{absolute}}$  may be better suited to rule in diagnosis. It has been shown that the PPV of 1h  $\Delta_{\text{absolute}}$  20 ng/L was 86.5% and that this increased to 90.5% when ECG ischaemia was included (224). This information may be useful to attempt a quick rule in diagnosis using POCT devices for cTn, H-FABP and ECG, which could include 1h  $\Delta_{\text{absolute}}$  if the cTn at presentation is not yet high enough to rule in AMI diagnosis. A study could assess the utility of first attempting to rule in patients with cTn, H-FABP and ECG ischaemia and if a diagnosis cannot be made using 1h  $\Delta_{\text{absolute}}$ , H-FABP and ECG ischaemia to rule in. The first rule in composite does contravene observing the necessary rise and fall pattern of cTn and true rule in of AMI according to international guidelines may require more observation. However, there is evidence that the addition of deltas does not improve diagnostic rule in accuracy (214).

#### 8.2.6 Prediction of 30-day MACE with cTn 0h & 3h samples

The prognostic accuracy of the 3 assays was assessed for their accuracy for 3 composite endpoints, composite MACE group included all outcomes; AV 1 included all-cause mortality, AMI, revascularisation, PCI, CABG and stenosis; AV2 included cardiac arrest, arrhythmia and acute heart failure. The accurate prognosis of MACE is important as even small rises in cTn can indicate poor long-term outcomes and intervention is beneficial for high-risk patients and detrimental to low-risk patients

(225). The differences between the 0h, 3h and max values sampling were minimal, as was the differences between the accuracy of the assays for the different composite endpoints.

Using the 10% CV cut-offs, the Roche assay produced average sensitivities and specificities for 0h (65.0%, 95% CI 55.9 – 73.4 and 55.8%, 95% CI 51.4 – 60.2, respectively), which did not increase at 3h (65.9%, 95% CI 56.8 – 74.2 and 53.1%, 95% CI 48.7 – 57.5, respectively). The NPVs for 0h and 3h were higher (87.0%, 95% CI 83.8 – 89.6 and 86.7%, 95% CI 83.4 – 89.4, respectively) suggesting a high proportion of patients below the cut-off could be ruled out of 30-day MACE. By using the same cut-off, the AV1 prognosis had higher sensitivity (0h: 89.3%, 95% CI 78.1 – 96.0 and 3h: 83.3 (71.5 – 91.7), which suggests that the rule out of AMI-associated events is higher than non-AMI associated events and the cause of the rise of the cTn could be caused by another ischaemic condition. The NPV for AV1 was higher at 98.2% (95% CI, 96.2 – 99.1) and 97.2% (95% CI, 95.2 – 98.4) for 0h and 3h, respectively, again suggesting more confidence in AV1 rule out. AV2 prognosis shows a reduction in sensitivity to composite MACE levels (0h: 59.3, 95% CI 38.8 – 77.6 and 3h: 55.6%, 95% CI 35.3 – 74.5) and the same occurred with specificity (50.3%, 95% CI 46.0 – 54.5 and 52.2%, 95% CI 48.0 – 56.5, respectively). Interestingly, the NPV remained high at 96.2% (95% CI, 94.2 – 97.6) and 96.1% (95% CI, 94.1 – 97.4), respectively, which may point to the separation of more similar conditions for prognosis to achieve better accuracy.

As with the diagnostic analyses, the Singulex assay displayed high sensitivities and NPVs with very low specificities and PPVs due to its low cut-off. For composite



MACE, the sensitivities for 0h, 3h and max values were all high (96.3%, 95% CI 91.6 – 98.8, 97.8%, 95% CI 93.6 – 100.0 and 98.5%, 95% CI 94.7 – 99.8, respectively) as were the NPVs for 3h and max values, which were 94.6% (95% CI, 84.6 – 98.2) and 93.6% (95% CI, 77.8 – 98.4) but was very low for 0h at 8.6% (95% CI, 7.8 – 9.4). This could mean for accurate prognosis of composite MACE, it is necessary to increase the interval to 3h to increase confidence in rule out when using the Singulex assay. This could be down to the variation seen at the low levels measured by Singulex and at the chosen cut-off.

For AV1 prognosis, the sensitivities were high and was found to be highest for max values (0h: 98.1, 95% CI 89.9 – 100.0, 3h: 96.2%, 95% CI 86.8 – 99.5 and max values: 100.0%, 95% CI 94.0 – 100), which also demonstrated 100% NPV. Therefore, by using the Singulex assay over 3h, all patients under the cut-off could be ruled out of 30-day AV1. As with the Roche assay, the sensitivities of AV2 (all 96.3%, 95% CI 81.0 – 99.9) were higher than composite MACE but lower than AV1, again showing that prognosis could be split by conditions to increase accuracy for different conditions.

The iSTAT assay followed the same pattern as with diagnosis with high specificities and low sensitivities. For composite MACE, the highest specificity was found for 0h (97.1%, 95% CI 95.2 – 98.4) but only marginally as the difference between 0h and 3h and max values was marginal (95.8%, 95% CI 93.7 – 97.4 and 95.4%, 95% CI 93.2 – 97.1, respectively). However, the PPVs were average (64.1%, 95% CI 48.9 – 76.9, 59.2%, 95% CI 45.9 – 71.2 and 55.1%, 95% CI 42.0 – 67.5, respectively) suggesting a limit value of rule in for composite MACE at this cut-off. NPVs were also high (82.5%, 95% CI 81.2 – 83.8, 82.9%, 95% CI 81.5 – 84.3 and 82.6%, 95% CI 81.1 –

83.9, respectively) but the sensitivity (20.2%, 95% CI 13.5 – 28.3, 23.4%, 95% CI 16.3 – 31.8 and 21.8%, 95% CI 14.9 – 30.1, respectively) would limit the amount of patients correctly identified (14%). AV2 displayed very low sensitivities and PPVs (all < 10%) but high specificity (0h: 93.6%, 95% CI 91.2 – 95.5 and 3h and max values: 92.1%, 95% CI 89.6 – 94.2) and NPVs (0h: 95.6%, 95% CI 95.3 – 96.0 and 3h and max values: 95.7%, 95% CI 95.2 – 96.2). This would allow confidence in the rule in of AV2 condition within 30 days but the low NPV would again limit the number of patients correctly identified.

Rapid rule out for a 3-month follow-up period is possible with NSTEMI patients within 3h. When comparing 4 hs-cTn assays and 3 s-cTn assays, all assays had 99.0% – 100% NPVs at 0h, for late presenters (> 6h after symptom onset), which only marginally increased when the interval was increased to 3h and no late presenters who were rule out died during the 3 month follow-up. Although this study observed only late presenters, it could provide a different avenue of prognosis for late presenters and rapid rule out of those under the cut-off. This study is similar to the current analyses and stratification by time since symptom onset could have improved prognostic accuracy. However, patients' accounts of symptoms can be unreliable as the symptoms of AMI can manifest in many different ways and therefore caution should be applied.

A large cohort of 65,696 patients evaluated the accuracy of a hs-TnT assay between 2006-2013 (226). The cohort included all those who experienced chest pain (exclusion criteria notwithstanding) not only NSTEMI and assessed the accuracy of the assay upon the discharged patients to focus on 30-day MACE. The patients were

split into groups that had been immediately discharged and those who had been admitted but later discharged. The hs-TnT assay discharged fewer patients than the conventional cTnT assay (30-day MACE incidence 0.60% vs 0.90%,  $p < 0.001$ ) showing not only greater analytical sensitivity but greater clinical sensitivity. The univariate analysis on the group that was discharged after an initial admission had a much higher HR than those who were immediately discharged (2.18 vs 0.69, respectively). This would be due to the number and severity of symptoms of those who were kept in would be more indicative of AMI and more likely to develop MACE within 30-days (227).

Aldous et al (228) reported risk of death, non-fatal AMI and HF according to a hs-TnT and cTnT over one year. The hs-cTnT was superior in predicting death and HF (HR 5.4 and 27.8) but not for non-fatal MI (HR 4.0). The more analytically sensitive hs-TnT assay was shown to be more prognostically accurate possibly because even small rises in cTn can predict poor long-term outcomes and the cTnT missed patients who fell below the cTnT assay's 99<sup>th</sup> percentile cut-off.

#### 8.2.7 Prediction of 30-day MACE with cTn $\Delta_{\text{absolute}}$ , $\% \Delta_{\text{baseline}}$ and $\% \Delta_{\text{mean}}$

There was a majority of males in the cohort (60.6%) but proportionally the number of males experiencing MACE was less than expected, although not significantly so ( $p = 0.242$ ). This concurs with other studies that show females over-experience MACE in comparison to males.

By using  $\Delta_{\text{absolute}}$  cut-off at 10% CV, the Roche assay did not yield clinically useful prognostic accuracy for any of the composite outcomes. For this variable, the highest sensitivity was found for composite MACE at 30.7% (95% CI, 22.7 – 39.6),

and also yielded the highest specificity (92.3%, 95% CI 89.7 – 94.4). The  $\% \Delta_{\text{baseline}}$  and  $\% \Delta_{\text{mean}}$  had the highest sensitivity for AV2 (both 63.0%, 95% CI 42.4 – 80.6) and highest specificity (76.7%, 95% CI 72.3 – 80.7 and 44.2%, 95% CI 39.4 – 49.2, respectively). The difference in specificity between  $\% \Delta_{\text{baseline}}$  and  $\% \Delta_{\text{mean}}$  may arise from the large magnitudes of change that  $\% \Delta_{\text{baseline}}$  can calculate in comparison to  $\% \Delta_{\text{mean}}$  as the  $\% \Delta_{\text{mean}}$  results can only reach 200%. This way the  $\% \Delta_{\text{mean}}$  will moderate outliers far more than  $\% \Delta_{\text{baseline}}$  but may also result in the identification of fewer patients with AV2 outcomes.

$\% \Delta_{\text{baseline}}$  and  $\% \Delta_{\text{mean}}$  were most accurate the Singulex assay especially the AV1 and 2 groups. The sensitivity for 30-day composite MACE for  $\Delta_{\text{absolute}}$ ,  $\% \Delta_{\text{baseline}}$  and  $\% \Delta_{\text{mean}}$  were all 100%. This is strengthened by the NPVs that are also at 100% suggesting that all negative tests are true negative tests allowing confident rule out. By using max values in to predict AV1 by the Singulex assay, the sensitivity and NPVs are also both 100%. The Singulex assay also showed 100% sensitivity and NPV for 30-day AV2 prognosis, but only for  $\% \Delta$ . Again, the specificities are very low (5.7%, 95% CI 4.0 – 8.0 and 5.2%, 95% CI 3.5 – 7.4 for  $\% \Delta_{\text{baseline}}$  and  $\% \Delta_{\text{mean}}$ , respectively) but in a rule out diagnosis, this is not a significant concern. It is unusual that the  $\% \Delta$  outperformed  $\Delta_{\text{absolute}}$  in a NSTEMI cohort as  $\Delta_{\text{absolute}}$  outperforms  $\% \Delta$  at lower concentrations. However, according to the Singulex assay, the 30-day composite MACE cohort did have a wide range of cTn baseline concentrations with a mean of 340 pg/ml, which is greater than the threshold at which the prognostic accuracy of  $\Delta_{\text{absolute}}$  is greater than  $\% \Delta$  (190).

The very low specificities comes from the fact that the Singulex is so variable that the low cut-offs are successful in identifying those without AMI but will also include many who are of moderate risk. The large variation in its performance means that whether a patient is put into high or low risk groups is almost random, as the crosstabs show. The survival analyses agree with this, as there is no significant difference between 30-day events between patients above and below the cut-offs. It is very useful for ruling patients out but it is random when compared with the final adjudicated diagnosis or 30-day MACE outcomes.

The analytical sensitivity of the ISTAT assay has again shown higher specificities and lower sensitivities than the other two assays. This was shown more when composite MACE and AV2 were measured by  $\Delta_{\text{absolute}}$  (19.4%, 95% CI 12.8 – 27.4 and 4.0%, 95% CI 0.1 – 20.4, respectively). However, the  $\Delta_{\text{absolute}}$  specificities for composite MACE, AV1 and AV2 were higher (96.5%, 95% CI 94.4 – 97.9, 96.2%, 95% CI 94.2 – 97.6 and 93.2%, 95% CI 90.8 – 95.2, respectively) and with optimisation the specificity and NPVs could reach 100%. This would require an increase in the  $\Delta_{\text{absolute}}$  cut-off and with only 40 patients (5.5% of cohort) above the current cut-off of 100 pg/ml, it would only recognise only the highest risk of patients but these patients are of greatest risk. The low PPVs (composite MACE at 58.5%; AV1 at 48.8%; AV2 at 2.6%) also call in question how accurate the prognosis would be and for a 30-day prognosis this would cause unnecessary admissions. When using  $\% \Delta$  a higher cut-off will yield a greater delta in absolute terms and therefore specificity will be higher owing to the larger cTn change, especially at lower cTn baseline and mean values.

The  $\% \Delta_{\text{baseline}}$  and  $\% \Delta_{\text{mean}}$  sensitivities were more uniform than the Roche assay but did not perform better (composite MACE at 56.0%, 95% CI 46.1 – 65.5 and 56.8%, 95% CI 47.1 – 66.3; AV1 at 55.4%, 95% CI 41.5 – 68.7 and 71.4%, 95% CI 57.8 – 82.7; AV2 at 52.0%, 95% CI 31.3 – 72.2 for both, all respectively). The disparity between the  $\% \Delta_{\text{baseline}}$  and  $\% \Delta_{\text{mean}}$  AV1 sensitivities could be due to the same reason as with the Roche assay, which is the mitigating of outliers by the  $\% \Delta_{\text{mean}}$ .

The outcome that had the highest sensitivity, specificity, NPV and PPV and was most accurate across all assays was the AV1 composite outcome. This is because the conditions included in this composite outcome, all-cause mortality, AMI, revascularisation, PCI, CABG and stenosis are ACS-associated conditions, instead of AV2, which included cardiac arrest, arrhythmia and acute heart failure.

Hazard ratios were conducted to assess which risk factors was most associated with 30-day composite, which included age, sex, prior MI, prior angina, prior PCI, prior CABG, hypertension, hyperlipidaemia, chronic kidney disease, smoker and the non-kinetic cut-off and deltas for each of the assays. Only prior angina and Singulex  $\Delta_{\text{absolute}}$  were significantly associated with 30-day composite MACE (HR: 0.462,  $p = 0.022$ ; HR: 2.466,  $p = 0.006$ , respectively). The reduced risk of patients with prior angina at 30 days is due to patients managing their condition. Of the 193 patients with prior stable angina, 21 (11%) were not receiving treatment related to their condition (includes aspirin, oral nitrate, statins, ACE inhibitors, beta blockers,  $\text{Ca}^{2+}$  blockers, Nicorandil). Patients with other risk factors would also be receiving treatment for the conditions, which would also cause the HR to fall below 1, none of which were significant. It is interesting to note that with increasing age there was

a slight but insignificant reduction in risk at 30 days but this is also because with age treatments that would reduce risk of MACE increase.

Average time to event for composite MACE was performed for each of the assays for 0h and  $\Delta_{\text{absolute}}$ . These analyses showed very small variation between high and low groups for all assays, ranging from 29.68 – 30.00 days. Only the Singulex assay showed a significant difference between high and low cTn groups in which the high cTn group had less time to event than the low cTn group (29.68 days, 95% CI, 29.46 – 29.90 and 29.95 days, 95% CI, 29.91 – 30.00, respectively;  $p = 0.003$ ), as would be expected. However, due to the low number of events across the cohort (6 in total), it would be difficult to represent how accurate each assay is at predicting average time to event and cumulative event rate.

Apple et al (210) used  $\% \Delta$  of 10%, 20% and 30% on a cohort of 397 for 60-day MACE and found highest cumulative event rate was with patients whose second cTn sample was  $> 0.034 \mu\text{g/L}$  (49.2%) and in patients whose  $\% \Delta$  was increased by  $> 30\%$  (60.5%) and both were independent predictors of MACE. Non-kinetic values showed the strongest prognostic accuracy in this paper but combined the  $6\text{h} > 0.034 \mu\text{g/L} + \Delta\text{cTnI} > 30\%$  was the most prognostically accurate with 69.4% of cohort having an event at 60-days.

In a study using a longer sample-sample interval of 24h,  $\% \Delta$  were set at +20%, +50% and +100% and showed higher proportional rates of a composite of AMI and death at 6 months (229). In the  $\text{cTnI} > 0.07 \mu\text{g/L}$  group 3.1% had events and this increased for  $\text{cTnI} > 0.07 \mu\text{g/L} + \geq 20\% \% \Delta$  to 14.4% of patients above threshold had an event. However, this did not increase with  $\text{cTnI} > 0.07 \mu\text{g/L} + \geq 100\% \% \Delta$  was 14.5%. Even

though the  $\% \Delta$  had increased, the effect on prognostic accuracy had not. The  $\geq 20\%$  did positively associate with AMI events over ten years (log rank  $p < 0.001$ ), showing that even moderate rises of cTnI show poor long-term outcomes.

In another long-term study associating cTn deltas with outcomes, Kaplan-Meier analysis showed only patients in the highest tertile ( $\Delta_{\text{absolute}} > 104$  ng/L) were significantly associated with worse outcomes after 30-days and those in the lowest tertile ( $\Delta_{\text{absolute}} < 5.4$  ng/L) were not (230). This concurs with the current analysis where only the  $\Delta_{\text{absolute}}$  Singulex was significantly predictive for 30-day composite MACE (HR = 2.466) Over one year, any detectable cTn was associated with poorer long-term outcomes with hazard ratios increasing as cTn deltas increased ( $\% \Delta < 43\%$ ;  $\% \Delta > 728\%$ ) but the HR for  $\Delta_{\text{absolute}}$  was greater than for  $\% \Delta$  (2.95 and 1.89, respectively).

The difference in plaque morphology can lead to a difference in how AMI manifests Ruptured coronary plaques and multiple thrombi are more associated with early events after presentation and chronic atherosclerosis is more associated with later events after presentation (231). Imaging techniques could be incorporated for better prognostic accuracy for patients and would further reduce unnecessary hospitalisations. Early PCI improves outcomes but more likely to need another revascularisation at 6 months (88).

#### 8.2.8 Prediction of 30-day MACE using baseline cTn in predictor composites with cTn deltas, acute ischaemia, and H-FABP diagnosis for AMI diagnosis for cardiac-associated conditions

As with the composite predictor for diagnosis, the same method was applied but for 30-day composite MACE to assess this novel composite for accuracy across the 3



assays. As with the diagnosis accuracy of these composites, the Singulex assay had high sensitivities, the iSTAT assay had high specificities and the Roche assay had more consistent results but with some composites showing high rule out capability.

The average predictive accuracy for the Roche assay for cTn + ECG (sensitivity: 64.1%, 95% CI 55.6 – 72.0, specificity: 52.8%, 95% CI 48.6 – 56.9, PPV: 24.9%, 95% CI 22.2 – 27.8 and NPV: 85.8%, 95% CI 82.7 – 88.3) did not improve with cTn +  $\Delta_{\text{absolute}}$  but cTn +  $\% \Delta_{\text{baseline}}$  did improve with regards to rule out capability with sensitivity and NPV both at 100.0%. All cTn + ECG + deltas expressed 100% sensitivity and NPV also but the addition of H-FABP had a detrimental effect on sensitivities for  $\Delta_{\text{absolute}}$ ,  $\% \Delta_{\text{baseline}}$  and  $\% \Delta_{\text{mean}}$  (68.3%, 95% CI 60.0 – 75.9, 99.3%, 95% CI 96.1 – 100.0 and 75.4%, 95% CI 67.4 – 82.2, respectively). This could be due to H-FABP being a short-term predictor according to rapid release into the system. The specificity of composites including  $\% \Delta_{\text{baseline}}$  was markedly less than  $\% \Delta_{\text{mean}}$  (cTn +  $\% \Delta_{\text{baseline}}$  0.4%, 95% CI 0.0 – 1.3 and cTn +  $\% \Delta_{\text{mean}}$  35.9%, 95% CI 32.0 – 40.0). This could be down to the mitigating factor of the  $\% \Delta_{\text{mean}}$  only allowing values to reach 200%, which  $\% \Delta_{\text{baseline}}$  does not have and small increases in absolute terms could be large as a percentage misprognosing patients.

For the Singulex assay, the cTn + ECG sensitivity was high (95.8%, 95% CI 91.0 – 98.4) and the specificity low (10.3%, 95% CI 8.0 – 13.1) and the introduction of deltas to make cTn + delta composites did not improve sensitivity but had an effect on  $\% \Delta_{\text{baseline}}$  and  $\% \Delta_{\text{mean}}$  specificity (1.6%, 95% CI 0.7 – 3.0 and 3.0%, 95% CI 1.7 – 4.7, respectively). This could be due to the effect of percentages exaggerating differences at lower concentrations, at which the Singulex assay can measure. The

combination of the low cTn cut-off and low  $\Delta_{\text{baseline}}$  and  $\Delta_{\text{mean}}$  cut-offs enhance this more than the specificity of cTn +  $\Delta_{\text{absolute}}$  (9.4%, 95% CI 7.2 – 12.1), which is very low but was not as effected as the  $\Delta$ . All cTn + ECG + deltas showed perfect rule out capability with 100% sensitivity and NPV, with consistently low specificity and PPVs once more. The addition of H-FABP reduced the sensitivities (97.2%, 95% CI 92.9 – 99.2, 98.6%, 95% CI 95.0 – 99.8 and 98.6%, 95% CI 95.0 – 99.8, respectively) and NPVs (93.0%, 95% CI 83.0 – 97.3, 84.6%, 95% CI 55.2 – 96.1 and 90.5%, 95% CI 69.1 – 97.6, respectively). The + H-FABP results are greater than the Roche assay results shown above but the reduction in rule out capability for 30 day MACE could also be due to the rapid release and decrease in the serum of H-FABP.

For the iSTAT assay, the specificities were mostly higher than the sensitivities with consistent NPVs either side of 85%. The addition of each variable to the composite had a negative effect on specificity, e.g. for  $\Delta_{\text{absolute}}$ , cTn +  $\Delta_{\text{absolute}}$  was 95.7% (95% CI 93.7 – 97.3), cTn + ECG +  $\Delta_{\text{absolute}}$  was 90.2% (95% CI, 87.3 – 92.6) and cTn + ECG +  $\Delta_{\text{absolute}}$  + H-FABP was 79.8% (95% CI, 76.1 – 83.1). The opposite was true for sensitivity with it increasing with additional variables, e.g. for  $\Delta_{\text{absolute}}$  was 23.0% (95% CI, 16.2 – 31.0), 32.6% (95% CI, 24.8 – 41.2) and 41.5% (95% CI, 33.1 – 50.3), respectively. For a high cut-off assay, this is consistent with the data because added variables will increase false positives missed by cTn, as seen with the PPVs that decreased accordingly.

The Singulex assay performed best when considering the rule out of patients from 30-day MACE. As said previously, the poor specificity is not a large concern if a patient can be ruled out quickly and effectively. The Roche assay performed as well

for the cTn + ECG + delta as the Singulex assay showing a strong prognostic accuracy not only for the assays but also for the predictor composite itself. Further studies could assess the prognostic utility of this composite as a possible simple early rule out for 30-day MACE. However, more complex, tailored algorithms would be more accurate to this end.

One such algorithm is the MACS rule, which used univariate logistic regression to identify predictors for AMI and MACE. The rule combines hs-cTnT, h-FABP, ECG ischaemia, observed sweating, vomiting, systolic blood pressure < 100 mmHg, worsening angina and pain radiating to right arm or shoulder in a multivariate logistic model (232). The rule produced AUC of 0.95 for predicting MACE at 30 days and could rule out all patients in the very low risk group that made up 35.5% of the cohort from 30-day AMI with only 1 patient experiencing MACE in the same group. This lead to an overall sensitivity of 99.4% and NPV of 99.6% for MACE and 100% for both for AMI. A further study with an automated assay for h-FABP increased the number of patients who could be ruled out of 30-day AMI with 100% sensitivity to 40.5% of cohort with a 1.1% incidence of 30-day MACE (233). However, these analyses include STEMI and NSTEMI patients and therefore the percentage of patients who would be considered for rule out would be higher than a cohort of NSTEMI only patients. Yet, the use of continuous data in the form of hs-TnT and h-FABP provides more information than categorical data alone and which could point towards its very high AUC. As NSTEMI diagnosis can be problematic, the use of continuous and not categorical data could be very useful in the further improvement in NSTEMI diagnostic accuracy.

#### 8.2.9 Limitations

Adjudication of outcomes was done with standard cTn assays and not those featured in the analyses and this could lead to mis-classification bias when using the assays in practise. Validation studies would need to be done to assess their performances in active clinical practice. Secondly, many patients did not have two samples taken, especially for the point of care iSTAT device, and these exclusions could lead to selection bias. The outcome measures for diagnosis were binary, AMI and no AMI, and does not include the myriad of ACS available. In future, the cohort could be subdivided further by cTn measurements to determine which ACS the patients is experiencing. However, even with ultra- or hyper-sensitive-cTn assays, subdividing by cTn alone may not be able to categorise patients effectively or more emphasis on rule in diagnoses may be needed for this end.

The short 30-day prediction time lead to a limited number of events, which effected the Kaplan-Meier analysis and differences between high and low cTn groups was minimal. The follow-up data was incomplete, and had few events regardless adding to apparent inconsistencies in the data. Inconsistency could also have arisen from sample collection and storage; the samples were used by multiple groups in a busy environment that could have lead to sample degradation. The busy environment may have lead to incomplete data on duration of chest pain and therefore provided misleading information concerning TSSO and discrepancies seen across the 0h-3h time period.

#### 8.2.10 Future work

Large  $\% \Delta$  cut-offs at low concentrations and small  $\% \Delta$  cut-offs at high concentrations are due to the effect of biological variation. At low concentrations,

the effect of biological variation is large and is much less at higher concentrations (234). This can be used clinically as cut-offs can be changed depending on the baseline cTn to make diagnoses and MACE predictions more accurate. Low  $\% \Delta$  cut-offs at high concentrations could be used to quickly rule out patients who have chronically high cTn levels because only a very low  $\% \Delta$  would be observed in those patients due to their raised basal cTn level. However, this could be used as a rule in tool for patients who are already at risk of AMI arriving to the ED with raised cTn, which may not raise much higher. Without a significant rising or falling pattern it might be difficult to diagnose, especially in the uncommon instance of reinfarction. In addition, variation across time has been shown to increase and decrease (234, 235) further complicating its use in diagnosis.

In the same way that different assays have different specifications, the individual variation between and within patients (235) will also have implications on how effective the specific diagnosis cut-off or algorithm will be on different patients or groups of patients.

A very small  $\% \Delta$  could be seen as individual, biological, analytical or even circadian (236) variation and not to do with myocardial ischaemia. However, higher concentrations experience a plateau of  $\% CV$  and therefore consistency above 300 pg/ml. The above analyses include only NSTEMI patients, which does not experience such high levels of cTn as STEMI but cTn means for NSTEMI are found within this range (160) especially if sampling is done post-24h symptom onset (209). Pretorius and Ungerer (190) observed this phenomenon and tried to overcome the different  $\% CV$  and analytical characteristics of different assays to produce a

universal cut-off for NSTEMI by using z-values. The cut-off was determined from the z-value, which takes into the account the analytical and biological variation found in the assay and the reference population of patients by this equation (190):

$$Z = \frac{\Delta_{absolute}}{\sqrt{2SD_{Analytical}^2 + 2SD_{Biological}^2}}$$

This is based on the reference change value (RCV) equation:

$$RCV = \sqrt{2SD_{Analytical}^2 + 2SD_{Biological}^2}$$

Using RCVs could be important for groups of patients who have chronically elevated cTn as a raised baseline cTn would not be specific to AMI and a standardised rising and falling pattern must be observed for MACE prediction to be accurate. In a group of haemodialysis patients, RCV cut-offs were determined at +37% and -30% for hs-cTnI and +25% and -20% for hs-cTnT and patients exceeding the RCVs had HR = 1.9 and = 1.7 for all-cause mortality (237). Specifically for sudden cardiac death, hs-cTnI RCVs > +37% and -30% showed an adjusted HR = 2.6.

Not only do RCVs allow another route for diagnosis and MACE prediction but also they are useful in directly comparing analytical specifications of different assays and not through diagnostic tests. This would allow comparing concentrations at which 10% CVs, 99<sup>th</sup> percentiles and LoDs easier to compare making comparisons of diagnostic test more effective. In addition, by using RCVs, the cut-off is personalised to each patient creating a more tailored and specific diagnosis. The variations between patients will be different and therefore assigning reference population data will cause infrequent false negatives due to this difference. By taking into

account, a patient with very low intrapersonal variation may be wrongly adjudicated as AMI-free as the cTn delta was not high enough for a rule in diagnosis. By adjusting for this difference, a margin of error is removed and ACS diagnoses become closer to personalised medicine. In addition, RCV are not affected by how results are distributed whereas cTn  $\Delta_{\text{absolute}}$  and  $\% \Delta$  are more effective at opposing ends of the cTn baseline range giving RCVs more scope across all cTn concentrations.

### 8.3 Conclusion

The aim of these analyses was to produce a new clinical decision algorithm that included mCRP. However, the chemically complex nature of mCRP along with a non-commercial antibody made creating a reliable immunoassay problematic and too variable for clinical use. Its involvement in the degradation of the fibrous cap of atheromas suggests it would be a useful biomarker for rapid rule out or rule in. Alternatively, mCRP may be more of use in short-term MACE prediction as its role in degrading the fibrous cap is integral to and precedes MACE. However, it dissociates locally around sites of activated endothelium and therefore the systemic concentration will be low, which could require a very sensitive method of detection to discern between pathological and non-pathological rises in mCRP, as occurred with AMI diagnosis and cTn.

Although cTn is a product of ACS and does not precede events unlike mCRP, the use of the ultra-hs-cTnI Singulex analyser did produce perfect rule out at presentation for AMI with 21% of patients below the specified cut-off. This was much higher than the current Roche assay in use at the MRI and could allow more patients to be ruled out of AMI more quickly with a single test. However, validation in a clinical study

could wait until a precision profile was expanded to include the concentrations at which the assay displays its analytical sensitivities. This would increase clinicians' confidence concerning repeatability of the assay and in turn the safety of the patients.

The point of care iSTAT assay showed promising rule in capability, which is necessary to quickly identify patients who are at high risk and require immediate assistance. Its performance in the predictor composite did not consistently enhance rule out accuracy, unlike the Roche or Singulex assays. However, by using the iSTAT to identify high-risk patients, it could be used alongside other iSTAT cartridges, such as the h-FABP to identify high-risk patients even earlier. Using an assortment of tools to positively diagnose patients consolidates more and varied data resulting in more accurate diagnoses.

Furthermore, by categorising patients into risk groups based on the baseline cTn concentration and tailoring delta cut-offs to each individual group, diagnostic accuracy increases. Additional tailoring can be done with the use of RCVs, which provides each patient with a personalised cut-off. Although this may cause difficulty by taking time to calculate the RCVs, this could be automated for ease in busy EDs. This form of personalised medicine effectively negates the variation that causes uncertainties in diagnoses to provide clinicians with a more confident diagnosis for that particular patient and not solely based on reference populations.

The Gold Standard of ACS diagnosis is cTn due to its cardiac specificity and with ever more sensitive cTn assays, it will remain as the most clinically useful biomarker. This does not suggest that cTn should be used alone, by combining



different diagnostic tools and biomarkers ACS diagnosis could become more personalised and therefore more accurate.





# cTnI Assay Instructions For Use



Singulex.com/IFUs

## INTENDED USE

The Sgx Clarity™ cTnI Assay is an *in vitro* immunoassay test that quantitatively measures cardiac troponin (cTnI) in EDTA plasma using the Sgx Clarity System. The Sgx Clarity cTnI Assay is indicated to be used in conjunction with clinical evaluation for ruling out cardiac ischemia in patients suspected of having coronary artery disease.

## DEVICE DESCRIPTION

The Sgx Clarity cTnI Assay is composed of the following individual components (all sold separately):

- Sgx Clarity cTnI Reagent Pack
- Sgx Clarity cTnI Calibrator Kit
- Sgx Clarity System Elution Buffer
- Sgx Clarity System Wash Buffer Concentrate.

## SUMMARY AND EXPLANATION OF THE TEST

Coronary artery disease (CAD) is one of the leading causes of death worldwide.<sup>1</sup> Early detection of CAD and stress-induced cardiac ischemia is critical to global efforts towards reducing the CAD public health burden. Cardiac stress testing is currently the mainstay of noninvasive CAD diagnostics.<sup>2</sup> Nuclear stress testing with imaging, such as myocardial perfusion imaging single emission tomography (MPI-SPECT), has limitations including high costs, limited availability, and exposure to contrast agents and radiation.<sup>2-4</sup> Therefore, there is a need for simple, safe, and widely available alternative tools to detect stress-induced cardiac ischemia with a degree of accuracy that would enable rule-out of patients from such imaging tests. In addition to reducing healthcare costs, an equivalent alternative rule-out tool would reduce patient time in medical facilities and the number of specialist referrals needed.

Cardiac troponins I and T (cTnT) have a central role in the diagnosis and management of patients with suspected acute coronary syndrome (ACS).<sup>5,6</sup> Previous studies have demonstrated an association between cTnI levels and stress-induced cardiac ischemia.<sup>7,8</sup> The association between cardiac troponin and stress-induced ischemia was further established in the BASEL VIII study using a high-sensitivity cTnI Research Use Only (RUO) assay from Singulex in patients with suspected CAD being evaluated with MPI-SPECT—overall, the Singulex cTnI assay (RUO) demonstrated strong diagnostic accuracy, in particular for the rule-out of cardiac ischemia, and therefore the rule-out of standard stress-imaging procedures.<sup>9</sup> A separate subset of the EDTA plasma cohort from the BASEL VIII study was used to validate the Sgx Clarity cTnI Assay for its intended use and determine the diagnostic test characteristics at multiple cTnI concentrations.

## TEST PRINCIPLE




The Sgx Clarity cTnI Assay is an ultra-sensitive immunoassay that uses single photon fluorescence detection for the quantitation of cardiac troponin I (cTnI) in EDTA plasma samples. The sample is transferred by the Sgx Clarity System to an Sgx Clarity Reaction Vessel (RV), into which cTnI-specific antibody-coated paramagnetic microparticles (capture reagent) and fluorescently labeled cTnI-specific antibodies (detection reagent) are then added. The reactants are then incubated at 37 °C in the Reaction Vessel. During incubation, cTnI present in the sample binds to both the capture antibodies and the detection antibodies, forming an immune complex. Unbound material in the reaction mixture is washed away during the subsequent wash steps. Elution buffer is then added to dissociate the immune complexes (bound analyte and detection antibodies) from the paramagnetic microparticles and release fluorescently-labeled antibodies during the second incubation step of the protocol. After dissociation, the mixture is exposed to a magnetic field in order to separate the paramagnetic microparticles from the dissociated labeled antibodies. The resulting eluate, containing the dissociated detection antibodies, is transferred to an Sgx Clarity Detection Vessel (DV) where the labeled molecules are detected and counted. The signal count results are then compared to a calibration-adjusted Master Curve and converted into a cTnI concentration.

## OTHER RESOURCES


- For lot-specific information, refer to the package insert or reagent label associated with each reagent.
- For detailed instructions on how to operate the Sgx Clarity System, refer to the Sgx Clarity System Operator's Manual. To download electronic copies of the operator's manual, please visit [singulex.com/IFUs](http://singulex.com/IFUs). To request additional printed copies of the Sgx Clarity System Operator's Manual or these Instructions For Use, call +800 135 79 135.

## REAGENTS

### Assay Reagents

Reagent	Description	Associated Notices	REF	
Capture Reagent	A HEPES-buffered solution containing anti-troponin I mouse monoclonal antibody-coated paramagnetic microparticles with protein stabilizers and sodium azide as a preservative.	None	DX-CTNKIT-001 Sgx Clarity cTnI Reagent Pack	CE
Detection Reagent	A HEPES-buffered solution containing fluorescently-labeled anti-troponin I mouse monoclonal antibodies with protein stabilizers and sodium azide as a preservative.	None	DX-CTNKIT-001 Sgx Clarity cTnI Reagent Pack	CE
Sgx Clarity cTnI Calibrators	Human Serum and Plasma protein matrix containing buffers, antibiotics, and stabilizers adjusted to known cTnI concentrations with native human cTnI.	 	DX-CTNCAL-001 Sgx Clarity cTnI Calibrator Kit	CE
Sgx Clarity cTnI Controls (optional)	Human Serum and Plasma protein matrix containing buffers, antibiotics, and stabilizers adjusted to known cTnI concentrations with native human cTnI.		DX-CTNCTR-001, 002, 003, 004 Sgx Clarity cTnI Controls (Levels 1-4)	CE



### System Reagents




Reagent	Description	Associated Notices	REF	
Sgx Clarity System Elution Buffer	Aqueous solution with a glycine buffer system.		DX-CLRELB-001 Sgx Clarity System Elution Buffer	CE
Sgx Clarity System Wash Buffer Concentrate	Borate buffer solution containing ProClin 950 as a preservative.	None	DX-CLRWAS-001 Sgx Clarity System Wash Buffer Concentrate	CE

## REAGENT STORAGE AND STABILITY

Store reagents as follows for use on the Sgx Clarity System. For lot-specific information, consult the package insert or reagent label for each reagent. All unopened reagents are stable when stored as directed until labeled expiration date.

For instructions related to usage on the Sgx Clarity System, refer to the Sgx Clarity System Operator's Manual.

Reagent	Store upright at...	Open Stability
Sgx Clarity cTnI Reagent Pack:  Capture Reagent and Detection Reagent		56 hours at room temperature following first use or until the labeled expiration date, whichever comes first. (See "Sgx Clarity cTnI Reagent Pack Stability and Calibration Interval".) <b>Note:</b> Unless specified otherwise, "room temperature" is defined as (15–30 °C).
Sgx Clarity System Elution Buffer		NA: Single use reagent.

Reagent	Store upright at...	Open Stability
Sgx Clarity System Wash Buffer Concentrate	 15°C – 30°C	<b>Concentrated:</b> Until the labeled expiration date.  <b>Prepared (diluted):</b> 7 days following preparation or until the labeled expiration date of the Wash Buffer Concentrate, whichever comes first.
Sgx Clarity cTnI Calibrators (3 levels)	 2°C – 8°C	NA: Single use reagent.
Sgx Clarity cTnI Controls (Singulex / 4 levels)	 2°C – 8°C	30 days or until the labeled expiration date, whichever comes first.  <b>Note:</b> The Sgx Clarity System does not track open stability of Sgx Clarity cTnI Controls. It is the responsibility of site personnel to track this following first use.

## PRECAUTIONS

- For *In Vitro* Diagnostic Use.
- Use routine laboratory precautions and do not pipette by mouth.
- Do not eat, drink, or smoke in the laboratory work area, and wash hands thoroughly after use.
- **WARNING** - Sgx Clarity cTnI Calibrators (3 levels) and Sgx Clarity cTnI Controls (4 levels; optional) contain methanol and are subject to the following Hazard and Precautionary statements:
  - H303, May be harmful if swallowed
  - H311, May be harmful in contact with skin
  - H331, May be harmful if inhaled
  - P264, Wash hands thoroughly after handling
  - P270, Do not eat, drink, or smoke while using this product
  - P280, Wear protective gloves/protective clothing/eye protection/face protection
  - P261, Avoid breathing mist/vapors/spray
  - P271, Use only in a well-ventilated area

### Hazard Responses:

- P301 + P312, if swallowed, call a Poison Center or doctor/physician if you feel unwell
- P330, Rinse mouth
- P302+P352, IF ON SKIN: Gently wash with plenty of soap and water
- P312, Call a POISON CENTER or doctor/physician if you feel unwell
- P363, Wash contaminated clothing before reuse
- P304+P340, IF INHALED: Remove victim to fresh air and keep at rest in a position comfortable for breathing
- P311, Call a POISON CENTER or doctor/physician
- **WARNING** - Sgx Clarity cTnI Calibrators and Sgx Clarity cTnI Controls (if used) contain human blood products and should be considered potentially infectious—take the same precautions as are used with patient specimens.
- Sgx Clarity cTnI Reagent Packs, Sgx Clarity cTnI Controls, and Sgx Clarity cTnI Calibrators contain sodium azide, which can react with copper and lead plumbing to form explosive metal azides. If disposal into a drain is in compliance with local requirements, flush reagents with a large volume of water to prevent buildup of azides.
- Disposal – Dispose of biohazardous materials according to the practices of your institution. Discard all materials in a safe and acceptable manner, and in compliance with all governmental requirements.
- The Safety Data Sheet (SDS) for each reagent is available upon request.

## MATERIALS

### Materials Provided by Singulex

Material	Quantity/Capacity	REF or PN
Sgx Clarity cTnl Reagent Pack	1 pack (92 test capacity*)	DX-CTNKIT-001
Sgx Clarity Detection Vessels Box	25 DVs	DX-CLRDVS-001
Sgx Clarity Reaction Vessels Box	120 RVs	DX-CLRRVS-001
Sgx Clarity System Elution Buffer	20 × 30 mL	DX-CLRELB-001
Sgx Clarity System Wash Buffer Concentrate	1 × 1 L	DX-CLRWAS-001
Sgx Clarity cTnl Calibrator Kit (lot matched)	Level 1 (1 × 0.75 mL) Level 2 (1 × 1.20 mL) Level 3 (1 × 0.75 mL)	DX-CTNCAL-001
Sgx Clarity Spare Reagent Caps	250	DX-CLRCSM-001
Sgx Clarity Waste Blisters	40 (20 large and 20 small)	DX-CLRCSM-002
Spare Bottles for RV Buffer	12	DX-CLRCSM-003
13 mm × 75 mm Low Volume Sample Cup Holders	1,000	DX-CLRCSM-004
Low Volume Sample Cup (0.5 mL)	1,000	DX-CLRCSM-005
Disposable Tips (DiTi), 1000 µL	2,304	30064861
Disposable Tips (DiTi), 350µL	7,680	30083400
7.5 mL Disposable Graduated Transfer pipets	500	16001-188
Super Sani-Cloth Germicidal Disposable Wipes	1 pack (160 sheets)	Q55172
Presaturated Wipes	1 pack (30 sheets)	PS-919
Microcide SQ	1 Gallon	MICROCIDE

\*Sgx Clarity cTnl Reagent Packs contain enough volume to run at least 92 tests under most operating conditions, but the actual number of tests derived from any given pack will fluctuate according to variable evaporation rates and total open time. If processed at the acceptable upper temperature limit for the entire open stability period, the actual number of tests derived may be as few as 72.

### Materials Required But Not Provided by Singulex

Material	Quantity	REF or PN
Deionized water	Not applicable	Not applicable

### Optional Materials

Material	Quantity	Vendor / Description	REF or PN
Sgx Clarity cTnl Control Level 1	6 × 3.0 mL	Singulex	DX-CTNCTR-001
Sgx Clarity cTnl Control Level 2	6 × 3.0 mL	Singulex	DX-CTNCTR-002
Sgx Clarity cTnl Control Level 3	6 × 3.0 mL	Singulex	DX-CTNCTR-003
Sgx Clarity cTnl Control Level 4	6 × 3.0 mL	Singulex	DX-CTNCTR-004
Phosphate Buffered Saline, no additives (for dilution, if required)	1 × 500 mL	Thermo Fisher / Gibco PBS, pH 7.2	20012027
	1 × 500 mL	Thermo Fisher / Gibco PBS, pH 7.4	10010023
	100 tablets	Diagnostic BioSystems / pH 7.4	DMRE404-01
Centrifuge filter, 500 µL capacity	100	VWR	82031-360

## PROCEDURAL NOTES

### Specimen Collection and Handling

- EDTA plasma is the intended sample type for this assay.
- Follow the manufacturer's processing instructions for plasma collection tubes.
- Collect blood samples observing Standard Precautions for venipuncture.
- To avoid cross-contamination, use caution when handling patient specimens. The use of disposable pipettes or pipette tips is recommended.
- Keep sample tubes capped at all times when not in use.
- Tightly cap and refrigerate sample tubes at 2–8 °C.
- Equilibrate samples to room temperature prior to processing on the Sgx Clarity System.
- Inspect all specimens for bubbles. If present, remove bubbles prior to analysis, being careful not to remove too much specimen volume.
- Centrifuged specimens with a lipid layer on the top must be transferred to a Low Volume Sample Cup or secondary tube for processing on the Sgx Clarity System. Care must be taken to transfer only the clarified specimen without the lipemic material.
- Frozen Sample Handling:
  - Freeze samples  $\leq -70$  °C for long term storage, with maximum of 3 freeze/thaw cycles.
  - Mix thoroughly by gentle inversion after thawing until samples are visibly homogenous, without layering or stratification.
  - Frozen samples must be fully thawed and centrifuged at  $11,300 \times g$  for 10 minutes before analysis.
  - Following centrifugation, prepare the supernatant and transfer as follows:
    - **For low volume ( $\leq 0.5$  mL) samples:** Without disturbing the pellet, transfer the supernatant to a Low Volume Sample Cup and load onto the Sgx Clarity System in a  $13 \times 75$  mm Low Volume Sample Cup Holder per the instructions provided in the Sgx Clarity System Operator's Manual.
    - **For larger volume samples ( $> 0.5$  mL):** Without disturbing the pellet, transfer the supernatant to an appropriately-sized tube. Pipette up and down 10 times within the tube to mix thoroughly, then transfer 300  $\mu$ L to a Low Volume Sample Cup and load onto the Sgx Clarity System per the instructions provided in the Sgx Clarity System Operator's Manual.

Or:

- **As needed:** If supernatant retains visible particulate matter following centrifugation, samples may require filtration. In this case, transfer the supernatant to a VWR centrifuge filter (see "Optional Materials" on page 4) and centrifuge at 13,900 g for 10 min prior to transferring sample to Low Volume Sample Cup or tube as noted above.
- Before placing samples onto the system, ensure that the samples are:
  - Free of particulate matter.
  - Free of bubbles.
- Stability

The Sgx Clarity cTnI Assay has shown stability for EDTA plasma samples at room temperature (20–25 °C) for up to 24 hours, refrigerated (2–8 °C) for up to 120 hours, and 12 months at  $\leq -70$  °C with up to 3 freeze/thaw cycles.

## Reagent Preparation

Reagent	Preparation
Sgx Clarity cTnI Reagent Pack:  Capture Reagent and Detection Reagent	<ul style="list-style-type: none"> <li>Keep Sgx Clarity cTnI Reagent Pack vials capped when not in use.</li> <li>Once reagent vial caps have been removed for use of the reagent pack on the Sgx Clarity System, replace them with new Sgx Clarity Spare Reagent Caps before returning the reagent pack to storage.</li> <li>Do not combine leftover volume from one Sgx Clarity cTnI Reagent Pack with another.</li> <li>Prior to loading reagents onto the Sgx Clarity System:               <ul style="list-style-type: none"> <li>Remove from storage and allow to equilibrate to room temperature for 60 minutes.</li> <li>Mix the reagent pack by hand by gentle inversion at least 10 times prior to loading.</li> <li>Open each reagent vial and dispose of reagent caps (new reagent caps must be used upon returning the reagent pack to storage).</li> <li>Remove bubbles from the surface with a disposable transfer pipette as follows:                   <ul style="list-style-type: none"> <li>Use separate disposable pipettes for each reagent vial.</li> <li>Be careful not to aspirate the liquid reagent.</li> </ul> </li> </ul> </li> </ul> <p><b>Note:</b> Do not store Sgx Clarity cTnI Reagent Packs on the benchtop or on the Sgx Clarity System—always cap and return to storage at 2–8 °C when not in use.</p>
Sgx Clarity System Elution Buffer	<ul style="list-style-type: none"> <li>Remove from storage and allow to equilibrate to room temperature for 30 minutes.</li> </ul>
Sgx Clarity System Wash Buffer Concentrate	<ul style="list-style-type: none"> <li>To prepare a working solution, dilute Wash Buffer Concentrate 10X with deionized water (1 part Sgx Clarity Wash Buffer Concentrate / 9 parts deionized water), then mix thoroughly.</li> </ul> <p><b>Caution:</b> Failure to dilute Wash Buffer Concentrate as noted above prior to use on the Sgx Clarity System may impact assay results.</p>
Sgx Clarity cTnI Assay Calibrators (3 levels)	<ul style="list-style-type: none"> <li>Remove from storage and allow to equilibrate to room temperature for 30 minutes.</li> <li>Once at room temperature, mix by gentle inversion (10 times minimum).</li> <li>Keep tubes capped when not in use.</li> </ul>
Sgx Clarity cTnI Controls (Singulex / 4 levels)	<ul style="list-style-type: none"> <li>Remove from storage and allow to equilibrate to room temperature for 30 minutes.</li> <li>Once at room temperature, mix by gentle inversion (10 times minimum).</li> <li>Keep tubes capped when not in use.</li> </ul>

## Sgx Clarity cTnI Reagent Pack Stability and Calibration Interval

- Sgx Clarity cTnI Reagent Pack stability:
  - Open stability for cTnI Reagent Packs is 56 hours from first scan on the Sgx Clarity System, and assumes that cTnI Reagent Packs are immediately capped and returned to storage when not in use.
  - Discard Sgx Clarity cTnI Reagent Pack at the end of the stability interval. Stability is tracked in the Sgx Vision Software—see the Sgx Clarity System Operator's Manual for details.
- Calibration interval: 7 days
  - A new calibration is required:
    - When changing lot numbers of Sgx Clarity cTnI Reagent Packs.
    - When quality control results are repeatedly out of range.
    - When calibration interval is expired.
  - For full details regarding the calibration concept and instructions for calibrating cTnI Reagent Packs, refer to the Sgx Clarity System Operator's Manual.

## Master Standard Curve

Sgx Clarity cTnI Reagent Packs require a new lot-specific Master Curve with each new reagent pack lot. The Master Curve is provided in the Sgx Clarity cTnI Reagent Pack Package Insert, and is entered during reagent calibration per the instructions in the Sgx Clarity System Operator's Manual.



## Calibration

Prepare and load Sgx Clarity cTnI Calibrators onto the Sgx Clarity System per the instructions provided in the Sgx Clarity System Operator's Manual. **Note:** Sgx Clarity cTnI Calibrators are lot-matched with Sgx Clarity cTnI Reagent Pack lots, as noted in their respective package inserts. Sgx Clarity cTnI Reagent Packs may only be calibrated on the Sgx Clarity System using the matched Sgx Clarity cTnI Calibrator lot.

- Handling Sgx Clarity cTnI Calibrators:
  - Sgx Clarity cTnI Calibrators are stable when stored unopened at 2–8 °C until the expiration date.
  - Keep calibrator tubes capped when not in use.
  - Store in upright position.

**Note:** Always use a new Sgx Clarity cTnI Reagent Pack (never opened/loaded on the Sgx Clarity System) to establish reagent lot calibration. See the Sgx Clarity System Operator's Manual for detailed calibration instructions.

## Quality Control

- Singulex recommends the use of quality control materials provided by Singulex, or other commercially available quality control material with at least four levels. An acceptable level of performance is achieved when the control values obtained are within the acceptable control range, as defined by an appropriate internal laboratory quality control scheme.
- In addition to site requirements, required control levels and frequency of quality control runs may be dictated by local government regulations or accreditation requirements.
- Prior to use, control lots must be configured by an administrator-level user within the Sgx Vision Software. For detailed instructions on configuring control lots, refer to the Sgx Clarity System Operator's Manual.
- Required Control Volume
  - Required control volume is dependent on the number of replicates and the additional volume required for the Sgx Clarity System to initiate aspiration (dead space volume):

Number of Control Replicates	Low Volume Sample Cup* Dead Space Volume	Sample Processing Volume	Total Control Volume
1	200 µL	100 µL	300 µL
2	200 µL	200 µL	400 µL

\*0.5 mL Nalgene™ Vial

- Dispense 300 µL (if run in singlicate) or 400 µL (if run in duplicate) of each control level to a Low Volume Sample Cup and load onto the Sgx Clarity System per the instructions provided in the Sgx Clarity System Operator's Manual
- Configure and load all QC samples per the instructions provided in the Sgx Clarity System Operator's Manual.
- If the quality control results do not fall within the expected values provided by the manufacturer, or if they are not within the laboratory's established values, do not report patient results and take the following actions:
  - Verify that the materials are not expired.
  - Verify that the required maintenance was performed on the Sgx Clarity System.
  - Verify that the assay was performed according to these Instructions For Use.
  - Rerun the assay with fresh controls.
  - Perform a re-calibration and retest controls if a rerun of fresh controls fails.
  - If necessary, contact Singulex Technical Support.

## Sample Volume

This assay requires 100 µL of sample for a single test. This volume does not include the unusable volume in the sample container or primary tube (i.e. dead space volume). For the total sample volume required for the Sgx Clarity System (volume that must be present within the tube to ensure accurate pipetting), refer to the Sgx Clarity System Operator's Manual.

**Sample Dilution**

- Patient samples with troponin I levels reported as greater than 25,000 pg/mL must be diluted and retested to obtain numerical results if a numerical result is required.
  - If the sample result is beyond the reportable range of the Sgx Clarity cTnI Assay, perform a sample dilution using Phosphate Buffered Saline (PBS not included—refer to "Optional Materials" for recommended diluents).
  - An initial dilution of 1/10 is recommended (1 part sample to 9 parts PBS).
  - Enter the dilution factor upon loading onto the Sgx Clarity System per instructions provided in the Sgx Clarity System Operator's Manual.
- If a dilution factor is entered when scheduling the test, the Sgx Clarity System automatically calculates the result.

**Assay Procedure**

- All Sgx Clarity cTnI Assay processing steps are automated on the Sgx Clarity System. Prepare samples and reagents according to the instructions provided in these instructions for use, then load onto the Sgx Clarity System and initiate assay processing per instructions provided in the Sgx Clarity System Operator's Manual.

**ANALYTICAL PARAMETERS**

- The Sgx Clarity System reports the troponin I results in pg/mL.
- The Sgx Clarity cTnI Assay quantitative range is 0.14 pg/mL – 25,000 pg/mL.

**LIMITATIONS**

- Although the Sgx Clarity cTnI Reagents have been formulated to minimize heterophilic interference, heterophilic antibodies in human plasma may react with reagent immunoglobulins, interfering with *in vitro* diagnostics immunoassays.
- Patients routinely exposed to animals, or to animal serum or plasma products, may be prone to this type of assay interference and anomalous values may be observed when testing samples from these individuals.
- Samples from patients receiving preparations of mouse monoclonal antibodies for therapy or diagnosis may contain Human Anti-Mouse Antibodies (HAMA). These samples may show either falsely elevated or falsely depressed values when tested, even though the assay has been formulated to minimize interference from HAMA.
- The ultra-sensitive performance of this assay may, in rare instances, result in potential sensitivity to some environmental contaminants. Precautions have been taken in the design of the instrument and the assay to reduce this risk, however assay results that are not consistent with other clinical observations may require a retest to confirm the initial result. Results should always be assessed in conjunction with the patient's medical history, clinical examination, and other findings.

## PERFORMANCE CHARACTERISTICS

Data provided in this section were generated using the Sgx Clarity System. Assay results obtained in individual laboratories may vary from data presented here.

### Precision/Reproducibility

Precision of the Sgx Clarity cTnI Assay was tested following a two-part precision study informed by Chapters 3 and 4 of the CLSI EP05-A3 guideline for Evaluation of Precision of Quantitative Measurement Procedures. For the first part of the study (Table 1), 2 operators at one CLIA-certified laboratory tested 2 replicates per panel member of a 10-member panel on one Sgx Clarity System daily for 20 days using 3 different lots of Sgx Clarity cTnI Assay reagents. For the second part of the study (Table 2), 2 operators at each of 3 CLIA-certified laboratories tested 1 lot of Sgx Clarity cTnI assay reagents for 5 days with 3 replicates per panel member of a 10-member panel on a single Sgx Clarity System. The 10-member panel had members ranging from 1 pg/mL to 10,000 pg/mL.

**Table 1.** Precision Estimates for 20-day, Multi-Lot, Single-Site Study

Panel Member (pg/mL)	Lot	Mean	N	Day-to-Day		Repeatability	
				SD	%CV	SD	%CV
1	A	1.03	79	0.04	4.07	0.09	8.94
	B	0.98	78	0.02	2.05	0.08	7.98
	C	0.96	78	0.03	2.84	0.1	10
5	A	5.51	80	0.25	4.58	0.37	6.8
	B	5.28	80	0.25	4.74	0.3	5.64
	C	5.06	79	0.22	4.26	0.29	5.8
10	A	10.99	80	0.54	4.89	0.6	5.45
	B	10.57	80	0.26	2.48	0.47	4.45
	C	10.47	80	0.46	4.39	0.53	5.02
15	A	17.21	80	0	0	1.19	6.91
	B	16.69	79	0.24	1.45	0.69	4.15
	C	16.35	79	0.38	2.3	0.78	4.79
20	A	21.99	79	1.05	4.78	0.97	4.43
	B	21.15	80	0.47	2.21	1.02	4.84
	C	20.7	80	0.59	2.83	1	4.84
100	A	107.98	79	4.4	4.07	4.94	4.57
	B	96.68	80	2.13	2.21	3.73	3.86
	C	100.62	80	4.46	4.43	4.35	4.33
200	A	239.63	79	13.36	5.57	20.95	8.74
	B	224.56	80	6.25	2.78	15.53	6.92
	C	218.9	79	11.3	5.16	15.3	6.99
500	A	572.13	79	21.85	3.82	22.92	4.01
	B	527.07	80	8.96	1.7	16.67	3.16
	C	543.72	80	23.49	4.32	24.03	4.42
1000	A	1090.64	80	47.97	4.4	41.92	3.84
	B	988.95	79	17.64	1.78	34.88	3.53
	C	1046.89	80	44.33	4.23	50.99	4.87
10,000	A	11115.92	79	410.46	3.69	545.35	4.91
	B	9867.38	80	165.71	1.68	324.73	3.29
	C	10828.73	80	325.05	3	372.64	3.44

**Table 2.** Precision Estimates for 5-Day, Single-Lot, Multi-Site Study

Panel Member (pg/mL)	Site	Mean	Repeatability		Within Laboratory		Reproducibility	
			SD	CV(%)	SD	CV(%)	SD	CV(%)
1	1	1	0.09	9	0.1	10	0.13	12
	2	1.15	0.1	9	0.12	10		
	3	1.12	0.11	9.4	0.11	10		
	All Sites	1.09	0.1	9.2	0.11	10		
5	1	5.39	0.28	5.3	0.34	6.3	0.61	10
	2	5.98	0.38	6.3	0.45	7.5		
	3	6.21	0.54	8.7	0.55	8.8		
	All Sites	5.86	0.42	7.1	0.45	7.7		
10	1	10.7	0.52	4.9	0.6	5.6	0.87	7.6
	2	11.88	0.68	5.7	0.77	6.5		
	3	11.52	0.42	3.7	0.52	4.5		
	All Sites	11.36	0.55	4.8	0.64	5.6		
15	1	16.94	0.93	5.5	0.97	5.7	1.18	6.7
	2	17.95	0.98	5.4	0.98	5.4		
	3	17.96	1.03	5.7	1.22	6.8		
	All Sites	17.62	0.99	5.6	1.06	6		
20	1	21.44	1.2	5.6	1.36	6.3	1.49	6.7
	2	22.52	1.02	4.5	1.18	5.3		
	3	22.18	1.46	6.6	1.7	7.7		
	All Sites	22.04	1.25	5.7	1.43	6.5		
100	1	96.13	4.08	4.2	5.84	6.1	5.77	6
	2	96.97	6.33	6.5	6.41	6.6		
	3	97.57	4.89	5	5.27	5.4		
	All Sites	96.89	5.22	5.4	5.77	6		
200	1	224.62	16.3	7.3	17.3	7.7	17.43	7.7
	2	233.23	16.4	7	16.9	7.3		
	3	221.05	15	6.8	15.7	7.1		
	All Sites	226.3	16	7.1	16.6	7.4		
500	1	524.12	27.6	5.3	34.2	6.5	29.49	5.5
	2	546.24	21.1	3.9	23.2	4.2		
	3	549.34	21	3.8	22.2	4		
	All Sites	539.79	23.7	4.4	27.1	5		
1000	1	992.14	40.6	4.1	44.8	4.5	59.02	5.9
	2	1013.8	68.9	6.8	82.4	8.1		
	3	1008.4	41.4	4.1	42.3	4.2		
	All Sites	1004.8	52.7	5.2	59	5.9		
10000	1	9851	554	5.6	554	5.6	551.9	5.5
	2	9953.2	358	3.6	418	4.2		
	3	10048	499	5	683	6.8		
	All Sites	9950.9	488	4.9	552	5.5		

**Linearity/Reportable Range**

Linearity of the Sgx Clarity cTnI Assay run on the Sgx Clarity System was evaluated in accordance with CLSI EP6-A guideline using one reagent lot and one Sgx Clarity System testing EDTA plasma samples spiked with native cardiac troponin I analyte. The study reported here evaluated linearity using 11 sample dilutions of varying analyte concentrations spanning the range from 0.08 to 25,000 pg/mL. Four (4) replicates of each of 11 dilutions were tested and analyzed. For the range from 0.08 to 25,000 ng/mL, the 2<sup>nd</sup> and 3<sup>rd</sup> order polynomial fits were no better than a linear fit to within 10% nonlinearity. Therefore, the acceptable linearity includes the reportable range from 0.14 to 25,000 pg/mL cTnI for the Sgx Clarity cTnI Assay.

Hook Effect: The Sgx Clarity cTnI Assay demonstrated that there was no high dose hook effect up to 1000 ng/mL.

**Expected Values/Traceability**

- The Sgx Clarity cTnI Assay is traceable to the NIST Standard SRM2921.
- The Sgx Clarity cTnI Calibrators and Sgx Clarity cTnI Controls are prepared from commercially-available human cardiac troponin complex. Sgx Clarity cTnI Calibrators and Sgx Clarity cTnI Controls are value assigned against a cTnI Master Standard Curve, which is traceable to NIST SRM2921.

**Sensitivity/Detection Limit [LoD,LoB,LoQ]**

The limit of blank (LoB) and limit of detection (LoD) studies were performed following the recommendations in EP17-A2. Testing was performed over 3 days using 2 reagent lots, 1 instrument, and 2 calibration cycles.

To calculate the LoB, 4 blank samples were measured in replicates of 5 on each day of testing over 3 days for each reagent lot. To estimate the LoD, 4 low cTnI positive EDTA plasma samples were measured in replicates of 5 on each day of testing over 3 days for each reagent lot. Using a non-parametric model, the LoB was calculated to be 0.02 pg/mL and the LoD was calculated to be 0.08 pg/mL.

To estimate the LoQ, 10 EDTA plasma samples containing low levels of cTnI analyte were measured in replicates of 4 over 3 days on 1 instrument and 2 reagent lots. The LoQ was calculated using a precision profile/functional sensitivity approach, whereby the LoQ at 20% CV was calculated to be 0.14 pg/mL. The 10% functional sensitivity was calculated to be 0.53 pg/mL.

## Analytical Specificity

### • Potentially Interfering Substances

The following potentially interfering exogenous compounds, at the following concentrations (Table 3), did not interfere with Sgx cTnI Assay performance on the Sgx Clarity System (i.e., did not result in bias >10%).

**Table 3.** Exogenous Interference Substances That Do Not Interfere with the Sgx Clarity cTnI Assay

Potentially Interfering Substance	Interfering Substance Interferent Concentration
Acetaminophen	1134 µmol/L
Acetylsalicylic acid	2.54 µmol/L
Amlodipine besylate	245 nmol/L
Ampicillin	152 µmol/L
Ascorbic acid	342 µmol/L
Atenolol	37.6 µmol/L
Caffeine	308 µmol/L
Captopril	23 µmol/L
Chloramphenicol	155 µmol/L
Digoxin	7.8 nmol/L
Diltiazem hydrochloride	15 µmol/L
Dopamine hydrochloride	5.87 µmol/L
Enalaprilat	0.86 µmol/L
Furosemide	181 µmol/L
Hydrochlorothiazide	20.2 µmol/L
Indomethacin	100 µmol/L
Lisinopril	0.74 µmol/L
Nifedipine	1156 nmol/L
Quinidine	37 µmol/L
Ramipril	28.8 µmol/L
Spironolactone	1.44 µmol/L
Theophylline	222 µmol/L
Verapamil hydrochloride	4.4 µmol/L
Warfarin	32.5 µmol/L

### • HAMA: Studies conducted indicate that the Sgx Clarity cTnI Assay formulation reduces the effects of interference from heterophilic antibodies.

The following potentially interfering endogenous substances, at the concentrations listed below, did not interfere with Sgx Clarity cTnI Assay performance on the Sgx Clarity System (i.e., did not result in bias >10%).

**Table 4.** Summary of Endogenous Interference Substances That Do Not Interfere with the Sgx Clarity cTnI Assay

Potentially Interfering Substance	Interfering Substance Interferent Concentration
Biotin	290 ng/mL
Cholesterol	13 mmol/L
Unconjugated bilirubin	342 µmol/L
Conjugated bilirubin	342 µmol/L
Triglycerides (Intralipid)	37 mmol/L

The following are included as limitations:

- Samples showing visible signs of hemolysis may cause interference. Falsely depressed results were obtained when using samples with hemoglobin concentrations >5 g/L, the lowest concentration of hemoglobin tested. The specific amount of hemoglobin that can be present without causing a >10% bias will be determined in subsequent studies.
- Samples with high protein concentrations resulting in increased sample viscosity may cause interference. Falsely depressed results are obtained when using samples with bovine serum albumin concentrations >30 g/L, the lowest concentration of albumin tested. The specific amount of albumin that can be present without causing a >10% bias will be determined in subsequent studies.

### Cross-Reactivity

The Sgx Clarity cTnI Assay has no significant cross-reactivity (<1%) to cardiac TnI (cTnI) when cross-reactants listed in Table 5 were tested at 1000 ng/mL.

**Table 5.** Cross-Reactivity

Cross-Reactant Tested	Cross-Reactant Source	% Cross-Reactivity Sample 1 (≈2.5pg/mL)	% Cross-Reactivity Sample 2 (≈50pg/mL)
Skeletal Troponin T-1	Recombinant Protein	0.00%	0.00%
Skeletal Troponin T-3	Recombinant Protein	0.00%	0.00%
Cardiac Troponin C	Purified Protein	0.00%	0.00%
Skeletal Troponin I	Purified Protein	0.00%	0.00%
Cardiac Troponin T	Purified Protein	0.21%	0.21%
Cardiac Myosin Heavy Chain	Purified Protein	0.00%	0.00%
Cardiac Myosin Light Chain	Purified Protein	0.08%	0.08%
Cardiac Tropomyosin	Purified Protein	0.02%	0.02%

### Reference Range

Singulex conducted a reference range study based on guidance from Clinical and Laboratory Standards Institute (CLSI) document EP28-A3c. Donor samples were collected from 5 sites in the United States to establish the 99th percentile upper reference limit (URL) in a population of apparently healthy adults with no known disease of the cardiovascular system or chronic disease. Patients were excluded from the reference range if they had a history of CVD, angina complaints, heart failure, renal disease, diabetes, skeletal muscular disease, rheumatoid arthritis, vascular disease, chronic inflammatory disease, immediate family history of CVD, cancer, thyroid disease, chronic or systematic disease, recent CVD hospitalization, stroke, or an abnormal blood test result for NTproBNP or Creatinine. Extreme athletes and pregnant women were also excluded.

Result from this study demonstrated the 99<sup>th</sup> percentile upper reference limit (URL) to be < 8.67 pg/mL.

**Table 6.** 99<sup>th</sup> Percentile Upper Reference Limit of a Healthy Population

N	Age Range (years)	99 <sup>th</sup> Percentile
536	18-84	< 8.67 pg/mL

### Clinical Results - Rule-Out of Cardiac Ischemia

Using samples obtained from the Basel VIII cohort (Biochemical and Electrocardiographic Signatures in the Detection of Exercise-induced Myocardial Ischemia, NCT01838148), a study was performed to assess the diagnostic test characteristics of the Sgx Clarity cTnI Assay for ruling out myocardial ischemia in patients with suspected coronary artery disease (CAD).

Five hundred and fifty-five (555) consecutive patients with suspected stress-induced myocardial ischemia and without previously known CAD were tested with myocardial perfusion imaging utilizing single-photon emission computed tomography (MPI-SPECT). Clinical judgment assessing the probability of stress-induced myocardial ischemia was performed by the treating cardiologist on a visual analogue scale (VAS; range: 0%–100%) before (pre-stress VAS) and after (post-stress VAS) MPI-SPECT. Venous blood was collected prior to stress MPI-SPECT testing, and cardiac troponin I (cTnI) concentrations were measured in EDTA plasma using the Sgx Clarity cTnI Assay.

Diagnosis of stress-induced myocardial ischemia was adjudicated by two board-certified cardiologists based on interpretation of MPI-SPECT images combined with information obtained from elective coronary angiography, when available. The observed prevalence of myocardial ischemia was 19%.

The negative predictive value (NPV), positive predictive value (PPV), sensitivity, and specificity for multiple cTnI cutoff concentrations are summarized in Table 7.

**Table 7.** Cardiac Troponin I Measurement Using the Sgx Clarity cTnI Assay: Diagnostic Characteristics at Pre-Specified Cutoff Concentrations

Sgx Clarity cTnI Assay cutoffs (pg/mL)	Pre-VAS criteria	Incidence of criteria, n (%)	Sensitivity (95% CI)	Specificity (95% CI)	NPV (95% CI)	PPV (95% CI)
< 3.0	N/A	479 (86)	30 (22-39)	90 (87-93)	85 (81-88)	41 (30-52)
< 2.0	N/A	422 (76)	44 (35-54)	81 (77-84)	86 (83-89)	35 (27-43)
< 1.0	N/A	243 (44)	76 (67-83)	48 (44-53)	90 (85-93)	25 (21-30)
< 0.5	N/A	68 (12)	94 (88-97)	14 (11-17)	91 (82-96)	20 (17-24)
< 1.0	< 30%	105 (19)	95 (89-98)	22 (19-26)	95 (89-98)	22 (18-26)
< 0.5	< 30%	45 (8)	97 (92-99)	9 (7-12)	93 (82-98)	20 (17-24)

**Abbreviations used:** cTnI (cardiac troponin I); pre-VAS (clinical judgment before stress testing quantified on a visual analogue scale); CI (confidence interval).

The area under the receiver operating curve (AuROC) predicting stress-induced myocardial ischemia was determined for pre-, and post-stress test clinical judgment (VAS), pre-stress cTnI, and the combination of log-transformed pre-stress cTnI and VAS (Table 8).

**Table 8.** AUROC for Predicting Stress-Induced Myocardial Ischemia in 555 Patients Using Clinical Judgment (VAS) and cTnI Measurements with the Sgx Clarity cTnI Assay.

	AuROC	95% CI	P Value <sup>a</sup>	P Value <sup>b</sup>
<b>Pre-stress VAS%</b>	0.684	0.628-0.741	-	0.996
<b>Post-Stress VAS%</b>	0.704	0.644-0.764	0.996	-
<b>cTnI</b>	0.680	0.622-0.739	0.9170	0.5235
<b>Pre-stress VAS + log cTnI</b>	0.728	0.675-0.782	0.0160	0.2973

















<sup>a</sup>P values for comparison with the combination of pre-stress VAS.

<sup>b</sup>P values for comparison with post-stress VAS.

**Abbreviations used:** AuROC (area under the receiver operating curve); CI (confidence interval); pre-VAS (clinical judgment before stress testing quantified on a visual analogue scale); post-VAS (clinical judgment after stress testing quantified on a visual analogue scale); log cTnI (log transformed cardiac troponin I).



## KEY TO SYMBOLS

	Temperature Limit		Biological Hazard
	Consult Instructions For Use		CE Marking
	Contains n Content(s) of Each		For <i>In Vitro</i> Diagnostic Use
	Catalog Number		Single Use - Do Not Reuse
	Number of Tests		Expiration Date
	Part Number		Manufacturer
	Batch Code		Capture Reagent
	Detection Reagent		Calibrator

## BIBLIOGRAPHY

1. World Health Organization. World health statistics 2016: monitoring health for the SDGs, sustainable development goals. Retrieved from [http://www.who.int/gho/publications/world\\_health\\_statistics/2016/en/](http://www.who.int/gho/publications/world_health_statistics/2016/en/)
2. Fihn SD, et al. 2012 ACCF/AHA/ACP/AATS/ PCNA/SCAI/STS guideline for the diagnosis and management of patients with stable ischemic heart disease. *Circulation*. 2012; 126:e354–471.
3. Montalescot G, et al. 2013 ESC guidelines on the management of stable coronary artery disease: the Task Force on the management of stable coronary artery disease of the European Society of Cardiology. *European Heart Journal*. 2013; 34:2949-3003.
4. Ladapo JA, et al. Physician decision making and trends in the use of cardiac stress testing in the United States: an analysis of repeated cross-sectional data. *Annals of Internal Medicine*. 2014; 161:482-490.
5. Amsterdam EA, et al. 2014 ACC/AHA guideline for the management of patients with non–ST-elevation acute coronary syndromes: a report of the American College of Cardiology/American Heart Association Task Force on Practice Guidelines. *Circulation*. 2014; 130:e344–e426.
6. Melanson SE, et al. Earlier detection of myocardial injury in a preliminary evaluation using a new troponin I assay with improved sensitivity. *American Journal of Clinical Pathology*. 2007; 128:282-286.
7. Sabatine MS, et al. Detection of acute changes in circulating troponin in the setting of transient stress test-induced myocardial ischemia using an ultrasensitive assay: results from TIMI 35. *European Heart Journal*. 2009; 30:162-169.
8. Røsjø H, et al. Troponin I measured by high-sensitivity assay in patients with suspected coronary artery disease: data from the Akershus Cardiac Examination (ACE) 1 study. *Clinical Chemistry*. 2012; 58:1565-1573.
9. Tanglay Y, et al. Incremental value of a single high-sensitivity cardiac troponin I measurement to rule-out myocardial ischemia. *The American Journal of Medicine*. 2015; 128(6):638-46.



Manufactured For:  
Singulex, Inc.  
1701 Harbor Bay Parkway  
Alameda, CA 94502 USA

**Singulex®**



Qarad BV  
Flight Forum 40  
5657 DB Eindhoven  
The Netherlands



**TECHNICAL SUPPORT**  
+1 (510) 995-9040 +1 (855) 314-5757  
[ClaritySupport@singulex.com](mailto:ClaritySupport@singulex.com)

---

©2017 Singulex, Inc. All rights reserved.

Singulex® and Sgx Clarity™ are trademarks or registered trademarks of Singulex, Inc.

2017-06



# CARDIAC TROPONIN I/ (cTnI)

## Intended Use

The i-STAT® cardiac troponin I (cTnI) test is an *in vitro* diagnostic test for the quantitative measurement of cardiac troponin I (cTnI) in whole blood or plasma. Measurements of cardiac troponin I are used in the diagnosis and treatment of myocardial infarction and as an aid in the risk stratification of patients with acute coronary syndromes with respect to their relative risk of mortality.

## Method Explanation

The i-STAT cTnI test cartridge uses a two-site enzyme-linked immunosorbent assay (ELISA) method. Antibodies specific for human cardiac troponin I (cTnI) are located on an electrochemical sensor fabricated on a silicon chip. Also deposited in another location on the sensor silicon chip is an antibody/alkaline phosphatase enzyme conjugate specific to a separate portion of the cTnI molecule. The whole blood or plasma sample is brought into contact with the sensors allowing the enzyme conjugate to dissolve into the sample. The cTnI within the sample becomes labeled with alkaline phosphatase and is captured onto the surface of the electrochemical sensor during an incubation period of approximately seven minutes. The sample, as well as excess enzyme conjugate, is washed off the sensors. Within the wash fluid is a substrate for the alkaline phosphatase enzyme. The enzyme bound to the antibody/antigen/antibody sandwich cleaves the substrate releasing an electrochemically detectable product. The electrochemical (amperometric) sensor measures this enzyme product which is proportional to the concentration of cTnI within the sample.

## Contents

Each i-STAT cTnI cartridge provides a sample inlet, sensors to detect the cTnI as described above, and all the necessary reagents needed to perform the test. The cartridge contains a buffer and preservatives. A list of reactive ingredients is indicated below:

Reactive Ingredient	Biological Source	Minimum Quantity
Antibody/Alkaline Phosphatase Conjugate	Caprine IgG : Bovine Intestine	0.003 µg
IgG	Caprine IgG : Murine IgG	8 µg : 8 µg
Sodium Aminophenyl Phosphate	N/A	0.9 mg
Heparin	Porcine Intestine	0.45 IU
IgM	Murine IgM	0.3 µg

## **Metrological Traceability**

The i-STAT System test for cardiac troponin-I (cTnI) measures cardiac troponin-I amount-of-substance concentration in plasma or the plasma fraction of whole blood (dimension ng mL<sup>-1</sup>) for *in vitro* diagnostic use. Cardiac troponin-I values assigned to i-STAT's controls and calibration verification materials are traceable to i-STAT's working calibrator prepared from human cardiac troponin-ITC complex (Hy-Test Ltd., Turku, Finland, catalogue #8T62). i-STAT System controls and calibration verification materials are validated for use only with the i-STAT System and assigned values may not be commutable with other methods. Further information regarding metrological traceability is available from Abbott Point of Care Inc.

## **Reportable Range**

The i-STAT cTnI test will report 0.00 to 50.00 ng/mL (µg/L). Samples above the reportable range will yield ">50.00 ng/mL" on the analyzer display screen. However, the performance characteristics of the i-STAT cTnI measurement have not been established for cTnI values above 35.00 ng/mL (µg/L).

## **Reference Range**

Whole blood and plasma samples from 162 apparently healthy donors were assayed in duplicate using three different lots of i-STAT cTnI cartridges. The 0 to 97.5% range of results spanned 0.00 ng/mL (µg/L) to 0.03 ng/mL (µg/L). The 0 to 99% range of results spanned 0.00 ng/mL (µg/L) to 0.08 ng/mL (µg/L).

Note: Each facility should establish its own reference range using the i-STAT cTnI assay.

## **Clinical Significance**

Biochemical cardiac markers, including cTnI, are useful for both the diagnosis of myocardial infarction and the risk stratification that can help guide the choice of therapeutic options.

For optimal diagnostic usefulness, a cardiac marker should be specific for cardiac tissue, should be rapidly released into the bloodstream with a direct proportional relationship between the extent of myocardial injury and the measured level of the marker, and should persist in blood for a sufficient length of time to provide a convenient diagnostic time window.<sup>1</sup> The cardiac-specific troponins, troponin I (cTnI) and troponin T (cTnT) are considered the biochemical markers of choice in the evaluation of acute coronary syndromes (ACS) including ST-elevation myocardial infarction, non-ST-elevation myocardial infarction, and unstable angina.<sup>2,3</sup> Elevated levels of cardiac-specific troponins convey prognostic information beyond that supplied by the patients clinical signs and symptoms, the ECG at presentation, and the pre-discharge exercise test.<sup>1</sup> Antman et al. reported that patients with elevated levels of cTnI had a statistically significant increase in mortality ( $p < 0.001$ ).<sup>4</sup> Other studies have shown increases in other non-fatal cardiac events such as non-fatal MI, congestive heart failure, and urgent revascularization with increasing levels of cTnI.<sup>5,6,7</sup>

The ability for cTnI to be measured at low concentrations allows therapeutic intervention to be considered at any elevation above the normal range. Patients that present with no ST-elevation on their ECG but who have even slight elevation in cTnI or cTnT may receive a greater treatment benefit from certain drugs such as GP IIb/IIIa inhibitors or low molecular weight heparin.<sup>8,9,10</sup>

A Global Task Force with joint leadership from the European Society of Cardiology (ESC), the American College of Cardiology Foundation (ACCF), the American Heart Association (AHA) and the World Heart Federation (WHF) refined past criteria of myocardial infarction with a universal definition of myocardial infarction that supports the use of cTnI as a preferred biomarker for myocardial injury. The universal definition of MI according to this task force is defined as a typical rise and gradual fall of cardiac biomarkers (preferably troponin) with at least one value above the 99th percentile of the upper reference limit (URL) together with evidence of myocardial ischemia with at least one of the following: ischemic symptoms, pathological Q waves on electrocardiogram (ECG), ischemic ECG changes, or imaging evidence of new loss of viable myocardium or new regional wall motion abnormality.<sup>2</sup> An elevated troponin value alone is not sufficient to diagnose a myocardial infarction. Rather, the patient's clinical presentation (history, physical

exam) and ECG should be used in conjunction with troponin in the diagnostic evaluation of suspected myocardial infarction.<sup>3</sup> A serial sampling protocol is recommended to facilitate the identification of temporal changes in troponin levels characteristic of MI.<sup>2,3,11</sup>

Since cTnI is not unequivocally detectable by commercial assays in samples from healthy persons, measurements beyond the upper limit of the reference range have a significant probability of being associated with ischemia or necrosis;<sup>12</sup> this probability increases with the measured troponin concentration. Nonetheless, by definition, results beyond the reference range will occur in a normal population in healthy individuals in the absence of myocardial necrosis, i.e., a result beyond the 99th percentile does not confirm the presence of troponin with absolute certainty. Each institution should determine the reference range and decision levels appropriate to its specific patient population and clinical practice.

Acute myocardial injury is evidenced by temporal changes in troponin levels while consistent elevations of troponin may be suggestive of other chronic cardiac or non-cardiac conditions. There are many clinical conditions that can lead to an elevated troponin level without ischemic coronary artery disease. Such conditions include blunt trauma, myocarditis, congestive heart failure, left ventricular hypertrophy etc.<sup>13,14</sup> These clinical conditions should be considered when interpreting results. The use of serial sampling with a consistent troponin methodology can identify temporal troponin changes, as well as provide additional information that can assist in the clinical diagnosis for those patients with low-level results. Where there are inconsistencies in the clinical information or where diagnostic criteria are not fully satisfied, the possibility of biased results should be recognized – see Test Limitations.

### Performance Characteristics

Precision data were collected in multiple sites as follows: Duplicates of each control were tested daily for a period of 20 days, resulting in a total of 40 replicates. The average statistics are presented below.

Method comparison data were collected using CLSI guideline EP9-A2.<sup>15</sup> Venous blood samples were collected in heparinized evacuated tubes and analyzed in duplicate on the i-STAT System. A portion of the specimen was centrifuged and the separated plasma was analyzed in duplicate on the comparative method within 1 hour of collection.

Deming regression analysis<sup>16</sup> was performed on the first replicate of each sample. In the method comparison table, n is the number of specimens in the first data set, Sxx and Syy refer to estimates of imprecision based on the duplicates of the comparative and the i-STAT methods respectively. Sy.x is the standard error of the estimate, and r is the correlation coefficient.\*

Method comparisons will vary from site to site due to differences in sample handling, comparative method calibration and other site specific variables.

Interference studies were based on CLSI guideline EP7.<sup>17</sup>

\*The usual warning relating to the use of regression analysis is summarized here as a reminder. For any analyte, “if the data is a narrow range, the estimate of the regression parameters are relatively imprecise and may be biased. Therefore, predictions made from estimates may be invalid”.<sup>13</sup> The correlation coefficient, r, can be used as a guide to assess the adequacy of the comparative method range in overcoming the problem. As a guide, the range of data can be considered adequate if  $r > 0.975$ .

### Precision Data (ng/mL)

Control	Mean	SD	%CV
Level 1	0.53	0.04	7.8
Level 2	2.17	0.18	8.5
Level 3	31.82	2.42	7.6

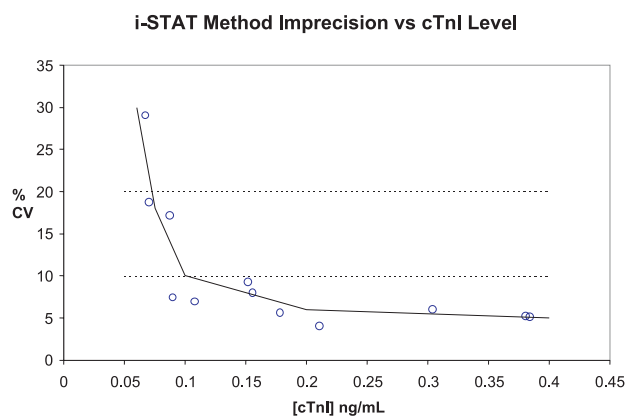
## Method Comparison (ng/mL)

	Dade Behring Stratus® CS
n	189
Sxx	0.28
Syy	0.31
Slope	0.883
Int't	0.029
Sy.x	1.40
Xmin	0.00
Xmax	46.27
r	0.975

## Analytical and Functional Sensitivities

The analytical sensitivity of the cTnI method is 0.02 ng/mL, which is the lowest cTnI level that can be distinguished from zero. The analytical sensitivity is defined as the concentration at two standard deviations from a sample at 0.00 ng/mL.

Another characteristic of an analytical measurement is the functional sensitivity, which is defined as the cTnI level at which the test method displays a particular percent coefficient of variation (%CV). Estimates of the 20% and 10% functional sensitivity for the cTnI method were determined from whole blood measurements. The 20% and 10% functional sensitivities for the cTnI method are 0.07 ng/mL and 0.10 ng/mL, respectively (see graph below).



### Analytical Specificity

The cTnI method is specific for cardiac troponin I. The following muscle proteins were tested and found to have an insignificant effect on the measured cTnI.

Crossreactant	Concentration	Percent Crossreactivity
Troponin C (cardiac)	1000 ng/mL	<0.002%
Troponin T (cardiac)	1000 ng/mL	0.65%
Troponin I (skeletal)	1000 ng/mL	<0.002%
Troponin T (skeletal)	1000 ng/mL	<0.002%

### Recovery

The dilution linearity of the i-STAT cTnI test was investigated using heparinized whole blood and plasma samples derived from 3 separate donors. For each donor, the original cTnI negative sample and a cTnI spiked sample were prepared. This process yielded three cTnI positive whole blood samples that were then assayed in duplicate for each of three separate i-STAT cTnI cartridge lots. These whole blood samples were then diluted using an equal mass of the original unspiked whole blood and assayed in duplicate. From this whole blood data, the cTnI recovery was calculated.

The plasma derived from these three donors was combined in equal masses and all pairwise combinations. These combinations were then assayed in duplicate for each of three separate i-STAT cTnI cartridge lots. The cTnI recovery for each pair was calculated using the average of the 6 results. The % recoveries are listed in the Tables below.

#### Whole blood

Sample	Concentration	Diluted Concentration	% Recovery
A	2.05	1.04	101%
B	6.31	3.14	100%
C	27.04	14.05	104%

#### Plasma

Sample	Concentration	Diluted Concentration	% Recovery
A	2.41	-----	-----
B	7.50	-----	-----
C	29.35	-----	-----
A+B	-----	4.69	95%
B+C	-----	18.90	103%
A+C	-----	16.89	106%

## Test Limitations

The frequency of suppressed results is affected by atmospheric pressure. Suppressed result rates may increase with higher elevations (decreased barometric pressure) and may become persistent if testing is performed at more than 7500 feet above sea level. Where unavailability of results is unacceptable, i-STAT recommends having an alternate test method available.

Samples from patients who have been exposed to animals or who have received therapeutic or diagnostic procedures employing immunoglobulins or reagents derived from immunoglobulins may contain antibodies, e.g., HAMA or other heterophile antibodies, which may interfere with immunoassays and produce erroneous results.<sup>18-24</sup> The generation of potentially interfering antibodies in response to bacterial infections has been reported.<sup>16</sup> While this product contains reagents that minimize the effect of these interferents and QC algorithms designed to detect their effects, the possibility of interference causing erroneous results should be evaluated carefully in cases where there are inconsistencies in the clinical information. Results from the i-STAT cTnI assay should be considered in the context of the entirety of the available clinical information. Medical decisions should not be based on a single i-STAT measurement.<sup>14</sup>

Cardiac troponin may not appear in circulation for 4-6 hours following the onset of symptoms of MI. Consequently, a single negative result is insufficient to rule out MI. The use of a serial sampling protocol is recommended practice.<sup>11</sup>

The results of different troponin assays are not generally comparable: cTnI and cTnT are distinct molecules and results are not interchangeable, nor comparable. In addition, significant variation in absolute troponin values may be observed for a given patient specimen with different analytic methods.<sup>13</sup>

Partially clotted samples can result in elevated cTnI results above the reference range, as well as quality check code errors. To prevent this from occurring, upon drawing the whole blood sample into a heparinized collection tube, the sample should be inverted gently at least 10 times to ensure even dissolution of the heparin anticoagulant.

Grossly hemolyzed samples can cause a decreased alkaline phosphatase activity, resulting in decreased detection of cTnI, increased assay backgrounds, and/or quality check codes.

Hematocrits in the range of 0-65% PCV have been demonstrated not to affect results. Samples with hematocrit levels above this range have demonstrated increases in the test imprecision and quality check codes.

The analyzer must remain on a level surface with the display facing up during testing. Motion of the analyzer during testing can increase the frequency of suppressed results or quality check codes. A level surface includes running the handheld in the downloader/recharger.



### Interference Testing

The following substances were found to have no significant effect (less than 10%) on the cTnI method, when added to a plasma pool containing approximately 2 ng/mL of cardiac troponin I, at the concentrations indicated:

Compound	Test Level ( $\mu\text{mol/L}$ unless otherwise indicated)
Acetaminophen	1660
Allopurinol	294
Ascorbic Acid	227
Acetyl Salicylic Acid	3330
Atenolol	37.6
Caffeine	308
Captopril	23
Chloramphenicol	155
Diclofenac	169
Digoxin	6.15
Dopamine	5.87
Enalaprilat	0.86
Erythromycin	81.6
Furosemide	181
Sodium Heparin*	36 U/mL
Ibuprofen	2425
Isosorbide dinitrate	636
Methyldopa	71
Nicotine	6.2
Nifedipine	1.156
Phenytoin	198
Propranolol	7.71
Salicylic Acid	4340
Theophylline	222
Verapamil	4.4
Warfarin	64.9

\*Heparin at 90 U/mL was found to decrease the cTnI level by approximately 20%.

## References

1. Braunwald, E, *et al.* ACC/AHA 2002 guideline update for the management of patients with unstable angina and non-ST-segment elevation myocardial infarction: a report of the American College of Cardiology/American Heart Association Task Force on Practice Guidelines (Committee on the Management of Patients with Unstable Angina). 2002. Available at: <http://content.onlinejacc.org/article.aspx?articleid=1130417>.
2. Thygesen K, Alpert JS, White HD, *et al.* Universal definition of myocardial infarction. *Circulation*. 2007; 116:2634-2653.
3. Anderson JL, Adams CD, Antman EM, *et al.* ACC/AHA 2007 Guidelines for the management of patients with unstable angina/non-ST-elevation myocardial infarction: a report of the American College of Cardiology/American Heart Association Task Force on Practice Guidelines (Writing Committee to Revise the 2002 Guidelines for the Management of Patients With Unstable Angina/Non-ST-Elevation Myocardial Infarction). *Circulation*. 2007;116:e148-e304.
4. Antman EM, Tanasijevic, MJ, Thompson B, *et al.* Cardiac-specific troponin I levels to predict the risk of mortality in patients with acute coronary syndromes. *NEJM* 1996, 335(18): 1342-1349.
5. Galvani M, Ottani F, Ferrini D, *et al.* Prognostic influence of elevated values of cardiac troponin I in patients with unstable angina. *Circulation* 1997, 95: 2053-2059.
6. Morrow DA, Rifai N, Tanasijevic MJ, *et al.* Clinical efficacy of three assays for cardiac troponin I for risk stratification in acute coronary syndromes: A thrombolysis in myocardial infarction (TIMI) IIB substudy. *Clin Chem* 2000, 46(4): 453-460.
7. Sabatine MS, Morrow DA, de Lemos JA, *et al.* Multimarker approach to risk stratification in non-ST-elevation acute coronary syndromes: Simultaneous assessment of troponin I, C-reactive protein, and B-type natriuretic peptide. *Circulation* 2002, 105: 1760-1763.
8. Cannon CP, Weintraub WS, Demopoulos LA, *et al.* Comparison of early invasive and conservative strategies in patients with unstable coronary syndromes treated with the glycoprotein IIb/IIIa inhibitor tirofiban. *NEJM* 2001, 344(25): 1879-1887.
9. Morrow DA, Antman EM, Tanasijevic MJ, *et al.* Cardiac troponin I for stratification of early outcomes and the efficacy of enoxaparin in unstable angina: A TIMI-IIB substudy. *JACC* 2000, 36: 1812-1817.
10. Hamm CW, Heeschen C, Goldmann B, *et al.* Benefit of abciximab in patients with refractory unstable angina in relation to serum troponin T levels (CAPTURE Study Investigators). *NEJM* 1999, 340: 1623-1629.
11. Babuin and Jaffe. Troponin: the biomarker of choice for the detection of cardiac injury. *Can. Med. Assoc. J.* 2005; 173:1191.
12. Hickman *et al.* Cardiac troponin may be released by ischemia alone, without necrosis. *Clin Chem Acta* 2010; 411: 318-323.
13. See "Troponin: What Laboratorians Should know to Manage Elevated Results" at <http://www.fda.gov/MedicalDevices/Safety/AlertsandNotices/TipsandArticlesonDeviceSafety/ucm109362.htm>.
14. Wu *et al.* NACB Standards of Laboratory Practice: Recommendations for the use of cardiac markers in coronary artery disease. *Clin. Chem.* 1999; 45:1104.
15. CLSI. *Method Comparison and Bias Estimation Using Patient Samples; Approved Guideline – Second Edition*. CLSI document EP9-A2 [ISBN 1-56238-472-4]. CLSI, 940 West Valley Road, Suite 1400, Wayne, Pennsylvania 19087-1898, USA 2002.
16. P.J. Cornbleet and N. Gochman, "Incorrect Least-Squares Regression Coefficients in Method-Comparison Analysis," *Clinical Chemistry* 25:3, 432 (1979).
17. CLSI. *Interference Testing in Clinical Chemistry; Approved Guideline*. CLSI document EP7-A [ISBN 1-56238-480-5]. CLSI, 940 West Valley Road, Suite 1400, Wayne, Pennsylvania 19087-1898, USA 2002.
18. Clinical and Laboratory Standards Institute (CLSI) *Immunoassay Interference by Endogenous Antibodies; Proposed Guideline*. CLSI document I/LA30-P (ISBN 1-56238-633-6) Clinical and Laboratory Standards Institute, 940 West Valley Road, Suite 1400, Wayne, Pennsylvania 19087-1898 USA, 2007.

19. Bjerner et al. Immunometric Assay Interference: Incidence and Prevention. Clin. Chem. 2002; 48:613.
20. Kricka, Interferences in Immunoassays – Still a Threat. Clin. Chem. 2000; 46:1037.
21. Schroff et al. Human anti-murine immunoglobulin responses in patients receiving monoclonal antibody therapy. Cancer Res. 1985;45:879.
22. Primus et al. “Sandwich”-type immunoassay of carcinoembryonic antigen in patients receiving murine monoclonal antibodies for diagnosis and therapy. Clin Chem. 1988; 34:261.
23. Nahm et al. Heteroantibody: phantom of the immunoassay. Clin. Chem. 1990; 36:829.
24. Boscato et al. Heterophilic antibodies: a problem for all immunoassays. Clin. Chem. 1988; 34:27.

i-STAT is a registered trademark of the Abbott Group of Companies in various jurisdictions.



Abbott Point of Care Inc.  
Abbott Park, IL 60064 • USA



Emergo Europe  
Molenstraat 15  
2513 BH, The Hague  
The Netherlands  
Tel: (31)70 345 8570  
Fax: (31)70 346 7299



©2013 Abbott Point of Care Inc. All rights reserved. Printed in USA.

## References

1. Rafieian-Kopaei M, Setorki M, Doudi M, Baradaran A, Nasri H. Atherosclerosis: process, indicators, risk factors and new hopes. *Int J Prev Med*. 2014;5(8):927-46.
2. Stone PH, Saito S, Takahashi S, Makita Y, Nakamura S, Kawasaki T, et al. Prediction of progression of coronary artery disease and clinical outcomes using vascular profiling of endothelial shear stress and arterial plaque characteristics: the PREDICTION Study. *Circulation*. 2012;126(2):172-81.
3. Jones R, Payne B. *Clinical Investigation and Statistics in Laboratory Medicine*. Cambridge: Piggott Printers; 1997. 196 p.
4. Peisajovich A, Marnell L, Mold C, Du Clos TW. C-reactive protein at the interface between innate immunity and inflammation. *Expert Rev Clin Immunol*. 2008;4(3):379-90.
5. Koenig W, Khuseynova N. Biomarkers of atherosclerotic plaque instability and rupture. *Arterioscler Thromb Vasc Biol*. 2007;27(1):15-26.
6. Eisenhardt SU, Habersberger J, Peter K. Monomeric C-reactive protein generation on activated platelets: the missing link between inflammation and atherothrombotic risk. *Trends Cardiovasc Med*. 2009;19(7):232-7.
7. Body R, Carley S, McDowell G, Jaffe AS, France M, Cruickshank K, et al. Rapid exclusion of acute myocardial infarction in patients with undetectable troponin using a high-sensitivity assay. *J Am Coll Cardiol*. 2011;58(13):1332-9.
8. National Clinical Guideline Centre for Acute and Chronic Conditions. Chest pain of recent onset: NICE Guideline. 2010.
9. Marini MG, Cardillo MT, Caroli A, Sonnino C, Biasucci LM. Increasing specificity of high-sensitivity troponin: new approaches and perspectives in the diagnosis of acute coronary syndromes. *J Cardiol*. 2013;62(4):205-9.
10. He LP, Tang XY, Ling WH, Chen WQ, Chen YM. Early C-reactive protein in the prediction of long-term outcomes after acute coronary syndromes: a meta-analysis of longitudinal studies. *Heart*. 2010;96(5):339-46.
11. Molins B, Peña E, de la Torre R, Badimon L. Monomeric C-reactive protein is prothrombotic and dissociates from circulating pentameric C-reactive protein on adhered activated platelets under flow. *Cardiovasc Res*. 2011;92(2):328-37.
12. Torres M, Moayed S. Evaluation of the acutely dyspneic elderly patient. *Clin Geriatr Med*. 2007;23(2):307-25, vi.
13. Corban MT, Eshtehardi P, Suo J, McDaniel MC, Timmins LH, Rassoul-Arzrumly E, et al. Combination of plaque burden, wall shear stress, and plaque phenotype has incremental value for prediction of coronary atherosclerotic plaque progression and vulnerability. *Atherosclerosis*. 2014;232(2):271-6.
14. Li X, Fang P, Li Y, Kuo YM, Andrews AJ, Nanayakkara G, et al. Mitochondrial Reactive Oxygen Species Mediate Lysophosphatidylcholine-Induced Endothelial Cell Activation. *Arterioscler Thromb Vasc Biol*. 2016;36(6):1090-100.
15. Aviram M, Fuhrman B. LDL oxidation by arterial wall macrophages depends on the oxidative status in the lipoprotein and in the cells: role of prooxidants vs. antioxidants. *Mol Cell Biochem*. 1998;188(1-2):149-59.
16. Body R, Slevin M, McDowell G. Biomarkers of Atherosclerosis and Acute Coronary Syndromes - A Clinical Perspective. Gaxiola E, editor. <https://www.intechopen.com/books/editor/traditional-and-novel-risk-factors-in-atherothrombosis>. InTech; 2012.
17. Stancel N, Chen CC, Ke LY, Chu CS, Lu J, Sawamura T, et al. Interplay between CRP, Atherogenic LDL, and LOX-1 and Its Potential Role in the Pathogenesis of Atherosclerosis. *Clin Chem*. 2016;62(2):320-7.
18. Wentzel J, Groen H, van der Giessen R, Rodríguez-Granillo G, Gijzen F, G. van der Giessen A, et al. Vascular Remodeling During Atherosclerotic Plaque Build Up Is Controlled by the Plaque Free Part of the Vessel Wall 2008.

19. White SJ, Hayes EM, Lehoux S, Jeremy JY, Horrevoets AJ, Newby AC. Characterization of the differential response of endothelial cells exposed to normal and elevated laminar shear stress. *J Cell Physiol.* 2011;226(11):2841-8.
20. Hazell GG, Peachey AM, Teasdale JE, Sala-Newby GB, Angelini GD, Newby AC, et al. PI16 is a shear stress and inflammation-regulated inhibitor of MMP2. *Sci Rep.* 2016;6:39553.
21. Nourshargh S, Alon R. Leukocyte migration into inflamed tissues. *Immunity.* 2014;41(5):694-707.
22. Pober JS, Sessa WC. Evolving functions of endothelial cells in inflammation. *Nat Rev Immunol.* 2007;7(10):803-15.
23. Dejana E, Spagnuolo R, Bazzoni G. Interendothelial junctions and their role in the control of angiogenesis, vascular permeability and leukocyte transmigration. *Thromb Haemost.* 2001;86(1):308-15.
24. O'Sullivan LA, Liongue C, Lewis RS, Stephenson SE, Ward AC. Cytokine receptor signaling through the Jak-Stat-Socs pathway in disease. *Mol Immunol.* 2007;44(10):2497-506.
25. Kiyon Y, Tkachuk S, Hilfiker-Kleiner D, Haller H, Fuhrman B, Dumler I. oxLDL induces inflammatory responses in vascular smooth muscle cells via urokinase receptor association with CD36 and TLR4. *J Mol Cell Cardiol.* 2014;66:72-82.
26. Sangkuhl K, Shuldiner AR, Klein TE, Altman RB. Platelet aggregation pathway. *Pharmacogenet Genomics.* 2011;21(8):516-21.
27. Moreno PR. Vulnerable plaque: definition, diagnosis, and treatment. *Cardiol Clin.* 2010;28(1):1-30.
28. Moreno PR, Purushothaman M, Purushothaman KR. Plaque neovascularization: defense mechanisms, betrayal, or a war in progress. *Ann N Y Acad Sci.* 2012;1254:7-17.
29. W van Lammeren G, L Moll F, Borst GJ, de Kleijn DP, P M de Vries JP, Pasterkamp G. Atherosclerotic plaque biomarkers: beyond the horizon of the vulnerable plaque. *Curr Cardiol Rev.* 2011;7(1):22-7.
30. Luttun A, Tjwa M, Moons L, Wu Y, Angelillo-Scherrer A, Liao F, et al. Revascularization of ischemic tissues by PlGF treatment, and inhibition of tumor angiogenesis, arthritis and atherosclerosis by anti-Flt1. *Nat Med.* 2002;8(8):831-40.
31. Bunn RC, Fowlkes JL. Insulin-like growth factor binding protein proteolysis. *Trends Endocrinol Metab.* 2003;14(4):176-81.
32. Body R, Ferguson C. Towards evidence-based emergency medicine: best BETs from the Manchester Royal Infirmary. Pregnancy-associated plasma protein A: a novel cardiac marker with promise. *Emerg Med J.* 2006;23(11):875-7.
33. Fu X, Kassim SY, Parks WC, Heinecke JW. Hypochlorous acid oxygenates the cysteine switch domain of pro-matrilysin (MMP-7). A mechanism for matrix metalloproteinase activation and atherosclerotic plaque rupture by myeloperoxidase. *J Biol Chem.* 2001;276(44):41279-87.
34. Shabani F, McNeil J, Tippet L. The oxidative inactivation of tissue inhibitor of metalloproteinase-1 (TIMP-1) by hypochlorous acid (HOCl) is suppressed by anti-rheumatic drugs. *Free Radic Res.* 1998;28(2):115-23.
35. Galis ZS, Khatri JJ. Matrix metalloproteinases in vascular remodeling and atherogenesis: the good, the bad, and the ugly. *Circ Res.* 2002;90(3):251-62.
36. Blankenberg S, Rupprecht HJ, Poirier O, Bickel C, Smieja M, Hafner G, et al. Plasma concentrations and genetic variation of matrix metalloproteinase 9 and prognosis of patients with cardiovascular disease. *Circulation.* 2003;107(12):1579-85.
37. Herder C, Baumert J, Thorand B, Martin S, Löwel H, Kolb H, et al. Chemokines and incident coronary heart disease: results from the MONICA/KORA Augsburg case-cohort study, 1984-2002. *Arterioscler Thromb Vasc Biol.* 2006;26(9):2147-52.
38. Wang J, Tang B, Liu X, Wu X, Wang H, Xu D, et al. Increased monomeric CRP levels in acute myocardial infarction: a possible new and specific biomarker for diagnosis and severity assessment of disease. *Atherosclerosis.* 2015;239(2):343-9.

39. Ridker PM, Buring JE, Shih J, Matias M, Hennekens CH. Prospective study of C-reactive protein and the risk of future cardiovascular events among apparently healthy women. *Circulation*. 1998;98(8):731-3.
40. Ridker PM, Cushman M, Stampfer MJ, Tracy RP, Hennekens CH. Inflammation, aspirin, and the risk of cardiovascular disease in apparently healthy men. *N Engl J Med*. 1997;336(14):973-9.
41. Inoue T, Kato T, Uchida T, Sakuma M, Nakajima A, Shibasaki M, et al. Local release of C-reactive protein from vulnerable plaque or coronary arterial wall injured by stenting. *J Am Coll Cardiol*. 2005;46(2):239-45.
42. Khreiss T, József L, Potempa LA, Filep JG. Conformational rearrangement in C-reactive protein is required for proinflammatory actions on human endothelial cells. *Circulation*. 2004;109(16):2016-22.
43. Khreiss T, József L, Potempa LA, Filep JG. Opposing effects of C-reactive protein isoforms on shear-induced neutrophil-platelet adhesion and neutrophil aggregation in whole blood. *Circulation*. 2004;110(17):2713-20.
44. Eisenhardt SU, Thiele JR, Bannasch H, Stark GB, Peter K. C-reactive protein: how conformational changes influence inflammatory properties. *Cell Cycle*. 2009;8(23):3885-92.
45. Filep JG. Platelets affect the structure and function of C-reactive protein. *Circ Res*. 2009;105(2):109-11.
46. Habersberger J, Strang F, Scheichl A, Htun N, Bassler N, Merivirta RM, et al. Circulating microparticles generate and transport monomeric C-reactive protein in patients with myocardial infarction. *Cardiovasc Res*. 2012;96(1):64-72.
47. Slevin M, Matou-Nasri S, Turu M, Luque A, Rovira N, Badimon L, et al. Modified C-reactive protein is expressed by stroke neovessels and is a potent activator of angiogenesis in vitro. *Brain Pathol*. 2010;20(1):151-65.
48. de la Torre R, Peña E, Vilahur G, Slevin M, Badimon L. Monomerization of C-reactive protein requires glycoprotein IIb-IIIa activation: pentraxins and platelet deposition. *J Thromb Haemost*. 2013;11(11):2048-58.
49. Ji SR, Ma L, Bai CJ, Shi JM, Li HY, Potempa LA, et al. Monomeric C-reactive protein activates endothelial cells via interaction with lipid raft microdomains. *FASEB J*. 2009;23(6):1806-16.
50. Slevin M, Krupinski J. A role for monomeric C-reactive protein in regulation of angiogenesis, endothelial cell inflammation and thrombus formation in cardiovascular/cerebrovascular disease? *Histol Histopathol*. 2009;24(11):1473-8.
51. Tenaglia AN, Peters KG, Sketch MH, Annex BH. Neovascularization in atherectomy specimens from patients with unstable angina: implications for pathogenesis of unstable angina. *Am Heart J*. 1998;135(1):10-4.
52. Koole D, Heyligers J, Moll FL, Pasterkamp G. Intraplaque neovascularization and hemorrhage: markers for cardiovascular risk stratification and therapeutic monitoring. *J Cardiovasc Med (Hagerstown)*. 2012;13(10):635-9.
53. Hellings WE, Peeters W, Moll FL, Piers SR, van Setten J, Van der Spek PJ, et al. Composition of carotid atherosclerotic plaque is associated with cardiovascular outcome: a prognostic study. *Circulation*. 2010;121(17):1941-50.
54. Braig D, Nero TL, Koch HG, Kaiser B, Wang X, Thiele JR, et al. Transitional changes in the CRP structure lead to the exposure of proinflammatory binding sites. *Nat Commun*. 2017;8:14188.
55. Wang HW, Sui SF. Dissociation and subunit rearrangement of membrane-bound human C-reactive proteins. *Biochem Biophys Res Commun*. 2001;288(1):75-9.
56. Okemefuna AI, Stach L, Rana S, Buetas AJ, Gor J, Perkins SJ. C-reactive protein exists in an NaCl concentration-dependent pentamer-decamer equilibrium in physiological buffer. *J Biol Chem*. 2010;285(2):1041-52.
57. Ji SR, Wu Y, Zhu L, Potempa LA, Sheng FL, Lu W, et al. Cell membranes and liposomes dissociate C-reactive protein (CRP) to form a new, biologically active structural intermediate: mCRP(m). *FASEB J*. 2007;21(1):284-94.

58. Sun H, Koike T, Ichikawa T, Hatakeyama K, Shiomi M, Zhang B, et al. C-reactive protein in atherosclerotic lesions: its origin and pathophysiological significance. *Am J Pathol.* 2005;167(4):1139-48.
59. Eisenhardt SU, Habersberger J, Murphy A, Chen YC, Woollard KJ, Bassler N, et al. Dissociation of pentameric to monomeric C-reactive protein on activated platelets localizes inflammation to atherosclerotic plaques. *Circ Res.* 2009;105(2):128-37.
60. Oh SJ, Na Kim E, Jai Kim C, Choi JS, Kim KB. The effect of C-reactive protein deposition on myocardium with ischaemia-reperfusion injury in rats. *Interact Cardiovasc Thorac Surg.* 2017;25(2):260-7.
61. Xie L, Chang L, Guan Y, Wang X. C-reactive protein augments interleukin-8 secretion in human peripheral blood monocytes. *J Cardiovasc Pharmacol.* 2005;46(5):690-6.
62. Devaraj S, Davis B, Simon SI, Jialal I. CRP promotes monocyte-endothelial cell adhesion via Fcγ receptors in human aortic endothelial cells under static and shear flow conditions. *Am J Physiol Heart Circ Physiol.* 2006;291(3):H1170-6.
63. Fujii H, Li SH, Szmítzko PE, Fedak PW, Verma S. C-reactive protein alters antioxidant defenses and promotes apoptosis in endothelial progenitor cells. *Arterioscler Thromb Vasc Biol.* 2006;26(11):2476-82.
64. Woollard KJ, Phillips DC, Griffiths HR. Direct modulatory effect of C-reactive protein on primary human monocyte adhesion to human endothelial cells. *Clin Exp Immunol.* 2002;130(2):256-62.
65. Khreiss T, József L, Hossain S, Chan JS, Potempa LA, Filep JG. Loss of pentameric symmetry of C-reactive protein is associated with delayed apoptosis of human neutrophils. *J Biol Chem.* 2002;277(43):40775-81.
66. Meuwissen M, van der Wal AC, Niessen HW, Koch KT, de Winter RJ, van der Loos CM, et al. Colocalisation of intraplaque C reactive protein, complement, oxidised low density lipoprotein, and macrophages in stable and unstable angina and acute myocardial infarction. *J Clin Pathol.* 2006;59(2):196-201.
67. Molins B, Peña E, Vilahur G, Mendieta C, Slevin M, Badimon L. C-reactive protein isoforms differ in their effects on thrombus growth. *Arterioscler Thromb Vasc Biol.* 2008;28(12):2239-46.
68. Fordjour PA, Wang Y, Shi Y, Agyemang K, Akinyi M, Zhang Q, et al. Possible mechanisms of C-reactive protein mediated acute myocardial infarction. *Eur J Pharmacol.* 2015;760:72-80.
69. Mihlan M, Stippa S, Józsi M, Zipfel PF. Monomeric CRP contributes to complement control in fluid phase and on cellular surfaces and increases phagocytosis by recruiting factor H. *Cell Death Differ.* 2009;16(12):1630-40.
70. Kovacs A, Tornvall P, Nilsson R, Tegnér J, Hamsten A, Björkegren J. Human C-reactive protein slows atherosclerosis development in a mouse model with human-like hypercholesterolemia. *Proc Natl Acad Sci U S A.* 2007;104(34):13768-73.
71. Turu MM, Slevin M, Matou S, West D, Rodríguez C, Luque A, et al. C-reactive protein exerts angiogenic effects on vascular endothelial cells and modulates associated signalling pathways and gene expression. *BMC Cell Biol.* 2008;9:47.
72. Thiele JR, Habersberger J, Braig D, Schmidt Y, Goerendt K, Maurer V, et al. Dissociation of pentameric to monomeric C-reactive protein localizes and aggravates inflammation: in vivo proof of a powerful proinflammatory mechanism and a new anti-inflammatory strategy. *Circulation.* 2014;130(1):35-50.
73. Frangogiannis NG. Monomeric C-reactive protein and inflammatory injury in myocardial infarction. *Cardiovasc Res.* 2012;96(1):4-6.
74. Badimon L, Vilahur G. Thrombosis formation on atherosclerotic lesions and plaque rupture. *J Intern Med.* 2014;276(6):618-32.
75. Li R, Ren M, Luo M, Chen N, Zhang Z, Luo B, et al. Monomeric C-reactive protein alters fibrin clot properties on endothelial cells. *Thromb Res.* 2012;129(5):e251-6.



76. Boras E, Slevin M, Alexander MY, Aljohi A, Gilmore W, Ashworth J, et al. Monomeric C-reactive protein and Notch-3 co-operatively increase angiogenesis through PI3K signalling pathway. *Cytokine*. 2014;69(2):165-79.
77. Goda T, Miyahara Y. Calcium-independent binding of human C-reactive protein to lysophosphatidylcholine in supported planar phospholipid monolayers. *Acta Biomater*. 2017;48:206-14.
78. Goda T, Kjall P, Ishihara K, Richter-Dahlfors A, Miyahara Y. Biomimetic interfaces reveal activation dynamics of C-reactive protein in local microenvironments. *Adv Healthc Mater*. 2014;3(11):1733-8.
79. Goda T, Miyahara Y. Engineered zwitterionic phosphorylcholine monolayers for elucidating multivalent binding kinetics of C-reactive protein. *Acta Biomater*. 2016;40:46-53.
80. O'Flynn J, van der Pol P, Dixon KO, Prohászka Z, Daha MR, van Kooten C. Monomeric C-reactive protein inhibits renal cell-directed complement activation mediated by properdin. *Am J Physiol Renal Physiol*. 2016;310(11):F1308-16.
81. Li HY, Wang J, Meng F, Jia ZK, Su Y, Bai QF, et al. An Intrinsically Disordered Motif Mediates Diverse Actions of Monomeric C-reactive Protein. *J Biol Chem*. 2016;291(16):8795-804.
82. Obradovic MM, Trpkovic A, Bajic V, Soskic S, Jovanovic A, Stanimirovic J, et al. Interrelatedness between C-reactive protein and oxidized low-density lipoprotein. *Clin Chem Lab Med*. 2015;53(1):29-34.
83. Sabatine MS, Cannon CP. Approach to the patient with chest pain. *Braunwald's Heart Disease: A Textbook of Cardiovascular Medicine* 9th ed Philadelphia, Pa: Saunders Elsevier. 2011.
84. Culić V, Eterović D, Mirić D, Silić N. Symptom presentation of acute myocardial infarction: influence of sex, age, and risk factors. *Am Heart J*. 2002;144(6):1012-7.
85. Brieger D, Eagle KA, Goodman SG, Steg PG, Budaj A, White K, et al. Acute coronary syndromes without chest pain, an underdiagnosed and undertreated high-risk group: insights from the Global Registry of Acute Coronary Events. *Chest*. 2004;126(2):461-9.
86. Canto JG, Fincher C, Kiefe CI, Allison JJ, Li Q, Funkhouser E, et al. Atypical presentations among Medicare beneficiaries with unstable angina pectoris. *Am J Cardiol*. 2002;90(3):248-53.
87. Savonitto S, Ardissino D, Granger CB, Morando G, Prando MD, Mafrici A, et al. Prognostic value of the admission electrocardiogram in acute coronary syndromes. *JAMA*. 1999;281(8):707-13.
88. Ronner E, Boersma E, Laarman GJ, Somsen GA, Harrington RA, Deckers JW, et al. Early angioplasty in acute coronary syndromes without persistent ST-segment elevation improves outcome but increases the need for six-month repeat revascularization: an analysis of the PURSUIT Trial. Platelet glycoprotein IIb/IIIa in Unstable angina: Receptor Suppression Using Integrilin Therapy. *J Am Coll Cardiol*. 2002;39(12):1924-9.
89. Braunwald E. Unstable angina. A classification. *Circulation*. 1989;80(2):410-4.
90. Pryor DB, Shaw L, McCants CB, Lee KL, Mark DB, Harrell FE, et al. Value of the history and physical in identifying patients at increased risk for coronary artery disease. *Ann Intern Med*. 1993;118(2):81-90.
91. Ho KT, Miller TD, Hodge DO, Bailey KR, Gibbons RJ. Use of a simple clinical score to predict prognosis of patients with normal or mildly abnormal resting electrocardiographic findings undergoing evaluation for coronary artery disease. *Mayo Clin Proc*. 2002;77(6):515-21.
92. Six AJ, Backus BE, Kelder JC. Chest pain in the emergency room: value of the HEART score. *Neth Heart J*. 2008;16(6):191-6.
93. Backus BE, Six AJ, Kelder JC, Mast TP, van den Akker F, Mast EG, et al. Chest pain in the emergency room: a multicenter validation of the HEART Score. *Crit Pathw Cardiol*. 2010;9(3):164-9.
94. Antman EM, Cohen M, Bernink PJ, McCabe CH, Horacek T, Papuchis G, et al. The TIMI risk score for unstable angina/non-ST elevation MI: A method for prognostication and therapeutic decision making. *JAMA*. 2000;284(7):835-42.
95. guidance N. *Chest Pain of Recent Onset: Assessment and diagnosis (update)*. CG95. <https://www.nice.org.uk/guidance/cg952016> [

96. Bandstein N, Ljung R, Johansson M, Holzmann MJ. Undetectable high-sensitivity cardiac troponin T level in the emergency department and risk of myocardial infarction. *J Am Coll Cardiol*. 2014;63(23):2569-78.
97. Zhelev Z, Hyde C, Youngman E, Rogers M, Fleming S, Slade T, et al. Diagnostic accuracy of single baseline measurement of Elecsys Troponin T high-sensitive assay for diagnosis of acute myocardial infarction in emergency department: systematic review and meta-analysis. *BMJ*. 2015;350:h15.
98. Carlton EW, Cullen L, Than M, Gamble J, Khattab A, Greaves K. A novel diagnostic protocol to identify patients suitable for discharge after a single high-sensitivity troponin. *Heart*. 2015;101(13):1041-6.
99. Body R, Burrows G, Carley S, Cullen L, Than M, Jaffe AS, et al. High-sensitivity cardiac troponin t concentrations below the limit of detection to exclude acute myocardial infarction: a prospective evaluation. *Clin Chem*. 2015;61(7):983-9.
100. Carlton E, Greenslade J, Cullen L, Body R, Than M, Pickering JW, et al. Evaluation of High-Sensitivity Cardiac Troponin I Levels in Patients With Suspected Acute Coronary Syndrome. *JAMA Cardiol*. 2016;1(4):405-12.
101. Pickering JW, Than MP, Cullen L, Aldous S, Ter Avest E, Body R, et al. Rapid Rule-out of Acute Myocardial Infarction With a Single High-Sensitivity Cardiac Troponin T Measurement Below the Limit of Detection: A Collaborative Meta-analysis. *Ann Intern Med*. 2017;166(10):715-24.
102. Body R, Mueller C, Giannitsis E, Christ M, Ordonez-Llanos J, de Filippi CR, et al. The Use of Very Low Concentrations of High-sensitivity Troponin T to Rule Out Acute Myocardial Infarction Using a Single Blood Test. *Acad Emerg Med*. 2016;23(9):1004-13.
103. Chapman AR, Anand A, Boeddinghaus J, Ferry AV, Sandeman D, Adamson PD, et al. Comparison of the Efficacy and Safety of Early Rule-Out Pathways for Acute Myocardial Infarction. *Circulation*. 2017;135(17):1586-96.
104. Takeda S, Yamashita A, Maeda K, Maeda Y. Structure of the core domain of human cardiac troponin in the Ca(2+)-saturated form. *Nature*. 2003;424(6944):35-41.
105. Hwang PM, Cai F, Pineda-Sanabria SE, Corson DC, Sykes BD. The cardiac-specific N-terminal region of troponin I positions the regulatory domain of troponin C. *Proc Natl Acad Sci U S A*. 2014;111(40):14412-7.
106. Dhoot GK, Gell PG, Perry SV. The localization of the different forms of troponin I in skeletal and cardiac muscle cells. *Exp Cell Res*. 1978;117(2):357-70.
107. Dhoot GK, Perry SV. Distribution of polymorphic forms of troponin components and tropomyosin in skeletal muscle. *Nature*. 1979;278(5706):714-8.
108. Parmacek MS, Leiden JM. Structure, function, and regulation of troponin C. *Circulation*. 1991;84(3):991.
109. Szczesna D, Guzman G, Miller T, Zhao J, Farokhi K, Ellemberger H, et al. The role of the four Ca<sup>2+</sup> binding sites of troponin C in the regulation of skeletal muscle contraction. *J Biol Chem*. 1996;271(14):8381-6.
110. Filatov VL, Katrukha AG, Bulargina TV, Gusev NB. Troponin: structure, properties, and mechanism of functioning. *Biochemistry (Mosc)*. 1999;64(9):969-85.
111. Raggi A, Grand RJ, Moir AJ, Perry SV. Structure-function relationships in cardiac troponin T. *Biochim Biophys Acta*. 1989;997(1-2):135-43.
112. Cummins P, Perry SV. Troponin I from human skeletal and cardiac muscles. *Biochem J*. 1978;171(1):251-9.
113. Schreier T, Kedes L, Gahlmann R. Cloning, structural analysis, and expression of the human slow twitch skeletal muscle/cardiac troponin C gene. *J Biol Chem*. 1990;265(34):21247-53.
114. Anderson PA, Malouf NN, Oakeley AE, Pagani ED, Allen PD. Troponin T isoform expression in humans. A comparison among normal and failing adult heart, fetal heart, and adult and fetal skeletal muscle. *Circ Res*. 1991;69(5):1226-33.

115. Willging S, Keller F, Steinbach G. Specificity of cardiac troponins I and T in renal disease. *Clin Chem Lab Med*. 1998;36(2):87-92.
116. Buiten MS, de Bie MK, Rotmans JI, Dekker FW, van Buren M, Rabelink TJ, et al. Serum Cardiac Troponin-I is Superior to Troponin-T as a Marker for Left Ventricular Dysfunction in Clinically Stable Patients with End-Stage Renal Disease. *PLoS One*. 2015;10(8):e0134245.
117. Bhayana V, Gougoulas T, Cohoe S, Henderson AR. Discordance between results for serum troponin T and troponin I in renal disease. *Clin Chem*. 1995;41(2):312-7.
118. Lavoinne A, Hue G. Serum cardiac troponins I and T in early posttraumatic rhabdomyolysis. *Clin Chem*. 1998;44(3):667-8.
119. Saggin L, Gorza L, Ausoni S, Schiaffino S. Troponin I switching in the developing heart. *J Biol Chem*. 1989;264(27):16299-302.
120. Jin JP. Alternative RNA splicing-generated cardiac troponin T isoform switching: a non-heart-restricted genetic programming synchronized in developing cardiac and skeletal muscles. *Biochem Biophys Res Commun*. 1996;225(3):883-9.
121. Toyota N, Shimada Y. Differentiation of troponin in cardiac and skeletal muscles in chicken embryos as studied by immunofluorescence microscopy. *J Cell Biol*. 1981;91(2 Pt 1):497-504.
122. Katus HA, Looser S, Hallermayer K, Remppis A, Scheffold T, Borgya A, et al. Development and in vitro characterization of a new immunoassay of cardiac troponin T. *Clin Chem*. 1992;38(3):386-93.
123. de Winter RJ, Koster RW, Sturk A, Sanders GT. Value of myoglobin, troponin T, and CK-MBmass in ruling out an acute myocardial infarction in the emergency room. *Circulation*. 1995;92(12):3401-7.
124. Tucker JF, Collins RA, Anderson AJ, Hauser J, Kalas J, Apple FS. Early diagnostic efficiency of cardiac troponin I and Troponin T for acute myocardial infarction. *Acad Emerg Med*. 1997;4(1):13-21.
125. Müller-Bardorff M, Hallermayer K, Schröder A, Ebert C, Borgya A, Gerhardt W, et al. Improved troponin T ELISA specific for cardiac troponin T isoform: assay development and analytical and clinical validation. *Clin Chem*. 1997;43(3):458-66.
126. Jaffe AS, Ravkilde J, Roberts R, Naslund U, Apple FS, Galvani M, et al. It's time for a change to a troponin standard. *Circulation*. 2000;102(11):1216-20.
127. Gerhardt W, Nordin G, Ljungdahl L. Can troponin T replace CK MBmass as "gold standard" for acute myocardial infarction ("AMI")? *Scand J Clin Lab Invest Suppl*. 1999;230:83-9.
128. Myocardial infarction redefined--a consensus document of The Joint European Society of Cardiology/American College of Cardiology Committee for the redefinition of myocardial infarction. *Eur Heart J*. 2000;21(18):1502-13.
129. Smith SC, Ladenson JH, Mason JW, Jaffe AS. Elevations of Cardiac Troponin I Associated With Myocarditis. *Circulation*. 1997;95(1):163.
130. Adams JE, Bodor GS, Dávila-Román VG, Delmez JA, Apple FS, Ladenson JH, et al. Cardiac troponin I. A marker with high specificity for cardiac injury. *Circulation*. 1993;88(1):101-6.
131. Eggert KM, Oldgren J, Nordenskjöld A, Lindahl B. Diagnostic value of serial measurement of cardiac markers in patients with chest pain: limited value of adding myoglobin to troponin I for exclusion of myocardial infarction. *Am Heart J*. 2004;148(4):574-81.
132. Jaffe AS, Landt Y, Parvin CA, Abendschein DR, Geltman EM, Ladenson JH. Comparative sensitivity of cardiac troponin I and lactate dehydrogenase isoenzymes for diagnosing acute myocardial infarction. *Clin Chem*. 1996;42(11):1770-6.
133. Katus HA, Remppis A, Scheffold T, Diederich KW, Kuebler W. Intracellular compartmentation of cardiac troponin T and its release kinetics in patients with reperfused and nonreperfused myocardial infarction. *Am J Cardiol*. 1991;67(16):1360-7.
134. Galvani M, Ottani F, Ferrini D, Ladenson JH, Destro A, Baccos D, et al. Prognostic influence of elevated values of cardiac troponin I in patients with unstable angina. *Circulation*. 1997;95(8):2053-9.

135. Stubbs P, Collinson P, Moseley D, Greenwood T, Noble M. Prognostic significance of admission troponin T concentrations in patients with myocardial infarction. *Circulation*. 1996;94(6):1291-7.
136. Hamm CW, Goldmann BU, Heeschen C, Kreymann G, Berger J, Meinertz T. Emergency room triage of patients with acute chest pain by means of rapid testing for cardiac troponin T or troponin I. *N Engl J Med*. 1997;337(23):1648-53.
137. Wu AH, Feng YJ, Contois JH, Azar R, Waters D. Prognostic value of cardiac troponin I in patients with chest pain. *Clin Chem*. 1996;42(4):651-2.
138. Ravkilde J, Nissen H, Hørder M, Thygesen K. Independent prognostic value of serum creatine kinase isoenzyme MB mass, cardiac troponin T and myosin light chain levels in suspected acute myocardial infarction. Analysis of 28 months of follow-up in 196 patients. *J Am Coll Cardiol*. 1995;25(3):574-81.
139. Holmes DR, Hartzler GO, Smith HC, Fuster V. Coronary artery thrombosis in patients with unstable angina. *Br Heart J*. 1981;45(4):411-6.
140. Vetovec GW, Cowley MJ, Overton H, Richardson DW. Intracoronary thrombus in syndromes of unstable myocardial ischemia. *Am Heart J*. 1981;102(6 Pt 2):1202-8.
141. Zack PM, Ischinger T, Aker UT, Dincer B, Kennedy HL. The occurrence of angiographically detected intracoronary thrombus in patients with unstable angina pectoris. *Am Heart J*. 1984;108(6):1408-12.
142. Bresnahan DR, Davis JL, Holmes DR, Smith HC. Angiographic occurrence and clinical correlates of intraluminal coronary artery thrombus: role of unstable angina. *J Am Coll Cardiol*. 1985;6(2):285-9.
143. Mann JM, Kaski JC, Pereira WI, Arie S, Ramires JA, Pileggi F. Histological patterns of atherosclerotic plaques in unstable angina patients vary according to clinical presentation. *Heart*. 1998;80(1):19-22.
144. Davies MJ, Thomas AC, Knapman PA, Hangartner JR. Intramyocardial platelet aggregation in patients with unstable angina suffering sudden ischemic cardiac death. *Circulation*. 1986;73(3):418-27.
145. Falk E. Unstable angina with fatal outcome: dynamic coronary thrombosis leading to infarction and/or sudden death. Autopsy evidence of recurrent mural thrombosis with peripheral embolization culminating in total vascular occlusion. *Circulation*. 1985;71(4):699-708.
146. Apple FS, Wu AH, Jaffe AS. European Society of Cardiology and American College of Cardiology guidelines for redefinition of myocardial infarction: how to use existing assays clinically and for clinical trials. *Am Heart J*. 2002;144(6):981-6.
147. Panteghini M, Pagani F, Yeo KT, Apple FS, Christenson RH, Dati F, et al. Evaluation of imprecision for cardiac troponin assays at low-range concentrations. *Clin Chem*. 2004;50(2):327-32.
148. Macht M, Fiedler W, Kürzinger K, Przybylski M. Mass spectrometric mapping of protein epitope structures of myocardial infarct markers myoglobin and troponin T. *Biochemistry*. 1996;35(49):15633-9.
149. Katrukha AG, Bereznikova AV, Esakova TV, Pettersson K, Lövgren T, Severina ME, et al. Troponin I is released in bloodstream of patients with acute myocardial infarction not in free form but as complex. *Clin Chem*. 1997;43(8 Pt 1):1379-85.
150. Ferrieres G, Calzolari C, Mani JC, Laune D, Trinquier S, Laprade M, et al. Human cardiac troponin I: precise identification of antigenic epitopes and prediction of secondary structure. *Clin Chem*. 1998;44(3):487-93.
151. Filatov VL, Katrukha AG, Bereznikova AV, Esakova TV, Bulargina TV, Kolosova OV, et al. Epitope mapping of anti-troponin I monoclonal antibodies. *Biochem Mol Biol Int*. 1998;45(6):1179-87.
152. Bates KJ, Hall EM, Fahie-Wilson MN, Kindler H, Bailey C, Lythall D, et al. Circulating immunoreactive cardiac troponin forms determined by gel filtration chromatography after acute myocardial infarction. *Clin Chem*. 2010;56(6):952-8.

153. Wu AH, Feng YJ, Moore R, Apple FS, McPherson PH, Buechler KF, et al. Characterization of cardiac troponin subunit release into serum after acute myocardial infarction and comparison of assays for troponin T and I. American Association for Clinical Chemistry Subcommittee on cTnI Standardization. *Clin Chem*. 1998;44(6 Pt 1):1198-208.
154. Panteghini M, Gerhardt W, Apple FS, Dati F, Ravkilde J, Wu AH. Quality specifications for cardiac troponin assays. *Clin Chem Lab Med*. 2001;39(2):175-9.
155. Cullen L, Parsonage WA, Greenslade J, Lamanna A, Hammett CJ, Than M, et al. Delta troponin for the early diagnosis of AMI in emergency patients with chest pain. *Int J Cardiol*. 2013;168(3):2602-8.
156. Macrae AR, Kavsak PA, Lustig V, Bhargava R, Vandersluis R, Palomaki GE, et al. Assessing the requirement for the 6-hour interval between specimens in the American Heart Association Classification of Myocardial Infarction in Epidemiology and Clinical Research Studies. *Clin Chem*. 2006;52(5):812-8.
157. Keller T, Zeller T, Peetz D, Tzikas S, Roth A, Czyz E, et al. Sensitive troponin I assay in early diagnosis of acute myocardial infarction. *N Engl J Med*. 2009;361(9):868-77.
158. Reichlin T, Hochholzer W, Bassetti S, Steuer S, Stelzig C, Hartwiger S, et al. Early diagnosis of myocardial infarction with sensitive cardiac troponin assays. *N Engl J Med*. 2009;361(9):858-67.
159. Giannitsis E, Kurz K, Hallermayer K, Jarausch J, Jaffe AS, Katus HA. Analytical validation of a high-sensitivity cardiac troponin T assay. *Clin Chem*. 2010;56(2):254-61.
160. Reichlin T, Irfan A, Twerenbold R, Reiter M, Hochholzer W, Burkhalter H, et al. Utility of absolute and relative changes in cardiac troponin concentrations in the early diagnosis of acute myocardial infarction. *Circulation*. 124. United States 2011. p. 136-45.
161. Keller T, Zeller T, Ojeda F, Tzikas S, Lillpopp L, Sinning C, et al. Serial changes in highly sensitive troponin I assay and early diagnosis of myocardial infarction. *JAMA*. 2011;306(24):2684-93.
162. Giannitsis E, Becker M, Kurz K, Hess G, Zdunek D, Katus HA. High-sensitivity cardiac troponin T for early prediction of evolving non-ST-segment elevation myocardial infarction in patients with suspected acute coronary syndrome and negative troponin results on admission. *Clin Chem*. 2010;56(4):642-50.
163. Thygesen K, Mair J, Giannitsis E, Mueller C, Lindahl B, Blankenberg S, et al. How to use high-sensitivity cardiac troponins in acute cardiac care. *Eur Heart J*. 2012;33(18):2252-7.
164. Thygesen K, Alpert JS, Jaffe AS, Simoons ML, Chaitman BR, White HD, et al. Third universal definition of myocardial infarction. *Glob Heart*. 2012;7(4):275-95.
165. Apple FS, Jesse RL, Newby LK, Wu AH, Christenson RH, Biochemistry NAOc, et al. National Academy of Clinical Biochemistry and IFCC Committee for Standardization of Markers of Cardiac Damage Laboratory Medicine Practice Guidelines: Analytical issues for biochemical markers of acute coronary syndromes. *Circulation*. 2007;115(13):e352-5.
166. Body R, McDowell G, Carley S, Ferguson J, Mackway-Jones K. Diagnosing acute myocardial infarction with troponins: how low can you go? *Emerg Med J*. 2010;27(4):292-6.
167. Jaffe AS. Chasing troponin: how low can you go if you can see the rise? *J Am Coll Cardiol*. 2006;48(9):1763-4.
168. Jaffe AS, Apple FS. Refining our criteria: a critical challenge. *Am J Clin Pathol*. 2009;131(1):11-3.
169. Apple FS, Morrow DA. Delta cardiac troponin values in practice: are we ready to move absolutely forward to clinical routine? *Clin Chem*. 58. United States 2012. p. 8-10.
170. Kleine AH, Glatz JF, Van Nieuwenhoven FA, Van der Vusse GJ. Release of heart fatty acid-binding protein into plasma after acute myocardial infarction in man. *Mol Cell Biochem*. 1992;116(1-2):155-62.
171. Veerkamp JH. Fatty acid transport and fatty acid-binding proteins. *Proc Nutr Soc*. 1995;54(1):23-37.

172. Glatz JF, van Bilsen M, Paulussen RJ, Veerkamp JH, van der Vusse GJ, Reneman RS. Release of fatty acid-binding protein from isolated rat heart subjected to ischemia and reperfusion or to the calcium paradox. *Biochim Biophys Acta*. 1988;961(1):148-52.
173. Ghani F, Wu AH, Graff L, Petry C, Armstrong G, Prigent F, et al. Role of heart-type fatty acid-binding protein in early detection of acute myocardial infarction. *Clin Chem*. 2000;46(5):718-9.
174. Pelsers MM, Hermens WT, Glatz JF. Fatty acid-binding proteins as plasma markers of tissue injury. *Clin Chim Acta*. 2005;352(1-2):15-35.
175. Glatz JF, Kleine AH, van Nieuwenhoven FA, Hermens WT, van Dieijen-Visser MP, van der Vusse GJ. Fatty-acid-binding protein as a plasma marker for the estimation of myocardial infarct size in humans. *Br Heart J*. 1994;71(2):135-40.
176. Wodzig KW, Kragten JA, Hermens WT, Glatz JF, van Dieijen-Visser MP. Estimation of myocardial infarct size from plasma myoglobin or fatty acid-binding protein. Influence of renal function. *Eur J Clin Chem Clin Biochem*. 1997;35(3):191-8.
177. Van Nieuwenhoven FA, Kleine AH, Wodzig WH, Hermens WT, Kragten HA, Maessen JG, et al. Discrimination between myocardial and skeletal muscle injury by assessment of the plasma ratio of myoglobin over fatty acid-binding protein. *Circulation*. 1995;92(10):2848-54.
178. H-FABP. What is H-FABP? <http://www.h-fabp.com/what-is-h-fabp/2017> [
179. Azzazy HM, Pelsers MM, Christenson RH. Unbound free fatty acids and heart-type fatty acid-binding protein: diagnostic assays and clinical applications. *Clin Chem*. 2006;52(1):19-29.
180. Body R, McDowell G, Carley S, Wibberley C, Ferguson J, Mackway-Jones K. A FABP-ulous 'rule out' strategy? Heart fatty acid binding protein and troponin for rapid exclusion of acute myocardial infarction. *Resuscitation*. 2011;82(8):1041-6.
181. McMahon CG, Lamont JV, Curtin E, McConnell RI, Crockard M, Kurth MJ, et al. Diagnostic accuracy of heart-type fatty acid-binding protein for the early diagnosis of acute myocardial infarction. *Am J Emerg Med*. 2012;30(2):267-74.
182. Orak M, Ustündağ M, Güloğlu C, Ozhasenekler A, Alyan O, Kale E. The role of the heart-type fatty acid binding protein in the early diagnosis of acute coronary syndrome and its comparison with troponin I and creatine kinase-MB isoform. *Am J Emerg Med*. 2010;28(8):891-6.
183. Figiel Ł, Kasprzak JD, Peruga J, Lipiec P, Drozd J, Krzemińska-Pakuła M, et al. Heart-type fatty acid binding protein--a reliable marker of myocardial necrosis in a heterogeneous group of patients with acute coronary syndrome without persistent ST elevation. *Kardiologia Polska*. 2008;66(3):253-9, discussion 60-1.
184. Agnello L, Bivona G, Novo G, Scazzone C, Muratore R, Levantino P, et al. Heart-type fatty acid binding protein is a sensitive biomarker for early AMI detection in troponin negative patients: a pilot study. *Scandinavian Journal of Clinical and Laboratory Investigation*. 2017;77(6):428-32.
185. Liu Y, Jiang Z, Luo J, Peng X, Yi Z. Clinical study of H-FABP for risk stratification and prognosis in patients with early cTnT-negative ACS. *International Journal of Clinical and Experimental Medicine*. 2017;10(3):4873-80.
186. Li CJ, Li JQ, Liang XF, Li XX, Cui JG, Yang ZJ, et al. Point-of-care test of heart-type fatty acid-binding protein for the diagnosis of early acute myocardial infarction. *Acta Pharmacol Sin*. 2010;31(3):307-12.
187. Kim Y, Kim H, Kim SY, Lee HK, Kwon HJ, Kim YG, et al. Automated heart-type fatty acid-binding protein assay for the early diagnosis of acute myocardial infarction. *Am J Clin Pathol*. 2010;134(1):157-62.
188. Singulex. Singulex Clarity <http://www.singulexclarity.eu/> [
189. Abbott. iSTAT test cartridges <https://www.pointofcare.abbott/int/en/offerings/istat/istat-test-cartridges2017> [
190. Pretorius CJ, Wilgen U, Ungerer JP. Serial cardiac troponin differences measured on four contemporary analyzers: relative differences, actual differences and reference change values compared. *Clin Chim Acta*. 2012;413(21-22):1786-91.

191. Apple FS. A new season for cardiac troponin assays: it's time to keep a scorecard. *Clin Chem.* 2009;55(7):1303-6.
192. Taylor KE, van den Berg CW. Structural and functional comparison of native pentameric, denatured monomeric and biotinylated C-reactive protein. *Immunology.* 2007;120(3):404-11.
193. Potempa LA, Yao ZY, Ji SR, Filep JG, Wu Y. Solubilization and purification of recombinant modified C-reactive protein from inclusion bodies using reversible anhydride modification. *Biophys Rep.* 2015;1:18-33.
194. Crawford JR, Trial J, Nambi V, Hoogeveen RC, Taffet GE, Entman ML. Plasma Levels of Endothelial Microparticles Bearing Monomeric C-reactive Protein are Increased in Peripheral Artery Disease. *J Cardiovasc Transl Res.* 2016.
195. Crawford JR, Trial J, Nambi V, Hoogeveen RC, Taffet GE, Entman ML. Plasma Levels of Endothelial Microparticles Bearing Monomeric C-reactive Protein are Increased in Peripheral Artery Disease. *J Cardiovasc Transl Res.* 2016;9(3):184-93.
196. Wu AH, Jaffe AS. The clinical need for high-sensitivity cardiac troponin assays for acute coronary syndromes and the role for serial testing. *Am Heart J.* 2008;155(2):208-14.
197. Sabatine MS, Morrow DA, de Lemos JA, Jarolim P, Braunwald E. Detection of acute changes in circulating troponin in the setting of transient stress test-induced myocardial ischaemia using an ultrasensitive assay: results from TIMI 35. *Eur Heart J.* 2009;30(2):162-9.
198. Biener M, Mueller M, Vafaie M, Keller T, Blankenberg S, White HD, et al. Comparison of a 3-hour versus a 6-hour sampling-protocol using high-sensitivity cardiac troponin T for rule-out and rule-in of non-STEMI in an unselected emergency department population. *Int J Cardiol.* 2013;167(4):1134-40.
199. Apple FS, Collinson PO, Biomarkers ITFoCAoC. Analytical characteristics of high-sensitivity cardiac troponin assays. *Clin Chem.* 2012;58(1):54-61.
200. Bassand JP, Hamm CW, Ardissino D, Boersma E, Budaj A, Fernández-Avilés F, et al. Guidelines for the diagnosis and treatment of non-ST-segment elevation acute coronary syndromes. *Eur Heart J.* 2007;28(13):1598-660.
201. Jaffe AS, Apple FS, Morrow DA, Lindahl B, Katus HA. Being rational about (im)precision: a statement from the Biochemistry Subcommittee of the Joint European Society of Cardiology/American College of Cardiology Foundation/American Heart Association/World Heart Federation Task Force for the definition of myocardial infarction. *Clin Chem.* 2010;56(6):941-3.
202. Lam Q, Black M, Youdell O, Spilsbury H, Schneider HG. Performance evaluation and subsequent clinical experience with the Abbott Automated Architect STAT Troponin-I assay. *Clin Chem.* 2006;52(2):298-300.
203. Goorden SM, van Engelen RA, Wong LS, van der Ploeg T, Verdel GJ, Buijs MM. A novel troponin I rule-out value below the upper reference limit for acute myocardial infarction. *Heart.* 2016;102(21):1721-7.
204. Than M, Herbert M, Flaws D, Cullen L, Hess E, Hollander JE, et al. What is an acceptable risk of major adverse cardiac event in chest pain patients soon after discharge from the Emergency Department?: a clinical survey. *Int J Cardiol.* 2013;166(3):752-4.
205. Thygesen K, Mair J, Katus H, Plebani M, Venge P, Collinson P, et al. Recommendations for the use of cardiac troponin measurement in acute cardiac care. *Eur Heart J.* 2010;31(18):2197-204.
206. Agewall S, Giannitsis E, Jernberg T, Katus H. Troponin elevation in coronary vs. non-coronary disease. *Eur Heart J.* 2011;32(4):404-11.
207. Hamm CW, Giannitsis E, Katus HA. Cardiac Troponin Elevations in Patients Without Acute Coronary Syndrome. *Circulation.* 2002;106(23):2871-2.
208. Javed U, Aftab W, Ambrose JA, Wessel RJ, Mouanoutoua M, Huang G, et al. Frequency of elevated troponin I and diagnosis of acute myocardial infarction. *Am J Cardiol.* 2009;104(1):9-13.
209. Mueller M, Biener M, Vafaie M, Doerr S, Keller T, Blankenberg S, et al. Absolute and relative kinetic changes of high-sensitivity cardiac troponin T in acute coronary syndrome and in patients with increased troponin in the absence of acute coronary syndrome. *Clin Chem.* 2012;58(1):209-18.

210. Apple FS, Pearce LA, Smith SW, Kaczmarek JM, Murakami MM. Role of monitoring changes in sensitive cardiac troponin I assay results for early diagnosis of myocardial infarction and prediction of risk of adverse events. *Clin Chem*. 2009;55(5):930-7.
211. Apple FS, Smith SW, Pearce LA, Ler R, Murakami MM, Benoit MO, et al. Use of the bioMérieux VIDAS troponin I ultra assay for the diagnosis of myocardial infarction and detection of adverse events in patients presenting with symptoms suggestive of acute coronary syndrome. *Clin Chim Acta*. 2008;390(1-2):72-5.
212. Wu AH, Jaffe AS, Apple FS, Jesse RL, Francis GL, Morrow DA, et al. National Academy of Clinical Biochemistry laboratory medicine practice guidelines: use of cardiac troponin and B-type natriuretic peptide or N-terminal proB-type natriuretic peptide for etiologies other than acute coronary syndromes and heart failure. *Clin Chem*. 2007;53(12):2086-96.
213. Apple FS, Smith SW, Pearce LA, Murakami MM. Delta changes for optimizing clinical specificity and 60-day risk of adverse events in patients presenting with symptoms suggestive of acute coronary syndrome utilizing the ADVIA Centaur TnI-Ultra assay. *Clin Biochem*. 2012;45(10-11):711-3.
214. Mueller-Hennessen M, Mueller C, Giannitsis E, Biener M, Vafaie M, deFilippi CR, et al. Serial Sampling of High-Sensitivity Cardiac Troponin T May Not Be Required for Prediction of Acute Myocardial Infarction Diagnosis in Chest Pain Patients with Highly Abnormal Concentrations at Presentation. *Clin Chem*. 2017;63(2):542-51.
215. Sajeev JK, New G, Roberts L, Menon SK, Gunawan F, Wijesundera P, et al. High sensitivity troponin: Does the 50% delta change alter clinical outcomes in chest pain presentations to the emergency room? *Int J Cardiol*. 2015;184:170-4.
216. Mueller C, Giannitsis E, Christ M, Ordóñez-Llanos J, deFilippi C, McCord J, et al. Multicenter Evaluation of a 0-Hour/1-Hour Algorithm in the Diagnosis of Myocardial Infarction With High-Sensitivity Cardiac Troponin T. *Ann Emerg Med*. 2016;68(1):76-87.e4.
217. Sandoval Y, Smith SW, Thordsen SE, Bruen CA, Carlson MD, Dodd KW, et al. Diagnostic Performance of High Sensitivity Compared with Contemporary Cardiac Troponin I for the Diagnosis of Acute Myocardial Infarction. *Clin Chem*. 2017;63(10):1594-604.
218. Glatz JF, van der Vusse GJ. Cellular fatty acid-binding proteins: their function and physiological significance. *Prog Lipid Res*. 1996;35(3):243-82.
219. Storch J, Thumser AE. The fatty acid transport function of fatty acid-binding proteins. *Biochim Biophys Acta*. 2000;1486(1):28-44.
220. Niizeki T, Takeishi Y, Arimoto T, Takabatake N, Nozaki N, Hirono O, et al. Heart-type fatty acid-binding protein is more sensitive than troponin T to detect the ongoing myocardial damage in chronic heart failure patients. *J Card Fail*. 2007;13(2):120-7.
221. Kaczyńska A, Pelsers MM, Bochowicz A, Kostrubiec M, Glatz JF, Pruszczyk P. Plasma heart-type fatty acid binding protein is superior to troponin and myoglobin for rapid risk stratification in acute pulmonary embolism. *Clin Chim Acta*. 2006;371(1-2):117-23.
222. Lescuyer P, Allard L, Zimmermann-Ivol CG, Burgess JA, Hughes-Frutiger S, Burkhard PR, et al. Identification of post-mortem cerebrospinal fluid proteins as potential biomarkers of ischemia and neurodegeneration. *Proteomics*. 2004;4(8):2234-41.
223. Freund Y, Chenevier-Gobeaux C, Leumani F, Claessens YE, Allo JC, Doumenc B, et al. Heart-type fatty acid binding protein and the diagnosis of acute coronary syndrome in the ED. *Am J Emerg Med*. 2012;30(8):1378-84.
224. Neumann JT, Sörensen NA, Ojeda F, Renné T, Schnabel RB, Zeller T, et al. Early diagnosis of acute myocardial infarction using high-sensitivity troponin I. *PLoS One*. 2017;12(3):e0174288.
225. Morrow DA, Cannon CP, Rifai N, Frey MJ, Vicari R, Lakkis N, et al. Ability of minor elevations of troponins I and T to predict benefit from an early invasive strategy in patients with unstable angina and non-ST elevation myocardial infarction: results from a randomized trial. *JAMA*. 2001;286(19):2405-12.



226. Nejatian A, Omstedt Å, Höijer J, Hansson LO, Djärv T, Eggers KM, et al. Outcomes in Patients With Chest Pain Discharged After Evaluation Using a High-Sensitivity Troponin T Assay. *J Am Coll Cardiol*. 2017;69(21):2622-30.
227. Body R, McDowell G, Carley S, Mackway-Jones K. Do risk factors for chronic coronary heart disease help diagnose acute myocardial infarction in the Emergency Department? *Resuscitation*. 2008;79(1):41-5.
228. Aldous SJ, Richards M, Cullen L, Troughton R, Than M. Diagnostic and prognostic utility of early measurement with high-sensitivity troponin T assay in patients presenting with chest pain. *CMAJ*. 2012;184(5):E260-8.
229. Eggers KM, Jaffe AS, Venge P, Lindahl B. Clinical implications of the change of cardiac troponin I levels in patients with acute chest pain - an evaluation with respect to the Universal Definition of Myocardial Infarction. *Clin Chim Acta*. 2011;412(1-2):91-7.
230. Kavsak PA, Ko DT, Wang X, Macrae AR, Jaffe AS. Increasing cardiac troponin changes measured by a research high-sensitivity troponin I assay: absolute vs percentage changes and long-term outcomes in a chest pain cohort. *Clin Chem*. 2010;56(12):1902-4.
231. Amsterdam EA, Wenger NK, Brindis RG, Casey DE, Ganiats TG, Holmes DR, et al. 2014 AHA/ACC guideline for the management of patients with non-ST-elevation acute coronary syndromes: a report of the American College of Cardiology/American Heart Association Task Force on Practice Guidelines. *Circulation*. 2014;130(25):e344-426.
232. Body R, Carley S, McDowell G, Pemberton P, Burrows G, Cook G, et al. The Manchester Acute Coronary Syndromes (MACS) decision rule for suspected cardiac chest pain: derivation and external validation. *Heart*. 2014;100(18):1462-8.
233. Body R, Burrows G, Carley S, Lewis PS. The Manchester Acute Coronary Syndromes (MACS) decision rule: validation with a new automated assay for heart-type fatty acid binding protein. *Emerg Med J*. 2015;32(10):769-74.
234. Simpson AJ, Potter JM, Koerbin G, Oakman C, Cullen L, Wilkes GJ, et al. Use of observed within-person variation of cardiac troponin in emergency department patients for determination of biological variation and percentage and absolute reference change values. *Clin Chem*. 2014;60(6):848-54.
235. Aakre KM, Røraas T, Petersen PH, Svarstad E, Sellevoll H, Skadberg Ø, et al. Weekly and 90-minute biological variations in cardiac troponin T and cardiac troponin I in hemodialysis patients and healthy controls. *Clin Chem*. 2014;60(6):838-47.
236. Fournier S, Iten L, Marques-Vidal P, Boulat O, Bardy D, Beggah A, et al. Circadian rhythm of blood cardiac troponin T concentration. *Clin Res Cardiol*. 2017.
237. Sandoval Y, Herzog CA, Love SA, Cao J, Hu Y, Wu AH, et al. Prognostic Value of Serial Changes in High-Sensitivity Cardiac Troponin I and T over 3 Months Using Reference Change Values in Hemodialysis Patients. *Clin Chem*. 2016;62(4):631-8.